



The
University
Of
Sheffield.

Investigating the Post-transcriptional Regulation of Macrophage and Prostate Cancer Transcriptome by microRNAs with focus on Tribbles-1

Chiara Niespolo

Registration No: 160266054

A thesis submitted in partial fulfilment of the requirements for the degree of
Doctor of Philosophy

The University of Sheffield
Faculty of Medicine, Dentistry & Health

Department of Infection, Immunity & Cardiovascular Disease

April 2020

I am just a child who has never grown up. I still keep asking these 'how' and 'why' questions. Occasionally, I find an answer.

Stephen Hawking

Thesis format

Each chapter of this thesis is structured individually and consists of:

- I. A general introduction, providing a background to each results chapter (Chapter 1);
- II. General materials and methods, describing all the techniques, procedures and assay used in this work (Chapter 2);
- III. First results chapter, structured as a traditional thesis chapter but intended to be published (Chapter 3, first author);
- IV. Second results chapter, structured as a traditional thesis chapter but intended to be published (Chapter 4, co-first author);
- V. Two additional results chapters describing small, side projects fitting the aims of this thesis (Chapter 5,6);
- VI. A conclusive chapter, summarizing the main findings (Chapter 7);
- VII. Supporting information, additional methods and supplementary results, not included in the main chapters (Chapter 8).

List of contents, figures and tables is also provided at the beginning of the thesis.

Declaration

The work presented in this thesis has been generated and analysed by myself, unless otherwise stated. Help from Dr Jessica Johnston and Kajus Baidzajevs was greatly appreciated, as well as from Dr Alessandra Iscaro, Swapna Satam and Ziyanda Shologu who provided animal samples and prostate cancer specimens. Chapter 4 arises from a close collaboration with Sumeet Deshmukh and Dr Ian Sudbery, who performed the whole transcriptomics analysis. Chapter 3 and Chapter 4 are intended to be published, along with data not shown in this thesis. During the years, all the help and support received from IICD technicians was critical and I would like to thank them all, in particular Dr Markus Arians, Jonathan Kilby and Dr Ben Durham.

Associated Publications

Conference papers (published abstracts):

- I. Niespolo C, Shologu Z, Satam S, Iscaro A, Muthana M, Socorro S, Wilson HL, Kiss-Toth E, microRNAs regulating Tribbles-1: potential molecular targets in prostate cancer, *European Urology Supplements* 18(8):e3090-e3091 Oct 2019, 10.1016/s1569-9056(19)33337-8;
- II. Niespolo C, Salamanca Viloría J, Deshmukh S, Villacanas Perez O, Sudbery I, Wilson H, Kiss-Toth E, Investigating the MIR-101-3P/TRIB1 axis in macrophage immunometabolism, *BMJ Publishing Group Ltd and British Cardiovascular Society, Basic Science* May 2019, 10.1136/heartjnl-2019-bcs.188;
- III. Niespolo C, Viloría JS, Perez OV, Wilson HL, Kiss-Toth E, miR-101-3p controls TRIB1 expression in human macrophages: a potential target on atherosclerotic plaques, *Cardiovascular Research. Oxford University Press (OUP)*. 114: S8-S8. 01 Sep 2018, 10.1093/cvr/cvy216.029;
- IV. Niespolo C, Viloría JS, Perez OV, Wilson H, Kiss-Toth E, Post-transcriptional regulation of TRIB1 by miRNAs in primary macrophages *Heart*. 104: a86. 01 Jun 2018, 10.1136/heartjnl-2018-bcs.109.

Manuscripts in preparation

- I. Niespolo C, Johnston J, Kim T, Deshmukh S, Sudbery IM, Wilson H, Kiss-Toth E, TRIB1 Regulates Macrophage Polarisation in Vivo and in Vitro and is a Direct Target of miR-101-3p (*EMBO Reports*);
- II. Niespolo C*, Deshmukh S*, Wilson H, Kiss-Toth E, Sudbery IM, Super regulator miRNAs and SNP-dependent allelic imbalance: a comprehensive transcriptome analysis of pro-inflammatory macrophages (*Nature Immunology*).

Other Publications

Contribution, not presented in this thesis:

- I. Ingrid Gomez, Ben Ward, Celine Souilhol, Chiara Recarti, Mark Ariaans, Jessica Johnston, Amanda Burnett, Marwa Mahmoud, Le Anh Luong, Laura West, Merete Long, Sion Parry, Rachel Woods, Carl Hulston, Birke Benedikter, Chiara Niespolo, Rohit Bazaz, Sheila Francis, Endre Kiss-Toth, Marc van Zandvoort, Andreas Schober, Paul Hellewell, Paul C. Evans & Victoria Ridger, Neutrophil microvesicles drive atherosclerosis by delivering miR-155 to atheroprone endothelium, Nature Communications volume 11, Article number: 214 (2020), <https://doi.org/10.1038/s41467-019-14043-y>.

Acknowledgments

Above all, I would like to thank my supervisors Prof. Endre Kiss-Toth and Dr Heather Wilson, who have been not only exceptional supervisors, but also my parents over the last 3 years. They have been always supportive and caring, especially during hard times. I have learnt so much from both of them.

Thanks to Sumeet and Ian for our great collaboration and for teaching me the impossible (the RNA-seq analysis!).

A special acknowledgment goes to one of the smartest and sweetest persons I have ever met during my PhD: Dr Yang Li, my mentor and guide in the lab, a brilliant scientist and a lovely friend. Thanks for teaching me everything and for making the best dumplings in the world!

I would like to thank my friends and best lab mates Laura, Taewoo and Ahmed, who have been fundamental during these years. We started this journey together and we always supported each other, either in good or bad moments. Thanks also to all the I&M group members. It's been great working with you guys. I will miss you so much.

I must thank my best friends and my "rocks" Merete, Taghreed, Rehab, Lindsay and Anjana. The support and the love they gave me every single day meant the world to me. Without them, I would have been lost.

Thanks to Graham, my drinking buddy, the best TRAIN manager and trip organiser. And to the whole TRAIN Consortium, PIs and ESRs: I will miss you all. I had a great time with you.

Thanks to my lovely family and my friends "since ever", who never stopped believing in me and supporting me. It's been so hard staying away, but I am coming back soon (hopefully!).

Last, but not least, I should really thank myself, for my resilience, patience, strength and motivation during the hardest times. For not giving up, when I was unwell and everything around me seemed to fall into pieces.

Now, let's take this PhD home!

Table of contents

List of Figures	15
List of Tables	18
Appendices.....	20
List of Abbreviations	21
Abstract.....	23
Chapter 1. General Introduction.....	24
1.1. microRNAs as master regulators of gene expression	24
1.1.1. Genomics & biogenesis	24
1.1.2. Mechanisms & functions: the RNA-Induced Silencing Complex.....	27
1.1.3. Computational tools to predict microRNA-target interaction	30
1.1.4. microRNAs in health and disease	34
1.2. Macrophages, a plastic cell population.....	36
1.2.1. Origin and development.....	36
1.2.2. Function and activation states	37
1.2.3. Macrophages in health and disease.....	40
1.2.4. microRNAs regulating macrophage development and function.....	43
1.2.5. Limitations of the M1/M2 paradigm.....	44
1.3. Tribbles pseudo-kinases: regulators of inflammation, metabolism and cancer	46
1.3.1. Tribbles, a family of pseudo-kinases	46
1.3.2. Overview of Tribbles binding partners	46

1.3.3. Cell-context dependent functions of Tribbles.....	50
1.3.4. TRIB1-mediated control of macrophages.....	50
1.3.5. TRIB1 and Prostate Cancer	51
1.3.6. TRIB1: an unstable transcript	52
1.3.7. TRIB1 as a potential target of multiple microRNAs	53
1.4. Tribbles Research and Innovation Network (TRAIN).....	54
Chapter 2. General Materials and Methods.....	56
Part I, In Silico	56
2.1. microRNA-target prediction and databases management.....	56
2.1.1. miRNAs targeting TRIB1 genetic variants: Single Nucleotide Polymorphisms (SNPs)	58
2.1.2. Additional tools used	58
2.2. RNA-sequencing.....	58
2.2.1. Small non-coding RNA sequencing.....	59
2.2.2. Messenger RNA-sequencing	60
Part II, In Vitro.....	62
2.3. Cell culture and maintenance.....	62
2.3.1. Primary cells	62
2.3.1.1. Human monocyte-derived macrophages (MDMs)	62
Statement of Ethics	62
Blood Monocytes isolation and macrophages differentiation	62
Macrophages in vitro polarisation	63

2.3.2. Established cell lines.....	63
2.3.2.1. Immortalised BMDMs (iBMDMs).....	63
2.3.2.2. HEK293T cell line	63
2.3.2.3. Prostate cancer cell lines	64
2.4. Gene expression profiling	64
2.4.1. RNA extraction	64
2.4.2. cDNA synthesis	64
2.4.3. Real Time-quantitative PCR.....	65
2.4.4. Gene expression analysis: $2^{-\Delta Ct}$ method	65
2.5. Protein analysis	68
2.5.1. Protein Extraction	68
2.5.2. BCA Protein Quantification Assay	68
2.5.3. Western Blotting	68
2.6. Transient transfection.....	69
2.7. Molecular Cloning and Site-Directed Mutagenesis.....	70
2.7.1. Cloning reaction.....	71
2.7.1.1. pENTR Directional TOPO cloning.....	71
2.7.1.2. Gateway Cloning	72
2.7.2. Site-directed mutagenesis	73
2.8. Dual Luciferase Reporter Assay	73
2.9. Enzyme-linked immunosorbent assay (ELISA)	75

2.10. Viability Assay (MTT)	76
2.11. Immunofluorescence.....	77
2.12. Microscope Imaging and analysis.....	77
2.13. Cholesterol Efflux Assay	78
2.14. Flow cytometry	78
2.15. Statistics	78
Chapter 3. miR-101-3p negatively regulates Tribbles-1 in primary human macrophages	79
Declaration.....	79
Abstract.....	79
3.1. Introduction.....	80
3.2. Hypothesis and aims	81
3.3. Results.....	82
3.3.1. Endogenous TRIB1 expression in human polarised macrophages.....	82
3.3.2. TRIB1 overexpression in human macrophages	87
3.3.3. Post-transcriptional regulation of TRIB1: impact of the 3'UTR.....	90
3.3.4. Identification of miRNAs potentially targeting TRIB1	93
3.3.5. Experimental validation of miR-101-3p/TRIB1 interaction.....	101
3.3.6. Impact of miR-101-3p on human macrophages.....	107
3.4. Summary	112
Chapter 4. Integrated transcriptome analysis of small non-coding RNAs and mRNAs in pro-inflammatory macrophages	114

Declaration.....	114
Abstract.....	114
4.1. Introduction.....	115
4.2. Hypothesis and aims	116
4.3. Results.....	117
4.3.1. Small RNA sequencing data quality and analysis strategy.....	117
4.3.2. Differential expression of miRNAs in response to LPS and INF- γ in human primary macrophages	122
4.3.3. Identification of “super regulator” miRNAs: miRNA-target prediction analysis and datasets overlapping.....	127
4.3.4. Impact of “super regulator” miRNAs on macrophage transcriptome.....	137
4.4. Summary.....	148
Chapter 5. miRNAs targeting TRIB1 non-coding variants and identification of two novel eQTLs.....	150
Declaration.....	150
Abstract.....	150
5.1. Introduction.....	151
5.2. Hypothesis and aim of this study	153
5.3. Results.....	154
5.3.1. Impact of the 3’UTR of TRIB1 on mRNA stability	154
5.3.2. Identification of TRIB1 non-coding variants affecting miRNA-binding sites	155
5.3.3. Effect of TRIB1 3’UTR SNPs on gene reporter activity.....	160

5.3.4. Experimental validation of rs62521034/miR-29a-3p interaction	163
5.3.5. Identification of two novel trans-eQTLs.....	166
5.4. Summary.....	168
5.5. Limitations of the study	169
Chapter 6. miRNAs targeting TRIB1 in Prostate Cancer	171
Declaration.....	171
Abstract.....	171
6.1. Introduction.....	172
PCa overview	172
Genetics of PCa.....	173
Downregulation of microRNAs in PCa	173
The potential role of TRIB1 in PCa.....	174
6.2. Hypothesis and aim of the study.....	175
6.3. Results.....	176
6.3.1. Data mining of PCa datasets: cBioPortal for Cancer Genomics.....	176
6.3.2. Assessment of TRIB1 gene expression in human and mouse models of PCa by RT-qPCR	181
6.3.2. Identification of downregulated miRNAs potentially targeting TRIB1	184
6.3.3. Validation of miR-132-3p/TRIB1 interaction by gene reporter assay.....	189
6.3.4. Impact of miR-132-3p and TRIB1 on PC3 gene expression	191
6.4. Summary.....	195
6.5. Limitations of the study	197

Chapter 7. General discussion and conclusions	198
References.....	204
Chapter 8, Supporting Information	247
Appendix I, Chapter 2, General Materials and Methods.....	247
A1.4. Plasmids maps.....	250
A1.6. Site-directed mutagenesis primers	253
Appendix II, Supplementary data for Chapter 3.....	255
A2.1. Assessment of CD14 ⁺ monocyte purity: flow cytometry	255
A2.2. Immunofluorescence: isotype controls	256
A2.3. Assessment of co-transfection efficiency	257
Appendix III, Supplementary data for Chapter 4.....	260
A3.1. RNA quality and concentration: representative samples	260
A3.2. miRNA-seq: overrepresented sequence	262
A3.3. List of differentially expressed small RNAs.....	263
A3.4. List of differentially expressed genes	270
Appendix IV, Supplementary data for Chapter 5	275
A4.1. TRIB1 non-coding variants.....	275
A4.2. SNPs analysis with miRanda algorithm: workflow and scripts.....	276
Appendix V, Supplementary data for Chapter 6.....	281
A5.1. miRCancer database output	281

List of Figures

Figure 1.1. Schematic illustration of miRNAs biogenesis in mammals	26
Figure 1.2. miRNA binding site on target sequence and its downstream consequences	29
Figure 1.3. Schematic overview of free energy and RNA site accessibility.....	33
Figure 1.4. Overview of macrophage polarisation and function	39
Figure 1.5. The contribution of macrophages to health and disease.....	42
Figure 1.6. TRIB protein structure and interactions	48
Figure 2.1. Schematic overview of molecular cloning steps	71
Figure 2.2. Overview of the dual luciferase reporter assay	75
Figure 3.1. TRIB1 RNA expression in human tissues: GTExPortal	83
Figure 3.2. Assessment of TRIB1 RNA expression in polarised human macrophages by RT- qPCR.....	84
Figure 3.3. Assessment of TRIB1 protein expression in polarised human macrophages by immunofluorescence	85
Figure 3.4. Representative immunofluorescence images	86
Figure 3.5. Assessment of TRIB1 overexpression in MDMs by RT-qPCR.....	88
Figure 3.6. Impact of TRIB1 overexpression on MDMs phenotype	89
Figure 3.7. Impact of the 3'UTR of TRIB1 on gene reporter activity.....	91
Figure 3.8. Confirmation of DICER1 and AGO2 knock-down by RT-qPCR.....	91
Figure 3.9. Effect of DICER1 and AGO2 knock-down on TRIB1 mRNA expression.....	92
Figure 3.10. Effect of DICER1 knock-down on TRIB1 protein expression	92
Figure 3.11. Endogenous expression of candidate miRNAs in human polarised MDMs: small RNA-seq	96
Figure 3.12. Confirmation of miRNAs overexpression in MDMs by RT-qPCR.....	97
Figure 3.13. Assessment of TRIB1 endogenous expression in transfected MDMs by RT- qPCR.....	98
Figure 3.14. Assessment of mTrib1 endogenous expression in transfected iBMDMs by RT- qPCR.....	98
Figure 3.15. KEGG enrichment pathway analysis of macrophage-specific genes targeted by miR-101-3p and miR-132-3p.....	100
Figure 3.16. Impact of miR-101-3p on gene reporter activity.....	103
Figure 3.17. Phylogenetic conservation of miR-101-3p binding site on the 3'UTR of TRIB1	103

Figure 3.18. Impact of miR-101-3p on TRIB1 3'UTR mutant.....	104
Figure 3.19. Confirmation of site-directed mutagenesis: miR-101-3p binding site deletion	104
Figure 3.20. Impact of miR-101-3p inhibitor on <i>TRIB1</i> gene reporter activity.....	105
Figure 3.21. Effect of miR-101-3p mimic on Trib1 protein expression.....	105
Figure 3.22. Assessment of miR-101-3p specificity: miR-101/TRIB1 target site blocker ...	106
Figure 3.23. Impact of miR-101-3p mimic on DUSP1 and ABCA1 genes in human macrophages	108
Figure 3.24. miR-101-3p effect on pro-inflammatory IL-6 and IL-8	109
Figure 3.25. miR-101-3p impact on M1 polarisation markers expression by RT-qPCR	110
Figure 3.26. miR-101-3p impact on M2 polarisation markers expression by RT-qPCR	111
Figure 4.1. Sequencing error distribution rate	118
Figure 4.2. Overview of analysis strategy	121
Figure 4.3. Percentage of RNA types sequenced.....	123
Figure 4.4. PCA plot of small RNA-seq	123
Figure 4.5. Differential expression of small RNAs in pro-inflammatory M1 macrophages	124
Figure 4.6. PCA plot of RNA-seq data.....	130
Figure 4.7. Volcano plot of RNA-seq data	130
Figure 4.8. Number of differentially expressed miRNA-target genes.....	133
Figure 4.9. Assessment of “super regulator” miRNAs by RT-qPCR	134
Figure 4.10. Gene Ontology and KEGG Pathway Enrichment analysis of DE miRNAs target genes	135
Figure 4.11. Gene Ontology terms of target genes of “super regulator” miRNAs	136
Figure 4.12. Target genes overlapping: Jaccard Index	136
Figure 4.13. Confirmation of miRNAs overexpression in transfected MDMs by RT-qPCR	140
Figure 4.14. Single PCA plots of RNA-seq data: super regulator miRNAs overexpression.	141
Figure 4.15. Global PCA plot of RNA-seq data: gender-dependent clustering?.....	142
Figure 4.16. Volcano plots of RNA-seq data: super regulators overexpression.....	142
Figure 4.17. Number of target genes up- and downregulated in response to miRNA overexpression	143
Figure 4.18. Gene ontology terms of genes differentially expressed in response to miRNA mimics.....	144
Figure 4.19. MTT assay on MDMs transfected with miRNAs mimics.....	145
Figure 5.1. Impact of the 3'UTR of TRIB1 on mRNA stability.....	154
Figure 5.2. Example of SNP sequence before and after Python processing.....	156

Figure 5.3. Confirmation of TRIB1 3'UTR mutants: Sanger sequencing results	161
Figure 5.4. Effect of TRIB1 non-coding SNPs on gene reporter activity.....	162
Figure 5.5. miRNA-target alignment calculated by the algorithm miRanda.....	164
Figure 5.6. Experimental validation of rs62521034/miR-29a-3p interaction.....	165
Figure 5.7. TRIB1 expression negatively correlates with MRSP21 and NLRC4 in GSE81046 dataset	167
Figure 6.1. Screenshot of cBioPortal for Cancer Genomics showing the summary of TRIB1 alterations in PCa	178
Figure 6.2. Data mining of PCa datasets show TRIB1 gene amplification	179
Figure 6.3. Overall Survival Kaplan-Meier estimate.....	180
Figure 6.4. Assessment of TRIB1 RNA expression in human and mouse models of PCa ...	182
Figure 6.5. Assessment of murine Trib1 primers' target specificity using BLAST Primers tool	183
Figure 6.6. Identification of downregulated miRNAs targeting TRIB1	185
Figure 6.7. Assessment of candidate miRNAs expression in prostate cancer cell lines by RT- qPCR.....	188
Figure 6.8. miR-132-3p/TRIB1 experimental validation	190
Figure 6.9. Assessment of TRIB1 RNA expression by RT-qPCR after miR-132-3p overexpression and TRIB1 knockdown in PC3 cell line	192
Figure 6.10. Impact of miR-132-3p and TRIB1 on pro-inflammatory cytokines in PC3 cell line.....	193
Figure 6.11. Impact of miR-132-3p and TRIB1 on cancer-related genes in PC3 cell line....	194
Figure 7.1. miRNAs targeting TRIB1 in macrophages and prostate cancer	200

List of Tables

Table 1.1. List of online repositories for miRNA-target identification and SNP detection	32
Table 1.2. TRIB protein-protein interactions and their biological effect	49
Table 2.1. List of miRNA-target prediction tools.....	57
Table 2.2. Experimental conditions for the RNA-seq experiment.....	61
Table 2.3. Packages, functions and database used to carry out the RNA-seq analysis	61
Table 2.4. cDNA synthesis protocols	66
Table 2.5. RT-qPCR reagents and protocol: Primer Design.....	66
Table 2.6. RT-qPCR reagents and protocol: QIAGEN.....	66
Table 2.7. RT-qPCR running protocol: Primer Design	67
Table 2.8. RT-qPCR running protocol: QIAGEN	67
Table 2.9. Transient transfection assays	70
Table 3.1. miRNA-TRIB1 target prediction analysis	95
Table 3.2. Characteristics of candidate miRNAs.....	95
Table 3.3. Reactome pathway analysis of candidate miRNAs target genes	99
Table 4.1. Data quality summary	119
Table 4.2. Data filtering summary	120
Table 4.3. List of upregulated miRNAs.....	125
Table 4.4. List of downregulated miRNAs	126
Table 4.5. Number of target genes of upregulated miRNAs	131
Table 4.6. Number of target genes of downregulated miRNAs	132
Table 4.7. List of “super regulator” miRNAs with more than 500 target genes in macrophages	133
Table 4.8. Adjusted p-values-filtered differentially expressed genes.....	146
Table 4.9. Log fold change values-filtered differentially expressed genes	147
Table 5.1. List of TRIB1 3’UTR SNPs creating new miRNA-binding sites.....	157
Table 5.2. Output generated by PolymiRTS database 3.0	159
Table 5.3. TRIB1 non-coding variants selected for experimental validation	160
Table 5.4. miR-29a/b and TRIB1 involvement in cancer and metabolism	165
Table 5.5. Identification of two novel trans-eQTLs	166
Table 6.1. cBioPortal for Cancer genomics: selected studies.....	177
Table 6.2. Overview of the human prostate cell lines used in the present study.....	181
Table 6.3. Candidate miRNAs downregulated in PCa and predicted to target the 3’UTR ...	186

of TRIB1	186
Table 6.4. TargetScan miRNA-TRIB1 analysis output.....	187
Table 6.5. Experimentally validated targets of miR-132-3p and their effect on PCa.....	190
Table 6.6. List of genes analysed in transfected PC3 cell line	192

Appendices

A1.1. List of reagents and kits	247
A1.2. List of machines and equipment	249
A1.3. List of antibodies used in western blot and immunofluorescence	249
A1.4.1. Firefly reporter plasmid map.....	250
A1.4.2. Renilla reporter plasmid map.....	250
A1.4.3. TRIB1 3'UTR renilla reporter plasmid map.....	251
A1.4.4. Plasmids used for overexpression experiment	251
A1.5. List of RT-qPCR primers	252
A1.6.1. Forward and reverse primers used for site-directed mutagenesis of miR-101-3p binding site.....	253
A1.6.2. Forward and reverse primers used to generate SNPs in the 3'UTR of TRIB1	254
A2.1. Assessment of CD14+ monocyte population purity	255
A2.2. Immunofluorescence isotype controls	256
A2.3.1. Flow cytometry: non-transfected HEK293T cells	257
A2.3.2. Flow cytometry: DNA transfection in HEK293T cells	258
A2.3.3. Flow cytometry: DNA and RNA co-transfection in HEK293T cells	258
A2.3.4. Flow cytometry: DNA and RNA siGLO co-transfection in HEK293T cells	259
A2.3.5. Flow cytometry: fluorescence percentage and MFI.....	259
A3.1.1. RNA agarose gel electrophoresis: RNA quality assessment	260
A3.1.2. Agilent 2100 bioanalyser: RNA quality assessment.....	261
A3.2. MultiQC report: overrepresented sequences.....	262
A3.3.1. List of small RNAs upregulated in M1 macrophages.....	263
A3.3.2. List of small RNAs downregulated in M1 macrophages.....	268
A3.4.1. List of genes significantly downregulated in miR-155-5p overexpressing macrophages	270
A3.4.2. List of genes significantly downregulated in miR-125a-3p overexpressing macrophages	274
A3.4.3. List of genes significantly downregulated in miR-186-5p overexpressing macrophages	274
A4.1. List of TRIB1 non-coding variants	275
A5.1. miRCancer Output: dysregulated miRNAs in PCA.....	281

List of Abbreviations

AML	Acute myeloid leukaemia
BMDMs	Bone marrow derived macrophages
CDS	Coding sequence
CPM	Counts per million
Ct	Cycle threshold
DE	Differential expression/differentially expressed
DLR	Dual luciferase reporter
eQTLs	Expression quantitative trait loci
FC	Fold change
FDR	False discovery rate
GO	Gene ontology
iBMDMs	Immortalised bone marrow derived macrophages
INDELs	Insertion-deletion polymorphisms
IUPAC	International Union of Pure and Applied Chemistry
KEGG	Kyoto Encyclopedia of Genes and Genomes
MDMs	Monocyte derived macrophages (human primary macrophages)
miRNA	microRNA
mRNA	Messenger RNA
OD	Optical density
padj	Adjusted p value
PBMCs	Peripheral blood mononuclear cells
PCa	Prostate cancer
PCA	Principal component analysis
piR	Piwi-interacting RNA
QC	Quality control
RIN	RNA integrity number
RISC	RNA induced silencing complex
SEM	Standard error mean
SNPs	Single nucleotide polymorphisms
STR	Short Tandem Repeat
TAMs	Tumour associated macrophages
TME	Tumour microenvironment

TMP	Transcript per million
TRAIN	Tribbles research and innovation network
TRIB	Tribbles
tRNA	Transfer RNA
TSB	Target site blocker
UTR	Untranslated region

Abstract

The TRIB1 gene has been implicated in several human pathologies, including cancer, lipid disorders and cardiovascular disease. It is well appreciated that TRIB1 is a critical regulator of macrophage polarisation, favouring the activation of an anti-inflammatory phenotype. Recent studies also pointed to a role of TRIB1 in the pathogenesis of prostate cancer, although the mechanisms behind its overexpression remain elusive.

TRIB1 protein is produced from a highly unstable mRNA, with a half-life shorter than 1 hour, suggesting it may be subject to post-transcriptional regulation. The TRIB1 transcript includes a long, conserved 3'UTR, potentially enriched with putative miRNA-binding sites and polymorphisms. The latter could contribute to the regulation of TRIB1 expression, via either creating or abolishing miRNA-binding sites. However, the post-transcriptional regulation of TRIB1 by miRNAs has not been comprehensively investigated.

The work presented in this thesis explored the post-transcriptional regulation of TRIB1 by miRNAs, using a combination of bioinformatics and experimental tools, with focus on macrophage and prostate cancer biology. We identified multiple miRNAs predicted to target the 3'UTR of TRIB1 with good alignment scores and free energy values. We experimentally validated the interaction between miR-101-3p and TRIB1 in human macrophages and demonstrated that the overexpression of miR-101-3p and TRIB1 caused opposite genetic signatures, suggesting the biological importance of their interaction. Similarly, we identified 21 miRNAs targeting TRIB1, which are either downregulated or silenced in prostate cancer and could possibly account for the elevated expression of TRIB1. We focussed on the activity of the oncomiR miR-132-3p and observed that it is able to modulate the expression of TRIB1 and its downstream genes.

Additionally, a collaborative study on macrophage transcriptomes was performed using multiple RNA-seq experiments, leading to the identification of “super regulators” miRNAs and their targetome in pro-inflammatory macrophages.

Lastly, a brief preliminary research was also conducted on genetic variants affecting the 3'UTR of TRIB1: we found that TRIB1 SNPs create novel miRNA-binding sites and impairs the expression of distant genes, thus acting as potential trans-eQTLs. However, this remains to be elucidated further.

Chapter 1. General Introduction

1.1. microRNAs as master regulators of gene expression

MicroRNAs (miRNAs) are small non-coding, single stranded RNAs (generally 21-25 nucleotides long) that play a fundamental role in the regulation of gene expression, acting as key molecules in RNA-mediated silencing mechanisms. The first miRNA was discovered in 1993 by Lee and colleagues. They were screening for mutations in the *Caenorhabditis elegans* larval development and found that the gene *lin-4* does not code for a protein but for a small RNA complementary to multiple sites in the 3' untranslated region (3'UTR) of the *lin-14* messenger RNA (mRNA) (Lee *et al.*, 1993, Wightman *et al.*, 1993). This complementarity resulted in the impairment of the translation of the *lin-14* mRNA into the LIN-14 protein. It was the first evidence of anti-sense RNA-RNA interaction and since then a large number of small non-coding RNAs and their targets have been discovered and characterized. miRNAs have been found in both animals and plants, as well as in some viruses and they are highly conserved among different species (Bartel *et al.*, 2003, Zhang *et al.*, 2006). There are over 48,000 mature miRNA products in 271 species recorded in *miRBase* (version 22, released in October 2018), a searchable online database of published miRNAs and annotations (Kozomara *et al.*, 2019). Highlighting the importance of miRNAs in human physiology, it has been estimated that more than half of the protein coding-genes are negatively regulated by miRNAs and that a single miRNA species can target hundreds of different mRNAs (Friedman *et al.*, 2009). Therefore, it is not surprising that dysregulated miRNA expression is associated with multiple human diseases (Calin *et al.*, 2006).

1.1.1. Genomics & biogenesis

The identification of miRNA coding genes has been largely approached by using the complementary DNA (cDNA) cloning method, in which small RNA molecules are first separated from the total RNA and then cloned to construct a cDNA library to be sequenced, as described in detail by Ambros and colleagues (Ambros *et al.*, 2004). However, this method is limited by not being sensitive to discover miRNAs whose expression is not abundant or is restricted only to some cell/tissue types. This can be overcome by using computational approaches and examining genomic sequences on the basis of phylogenetic conservation criteria (Bartel *et al.*, 2004, Kim *et al.*, 2006). Several studies showed that genes encoding for miRNAs are located in intergenic regions and they are distant from annotated genes, thus

forming independent transcriptional units (*Lagos-Quintana et al., 2001, Lau et al., 2001, Lee et al., 2001*). However, it is also known that some miRNAs are processed from the introns of protein coding genes (*Ambros et al., 2003*), as well as introns and exons of “non-coding” genes (*Rodriguez et al., 2004*). Interestingly, Cai and colleagues found that 9 human miRNAs are excised from the 3'UTR of transcripts (*Cai et al., 2004*). miRNA coding genes are usually transcribed by RNA polymerase II (*Lee et al., 2004*), despite some evidence suggesting that the transcription of miRNA genes can be also mediated by the RNA polymerase III (*Borchert et al., 2006*). The canonical mechanism of miRNA biogenesis in mammals is illustrated in **Figure 1.1**. The first maturation step occurs inside the nucleus after the transcription of the miRNA coding gene. The product of transcription is a long capped and polyadenylated primary miRNA (pri-miRNA) characterized by the presence of stem loop structures. The pri- miRNA is processed into a precursor miRNA (pre-miRNA) of approximately 60-70 nucleotides by the RNase III endonuclease DROSHA that cleaves both strands at the level of the stem loops. To process the pri-miRNA the protein PASHA (DGCR8) is also required (*Tomari et al., 2005*). The pre-miRNAs are then transported to the cytoplasm by Exportin 5 (EXP-5), a GTP-dependent nucleo/cytoplasmic transporter. The latter recognizes a 2-nucleotide 3' overhang created by DROSHA at the 3' end of the pre-miRNAs, which therefore defines one end of the mature miRNA. Once in the cytoplasm, another RNase III endonuclease, DICER, processes the precursors into small double-stranded RNA duplexes containing both the mature sequence of the miRNA and its complementary strand (*Bartel et al., 2004, He et al., 2004*). The dsRNA duplex is also referred to as a miRNA: miRNA* duplex, where miRNA is the mature miRNA and miRNA* (also known as star-strand) corresponds to the complementary arm. They are commonly termed 5p and 3p, depending on which end of the stem loop they derive from. Generally, only one strand, probably the most unstable, is incorporated in the RNA-induced silencing complex (RISC), whereas the other one is released and degraded (*Du et al., 2005*). However, it has been reported that in some cases both strands can be loaded into the RISC: for example, Huang and colleagues have recently demonstrated that both miR-582-3p and miR-582-5p are functional. They have been shown to repress prostate cancer metastasis to bone by targeting and downregulating several components of the TGF- β signalling pathway (*Huang et al., 2019*). The RISC complex is composed of different conserved proteins, including Argonaute (AGO) proteins that form the catalytic core of the RISC complex (*Pratt et al., 2009*).

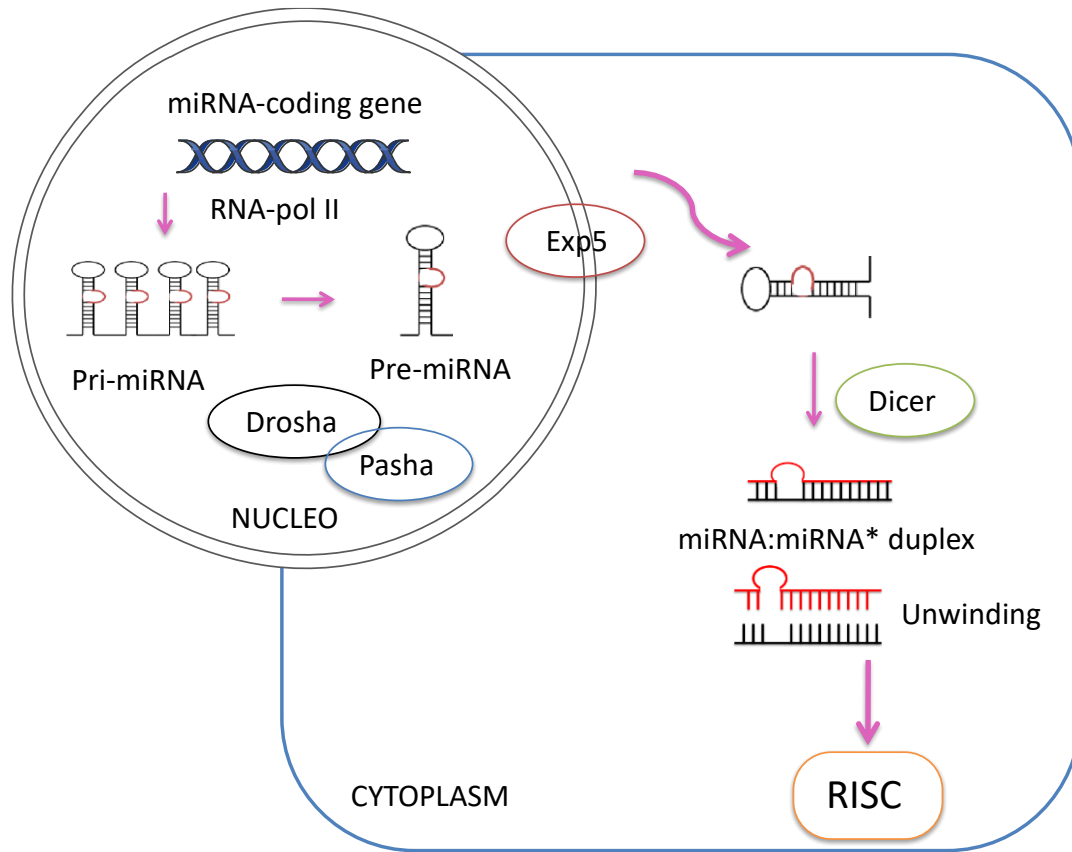


Figure 1.1. Schematic illustration of miRNAs biogenesis in mammals

miRNA-coding genes are transcribed by RNA pol II into a pri-miRNA. This is further cleaved by DROSHA that together with the protein PASHA creates a pre-miRNA of 60-70 nucleotides. In turn, this is translocated to the cytoplasm by the GTP-dependent nucleo/cytoplasm cargo transporter EXP-5. Once in the cytoplasm, the pre-miRNA is processed by DICER that forms a miRNA: miRNA* duplex. In general, only one miRNA strand will be incorporated in the RISC complex.

1.1.2. Mechanisms & functions: the RNA-Induced Silencing Complex

Initially, it was believed that miRNAs do not cause transcript degradation but only repress protein translation. In fact, the first miRNA identified in *Caenorhabditis elegans*, lin-4, was only shown to repress LIN-4 protein synthesis and seemed to not affect messenger RNA levels (Lee *et al.*, 1993, Wightman *et al.*, 1993). However, it is now well appreciated that via association with the effector proteins of the RISC, miRNAs guide and mediate silencing of gene expression by either suppressing protein translation and/or promoting target mRNA cleavage (Bartel *et al.*, 2004). Both mechanisms are the consequence of “target recognition”, the Watson-Crick complementarity between the “seed” sequence, 6-8 nucleotides (typically 2nd-8th) at the 5' end of the miRNA and the transcript sequence (Lewis *et al.*, 2003, Grimson *et al.*, 2007) (shown in **Figure 1.2.A**). The majority of miRNA-binding sites have been identified in the 3'UTR of genes (Bartel *et al.*, 2009). However, functional binding can also occur in the 5' UTR, as well as in the coding region (CDS) (Kloosterman *et al.*, 2004, Lytle *et al.*, 2007, Fang *et al.*, 2011). It has been proposed that the balance between mRNA degradation and protein synthesis inhibition is determined by the extent of the base-pairing between the miRNA and the mRNA. The messenger RNA is cleaved when the miRNA perfectly matches its target-sequence, whereas a partial base-pairing is more likely to promote translational repression (Hutvagner *et al.*, 2002, Zeng *et al.*, 2002, Zeng *et al.*, 2003, Doench *et al.*, 2003). Although they mediate target recognition, which represents the triggering step for gene silencing mechanisms, miRNAs do not work alone. **Figure 1.2.B** schematizes the canonical mechanism of action of miRNA-guided gene silencing and its main players. Structural studies showed that the mRNA degradation is mediated by Ago proteins which contain two characteristic domains: an N-terminal PAZ domain that recognise the 3' end of the guide-miRNA (Lingel *et al.*, 2005) and a C-terminal PIWI domain. The latter is similar to the ribonuclease H (nuclease activity) and for this reason thought to be responsible for the mRNA cleavage (Parker *et al.*, 2004, Song *et al.*, 2004). In mammals, all four Ago proteins (Ago1-4) contribute to miRNA- guided gene silencing, while in *Drosophila* only Ago1 protein plays this role (Ipsaro *et al.*, 2015). Further work has also shown that miRNAs promote target destabilization prior to degradation by recruiting deadenylases through GW182 protein which is also recognized by Ago (Fabian *et al.*, 2011). In fact, GW182 proteins are mainly characterized by the presence of an Argonaute-binding domain (ABD) and a silencing domain (SD) (Jonas *et al.*, 2015). The molecular mechanisms of miRNA-mediated translational suppression in animals are still poorly understood, particularly the step in which translation is

blocked. To date, several mechanisms have been proposed; they involve GW182 and the recruitment of translational repressors (*Iwakawa et al., 2015, Jonas et al., 2015*). However, even though recent reports have enhanced our understanding of the miRNA-mediated mechanisms of silencing, it is still believed that they may exert additional functions. In fact, it is beginning to emerge that miRNA activity may oscillate between activation and repression of target genes, as previously reported, particularly in cancer (*Vasudevan et al., 2007, Valinezhad et al., 2014*). Therefore, there is no doubt that miRNA-mediated mechanisms in regulating gene expression should be investigated further.

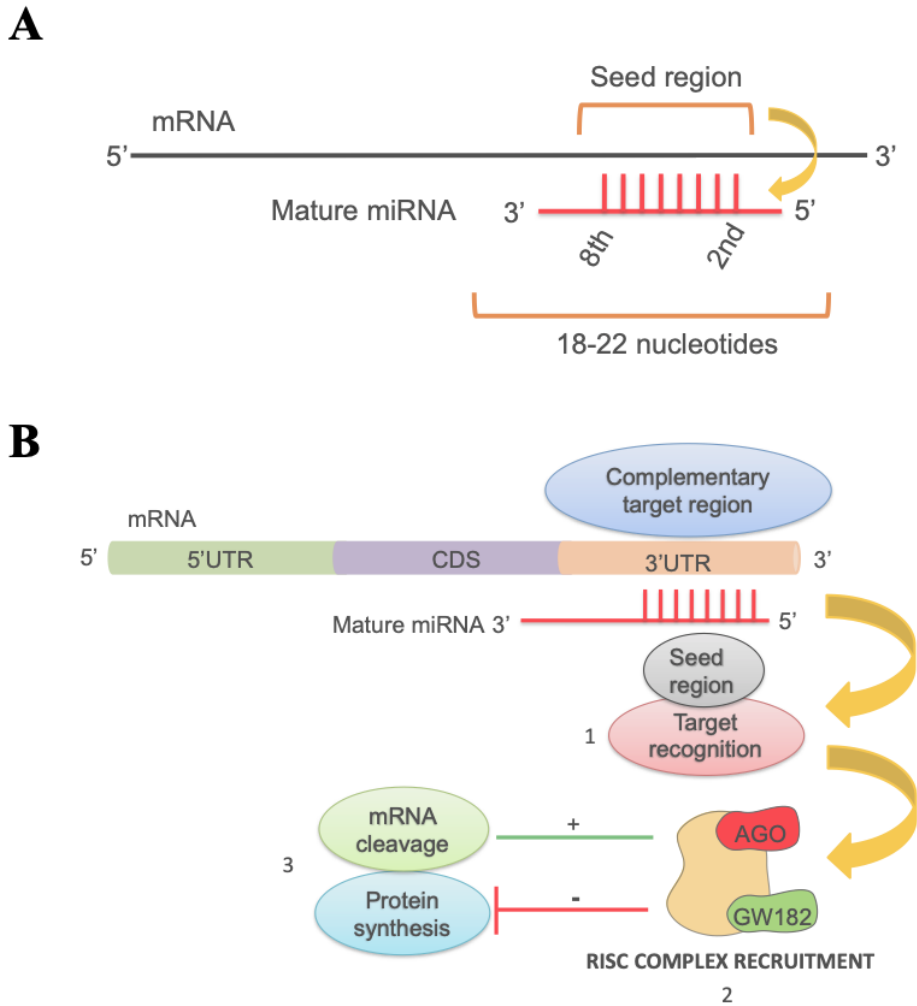


Figure 1.2. miRNA binding site on target sequence and its downstream consequences

The miRNA binding site on the target mRNA referred as “seed region” (A). Typically, this is located between the 2nd and the 8th nucleotide at the 5' end of the miRNA but its length varies among different molecules. The most common seed lengths are 6nt, 7nt and 8nt. The process of target recognition (1) is followed by the recruitment of the RISC proteins Ago and GW182 (2) which together with other repressors mediate the cleavage of mRNA and the inhibition of protein translation (3) (B).

1.1.3. Computational tools to predict microRNA-target interaction

It is thought that genes with longer 3'UTRs have a higher number of miRNA-binding sites, compared to genes with shorter 3'UTRs. Moreover, genes with longer 3'UTRs are more conserved and often involved in developmental processes (Cheng *et al.*, 2009), whereas housekeeping genes contributing to basic cellular mechanisms, although conserved, have shorter 3'UTRs, thereby avoiding stringent miRNA-mediated post-transcriptional regulation (Stark *et al.*, 2005). However, it is well established that a single miRNA has the potential to bind to multiple genes and, conversely, one gene can be targeted by multiple miRNAs. Moreover, it is likely that single miRNA binds to different sequences in the same 3'UTR and these binding sites might also overlap with each other. As mentioned earlier, miRNAs also bind to the 5'UTR and CDS of transcripts. In addition, one must consider the presence of Single-Nucleotide-Polymorphisms (SNPs) as well as Multiple-Nucleotide-Polymorphisms (MNP) and small insertions/deletions (INDELS). In fact, mutations in either of the sequences (miRNA and target) can affect the miRNA-target interaction by creating and abolishing the binding site, as well as modifying the binding affinity (Chen *et al.*, 2008, Wei *et al.*, 2012). For this reason, prior to applying experimental approaches it is useful to characterize and predict miRNA-target interactions “*in silico*”, as well as the putative presence of known polymorphisms. To this aim, in the last few years, a number of bioinformatics and computational tools have been developed. The current databases used to identify and predict miRNA-target interactions, including SNPs databases, are briefly listed in **Table 1.1.** along with a short description. They are characterized by intuitive function and a friendly interface and can be easily accessed by less experienced users. Mostly, target prediction tools are accessible via free web-sources but some of them can also be downloaded as software and packages (R, C, Python, Java) for independent external searches (Riffo-Campos *et al.*, 2016). All of them rely on the function of different, dedicated algorithms that can be divided into two main categories: rule-based algorithms and data-driven algorithms (Yue *et al.*, 2009). Rule based algorithms consider biological parameters including the seed region matching (Watson-Crick complementarity), the conservation status between different species and the thermodynamic features of RNA-RNA interaction (Riffo-Campos *et al.*, 2016, Peterson *et al.*, 2014). The latter refer to the minimization of the free energy or Gibbs free energy (showing how strong the miRNA binds to its target) and the site accessibility (the degree of openness of the 3'UTR bound to a miRNA, representing how much the binding site is accessible) (Mathews *et al.*, 1999, Kertesz *et al.*, 2007) (**Figure 1.3.A-B**). Indeed, the majority of target prediction

tools incorporate the Vienna RNA package and the PITA program, designed to calculate the free energy and the accessibility energy (*Lorenz et al., 2011, Kertesz et al., 2007*). Data-driven algorithms follow the same rules but they are further complemented with experimental findings (validated interactions) (*Yue et al., 2009*). Interestingly, several databases contain both predicted and validated modules and they also provide users with additional information (e.g. miRWalk 2.0 contains tissue specific expression, cell line specific expression, gene-enrichment analysis, wiki-pathways, disease associated miRNAs, based on published literature) (*Dweep et al., 2015*).

Table 1.1. List of online repositories for miRNA-target identification and SNP detection

miRNA-target prediction and SNP/INDEL detection in either target genes and miRNAs is achieved by using dedicated tools. In most cases, entries can be retrieved by both miRNA and target gene symbols, as well as tissue/cell line/disease of interest. SNP: Single Nucleotide Polymorphism, INDEL: small insertion/deletion.

Database	Description	Type of algorithm	Reference
miRBase	Published miRNA sequences, target interactions and nomenclature	NA	Kozomara et al., 2014 Kozomara et al., 2019
miRWalk 2.0/3.0	Predicted and validated target interactions and miRNA tissue /disease specific expression (based on existing literature)	Rule-based, data-driven	Dweep et al., 2011 Sticht et al., 2018
miRDB	Target prediction and functional annotations in human, mouse, rat, dog, chicken	Rule-based, data-driven	Chen and Wang 2020 Wong et al., 2015 Liu et al., 2019
TargetScan	Prediction of miRNA-target in human, mouse, worm, fly and fish; conserved and poorly conserved interactions	Rule-based	Agarwal et al., 2015
RNA22	Interactive and pre-computed miRNA-target interactions	Rule-based, data-driven	Miranda KC et al., 2006
miRanda	Predicted miRNA-target interaction and miRNA specific tissue expression	Rule-based	Betel et al., 2010
DIANA TaRBase	Published experimentally validated miRNA-interactions; alignment details and conservation scores	Rule-based, data-driven	Vlachos et al., 2014 Karagkouni et al., 2018
DIANA microT-CDS	miRNA-target prediction and functional analysis	Data-driven	Paraskevopoulou et al., 2013
miRTarBase	Experimentally validated miRNA-target interactions	Data-driven	Chou et al., 2016
RePTar	miRNA-target interactions, including noncanonical seed pairing (3' compensatory binding site, full match binding sites, centered binding site)	Rule-based	Elefant et al., 2011
miRTar	miRNA-target interactions, biological functions and regulatory relationship	Data-driven	Hsu et al., 2011
miRdSNP	Disease-associated SNPs in 3'UTR sequences and miRNA target sites	Data-driven	Bruno et al., 2012
PolymiRTS	SNPs and INDELS in miRNAs and their targets also supported by experimental findings	Data-driven	Bhattacharya et al., 2014
StarBase ENCORI	Open-source platform of miRNA-ncRNA, miRNA-mRNA, ncRNA-RNA, RNA-RNA, RBP-ncRNA and RBP-mRNA interactions from CLIP-seq, degradome-seq and RNA-RNA interactome data	Data-driven	Li et al., 2014 Zhou et al., ENCORI

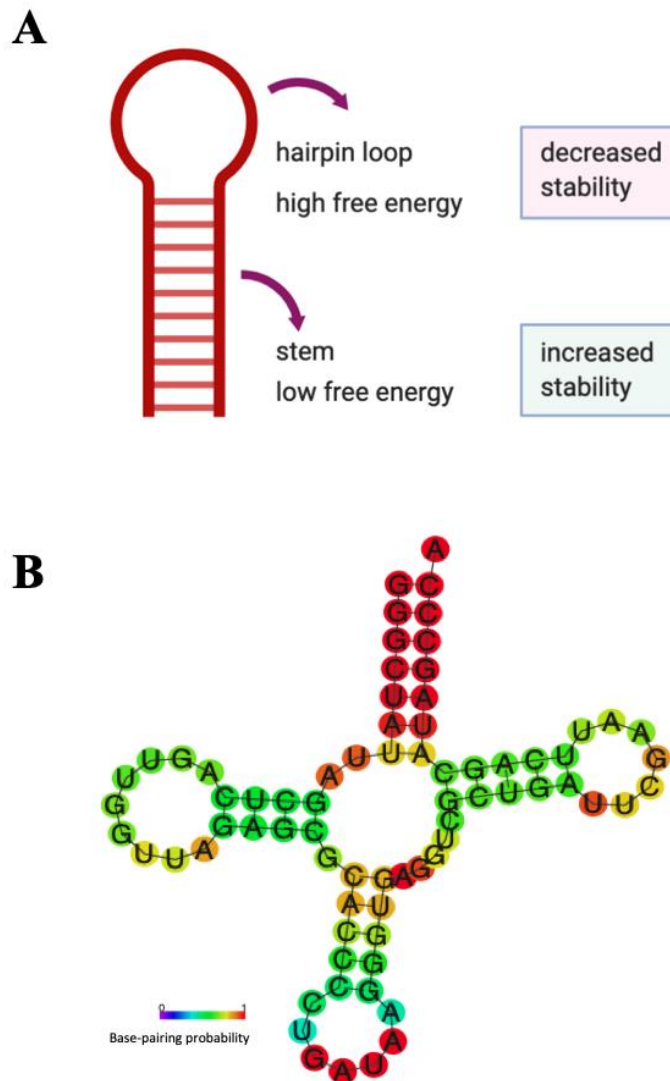


Figure 1.3. Schematic overview of free energy and RNA site accessibility

RNA secondary structure showing a region of high free energy characterized by the presence of a hairpin loop and a region of low free energy corresponding to the stem which increases stability (A) (adapted from Peterson et al., 2014); example of an RNA secondary structure illustrating the base-pairing probability, calculated by RNAFold WebServer (<http://rna.tbi.univie.ac.at/cgi-bin/RNAWebSuite/RNAfold.cgi>) (B).

1.1.4. microRNAs in health and disease

Being master regulators of gene expression, cell differentiation, proliferation and apoptosis, miRNAs are recognised to have a big impact on health and disease. Aberrant expression of miRNAs has been implicated in virtually all human diseases, from inherited conditions to cancer, autoimmunity, neurodegeneration, cardiovascular disease, metabolic disorders and many others (Ardekani *et al.*, 2010, Li *et al.*, 2012). A strong link between miRNAs and human diseases is seen in DiGeorge Syndrome, a genetic disorder characterized by a heterogeneous group of defects and clinical manifestations, including immunodeficiency, skeletal and cardiac anomalies, neuromuscular problems, hypocalcaemia and psychiatric illnesses. This syndrome is caused by a deletion in chromosomal region 22q11.2, where the gene encoding Pasha (DGCR8, also called DiGeorge Syndrome Chromosomal or Critical Region 8) is located. As discussed above (Section 1.1.1. Genomics & biogenesis), Pasha acts as partner of Drosha in the biogenesis of miRNAs. Therefore, patients affected by DiGeorge Syndrome show a pattern of dysregulated miRNA expression, resulting in aberrant gene expression and multi organ disease (de La Morena *et al.*, 2013, Landthaler *et al.*, 2004, Shiohama *et al.*, 2003). miRNAs are also required for normal development and organogenesis, as suggested by a multitude of studies involving Dicer mutant animals and cell lines. In fact, it has been shown that mice lacking Dicer1 die at embryonic stage, because of the lack of proliferation and differentiation of embryonic stem cells (Bernstein *et al.*, 2003). In zebrafish and Drosophila, deletion of Dicer1 also results in development arrest and impairment of stem cell proliferation (Hatfield *et al.*, 2005, Wienholds *et al.*, 2003). The same effect was observed in human embryonic stem cells (hESCs), where the loss of DICER1 induces apoptosis and impairs self-renewal, due to deficiency in mature miRNAs. In fact, transfection of selected miRNAs is able to rescue the phenotype of DICER1-depleted cells, regulating the expression of apoptotic genes (Teijeiro *et al.*, 2018). As the fundamental impact of miRNAs on health and disease became clear, much attention has focused on their potential role as biomarkers for disease diagnosis, prognosis and responses to therapy. To date, a number of circulating miRNAs have been established as diagnostic markers for different types of cancer, as well as in cardiovascular and infectious diseases. For example, it has been shown that in HIV-infected patients plasma levels of miR-29, miR-150 and miR-146b-5p are highly altered compared to healthy individuals (Faruq *et al.*, 2015, Monteleone *et al.*, 2015, Munshi *et al.*, 2014). Plasma miR-21-5p, miR-20a-5p, miR-141-3p, miR-145-5p, miR-155-5p and miR-223-3p have been identified as biomarkers for early diagnosis of non-small cell lung cancers (NSCLC) (Geng *et al.*, 2014, Arab *et al.*, 2017,

Zhang et al., 2017). Interestingly, miRNAs found in body fluids can also be used as diagnostic biomarkers. A number of miRNAs found in the saliva have been shown to be predictive of mild-traumatic brain injury and concussion, which is known to be difficult to diagnose (*Di Pietro et al., 2018*). Five serum miRNAs (miR-1, miR-20a, miR-27a, miR-34 and miR-423-5p) have been identified as strong diagnostic markers for gastric cancer (*Liu et al., 2011*), while miR-125a-5p, targeting HER2, serves as a prognostic marker and could be used as a potential therapy against gastric neoplasms (*Nishida et al., 2011*). Notably, the world's first miRNA-based therapeutic, miravirsen, is currently in phase II clinical trials for the treatment of hepatitis C liver infection (HCV). It is based on the inhibition of miR-122, the most abundant miRNA in the liver, which is known to be an important host factor for HCV pathogenesis (*Lindow et al., 2012*).

1.2. Macrophages, a plastic cell population

Macrophages are professional phagocytes, first discovered in the late 19th century by Ilya Metchnikoff (https://en.wikipedia.org/wiki/Ilya_Metchnikoff). They represent a key cell type of the innate immune system and according to environmental cues they can change their physiology and become either protective or detrimental in the context of human disease. The ability to integrate and respond to a wide range of extracellular signals, both pro- and anti-inflammatory, makes macrophages one of the most versatile and plastic cell types of the haematopoietic system (Wynn *et al.*, 2013, Gordon *et al.*, 2014). Macrophages function in a multitude of biological processes such as inflammation (promotion/resolution), immunosuppression, phagocytosis, apoptotic cell clearance (efferocytosis), wound healing, tumour promotion (tumour-associated macrophages, TAMs) and intercellular communication via the release of extracellular vesicles (Mosser *et al.*, 2008, Koh *et al.*, 2011, Quatromoni *et al.*, 2012, Ismail *et al.*, 2013, Martin *et al.*, 2014). This section summarises the main features of macrophages, focusing on their plasticity and involvement in a variety of human diseases.

1.2.1. Origin and development

Macrophages reside in all the tissues of the body and, as for all blood cells, they arise following a complex differentiation program. It was initially believed that macrophages only derive from circulating monocytes but recently it has become clear that they have a dual origin: a proportion of these cells originate from haematopoietic stem cells (HSCs) but most adult tissue resident macrophage populations are established during embryonic development and before definitive haematopoiesis (Epelman *et al.*, 2014, Davies *et al.*, 2015). In fact, through the power of fate-mapping strategies it has been revealed that tissue macrophages derive from cells existing within the yolk sac and the foetal liver (Schulz *et al.*, 2012, Yona *et al.*, 2013). The differentiation of macrophages from HSCs strictly depends on the activity of Myb, a haematopoietic transcription factor involved in myeloblastosis and leukemia (Sumner *et al.*, 2000, Lahortiga *et al.*, 2007, Nguyen *et al.*, 2016). However, macrophages derived from embryonic and extra-embryonic tissues do not require Myb activity, suggesting that they are genetically distinct from the blood precursor (Pattabiraman *et al.*, 2013, Schulz *et al.*, 2012). Embryonic and monocyte-derived macrophage lineages are found in the brain (microglia), lung (alveolar macrophages), liver (Kupffer cells), spleen (red pulp macrophages), heart (CCR2⁻ macrophages), skin (Langerhans cells), peritoneum and kidney. Macrophages populating the skin, heart (CCR2⁺ macrophages) and gut also differentiate from circulating monocytes that continuously replace them (Epelman *et al.*, 2014).

1.2.2. Function and activation states

Being leukocytes, macrophages are motile cells. They have the ability to migrate through the wall of blood vessels as monocytes into inflamed and damaged tissues, differentiating into macrophages. This process is known as chemotaxis and it requires complex cellular signalling (Jones *et al.*, 2000, Xuan *et al.*, 2015). More importantly, macrophages are characterized by the expression of Toll-Like Receptors (TLRs) through which they detect and internalise products of bacteria and pathogens. They also produce nitric oxide (NO) and reactive oxygen species (ROS) facilitating the killing of phagocytosed microorganisms and secrete bioactive lipids and multiple cytokines (Billack *et al.*, 2006). Cytokines produced by macrophages represent the link between innate and adaptive immunity and they can either promote or inhibit inflammation, as well as cause tissue damage. The activation of macrophages toward different phenotypes is called polarisation and it has been intensively studied in both human and animal models. However, this is not a fixed event and classifying macrophage phenotypes still remains a big challenge. According to the historical concept of polarisation, M1 macrophages are the classically activated cells which exhibit a pro-inflammatory status, whilst M2 macrophages display an anti-inflammatory phenotype and are mainly involved in tissue repair and homeostasis (Martinez *et al.*, 2008, Wang *et al.*, 2014). M1 macrophages are activated by pro-inflammatory cytokines such as $\text{INF-}\gamma$ and LPS which enhance the expression of TLRs thus favouring the phagocytic activity of macrophages. Moreover, these cells are characterized by high levels of opsonic receptors (CD16) and IL-12 and low levels of IL-10. In addition, by secreting high levels of IL-1 β , TNF- α , IL-15, IL-18, IL-23, IL-8 and IL-6, M1 macrophages significantly contribute to the activation and polarisation of Th1 cells and mediate pathogen killing and tumour resistance. On the contrary, M2 phenotype arises when macrophages are activated upon stimulation with anti-inflammatory cytokines, mainly IL-4 and IL-10. M2 macrophages are characterized by IL-10^{high} and IL-12^{low} expression and abundant levels of non-opsonic receptors, such as the mannose receptor and scavenger receptors. They are further classified in three subtypes M2a, M2b and M2c activated by different stimuli, including IL-4, IL-10, IL-13, TGF- β , glucocorticoids (GCs) and immune complexes (ICs). M2 macrophages not only exert an anti-inflammatory activity, but they also contribute to wound healing, immunoregulation, immunosuppression, tissue remodelling, clearance of apoptotic bodies and tumour progression (Mantovani *et al.*, 2004, Mantovani *et al.*, 2005, Martinez *et al.*, 2008, Viola *et al.*, 2019). From a metabolic point of view, it has been shown that murine macrophages are characterized by the metabolism of arginine, which is a complex amino acid involved in a

variety of biological processes, ranging from single cell regulation to the whole organism regulation. In M1 cells, arginine is used to produce NO, while in M2 macrophages it is mainly catabolised to produce ornithine, urea and polyamines. The production of NO is mediated by the inducible nitric oxide synthase (iNos), which is highly expressed by M1 cells and results in increased cell death. Instead, ornithine, urea and polyamines are generated by arginase (Arg), abundant in M2 cells, which in turn promote proliferation. These two enzymes are among the most employed markers enabling the functional characterization of M1 and M2 macrophages in mice (*Rath et al., 2014*). However, in human macrophages the expression and activity of iNos and arginase is still under debate. In fact, many groups have been able to detect them but others have not. It seems that the presence of arginine-metabolizing enzymes strictly depends on cell source (i.e. blood-derived macrophages and tissue resident macrophages), as well as the health status of the individual (*Thomas et al., 2014*). In addition to arginine metabolism, different macrophages display different lipid metabolism pathways. M1 macrophages rely on fatty acid synthesis (FAS), while M2 cell metabolism is mainly supported by fatty-acids oxidation (FAO), which is also thought to promote cellular longevity (*Remmerie et al., 2018*). Macrophage phenotypes and their main functions are illustrated in **Figure 1.4**.

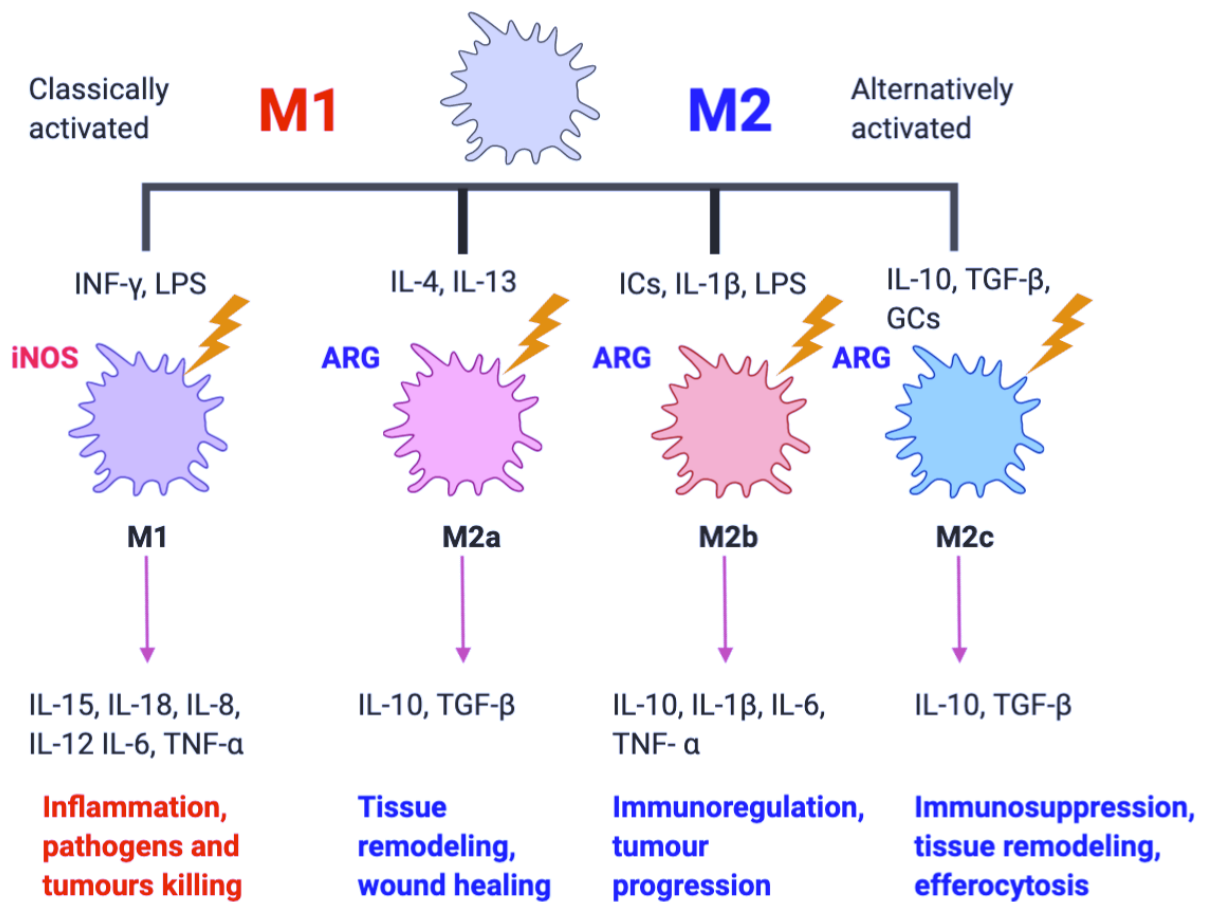


Figure 1.4. Overview of macrophage polarisation and function

Classically or M1-activated macrophages are induced by inflammatory stimuli, such as LPS and INF- γ and they are mediators of inflammation, pathogens killing and tumour resistance. Alternatively or M2-activated macrophages mainly respond to anti-inflammatory cytokines, glucocorticoids (GCs) and immunocomplexes (ICs). They exert a variety of functions, including tissue remodelling, immunosuppression and tumour progression.

1.2.3. Macrophages in health and disease

Traditionally considered the first line of defence against infectious diseases, macrophages play a crucial role in maintaining all tissues in a healthy condition, for example by directing the clearance of dead and dying cells, as well as toxic substances and pathogens. The physiological roles of macrophages have been intensively studied in metabolic tissues (adipose tissue and liver) where, polarised towards an anti-inflammatory M2 phenotype, they control and maintain insulin sensitivity and energy homeostasis, especially after an increased caloric intake (*Fujisaka et al., 2016*). However, in individuals affected by obesity the protective role of macrophages is subverted: they switch to the pro-inflammatory M1 phenotype, promoting a low-grade chronic inflammation, thus leading to insulin resistance, fibrosis and fatty liver disease (*Claria et al., 2011, Odegaard et al., 2013*). Both M1 and M2 macrophages play a key role in the pathogenesis of atherosclerosis, a chronic inflammatory disease caused by lipid retention in the arterial wall. Recruited at the site of the lesion, macrophages accumulate in the arterial intima where they uptake atherogenic lipoproteins via either scavenger receptors or micropinocytosis, promoting the formation of foam “fatty” cells, the hallmark of the atherosclerotic plaque. The population of macrophages found in the plaques is highly heterogeneous but it is believed that M1 macrophages are present in progressing plaques, at an early stage, while M2 macrophages, involved in the mechanisms of repair and stabilization, are found in regressing plaques (*Moore et al., 2013, Bobryshev et al., 2016*). A dual role for macrophages has been also established in cancer, where they take the name of tumour-associated macrophages (TAMs). Up to 50% of solid tumours are composed of macrophages: they have been shown to facilitate angiogenesis, immunosuppression, invasion and metastasis and for this reason they have formed a key area of investigation for the development of cell-based therapies and genetic reprogramming strategies (*Yang et al., 2018*). Several studies reported that either genetic or pharmacological inhibition of macrophage-colony stimulating factor (M-CSF) results in a strong reduction in the number of TAMs thus suppressing angiogenesis and tumour growth and progression in different cancer models (*Kubota et al., 2009, Pyonteck et al., 2012, Ryder et al., 2013*). TAMs derive from both circulating monocytes and embryonic tissues and they usually display different activation states, depending on the type of cancer, as well as the stage (*Zhu et al., 2017, Laviron et al., 2019*). Due to the high plasticity of TAMs, they cannot be defined by the classical M1/M2 nomenclature. It is, however, widely accepted that the population of macrophages found in tumours more closely resembles the phenotype of M2-like cells. In fact, TAMs express high levels of arginase, which,

as mentioned before, is required for cell proliferation and it is also linked to immunosuppression (*Bronte et al., 2005, Mantovani et al., 2013, Laviron et al., 2019*). Indeed, inhibiting arginase expression has a negative effect on tumour growth and has been shown to shift TAMs toward a pro-inflammatory phenotype (*Sharda et al., 2011, Steggerda et al., 2017*). Pro-inflammatory M1-macrophages are thought to be protective against cancer, due to their cytotoxic activity. It has been reported that M2 cells predominate over M1 in tumour tissue and cancer patients with higher infiltration of M1 cells in the tumour show a better overall survival, compared to patients with low M1 macrophages infiltration (*Ohri et al., 2009, Jackute et al., 2018*). In addition, mice lacking *Stat6*, a transcription factor required for M2 polarisation, produce M1 macrophages with high levels of iNOS and are resistant to metastatic disease compared to control mice (*Sinha et al., 2005*). Similarly, the pharmacological inhibition of STAT3, another transcription factor required for M2 activation, induces tumour cell apoptosis and enhanced tumour immunogenicity (*Xin et al., 2009*). Interferon regulatory factor 5 (IRF-5) in combination with its activating kinase IKK β has also been tested and was successful in generating anti-tumour immunity through M1 induction in models of melanoma, glioblastoma and ovarian cancer (*Zhang et al., 2019*). However, it is important to mention that the tumour microenvironment (TME) “educates” macrophages and TAMs often sharing features of both M1 and M2 varying among individual stages of tumour development (*Qian et al., 2010, Laoui et al., 2011, van Dalen et al., 2018*).

In addition to insulin resistance, cardiovascular disease and cancer, the plasticity of macrophages has also been implicated in autoimmunity, rheumatoid arthritis, kidney disease and neuroimmune disorders (*Kinne et al., 2000, Duffield et al., 2010, Fan et al., 2016*). The contribution of macrophages to human health and disease is schematized in **Figure 1.5**.

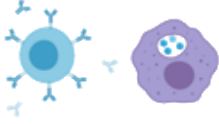
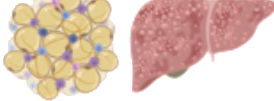
Health		Disease
Immunity		Inflammation, autoimmunity
Tissue Homeostasis		Cancer and metastasis
Cardiovascular System		Atherosclerosis
Metabolism		Obesity, Insulin Resistance, Fibrosis, Fatty Liver

Figure 1.5. The contribution of macrophages to health and disease

Macrophages play a crucial role in maintaining all tissues in a healthy state, acting as modulators of immunity, metabolism and tissue homeostasis. However, in the presence of a pathological insult their protective role is subverted: closely involved in a multitude of biological processes, macrophages can trigger a variety of human diseases including cancer, atherosclerosis, insulin resistance, fibrosis, fatty liver and autoimmunity.

1.2.4. microRNAs regulating macrophage development and function

In the past few years, miRNA regulation of macrophage development, function and polarisation has been the subject of intense research. It has been shown that murine macrophage development from haematopoietic precursor cells requires the expression of a specific subset of miRNAs (miR-146a, miR-342, miR-338, miR-155) which are induced by the transcription factor PU.1 (*Zhang et al., 1994*); miR-146, has also been tested in zebrafish, confirming its crucial and conserved role in macrophage differentiation (*Ghani et al., 2011*). However, the importance of miR-146 in macrophage differentiation appears to be controversial. Starczynowski and colleagues reported that over-expression of miR-146a in mouse hematopoietic precursor cells causes a reduced differentiation and survival of these cells, mimicking the cytotoxic effect of LPS long exposure (*Starczynowski et al., 2011*). PU.1 also suppresses a specific cluster of miRNAs (miR17-5p, miR-18a, miR-20a, miR-92) which have been shown to act in a feedback loop with the transcription factor acute myeloid leukemia-1 (AML1) during haematopoiesis (*Fontana et al., 2007, Ghani et al., 2011*). Several studies identified specific subsets of miRNAs that are differentially expressed in distinct macrophage phenotypes. By using a miRNA microarray analysis in cultured bone marrow derived macrophages (BMDMs), Zhang and colleagues identified a total of 109 miRNAs differentially expressed between M1 and M2 conditions (*Zhang et al., 2013*). M1 polarised macrophages are characterized by the expression of miR-181a, miR-155-5p, miR-204-5p, miR-451, whereas M2 macrophages differentially express miR-125-3p, miR-146-3p, miR-143-3p, miR-145-5p (*Zhang et al., 2013*). In particular, miR-155 has been intensively studied in M1 polarised macrophages. It has been shown that macrophages derived from miR-155 knockout mice do not express M1 related genes, even in response to stimulation with LPS and INF- γ (*Jablonski et al., 2016*). Moreover, the lack of miR-155 is linked to the dysregulation of approximately 650 genes previously associated with M1 phenotype (*Jablonski et al., 2015*). Accordingly, myeloid specific knockout of miR-155 enhances tumour growth in a breast cancer mouse model, due to the lack of M1 anti-tumoural immunity (*Zonari et al., 2013*). Macrophage polarisation has also been linked to the activity of miR-21, which has been found by several groups to suppress M1 cells and favour M2 macrophage polarisation (*Caescu et al., 2015, Wang et al., 2015*). Consistent with these findings, miR-21 expression is associated with poor survival in patients with specific cancers. miR-21 knockout mice develop smaller tumours compared to controls, suggesting that the lack of miR-21 activates genes able to re-educate TAMs towards an M1-like phenotype (*Xi et al., 2018*). Another M2-specific miRNA is miR-

124, which has been shown to upregulate CD206, Ym1, Fizz1, Arg1 and TGF- β and downregulate iNOS, CD86, TNF- α (Veremeyko *et al.*, 2013). Furthermore, miR-124 expression is strongly induced by IL-4 and IL-13 (Veremeyko *et al.*, 2013). Another miRNA controlling macrophage function is miR-101-3p, which directly target the 3'UTR of the dual specificity phosphatase (DUSP1) and the ATP-binding cassette transporter A1 (ABCA1). By negatively modulating these genes, miR-101-3p enhances inflammation and promote cholesterol accumulation in macrophages, thus offering a promising target to simultaneously antagonize inflammation and improve lipid metabolism (Wei *et al.*, 2015, Zhang *et al.*, 2015). Although many other miRNAs have been implicated in macrophages, there is little information about miRNA-mRNA networks in human macrophages and there are often opposing data. This raises the need for integrated transcriptomic analysis to identify multiple gene networks that can be used for both mechanistic investigations and novel drug development.

1.2.5. Limitations of the M1/M2 paradigm

The M1/M2 classification of functional macrophage phenotypes has been widely used to characterize macrophage populations *in vitro* and so far, has provided useful insights into the role of macrophage in health and disease. However, when it comes to complex *in vivo* environments, this model has significant limitations: macrophages generate heterogeneous and dynamic responses that are not easy to categorize, especially during some diseases (Martinez *et al.*, 2014, Laviron *et al.*, 2019). Martinez and Gordon suggested that M1 and M2 features do not exclude each other, but they can coexist, giving rise to a mixed phenotype that only depends on the balance of activating and inhibiting environmental signals. For this reason, the role of M1 and M2 should be considered beyond the historical, bipolar classification (Martinez *et al.*, 2014). Mitsi and colleagues have observed that steady state alveolar macrophages are characterized by both M1 and M2 signatures and this mixed phenotype can be changed by environmental stresses and stimuli, such as HIV infection (Mitsi *et al.*, 2018). Trombetta and colleagues also reported the existence of a mixed M1/M2 population in the lung of patients affected by systemic sclerosis (Trombetta *et al.*, 2018). Other examples of macrophage heterogeneity come from atherosclerosis and cancer (as previously discussed in section 1.2.3. Macrophages in health and disease). They are diseases in which both pro- and anti-inflammatory cells play decisive roles, more often in a stage- and environment-dependent manner. Both M1 and M2 makers have been detected in atherosclerotic plaques: M2 cells populate the stable region, while M1 cells are more abundant in the unstable plaque (*de*

Gaetano et al., 2016). Similarly, TAMs found in non-small cell lung cancer (NSCLC) consist of a mixed M1/M2 populations: Jackute and colleagues observed that the tumour tissue and stroma are mostly populated by M2 cells, but the tumour islets host cytotoxic M1 macrophages (*Jackute et al., 2018*). Recently, melanoma extracellular vesicles (EVs) have been shown to influence macrophage polarisation, towards a mixed M1/M2 phenotype (*Bardi et al., 2018*). In the light of these recent observations and to sum up, macrophage polarisation is a complex, dynamic and flexible process that depends on the surrounding environment. Therefore, classifying macrophages into M1 and M2 phenotypes often does not fully reflect what happens in physiological contexts.

1.3. Tribbles pseudo-kinases: regulators of inflammation, metabolism and cancer

Described for the first time in *Drosophila melanogaster* as regulators of mitosis and morphogenesis via *string/cdc25* (Mata *et al.*, 2000), Tribbles genes are now the subject of intense investigation in mammals, due to their involvement in numerous signalling pathways. Here, we briefly describe the function and key interacting partners of Tribbles proteins, mostly focusing on Tribbles-1 and discussing its critical role in the control of inflammation, metabolism and cancer.

1.3.1. Tribbles, a family of pseudo-kinases

Tribbles (TRIBs) genes encode for an evolutionary conserved family of pseudo-kinases that control a wide range of interacting signalling pathways. In mammals, three TRIB family members have been identified (TRIB1, TRIB2, TRIB3) and they have been associated with a significant number of human diseases, including cancer, cardiovascular disease, inflammation and immune-metabolic disorders (Hegedus *et al.*, 2006, Kiss-Toth 2011, Yokoyama *et al.*, 2011). Sequence alignments revealed a high conservation of TRIB proteins between human and mouse (identities: TRIB1, 97.5%, TRIB2, 99.2%, TRIB3, 81.2%) and a high degree of similarity among different human TRIBs (TRIB1/TRIB2, 71.3%, TRIB1/TRIB3, 53.3%, TRIB2/TRIB3, 53.7%). It is thought that TRIB proteins are mainly located in the nucleus, but can also interact with their partners in the cytoplasm. TRIB1 and TRIB2 are strongly associated with subsets of acute myeloid leukemia (AML), while TRIB3 has mainly been studied in the context of metabolic disorders, including insulin resistance, atherosclerosis (Yokoyama *et al.*, 2011) and cancer (Dong *et al.*, 2016, Yu *et al.*, 2019).

1.3.2. Overview of Tribbles binding partners

Structurally, TRIBs are three-domain proteins that contain an N-terminal PEST region, a pseudo-kinase domain and a C-terminal, COP1-binding region. However, they lack a functional adenosine 5'-triphosphate (ATP) binding site and therefore classified as catalytically inactive pseudo-kinase proteins. It has been proposed that through the pseudo-kinase domain, TRIBs act as adaptors or scaffold kinases facilitating the assembly with other proteins (Hegedus *et al.*, 2007, Lohan *et al.*, 2013). In addition, structural studies demonstrated that TRIB proteins have a unique C-terminal domain defined by two distinct motifs: the HPW

[F/L] motif binding to the MAPKK/MEK family members and the DQVXP [D/E] that targets the E3-ubiquitin ligases, including the constitutive photomorphogenic protein 1 (COP1) (Yoshida *et al.*, 2013, Eyers *et al.*, 2017) (**Figure 1.6.**). Through these motifs, TRIB proteins exert multiple functions in different cell types and tissues, important for the development of cancer and in the control of inflammatory signalling. TRIBs selectively regulate several members of the mitogen-activated protein kinase kinase (MAPKK) pathway, including ERKs, JNKs and p38 MAPK. It has been shown that TRIB1 is able to control the extent and specificity of MAPK activation depending on its expression level (Kiss-Toth *et al.*, 2004, Sung *et al.*, 2005, Guan *et al.*, 2016). By recruiting E3 ubiquitin ligases, TRIBs have been shown to promote target protein degradation. In fact, both TRIB1 and TRIB2 cause the degradation of C/EBP α and this has been associated with the development of acute myelogenous leukemia in murine models (Keeshan *et al.*, 2006, Dedhia *et al.*, 2010). Furthermore, by blocking C/EBP β , TRIB1 impairs TLR-mediated responses and leads to a dysregulation of LPS-inducible genes and NF-IL6 in murine macrophages (Yamamoto *et al.*, 2007). TRIB2 also promotes the proteolysis of C/EBP β and this together with the inhibition of AKT has a strong inhibitory effect on adipocytes differentiation in mice (Naiki *et al.*, 2007). Similarly, TRIB3 has been associated with the degradation of acetyl coenzyme carboxylase (ACC) in adipose tissue through the recruitment of COP1. In fact, adipose tissue lacking TRIB3 accumulates ACC (Qi *et al.*, 2006). In adipose tissue, TRIB3 also interacts with PPAR γ which results in the suppression of adipocytes differentiation (Takahashi *et al.*, 2008). Moreover, TRIB3 is thought to contribute to insulin resistance by inhibiting the phosphorylation of AKT. In fact, hepatic overexpression of TRIB3 leads to hyperglycemia and glucose intolerance (Du *et al.*, 2003). Notably, diabetic patients show an increased expression of TRIB3 compared to healthy controls suggesting a central role of TRIB3 in the pathogenesis of insulin resistance (Liu *et al.*, 2010). TRIB protein-protein interactions and their biological effect are briefly listed in **Table 1.2.**

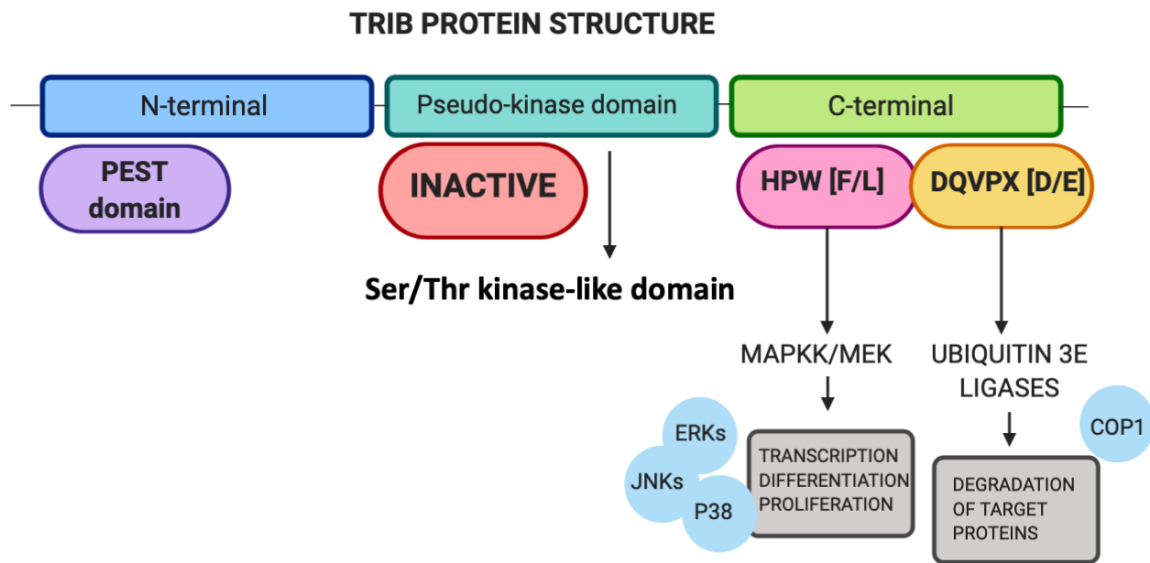


Figure 1.6. TRIB protein structure and interactions

TRIB proteins contain a N-terminal PEST domain, a Ser/Thr kinase-like domain lacking a functional ATP binding pocket and a C-terminal domain that mediate the interactions of TRIB with other factors. Due to the presence of two motifs HPW[F/L] and DQVXP[D/E] in the C-terminal domain, TRIBs interact with MAPKK/MEK family members and E3-ubiquitin ligases, respectively. Interactions with MAPKK/MEK mainly affect inflammatory and proliferative pathways, whilst via binding the ubiquitin E3 ligases, such as COP1, TRIBs regulate degradation of target proteins, affecting different biological processes.

Table 1.2. TRIB protein-protein interactions and their biological effect

TRIB interactions with target proteins mainly occur through their C-terminal domain, containing specific MAPKK/MEK and E3-ligases binding sites. Most biological effects are crucial in the context of inflammation and adipogenesis.

Tribbles	Protein	Biological Effect	Cell Type	Reference
TRIB1-3	MEK-1	ERK phosphorylation enhancement, myeloid leukemia	HeLa, U2OS, HEK293, NIH 3T3	Kiss-Toth et al., 2004, Yokoyama et al., 2010
TRIB2, TRIB3	AKT	Suppression of adipocytes differentiation and insulin resistance	Hepatocytes, 3T3-L1 adipocytes	Du et al., 2003, Naiki et al., 2007
TRIB1, TRIB2	C/EBP α	Acute myelogenous leukemia	Haematopoietic stem cells	Dedhia et al., 2010
TRIB1, TRIB3	MKK4	Inhibition of vascular smooth muscle cells migration	Vascular smooth muscle cells	Sung et al., 2007
TRIB3	CHOP	Endoplasmic reticulum (ER) stress and apoptosis induction	A375, HEK293, HepG2	Ohoka et al., 2005, Ohoka et al., 2007
TRIB3	SIAH1	Inhibition of TGF- β signaling	HEK293T	Zhou Y et al., 2008
TRIB1, TRIB2	C/EBP β	Suppression of adipocytes differentiation; TLR responses enhancement	Adipocytes, macrophages	Naiki et al., 2007, Yamamoto et al., 2007
TRIB3	PPAR γ	Suppression of adipogenesis	3T3-L1 adipocytes	Takahashi et al., 2008
TRIB1-3	COP1	Target proteins degradation	Adipocytes, 32Dcl3, HEK293T	Qi et al., 2006, Keeshan et al., 2010, Yoshida et al., 2013

1.3.3. Cell-context dependent functions of Tribbles

TRIBs can exert opposing roles in a cell-dependent manner. In fact, it is well appreciated that they can act both as oncogenes and oncosuppressors, activators and repressors of inflammation. Several groups have shown that TRIB3 is critical in breast cancer pathogenesis: it supports cancer cells stemness by regulating FOXO1-AKT interaction (*Yu et al., 2019*) and NOTCH1 signalling pathway (*Izrailit et al., 2013*); it is also thought to contribute to the development of breast cancer radiation resistance (*Lee et al., 2019*). TRIB3 knockdown in radiation-resistant breast cancer cell lines was shown to sensitize cells toward radiotherapy, by reducing NOTCH1 activation (*Lee et al., 2019*). High levels of TRIB3 have been also associated with other neoplasia, including colorectal (*Hua et al., 2019*) and lung cancer (*Zhou et al., 2013, Zhang et al., 2019*). However, in different contexts TRIB3 can behave as an oncosuppressor: Salazar and colleagues reported that TRIB3 is implicated in the anti-tumoral activity of cannabinoids, by regulating autophagy. They also found that genetic inhibition of TRIB3 enhances tumorigenesis in different cancer models and this is due to TRIB3's ability to control and modulate the extent of AKT activation (*Salazar et al., 2015*). Similarly, TRIB1 seems to have a dual role in regulating inflammation, depending on the context. Ostertag and colleagues have demonstrated that Trib1 mRNA is upregulated in response to inflammatory stimuli (i.e. LPS) in the whole white adipose tissue (WAT) depot of mice, but not in the macrophage-enriched fractions; moreover, Trib1 acts as activator of inflammation in adipose tissue as its deficiency in adipocytes impairs IL-6 and IL-1 β gene expression and also protects mice from high-diet induced obesity (*Ostertag et al., 2010*). On the contrary, the lack of Trib1 in the haematopoietic system causes an increase in pro-inflammatory cytokines, as well as hypertriglyceridemia and insulin resistance (*Akira et al., 2013*). The role of TRIB1 in inflammation is further discussed in the next section.

1.3.4. TRIB1-mediated control of macrophages

TRIB1 is a critical regulator of tissue resident macrophage differentiation. Tissue resident macrophages are M2-like cells which mainly display an anti-inflammatory phenotype under homeostatic condition. A massive reduction of M2 macrophages has been observed in bone marrow, spleen, lung and adipose tissue of mice lacking Trib1 in the haematopoietic system. This is due to the aberrant expression of C/EBP α , a TRIB1 downstream factor (*Satoh et al., 2013*). Interestingly, the lack of macrophages in these mice has also been associated with an increase in lipolysis and a reduction of adipose tissue mass. This pathological phenotype was

rescued when M2-macrophages were injected in the mice. Notably, when fed with a high fat diet, Trib1 knockout mice developed insulin resistance and hypertriglyceridemia. These results show that by regulating macrophages differentiation TRIB1 is also essential for the maintenance and functioning of adipose tissue, as well as lipid homeostasis (Sato *et al.*, 2013). TRIB1 also plays a role in macrophage migration. TRIB1 knock-down in RAW264.7 cells impairs macrophage migration behaviour mediated via C/EBP β and TNF- α and is also associated with a change in cell morphology (Liu *et al.*, 2013). It has been demonstrated that in absence of TRIB1, macrophages do not show MCP-1 induced chemotaxis, they detach and appear rounded with monocyte-like features (Liu *et al.*, 2013). In addition, it has been reported that Trib1 deficiency change bone marrow-derived macrophages (BMDMs) phenotype, by downregulating both M1 markers (Il6, Il1 β , Nos2) and M2 genes (Arg1, Fizz1, Cd206) (Arndt *et al.*, 2018). Recently, TRIB1 has been implicated in atherogenesis, particularly in macrophage foam cell formation (Fu *et al.*, 2017, Johnston *et al.*, 2019). Over-expression of TRIB1 in THP1-derived macrophages exposed to oxidized-LDL decreases intracellular lipid accumulation and increases cholesterol efflux (Fu *et al.*, 2017). In contrast, work recently published from our group by Johnston and colleagues showed that myeloid specific knockout of Trib1 is atheroprotective, while myeloid overexpression is detrimental *in vivo*. Trib1 overexpression upregulates the oxidized LDL receptor (OLR-1), increasing lipid uptake and foam cell formation in two distinct experimental models of atherosclerosis (Johnston *et al.*, 2019). Taken together these data suggest a pivotal role of TRIB1 in macrophage biology. However, considering the existence of contrasting results (Fu *et al.*, 2017, Johnston *et al.*, 2019) and the lack of experimental data in human macrophages, further investigation is needed.

1.3.5. TRIB1 and Prostate Cancer

Prostate cancer (PCa) is one of the most common malignancies in men with over 1 million new cases diagnosed per year, worldwide. PCa is a slow-growing cancer, it usually has a long progression and it can also remain asymptomatic for a long period. However, the majority of patients experience urinary dysfunction and sexual discomfort (Shen *et al.*, 2010). Although human PCa is considered to be highly heterogeneous, it has been reported that more than 95% of these cancers are classified as adenocarcinomas that, in common with most tumours, have the ability to spread from their original site and preferentially metastasize in the lungs, liver, pleura, adrenals, brain and bone (Shen *et al.*, 2010). Bone metastasis has been described as the most common for PCa, as well as the most severe for patients; it is also characterised by the

presence of peculiar osteoblast lesions (*Bubendorf et al., 2000, Logothetis et al., 2005*). Despite recent progress and the existence of different therapeutic strategies, the management of advanced and metastatic PCa still remains a big challenge (*Shen et al., 2010, Litwin et al., 2017*). Furthermore, the mutation rate in PCa is lower, compared to other cancer types. In fact, no single gene has been found to be responsible for the development of PCa but a significant number of genetic aberrations in multiple loci has been implicated (*Lawrence et al., 2014, Wang et al., 2018, Testa et al., 2019*). Among them it is important to mention mutations in androgen receptor (AR), phosphatase and tensin homolog (PTEN), Homeobox Protein NK-3 Homolog A (NKX3-1), adenomatous polyposis coli (APC), breast cancer susceptibility genes (BRCA1 and BRCA2), ATM Serine/Threonine Kinase (ATM) and Speckle Type BTB/POZ Protein (SPOP) (*Wang et al., 2018*).

TRIB1 has recently been reported to have a role in the tumorigenesis and progression of PCa. Mashima and colleagues found that TRIB1 is upregulated in PCa and required for the *in vitro* growth of the cancer under 3D conditions, by regulating the expression of endoplasmic reticulum (ER) chaperones (*Mashima et al., 2014*). Interestingly, the pseudo-kinase seems to promote M2 macrophage polarisation in the immune microenvironment of the tumour: in fact, the RNA expression of TRIB1 positively correlates with the amount of CD163⁺ macrophages infiltration (*Liu et al., 2019*). Moreover, data mining of PCa expression datasets shows overexpression and amplification of the TRIB1 gene, as well as correlation with risk, aggressiveness and survival. A short tandem repeat (STR) found in the 3'UTR of TRIB1 was significantly associated with prostate cancer risk and it is thought to alter TRIB1 mRNA expression and stability (*Moya et al., 2018*). However, despite published data and *in silico* analysis suggest an emerging role for TRIB1 in the pathogenesis of PCa, the mechanisms underlying its overexpression still remain unknown and require further investigation.

More information about miRNAs and TRIB1 in PCa is provided in the introduction section of Chapter 6, miRNAs regulating TRIB1 in PCa.

1.3.6. TRIB1: an unstable transcript

The TRIB1 mRNA is highly unstable, showing a half-life shorter than 1 hour (*Sharova et al., 2009*). This is often cell/tissue specific and likely due to the presence of endogenous post-transcriptional regulators. In mouse embryonic stem cells Sharova and colleagues identified TRIB1 among the top 50 genes with the most unstable mRNA half-life. They also reported that genes with unstable mRNAs often exert regulatory functions (transcription factors), while

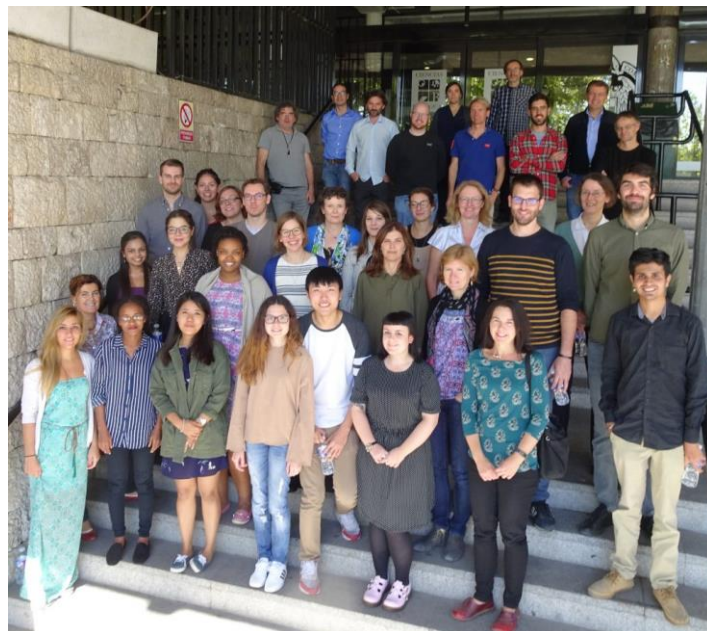
stable mRNA species with longer half-lives are genes related to cell structure and metabolism (Sharova *et al.*, 2009). TRIB1 gene expression is highly variable among different cell types and tissues, suggesting it might be subject to cell type-dependent post-transcriptional regulation (Sung *et al.*, 2006). In fact, the 3'UTR of TRIB1 mRNA represents more than 50% of the whole sequence (1.5 Kbp), it is highly conserved among different animal species and it is enriched in regulatory binding sites. Soubeyrand and colleagues have showed that blocking transcription through actinomycin-D dramatically reduced TRIB1 mRNA levels in HeLa and arterial smooth muscle cells (ASMCs) but inhibiting protein translation using cycloheximide and puromycin had the opposite effect (Soubeyrand *et al.*, 2016). This may be explained with the presence of a compensatory mechanism enhancing TRIB1 transcription when the protein translation is compromised. Nevertheless, the post-transcriptional regulation of TRIB1 expression remains largely unknown.

1.3.7. TRIB1 as a potential target of multiple microRNAs

Currently, there is little information about TRIB1 upstream regulators. However, *in silico* analysis show that TRIB1 is a potential target of multiple miRNAs, both in human and in mouse. To date, only a few interactions have been experimentally validated. In PCa, TRIB1 has been shown to be negatively modulated by miR-224, a miRNA often silenced in cancer. The expression level of miR-224 and TRIB1 negatively correlates in prostate tissue and their interaction results in the suppression of cell proliferation, invasion and metastasis (Lin *et al.*, 2014). Moreover, it has been shown that in hepatocellular carcinoma (HCC), where TRIB1 is usually overexpressed, miR-23a directly targets the 3'UTR of the pseudo-kinase, affecting HCC cell growth, through a mechanism involving p53 and β -catenin (Ye *et al.*, 2017). TRIB1 is also regulated by miR-202 in HepG2 and primary hepatocytes, as was shown in our research group (Ilyas *et al.*, 2015, unpublished, manuscript under development). We found an inverse correlation between miR-202 and TRIB1 expression levels in an inflammatory context (Ilyas *et al.*, 2015, unpublished). Considering its role in a multitude of signalling pathways and its short half-life, investigating TRIB1 post-transcriptional regulation by miRNAs seems a promising strategy to identify endogenous upstream regulators of the pseudo-kinase that might be used to modulate its expression in a tissue-specific context. Therefore, further work in this field is needed.

1.4. Tribbles Research and Innovation Network (TRAIN)

Tribbles Research and Innovation Network ([TRAIN, http://train-itn.eu](http://train-itn.eu)) is a project funded by the European Union's Horizon 2020 research and innovation programme that started in 2017, under the Marie Skłodowska Curie ITN Project Grant No 721532. TRAIN has brought together a group of scientists working at the interface of metabolism, immunity and cancer, for a total of 15 distinct multi-disciplinary research projects, spread across 6 European countries. The purpose of the TRAIN Consortium is to unravel the role of Tribbles pseudo-kinases in the development and progression of prostate cancer, with particular focus on metabolic and immune responses. The TRAIN scientific programme contains at least four different work packages: metabolism, immunity, cancer and genomics/system biology; all of them mainly focus on the function of TRIB1 and TRIB3 in macrophages, adipocytes, T-regulatory cells, Natural Killer cells and prostate cancer cells. My individual PhD project sits in the genomics/system biology package, as it is based on the identification and characterization of miRNAs targeting TRIB1, by using a combination of wet lab and bioinformatics procedures. The cell type of my focus is human macrophage as it is closely involved in immunity and metabolism, as well as in cancer. Therefore, the work presented in this thesis is mostly related to macrophage biology. However, to integrate my PhD individual project within the TRAIN Consortium interests I have performed some experiments using prostate cancer cell lines, which are described in Chapter 6, as a minor results chapter.



1.5. Hypothesis

Although the downstream interactors of TRIB1 are well characterised, the mechanisms underlying its regulation are still largely unknown. Considering the length of its 3'UTR, we hypothesised that TRIB1 undergoes post-transcriptional regulation by microRNAs. The purpose of this study is to identify and characterise miRNAs regulating TRIB1 expression by using a combination of computational and experimental approaches, with focus on human macrophages and prostate cancer *in vitro* models. Since TRIB1 genetic variants have been associated with disease traits and susceptibility, we also aim to investigate the potential impact of TRIB1 non-coding SNPs on miRNA-binding sites.

Chapter 2. General Materials and Methods

Part I, In Silico

2.1. microRNA-target prediction and databases management

microRNA-target prediction analysis was performed to identify miRNAs regulating TRIB1 expression. We used 7 prediction tools, listed in **Table 2.1.**; all of them were used online, except miRanda, which was downloaded and used locally as independent software.

miRanda is a dedicated algorithm developed for the detection of miRNA binding sites in target sequences. It reads RNA from a first input file containing mature miRNA sequences and DNA or RNA sequences from a second input file containing genes of interest. Between the two sets of sequences (Reference and Query), miRanda algorithm performs a dynamic local alignment and calculates the thermodynamic stability of RNA/RNA duplexes. This step takes advantage of the ViennaRNA package written by Ivo Hofacker (*Lorenz et al., 2011*) and included in the script. miRanda detection software (Version 3.3a, Computational Biology Center of Memorial Sloan-Kettering Cancer Center, <http://www.microrna.org/>) was downloaded in C and used as an open source method under the GPL. The following default parameters were used, according to the original script:

- Gap Open Penalty: -9.000000
- Gap Extend Penalty: -4.000000
- Score Threshold: 140.000000
- Energy Threshold: 1.000000 kCal/mol
- Scaling Parameter: 4.000000

miRanda input files were used in FASTA format: human mature miRNAs sequences were downloaded from miRbase 22.1 (<http://www.mirbase.org/ftp.shtml>), while TRIB1 3'UTR sequence (NM_025195.4, transcript variant 1) was taken from NCBI database (<https://www.ncbi.nlm.nih.gov/>). The output files generated by miRanda algorithm were post-processed and organised in tables by using Python (Python v3.6.2/BioPython v1.70). Tables were imported in MySQL database (pgAdmin version 4, Management Tools for PostgreSQL), along with the outputs generated by other prediction tools used (which were downloaded from the webpages of the tools). Results were filtered and analysed by using structural queries and

are explained in Chapter 3. The total number of miRNAs predicted to target the 3'UTR of TRIB1 was obtained following these filtering steps:

- Detect the number of miRNAs predicted by each algorithm;
- Eliminate duplicates (same miRNAs predicted by different algorithms);
- Select only “high confidence” miRNAs, taken from miRbase 22.1 (<ftp://mirbase.org/pub/mirbase/22.1/>).
- Further filter the list selecting only miRNAs which are present in at least 3 databases (miRanda, TargetScan and Starbase);

Scripts used to post-process miRanda output are listed in Chapter 8 (Appendix IV).

Table 2.1. List of miRNA-target prediction tools

Prediction tool/algorithm	Link	Reference
miRanda	http://www.microrna.org/microrna/home.do	Betel et al., 2008
TargetScan v.7.2	http://www.targetscan.org/vert_72/	Agarwal et al., 2015
StarBase ENCORI	http://starbase.sysu.edu.cn/	Li et al., 2014
miRDB	http://www.mirdb.org/	Chen and Wang 2020
miRwalk v.3	http://mirwalk.umm.uni-heidelberg.de/	Sticht et al., 2018
DIANA Tools, microT-CDS	http://diana.imis.athena-innovation.gr/DianaTools/index.php?r=microT_CDS/index	Paraskevopoulou et al., 2013, Reczko et al., 2012
DIANA Tools, Tarbase v.8	http://carolina.imis.athena-innovation.gr/diana_tools/web/index.php?r=tarbase8/index	Karagkouni et al., 2018
miRbase 22.1	http://www.mirbase.org/	Kozomara et al., 2019

2.1.1. miRNAs targeting TRIB1 genetic variants: Single Nucleotide Polymorphisms (SNPs)

To predict miRNAs potentially targeting TRIB1 SNPs we used the algorithm miRanda, as described earlier. As input file, we used a list of 90 genetic variants affecting the 3'UTR of TRIB1, downloaded from NCBI database. This list included both SNPs and small insertions/deletions (INDELS). However, these sequences were downloaded as short sequences containing IUPAC ambiguity codes, therefore we pre-processed them using Python to generate the full-length 3'UTR sequences carrying each SNP. After executing miRanda, we used Python to organise the output file into tables. We created a table for the reference transcript and a table for all the SNPs; we then imported the tables in MySQL and used structural queries to intersect each dataset and find, for example, common interactions and non-common interactions. Results are explained in Chapter 5, while the list of SNPs and scripts is provided in Chapter 8 (Appendix IV).

2.1.2. Additional tools used

As additional tools, we used the database PolymiRTS (<http://compbio.uthsc.edu/miRSNP/>) and the database miRCancer (<http://mircancer.ecu.edu/>). PolymiRTS is a web-based tool enabling the detection of miRNAs targeting SNPs and it is based on both TargetScan and experimental data (*Bhattacharya et al., 2014*) (see Chapter 5); miRCancer (*Xie et al., 2013*) was used to download a list of miRNAs dysregulated in prostate cancer according to published literature (see Chapter 6).

2.2. RNA-sequencing

RNA was isolated from human primary macrophages using the miRNeasy Mini Kit (QIAGEN) and sent to the sequencing company Novogene Co. Ltd (<https://en.novogene.com>) for two different type of RNA sequencing: a small non-coding RNA sequencing and a messenger RNA sequencing, which are the topic of Chapter 4. Prior to the sequencing, RNA samples were assessed for quality and concentration using Nanodrop, Agarose Gel Electrophoresis and Agilent 2100 (quality and concentration of representative samples are shown in Chapter 8, Appendix III). In the following sections we briefly describe the sequencing strategy, the bioinformatic pipelines and all the packages we used to analyse the data.

2.2.1. Small non-coding RNA sequencing

Small non-coding RNA sequencing was carried out on unpolarised (M0) and polarised (M1, pro-inflammatory phenotype) macrophages isolated from 8 healthy donors, for a total of 16 samples. The protocol of macrophage polarisation is specified below (Section 2.3.1.). For the cDNA library construction, 18-40 bp inserts were involved and for the sequencing an Illumina platform was used (NovaSeq platform, single-end 50 bp). Sequencing depth ranged from 18 to 25 million reads (recommended sequencing depth is ≥ 10 million reads). First, we performed a quality control check (QC) on fastq files, generated by the sequencer, using the package MultiQC (*Ewels et al., 2016*). We also carried out a trimming phase using Cutadapt to remove “contaminating” adapter sequences and improve the mappability of the reads. By using the aligner Bowtie2 we performed the mapping. However, instead of mapping the reads to a reference genome, we used sequences downloaded from RNACentral, a comprehensive database of non-coding RNAs (*RNAcentral Consortium, 2017*). This was necessary to avoid the alignment of small RNAs to unrelated, complementary sequences in the genome. After mapping, we used SAMTools to post-process the alignments and generate raw counts. The latter were then passed into the limma R package to generate CPM values (Counts Per Million). Differential expression (DE) analysis was performed using Deseq2 package (p value cut off 0.05; fold change threshold 1). A Principal Component Analysis (PCA) was also performed using the R functions “prcomp” and R package “factoextra”. PCA analysis shows clusters of samples according to their similarities and we generated PCA plots considering CPM values. Once DE microRNAs between M0 and M1 macrophages were identified, we used TargetScan algorithm to predict their target genes; the expression of these genes was then checked using an RNA seq experiment, previously generated in our lab (DOI: 10.17632/j2hmt7k9fh.1). We chose this dataset as it was carried out on human polarised macrophages (M0 vs M1) isolated from 8 healthy donors, following the same experimental protocol through which we generated our samples; moreover, both datasets are characterised by the same number of donors (n = 8). This RNA-seq was analysed starting from fastq files and following the same workflow described in the next section (Section 2.2.2. Messenger RNA sequencing). After overlapping the two sets of macrophage transcriptomic data, we carried out a downstream analysis to identify pathways and biological processes, using the R package GOSeq.

2.2.2. Messenger RNA-sequencing

Messenger RNA sequencing was performed on transiently transfected macrophages, isolated from 6 healthy volunteers for a total of 24 samples (as specified in **Table 2.2.**). According to the small RNA sequencing results, we selected miR-125a-3p, miR-155-5p and miR-186-5p as candidate miRNAs and transiently overexpressed them for our second sequencing experiment (see Chapter 4). For the cDNA library construction, inserts of 250-300 bp were used and sequencing was performed using an Illumina platform (paired-end 150 bp). As we did for the previous sequencing, we performed a QC on fastq file, followed by trimming and mapping using the reference genome. This time, the trimming was carried out using the tool Trimmomatic and the mapping was performed using the human reference genome (GRCh38). We used Salmon tool to perform the quantification. The DE analysis was performed by using DESeq2 (p value cut off=0.05; fold change threshold=1). **Table 2.3.** lists all the R packages and functions used to analyse both the small RNA seq and the RNA seq data, along with relevant links and publications. All the sequencing related graphs presented in Chapter 4 were generated using R scripting.

Table 2.2. Experimental conditions for the RNA-seq experiment

The table summarises the experimental conditions behind the mRNA-seq. We transiently transfected unpolarised macrophages (M0) isolated from 6 different individuals with candidate miRNA mimics and a negative control.

Cell type	4 transfection conditions (24 hours)
Monocyte-derived macrophages (isolated from 6 healthy volunteers)	miR-125a-3p Mimic, 50nM miR-155-5p Mimic, 50nM miR-186-5p Mimic, 50nM Negative Control Mimic, 50nM

Table 2.3. Packages, functions and database used to carry out the RNA-seq analysis

The table lists all the tools used to analyse RNA-seq data. DE= differential expression; PCA=principal component analysis; GO=gene ontology; KEGG: Kyoto Encyclopedia of Genes and Genomes.

Package/function/database	Used for	URL	Reference
MultiQC	Quality Control	https://multiqc.info/	<i>Ewels et al., 2016</i>
Cutadapt	Adapter trimming, miR-seq	https://cutadapt.readthedocs.io/en/stable/	<i>Martin et al., 2011</i>
Trimmomatic	Adapter trimming, RNA-seq	http://www.usadellab.org/cms/?page=trimmomatic	<i>Bolger et al., 2014</i>
RNA Central (v14)	Mapping, alignment (non-coding RNA sequences as reference genome)	https://rnacentral.org	<i>The RNA Central Consortium 2019</i>
GRCh38	Mapping, alignment	https://www.ncbi.nlm.nih.gov/assembly/GCF_000001405.26/	<i>Genome Reference Consortium Human Build 38</i>
Bowtie2	Mapping, alignment	http://bowtie-bio.sourceforge.net/bowtie2/index.shtml	<i>Langmead et al., 2012</i>
SAMtools	Quantification	http://www.htslib.org/	<i>Li et al., 2009</i>
Salmon tool	Quantification	https://salmon.readthedocs.io/en/latest/salmon.html	<i>Patro et al., 2017</i>
Limma	Quantification, post-processing	https://bioconductor.org/packages/release/bioc/html/limma.html	<i>Ritchie et al., 2015</i>
DESeq2	DE analysis	http://bioconductor.org/packages/release/bioc/html/DESeq2.html	<i>Love et al., 2014</i>
Prcomp	Generate PCA	https://stat.ethz.ch/R-manual/R-devel/library/stats/html/prcomp.html	<i>Mardia et al., 1979, Becker et al., 1988, Venables et al., 2002</i>
Factoextra	Visualise PCA	https://rpkgs.datanovia.com/factoextra/index.html	<i>Le et al., 2008</i>
GOSeq	GO and KEGG Enrichment Analysis	https://bioconductor.org/packages/release/bioc/html/goseq.html	<i>Young et al., 2010</i>

Part II, In Vitro

2.3. Cell culture and maintenance

2.3.1. Primary cells

2.3.1.1. Human monocyte-derived macrophages (MDMs)

Statement of Ethics

To isolate primary human blood monocytes, up to 80 mL of venous blood was taken from healthy donors. The study was ethically approved by the University of Sheffield Ethics Committee (Reference Number: 031330; previously SMBRER310) and written informed consent was obtained from all volunteers.

Blood Monocytes isolation and macrophages differentiation

Peripheral blood mononuclear cells (PBMCs) were isolated from whole blood using a Ficoll gradient centrifugation. All steps were performed at room temperature. In a 50 mL conical centrifuge tube, 40 mL of fresh whole blood was added along with 5 mL of 3.8% (w/v) Sodium Citrate to prevent coagulation; 30 mL of the mixture was slowly layered over 15 mL of Ficoll-Paque Plus (GE Healthcare) (2 volumes of blood per 1 volume of Ficoll) and centrifuged at 900xg for 20 minutes (accel and brake 1). Plasma was aspirated and the mononuclear cell layer was transferred to a new 50 mL conical tube filled with PBS-EDTA; the mixture was centrifuged at 265xg for 5 minutes. Red blood cells lysis buffer 1X (16.6 g NH₄Cl, 2 g KHCO₃, 400 uL 0.5 M EDTA, 200 mL distilled, sterile H₂O) was added for the removal of platelets and erythrocytes and left at room temperature for 5 minutes. Cells were further centrifuged and counted for the CD14⁺ positive magnetic selection using the Miltenyi Biotech MACS magnetic cell separation system and the anti-CD14 human antibody-beads. CD14⁺ monocytes purity was assessed by Flow Cytometry and cells were subsequently cultured in RPMI-1640 (Gibco) supplemented with 10% (v/v) of Low Endotoxin Heat Inactivated Foetal Bovine Serum, 1% (v/v) Penicillin/Streptomycin, 1% (v/v) L-Glutamine. Human recombinant macrophage-colony stimulating factor (M-CSF, Human, Prepotech) was added (100 ng/mL) to enable the differentiation of monocytes into macrophages. Cells were incubated for 7 days at 37°C, 5% CO₂.

Macrophages in vitro polarisation

After 7 days of differentiation, human macrophages were activated towards three different phenotypes by adding the following cytokines to the media:

- **M1 pro-inflammatory phenotype:** 20 ng/mL IFN- γ (Human, Peprotech) and 100 ng/mL E. coli lipopolysaccharide (Serotype R515 TLR grade TM, Enzo Life Sciences);
- **M2a anti-inflammatory phenotype:** 20 ng/mL IL-4 (Human, Peprotech);
- **M2c anti-inflammatory phenotype:** 20 ng/mL IL-10 (Human, Peprotech).

After 24 hours of treatment, cells were washed twice with PBS 1X and cell pellets were collected and stored at -80°C for further RNA/protein isolation.

2.3.2. Established cell lines

2.3.2.1. Immortalised BMDMs (iBMDMs)

Immortalised BMDMs were used for transient transfection of miRNA mimics (see Chapter 3). The line was generated from wild-type male mice as described by Hornung et al., 2008 and they were a gift from Professor David Brough (University of Manchester). The cells were grown in T75 flasks in DMEM (Gibco) supplied with 10% (v/v) of Low Endotoxin Heat Inactivated Foetal Bovine Serum, 1% (v/v) Penicillin/Streptomycin and 1% Sodium Pyruvate and passaged every 2 days, by using cell scraping.

2.3.2.2. HEK293T cell line

Human embryonic kidney cell line 293T (HEK293T) was used to perform transient transfection and luciferase reporter assay, as it is highly transfectable with either DNA and RNA constructs. Cells were grown in DMEM (Gibco) supplied with 10% (v/v) of Low Endotoxin Heat Inactivated Foetal Bovine Serum, 1% (v/v) Penicillin/Streptomycin, 1% Non-Essential Amino acids. Cells were passaged every 2 days in T25 flasks, by using Trypsin/EDTA.

2.3.2.3. Prostate cancer cell lines

Cell lines from prostate cancer (PC3, DU145, LNCAP, 22RV1) and normal epithelium (PNT1A, PWRE1, RWPE1) were cultured and used to investigate TRIB1 and miRNAs endogenous expression, as well as for transient transfection experiments (see Chapter 6). PC3 and DU145 cell lines were grown in DMEM (Gibco) supplemented with 10% (v/v) of Low Endotoxin Heat Inactivated Foetal Bovine Serum, 1% (v/v) Penicillin/Streptomycin, 1% Non-Essential Amino acids; LNCAP, 22RV1 and PNT1A were grown in RPMI-1640 (Gibco) supplemented with 10% (v/v) of Low Endotoxin Heat Inactivated Foetal Bovine Serum, 1% (v/v) Penicillin/Streptomycin, 1% (v/v) Glutamine, 1% (v/v) Non-Essential Amino acids; PWRE1 and RWPE1 were cultured in Keratinocyte Serum Free Media (K-SFM, Gibco) supplied with 1% (v/v) Penicillin/Streptomycin, 0.05 mg/mL bovine pituitary extract (BPE) and 5ng/mL human recombinant epidermal growth factor (EGF), both provided with the K-SFM kit. All cell lines were grown in T75 flasks and passaged every 2-3 days in a 1:5 ratio, by using Trypsin/EDTA.

2.4. Gene expression profiling

2.4.1. RNA extraction

Total RNA isolation was performed by using the miRNeasy Mini Kit (QIAGEN) according to manufacturer's instructions. The kit enables the purification of total RNA, including small RNA from approximately 18 nucleotides and are based on silica-spin columns which optimize the RNA binding. RNA concentration and purity were measured by NanoDropTM Spectrophotometer (260/280 ratio= 1.8/2.0; 260/230 ratio=1.8/2.0). Prior to the small-RNA sequencing and the mRNA sequencing, RNA integrity and concentration were also assessed by using Agarose Gel Electrophoresis (Gel Con: 1%; voltage: 180v; Run Time: 16min) and Bioanalyzer Agilent 2100 (RNA Integrity Number \geq 7.5) (details in Chapter 8, Appendix III).

2.4.2. cDNA synthesis

cDNA synthesis was performed by using the iScript cDNA synthesis kit (Biorad) and the miRCURY Universal cDNA synthesis kit (QIAGEN) according to manufacturer's instructions. The latter enable the reverse-transcription of all miRNAs in one single reaction which includes the following steps: (1) a poly-A tail is first added to the mature miRNA

template and (2) the cDNA is synthesized using a poly T primer with a 3' degenerate anchor and a 5' universal tag. Protocols, incubation and heat inactivation steps for both kits are listed below (**Table 2.4.**).

2.4.3. Real Time-quantitative PCR

Real Time qPCR was performed using SYBR Green Master Mix (Primer Design) for the messenger RNA; the miRCURY LNA miRNA PCR Assay (QIAGEN) was used for miRNAs. SYBR primers were designed and checked for specificity using the BLAST Primer Design Tool (<https://www.ncbi.nlm.nih.gov/tools/primer-blast>) and purchased from Sigma-Aldrich; miRNA Primer Mix were purchased from QIAGEN (sequences and details are listed in Chapter 8, Appendix I). Protocols are listed below (**Table 2.5.** and **Table 2.6.**). Results were analysed upon a CFX384 C1000 Touch Thermal Cycler (Biorad) using the PCR cycle conditions listed below (**Table 2.7.** and **Table 2.8.** and the $2^{-\Delta\text{Ct}}$) method described below.

2.4.4. Gene expression analysis: $2^{-\Delta\text{Ct}}$ method

Prior to the analysis, specificity of each primer pair was confirmed by Melt Curve Analysis, provided by the qPCR thermal cycler. Data were then exported in Excel and analysed by using the $2^{-\Delta\text{Ct}}$ method which enables the calculation of the expression of a gene relative to a housekeeping gene. The method consists in the following formulas:

1. Average Ct (or Cq) for each gene and sample;
2. ΔCt calculation for each sample:

$$\text{Ct}_{\text{gene of interest}} - \text{Ct}_{\text{housekeeping gene}}$$

3. $2^{-\Delta\text{Ct}}$ calculation for test sample and control sample:

$$= \text{power}(2, -\Delta\text{Ct})$$

Table 2.4. cDNA synthesis protocols

iScript cDNA synthesis (Biorad)	miRCURY Universal cDNA synthesis (QIAGEN)
5x iScript Reaction Mix: 4 uL	5x miRCURY RT Reaction Buffer: 2 uL
iScript Reverse Transcriptase: 1 uL	RNase-free water: 4.5 uL
Nuclease-free water: variable	10x miRCURY RT Enzyme Mix: 1 uL
RNA template (100 fg-1 ug total RNA)	Synthetic RNA spike ins, optional: 0,5 uL
Reactions volume: 20 uL	Template RNA (5 ng/uL): 2 uL
<input type="checkbox"/> Priming for 5 min at 25 °C.	<input type="checkbox"/> Incubate for 60 min at 42 °C.
<input type="checkbox"/> Reverse transcription for 20 min at 46 °C.	<input type="checkbox"/> Heat-inactivate the reverse transcriptase for 5 min at 95 °C.
<input type="checkbox"/> RT inactivation for 1 min at 95 °C.	<input type="checkbox"/> Immediately cool to 4 °C.
<input type="checkbox"/> Immediately cool to 4 °C.	<input type="checkbox"/> Store at 4 °C or freeze.
<input type="checkbox"/> Store at 4 °C or freeze.	

Table 2.5. RT-qPCR reagents and protocol: Primer Design

Component	SYBR Green Master Mix (Primer Design)
SYBR Green Master Mix	5 uL
Primer Forward 10uM	0,3 uL
Primer Reverse 10uM	0,3 uL
Diluted cDNA (0,2-1ng/uL)	5 uL
Total Reaction Volume	10,6 uL

Table 2.6. RT-qPCR reagents and protocol: QIAGEN

Component	miRCURY LNA miRNA PCR Assay (QIAGEN)
2x miRCURY SYBR Green Master Mix	5 uL
Nuclease-free water	1 uL
Primer Mix	1 uL
Diluted cDNA (1:60)	3 uL
Total Reaction Water	10 uL

Table 2.7. RT-qPCR running protocol: Primer Design

Process Step	Settings Primer Design
Polymerase	95°C, 2min
Activation/Denaturation	
Amplification	40 amplification cycles at 95°C, 15sec 60 °C ,1min
Melting Curve Analysis	Yes 60°C-95°C/0.5 °C Increment

Table 2.8. RT-qPCR running protocol: QIAGEN

Process Step	Settings QIAGEN
Polymerase	95°C, 2min
Activation/Denaturation	
Amplification	40 amplification cycles at 95°C, 10sec 56 °C ,1min
Melting Curve Analysis	Yes 60°C-95°C/0.5 °C Increment

2.5. Protein analysis

2.5.1. Protein Extraction

Proteins were extracted from cell pellets using the RIPA Buffer ready-to-use-solution (Sigma-Aldrich) and 1 uL/mL of Protease Inhibitor (100 uL each 1×10^6 cells). Cell lysates were further sonicated using the ultrasonic bath at voltage 220-240 and Hertz 50-60 for 15-30 minutes (Ultrawave, Cardiff, UK). Lysates were then centrifuged at $10.000 \times g$ for 20 minutes at 4°C ; proteins (supernatants) were transferred in a new tube while the debris was discarded.

2.5.2. BCA Protein Quantification Assay

Total protein concentration was measured compared to a protein standard (Bovine serum albumin, BSA) using the Pierce BCA Protein Assay kit according the manufacturer's instructions (Thermo Fisher Scientific). Concentration was estimated by a colorimetric microplate reader at 562nm. Data were analysed using GraphPad Prism 8.0 (GraphPad Software, La Jolla, CA, USA); the BSA standard curve was log transformed and plotted to allow the interpolation of unknown samples with 95% confidence intervals.

2.5.3. Western Blotting

Western Blotting was performed using the Invitrogen™ Novex XCell SureLock™ Mini- Cell (Invitrogen). 10-20 ug of sample protein was added to 5x Loading Buffer (10% SDS (w/v), 25% (v/v) beta-mercaptoethanol, 50% (v/v) glycerol, 0.01% (w/v) bromophenol blue, 0.125M Tris-HCl, pH 6.8) up to a final volume of 30 uL (volumes were adjusted with RIPA buffer) and incubated at 95°C for 10 minutes; 25 uL of proteins was then loaded into the wells of a NuPAGE 4-12% Bis-Tris SDS-PAGE gel Novex (Invitrogen) together with a standard protein size marker (SeeBlue, Plus2 Prestained Standard, Invitrogen). Electrophoresis was performed at 150 V for 60/80 minutes in NuPAGE MOPS/MES SDS Running Buffer (Novex, Invitrogen). Proteins were then transferred onto a nitrocellulose membrane at 35 V for 60 minutes in NuPAGE Transfer Buffer (5% (v/v) 20x transfer buffer, 0.1% (v/v) antioxidant, 20% (v/v) methanol (Novex, Invitrogen). Transfer efficiency was further determined by staining the membrane with Red-Ponceau S Solution (Sigma-Aldrich) for 5-10 minutes at room temperature. The membrane was washed in TBS-T (Tris Buffered Saline pH 8.0 powder dissolved in 1 L of distilled water, 0.1% (v/v) Tween 20, Sigma-Aldrich) and blocked at room

temperature for 1 hour in 5% Milk TBS-T. Primary antibody was diluted in 5% Milk TBS-T and left at 4°C, overnight. After the overnight incubation, the membrane was washed 3 times for 5 min in TBS-T and incubated with the HRP-conjugated secondary antibody (1:1000, 5% Milk TBS-T) at room temperature for 1 hour. The membrane was then washed again (3x5min in TBS-T). In order to use different primary antibodies (i.e. protein of interest and housekeeping) the membrane was cut when possible or stripped in ReBlot Plus Strong Antibody Stripping Solution 1X (EMD, Millipore) and re-blocked in 5% Milk TBS-T at room temperature for 1 hour. Prior to the development a chemiluminescent substrate (ECL Prime Western Blotting Detection Reagent, GE Healthcare) was added to the membrane for 60-90 seconds. Specific protein bands were detected by using either C-DiGit Blot Scanner (LI-COR Bioscience) and the ChemiDoc XRS+ Imaging System (Biorad). Primary and secondary antibodies and their working concentrations are specified in Chapter 8, Appendix I. Results were analysed in Excel through ImageStudio Digit version 5 (LI-COR Bioscience) and ImageLab version 6.0 (Biorad), as follows:

1. Calculate intensity for each protein band;
2. Background subtraction (adjusted intensity);
3. Normalise intensity for each test and control sample:

$$\text{Adjusted Intensity}_{\text{protein of interest}} / \text{Adjusted Intensity}_{\text{housekeeping}}$$

2.6. Transient transfection

Transient cell transfection was performed on both cell lines (HEK293T, iBMDMs, PC3) and primary cells (MDMs) by using different kits and different RNA and DNA constructs. Dharmafect DUO (Horizon Discovery) was used to co-transfect DNA (reporter plasmids) and RNA (miRNA mimics and inhibitors) in HEK293T cells for the dual luciferase reporter assay; Viromer Green and Viromer Blue kits (Cambridge Bioscience) were used to transiently transfect RNA constructs (miRNA mimics, inhibitors, siRNA and target-site blocker) into MDMs, iBMDMs and PC3. Lipofectamine 3000 (Invitrogen) was used to overexpress human TRIB1 into MDMs by using an expression plasmid. For each transfection protocol we followed the manufacturer's instruction (see **Table 2.9.**). All the details about DNA and RNA constructs used in this thesis are specified in Chapter 8 (Appendix I).

Table 2.9. Transient transfection assays

List of the 4 transfection systems used in the present thesis along with details about cell type, experiment format, DNA/RNA concentrations and incubation time; constructs concentrations and incubation time are also specified in the figure legend of each results chapter.

Transfection system	Cell type	Experiment format	DNA	RNA	Incubation time
Dharmafect DUO	HEK293T	96-well plate	Test plasmids 95ng/well Control 5 ng/well	Mimic 50 nM Inhibitor 25 nM	24 hours
Viromer Blue	PC3, LNCAP, iBMDMs	6-well plate 12-well plate	N/A	Mimic 50nM Inhibitor 50nM siRNA 50nM	24-48 hours
Viromer Green	MDMs	6-well plate 12-well plate	N/A	Mimic 50nM Inhibitor 50nM Target Site Blocker 50 nM	24 hours
Lipofectamine 3000	MDMs	6-well plate 12-well plate	human TRIB1 1-2,5 ug/well Control (GFP) 1-2,4 ug/well	N/A	24-48 hours

2.7. Molecular Cloning and Site-Directed Mutagenesis

Molecular cloning was performed to generate gene reporter plasmids. Each cloning experiment was carried out performing the following steps: (1) PCR amplification of sequence to be cloned, (2) PCR-fragment purification from gel, (3) cloning reaction with an entry vector and a destination gateway vector, (4) competent bacteria transformation and antibiotic selection, (5) bacterial colonies harvesting, (6) plasmid mini/midi prep, (7) restriction digestion analysis and (8) Sanger sequencing (**Figure 2.1.**). For Sanger sequencing, we have sent our samples to Source BioScience laboratory (Nottingham, UK) and further analysed the sequences by using the software DNASTAR LaserGene (<https://www.dnastar.com>).

Site-directed mutagenesis was performed to generate miRNA-binding site mutants and SNPs in the TRIB1 3'UTR reporter plasmid. PCR primers for mutagenesis were designed with mutations using the Agilent website (QuickChange Primer Design, <https://www.agilent.com/store/primerDesignProgram.jsp>) and purchased from Sigma-Aldrich; the mutagenesis reaction was prepared using the QuikChange II Site-Directed Mutagenesis Kit (Agilent) following the manufacturer's instruction.

Details about kits, reagents, bacteria and plasmids are specified in Chapter 8 (Appendix I). Protocols used for cloning and mutagenesis are described below.

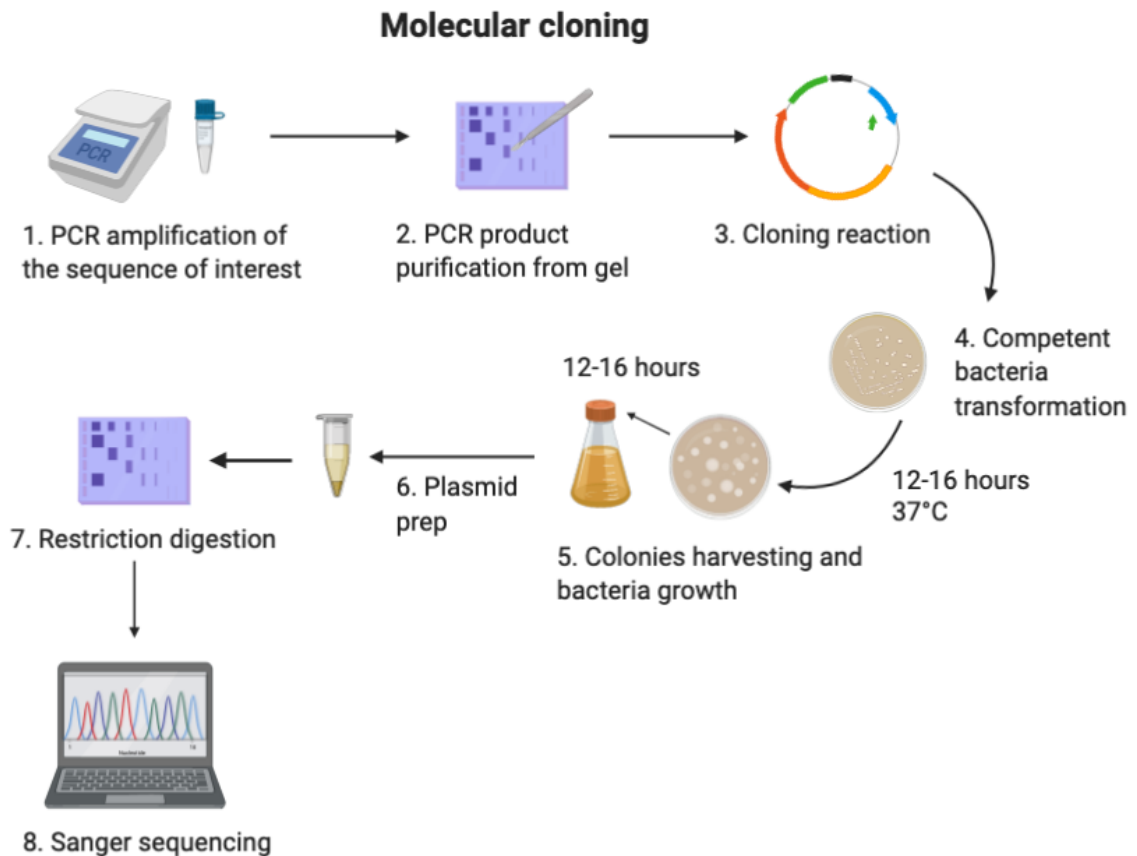


Figure 2.1. Schematic overview of molecular cloning steps

The sequence of interest is first amplified through a standard PCR (1); the PCR product is excised and purified from the gel (2) and then cloned in a specific vector (3). The obtained plasmid is used to transform competent bacteria (4). As soon as the bacteria grow (5), the plasmid is isolated using a commercial kit (6), digested (7) and sequenced (8).

2.7.1. Cloning reaction

Cloning was carried out using the pENTR Directional TOPO cloning kit (Invitrogen) and the Gateway LR Clonase kit (Invitrogen) according to manufacturer's instruction. Directional cloning enables to clone a blunt-end PCR fragment into an entry vector which is subsequently cloned into a gateway system through a set of recombination sequences. We first cloned the 3'UTR of TRIB1 in a TOPO vector; then we used EF1 GWB Renilla Luciferase plasmid as a gateway system to further clone the 3'UTR of TRIB1 downstream to the luciferase gene.

2.7.1.1. pENTR Directional TOPO cloning

The DNA fragment to be cloned was mixed together with a salt solution and a topo vector (4 uL of DNA fragment, 1 uL of salt solution and 1 uL of topo vector) and left at room temperature

for 10 minutes; 50 uL of bacteria (*E. Coli* C2987H) was then mixed with 3 uL of the cloning reaction and incubated on ice for 30 minutes, followed by 90 seconds at 42 °C and 5 minutes on ice again. Up to 1mL of lysogeny broth (LB) was then added and the mixture was incubated at 37 °C for 40 minutes. The tube was centrifuged at 6000 rpm for 5 minutes at room temperature and 100 uL of the mixture was plated on agar plates prepared with antibiotic. Plates were incubated over night at 37 °C. The next days, colonies were picked up with a pipette tip, mixed with super broth (SB) and left to grow at 37 °C in a water bath shaker. Plasmid mini and midi preps were carried out by using GenElute™ Plasmid Midiprep Kit/Miniprep Kit (Sigma Aldrich) following the manufacturer's instructions.

2.7.1.2. Gateway Cloning

The Gateway cloning was used to clone the 3'UTR of TRIB1 (entry clone) downstream of a renilla luciferase gene (destination vector, EF1 GWB Renilla Luciferase). The two plasmids were mixed together with LR clonase enzyme (1 uL plasmid1, 1 uL plasmid2, 0.5 uL LR clonase) and the mixture was incubated for 1 hour at room temperature; 1.5 uL of clonase reaction was then mixed with 50 uL of competent bacteria (*E. Coli* C2987H) and incubated as follows:

- 30' on ice;
- 30'' at 42°C;
- 5' on ice.

Up to 1 mL of SB was added to the mixture, which was incubated for 1 hour at 37 °C. The mixture was then centrifuged (2000xg for 5') and up to 100 uL of mixture was plated on agar plate prepared with antibiotic. Plates were incubated over night at 37 °C. The next day, colonies were harvested with a pipette tip, mixed with super broth (SB) and left to grow at 37 °C in a water bath shaker. Plasmid mini and midi preps were carried out by using GenElute™ Plasmid Midiprep Kit/Miniprep Kit (Sigma Aldrich) following the manufacturer's instructions. Plasmids were digested using restriction enzymes and sequenced (Sanger sequencing).

2.7.2. Site-directed mutagenesis

Being a PCR reaction, site-directed mutagenesis is mediated by oligonucleotide primers that introduce a mutation of interest (deletion, insertion, substitution) in a target sequence. After the mutagenesis reaction, we performed from step 4 to step 8 of the molecular cloning pipelines.

PCR machine settings for mutagenesis

1. Segment 1: 95°C for 2 minutes;
2. Segment 2: 95°C for 20 seconds; 55-60°C for 10 seconds; 68°C for 30 seconds/kb plasmid length; 18-30 cycles;
3. Segment 3: 68°C for 5 minutes;
4. Segment 4: hold at 4°C.

2.8. Dual Luciferase Reporter Assay

The Dual Luciferase Reporter Assay (DLR) is widely used as a quantitative assay to test the negative effect of a specific miRNA on a predicted target gene using a luciferase reporter clone (usually renilla and firefly luciferase enzymes from *Renilla reniformis* and *Photinus pyralis*, respectively). The experimental procedure first requires the cloning of the predicted target sequence (mostly the 3'UTRs) downstream of a luciferase reporter. Next, after transfecting the construct together with the miRNA into a cell line, the reporter activity is measured by adding a substrate. Negative changes in luciferase transcriptional activity will indicate whether or not the specific miRNA binds to its target, regulating its expression and stability which, in turn, affect the upstream gene. A schematic illustration of the DLR assay is shown in **Figure 2.2**. The DLR assay was performed in HEK293T cell line to assess the impact of the 3'UTR of TRIB1 on mRNA stability (reference alleles and genetic variants, see Chapter 5) and also to validate miRNA-target interactions (see Chapter 3, 5 and 6). We used renilla luciferase reporter plasmids (TRIB1 3'UTR and control plasmid without UTRs) and a firefly reporter as internal control. Each condition was performed in triplicate. The kit was purchased from Promega. The preparation of the reagents, the assay procedure and data analysis are described below.

Preparations:

Passive Lysis Buffer (PLB) 5x was diluted in distilled water in a 1:5 ratio to obtain the working concentration 1x and stored at 4°C; Luciferase Assay Reagent II (LAR II, Firefly) was prepared by resuspending the provided lyophilized Luciferase Assay Substrate in 10 mL of the supplied

Luciferase Assay Buffer II and stored at -80°C ; Stop & Glo reagent (Renilla) was prepared by adding 200 μL of 50X Stop & Glo Substrate to the 10 mL Stop & Glo Buffer and stored at -80°C .

Procedure:

After 24 hours of transient transfection performed in a 96-well plate, the media was removed and each well was washed twice in PBS 1x; 35 μL of PLB 1x was then added and cells were lysed by pipetting up and down. Up to 5 μL of cell lysates were transferred into a nunc-384 well plate; 5 μL of the first substrate (LARII, Firefly) were added to each well and the plate was read at 560 nm using a microplate reader (luminometric). After the first reading, 5 μL of the second substrate (Stop & Glo, Renilla) were added and the plate was read at 580 nm. Data generated by the plate reader were exported and analysed in Excel, as described below.

Data analysis:

Data were analysed by calculating the average of firefly and renilla readings (OD, optical density) for each replicate and condition. For the background subtraction, the OD readings generated by untransfected cells were subtracted to each test reading. To correct variations due to cell density, transfection efficiency and pipetting error, Firefly/Renilla ratio was calculated for each condition and the numbers generated were plotted in a column graph.

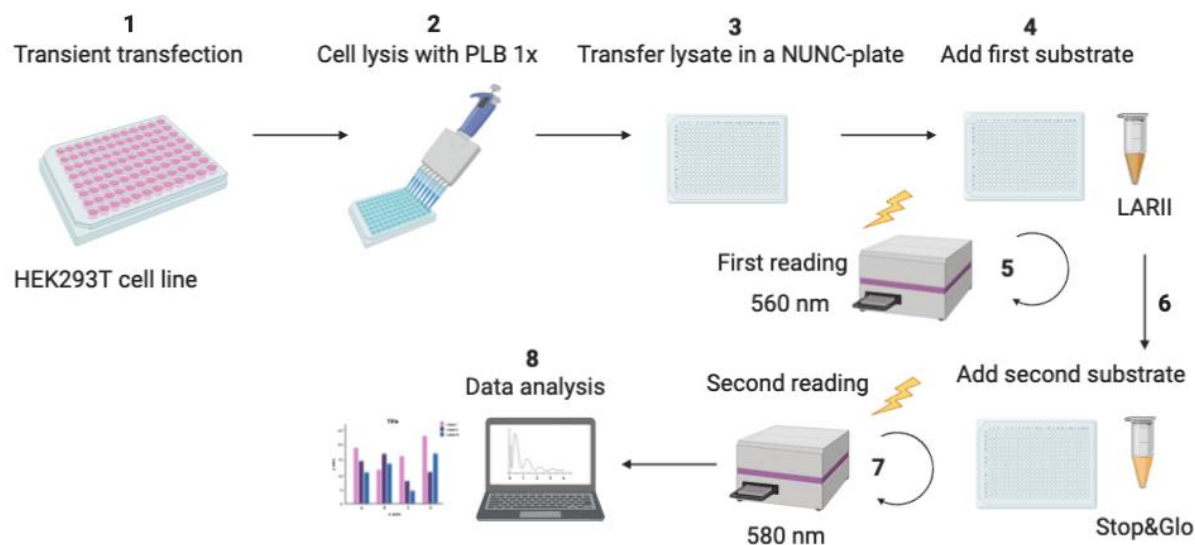


Figure 2.2. Overview of the dual luciferase reporter assay

After 24 hours transient transfection (1), HEK293T cells are lysed in 35 μ L of PLB 1x (2), 5 μ L of the lysate is transferred to a 384-well nunc plate (3). Then, the first substrate LARII (Firefly) is added and the plate is read at 560 nm (4,5); subsequently, the second substrate Stop & Glo (Renilla) is added and the plate is read again at 580 nm (6, 7). Data are exported and analysed in Excel (8).

2.9. Enzyme-linked immunosorbent assay (ELISA)

Enzyme-linked immunosorbent assay (ELISA) was used to assess the secretion of the pro-inflammatory interleukin-8 (IL-8) from polarised and treated human MDMs. This assay is widely used for the detection of secreted/extracellular proteins and it relies on the “sandwich” principle: detect and quantify antigens between two antibodies. In fact, ELISA assay involves the use of two antibodies: the capture antibody, which is immobilised to a solid support (usually a plastic 96-well plate) and the detection antibody, which is conjugated with an enzyme, able to generate a signal (light, colour, fluorescence) when its substrate is added. ELISA kits were purchased from R&D Systems company and the assay was performed according to manufacturer’s instruction. Each condition was performed in triplicate. The preparation of the plate, the assay procedure and data analysis are described below.

Plate Preparation: the Capture Antibody was diluted to the working concentration in PBS and added to a 96-well plate (100 μ L/well). The plate was then sealed and incubated at room

temperature overnight. The following day, the plate was washed three times with 300 uL of Wash Buffer (PBS 0.05% Tween) using an automated microplate washer. The plate was blocked with 300 uL of Reagent Diluent (PBS 1% BSA) for at least 1 hour at room temperature. After blocking, the plate was washed again three times with 300 uL of Wash Buffer.

Assay Procedure: all ELISA steps were performed at room temperature. Up to 100 uL of samples and standards diluted in Reagent Diluent were added to the plate, which was covered and incubated for 2 hours; the plate was washed and the Detection Antibody, diluted at its working concentration in Reagent Diluent, was added to each well for 2 hours; then 100 uL of the working dilution of Streptavidin-HRP was added to each well for 20 minutes. From this step on the plate was protected from direct light. The wash step was repeated and 100 uL of Substrate Solution (1:1) were added for 20 minutes. Without washing the plate, 50 uL of Stop Solution (2N Sulfuric Acid) were added to each well and the plate was read using a microplate reader set to 450 nm.

Data analysis: the data were exported and analysed in Excel. The average of OD readings (triplicate) for each condition (both standards and samples) was calculated; the OD values were then copied and pasted into a XY table in GraphPad Prism 8.0 and the concentration of the target protein was calculated by interpolating the test samples from the standard curve, with 95% confidence intervals.

2.10. Viability Assay (MTT)

Viability assay was carried out on MDMs transfected with miRNA mimics by using the commercial kit RealTime-Glo™ MT Cell Viability Assay (Promega) following the manufacturer's instructions. The kit measures reduction potential and enables an estimation of cell viability in a non-lytic context. NanoLuc Luciferase and MT Cell Viability Substrate are added to cell culture media. The MT Cell Viability Substrate enters the cells where it is reduced to form a NanoLuc Substrate, which exits the cell and is used by NanoLuc Luciferase in the media, realising luminescence. Only metabolically live cells can reduce the substrate and the luminescence is proportional to the number of live cells in culture.

2.11. Immunofluorescence

Immunofluorescence was carried out to determine TRIB1 protein expression in polarised MDMs. Cells were plated in 8 well chamber slides (100,000 cells per well); after 24 hours *in vitro* polarisation, cells were washed with PBS twice and fixed using 200 uL of 4% (w/v) PFA-PBS for 30-40 minutes. Cells were then washed with PBS twice and permeabilised using 200 uL of 0.1% (v/v) Triton-PBS for 15 minutes. After permeabilization, cells were washed again with PBS and then blocked with 2% (w/v) BSA-PBS for 1 hour. Primary antibody was then added in 200 uL of 1 % BSA-PBS and the chamber slide was incubated overnight at 4 °C. The following day, cells were washed with PBS and the secondary antibody was added in 200 uL of 1 % BSA-PBS and left it for 1 hour at room temperature. After washing in PBS, DAPI Solution (Thermo-Fisher Scientific) was added for 10 minutes at room temperature (1:1000 dilution in PBS). Cells were washed with PBS and the chambers were covered using coverslips and a mounting solution. Cells were left in the dark for at least 1 hour before imaging. The antibodies used for immunofluorescence are listed in Chapter 8 (Appendix I), along with their working dilution.

2.12. Microscope Imaging and analysis

Immunofluorescence experiments were analysed using the automated inverted microscope Leica AF6000LX, acquiring images using LAS-X software (Leica) and phase-contrast, blue, red and green filters. 3 or more images of each condition and isotype control per each donor were taken, saved in TIF and analysed with Fiji/ImageJ. The analysis was done by calculating the integrated density of regions of interest.

2.13. Cholesterol Efflux Assay

Cholesterol efflux assay was carried out in MDMs transfected with miRNA mimic and inhibitor. The assay was previously optimised in my lab by Dr Jessica Johnston. Cells were transfected with 50 nM of miRNA mimic/inhibitor for 24 hours and then treated with 2.5 μ M of TopFluor Cholesterol (23-(dipyromtheneboron difluoride)-24-norcholesterol (Avanti Polar Lipids) for 24 hours in RPMI 0.2% BSA fatty-acid free (Sigma-Aldrich) for other 24 hours. Media was changed RPMI 0.2% BSA fatty-acid free for 18 hours (equilibration step). After that, a cholesterol acceptor was added: 50 μ g/mL of HDL (Biorad) for 4 hours. At end of incubation, the media was collected and cells were lysed using a solution of 1% Cholic Acid in 100% Ethanol (Sigma-Aldrich). Both cells lysates and supernatants were added to a nunc 96 well plate (black) in triplicates and fluorescence was read using a microplate reader (excitation 490nm, emission 520nm). Data were analysed as follows in Excel (*Low et al., 2012*):

$$\% \text{ cholesterol efflux} = \text{SN} / (\text{lysate} * \text{dilution factor}) + \text{SN} * 100$$

$$\text{Final \% efflux} = \% \text{ cholesterol efflux} - \% \text{ blank efflux (no acceptor)}$$

where SN is the supernatant.

2.14. Flow cytometry

Flow cytometry was carried out to assess CD14⁺ monocyte purity and transfection efficiency, by using BD LSR II machine (BD Bioscience). In the flow cytometry experiment we used TO-PRO-1 Iodide (515/531) staining for live/dead cells (1:10000) (Invitrogen). Flow cytometry results are shown in Chapter 8 (Appendix II).

2.15. Statistics

All experiments were performed at least three times and data are presented as means \pm SEM. Graphs and statistical analysis were generated in GraphPad Prism 8.00 (GraphPad, San Diego, CA, USA). Statistical methods are specified in each figure legend. P-values < 0.05 were considered to be statistically significant. Each statistical test was performed as parametric and two-tailed.

Chapter 3. miR-101-3p negatively regulates Tribbles-1 in primary human macrophages

Declaration

This part of the work is intended to be published along with additional data not shown here (manuscript in preparation). The experiments and the bioinformatics analysis described in this chapter have been entirely performed by myself. The only exception is **Figure 3.15.**: the KEGG enrichment pathway analysis by using GOSeq was generated by my colleague Sumeet Deshmukh.

Abstract

Tribbles-1 (TRIB1) is an evolutionarily conserved pseudo-kinase protein that in mammals control a wide range of interacting signalling pathways. In myeloid cells, TRIB1 controls macrophage polarisation and dysregulated myeloid Trib1 expression has been shown to alter adipose homeostasis and atherosclerosis burden. However, mechanisms that regulate TRIB1 expression remain elusive. Taking advantages of *in-silico* predictions, we showed that the 3'untranslated region (3'UTR) of TRIB1 is enriched in microRNA-binding sites and when cloned downstream of a luciferase reporter gene, leads to a significant reduction of the reporter activity. Macrophage-specific knock-down of DICER1 and AGO2, key enzymes involved in miRNAs biogenesis and activity, causes an increase of TRIB1 RNA and protein, suggesting a role for microRNAs in its post-transcriptional regulation. We demonstrated that miR-101-3p, miR-132-3p and miR-214-5p are able to negatively modulate TRIB1 expression in macrophages and have validated the direct interaction of miR-101-3p and TRIB1 by employing site-directed mutagenesis. Through regulation of TRIB1, miR-101-3p induced an M1-like macrophage polarisation, altering the levels of pro-inflammatory markers. Our results suggest that the TRIB1-miR-101-3p interaction is biologically relevant in the context of human macrophage polarisation *in vitro* and should be further investigated *in vivo*, in the context of those diseases, in which the activation of macrophages towards different phenotypes plays a determinant role.

3.1. Introduction

Tribbles-1 (TRIB1) pseudo-kinase regulates cell function in a range of contexts, via regulating MAP kinase activation (*Kiss-Toth et al., 2004*) and mediating protein degradation via the COP1 ubiquitin ligase (*Yoshida et al., 2013*). Its expression is detectable in all tissues, but it is highly enhanced in the bone marrow and in the thyroid gland (The Human Protein Atlas, <https://www.proteinatlas.org>). In fact, TRIB1 has been shown to play a pivotal role in the differentiation of anti-inflammatory M2-macrophages, in the pathogenesis of early atherosclerosis and during adipose tissue inflammation (*Ostertag et al., 2010, Satoh et al., 2013, Johnston et al., 2019*). In murine bone-marrow derived macrophages, Trib1 deficiency has been reported to alter polarisation markers, impairing the transcription of both pro-inflammatory and anti-inflammatory genes (*Arndt et al., 2018*). Besides, TRIB1 is also an established oncogene in acute myeloid leukemia, a cancer that arise from monocytes (*Röthlisberger et al., 2007, Yoshida et al., 2013*).

At the gene level, TRIB1 is highly unstable, showing a mRNA half-life shorter than 1 hour (*Sharova et al., 2009*). Its expression is also highly variable among different cell types and tissues, suggesting it might be subject to cell type-dependent post-transcriptional regulation (*Sung et al., 2006*). The 3' untranslated region (3'UTR) of TRIB1 mRNA represents more than 50% of the whole sequence, it is highly conserved among different animal species and it is enriched in regulatory binding sites. Recently, Soubeyrand and colleagues have showed that blocking transcription through actinomycin-D dramatically reduced TRIB1 mRNA levels in different *in vitro* models (*Soubeyrand et al., 2016*). However, the regulation of human TRIB1 at the post-transcriptional level has not been investigated.

One of the main gene regulatory mechanisms described in eukaryotes is mediated by microRNAs (miRNAs) in a process called RNA Interference (RNAi). miRNAs are small non-coding RNAs that bind to the 3'UTR of target, complementary mRNAs and via association with effector proteins form the RNA-induced silencing complex (RISC). This ultimately leads to RNA degradation and inhibition of protein translation (*Bartel et al., 2004*). The role of miRNAs in macrophage development and function has been extensively studied (*Roy et al., 2016, Curtale et al., 2019*).

In the current work, we investigated for the first time the post-transcriptional regulation of TRIB1 by miRNAs. To date, only a few studies identified miRNAs regulating TRIB1 in the context of prostate and liver cancer (*Lin et al., 2014, Ye et al., 2017*). Considering its predominant role in myeloid cells we focussed on human macrophage function and

polarisation. In fact, the role of TRIB1 in human macrophages has not been extensively investigated and the majority of published studies are related to mice models and murine cell lines.

3.2. Hypothesis and aims

We hypothesised that TRIB1 is subject to post-transcriptional regulation by miRNAs in human macrophages. The aims of this study were (1) to investigate the expression and the function of TRIB1 in human macrophages; (2) to identify and validate macrophage-specific miRNAs potentially targeting TRIB1; (3) to test the impact of candidate miRNAs on macrophage biology.

3.3. Results

3.3.1. Endogenous TRIB1 expression in human polarised macrophages

TRIB1 expression has been reported to be highly variable among different cell types, both at the mRNA and protein levels and it appears to be regulated in response to inflammatory stimuli (Sung *et al.*, 2006, Soubeyrand *et al.*, 2016). By using GTEx Portal database (<https://gtexportal.org/home/>), we checked TRIB1 mRNA expression among 54 different human tissues; the top 5 tissues in which TRIB1 is expressed the most are thyroid (median Transcript Per Million, TPM 155), lung (median TPM 50.96), whole blood (median TPM 38.28), visceral adipose tissue (median TPM 37) and liver (median TPM 34.61) (**Figure 3.1.**). As TRIB1 is critical in the myeloid system (Yokoyama *et al.*, 2010, Satoh *et al.*, 2013), we measured its mRNA expression in human primary unpolarised (also referred as M0 and M^{un} macrophages) macrophages (MDMs), isolated from 18 different individuals of mixed age and gender, by using RT-qPCR. Prior to the RNA isolation, we polarised the cells towards M1, M2a and M2c phenotypes for 24 hours, as described in Chapter 2. The result is shown in **Figure 3.2.**: TRIB1 mRNA expression is highly variable among different individuals. However, it is significantly increased in M1^{LPS+INF- γ} and M2a^{IL-4} conditions, compared to M^{un} (2.6-fold change, p=0.02; 2.6-fold change, p=0.0002). *TRIB1* expression seems to increase also in response to IL-10 (M2c^{IL-10}) but the change is not statistically significant (1.4-fold change, p=0.3). We also investigated TRIB1 protein expression by using immunofluorescence. We first observed a nuclear localisation of TRIB1 in human macrophages, which was consistent with what have been reported before (Kiss-Toth *et al.*, 2006, Yokoyama *et al.*, 2010, Guan *et al.*, 2016). As expected, we observed variability among different donors (**Figure 3.3. B-F**) and we did not find any statistically significant changes in the expression of TRIB1 protein (**Figure 3.3. A**). This was potentially due to the low n number (n=5). Representative immunofluorescence pictures are shown in **Figure 3.4.**, while the isotype control staining for each condition is shown in Chapter 8 (Appendix II). TRIB1 is expressed in human macrophages differentiated from blood monocytes and it increases in response to both anti-inflammatory and pro-inflammatory polarising stimuli.

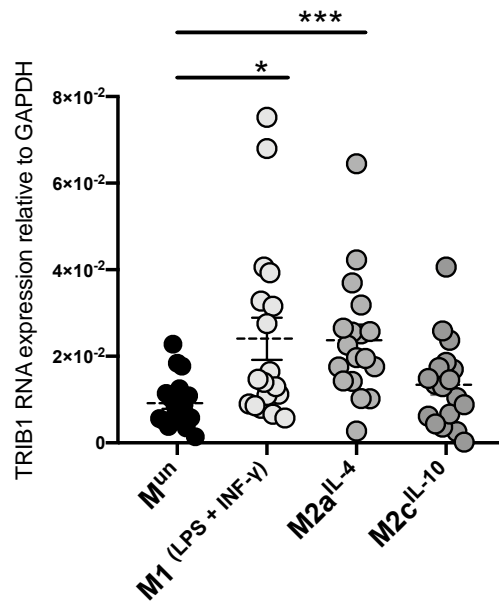


Figure 3.2. Assessment of TRIB1 RNA expression in polarised human macrophages by RT-qPCR

Relative TRIB1 RNA expression normalised to the housekeeping GAPDH, after 24 hours polarisation. Cells were treated with LPs and $INF-\gamma$ (M1), IL-4 (M2a) and IL-10 (M2c); M^{un} refers to untreated/unpolarised macrophages, used as a control. Data are presented as mean \pm SEM (One-way ANOVA with Dunnett's post-test, $n = 18$, *** $p < 0.001$, * $p < 0.05$, $p \geq 0.05$).

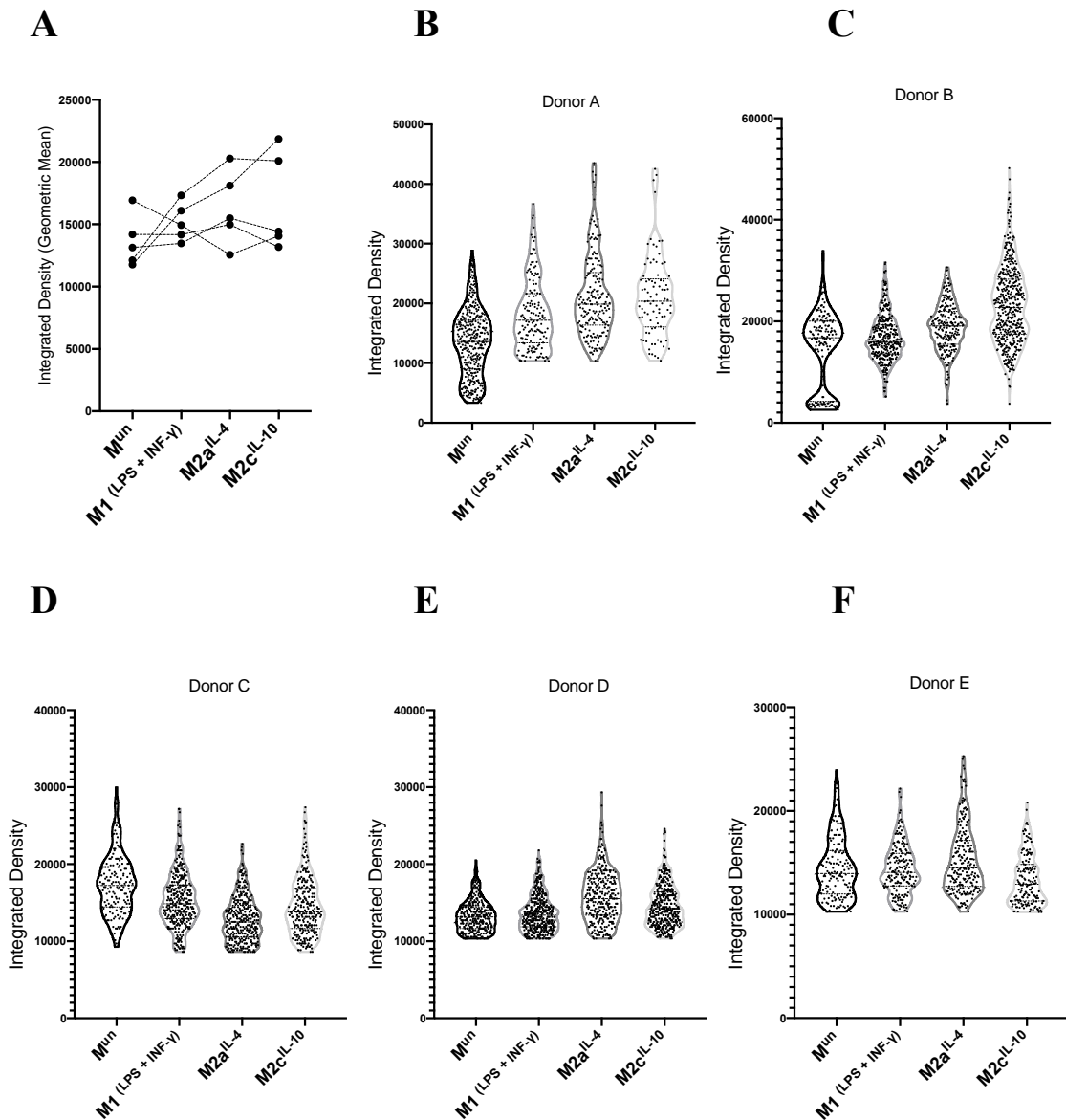


Figure 3.3. Assessment of TRIB1 protein expression in polarised human macrophages by immunofluorescence

Geometric Mean of integrated density of TRIB1-positive cells measured in Fiji/Image J in polarised human macrophages isolated from 5 different individuals; data are presented as mean \pm SEM (n = 5, One-way ANOVA with Dunnett's post-test, ns $p \geq 0.05$) (A). Integrated density of TRIB1-positive cells for each donor (B-F); each graph represents an n=1, so no statistical analysis was performed.

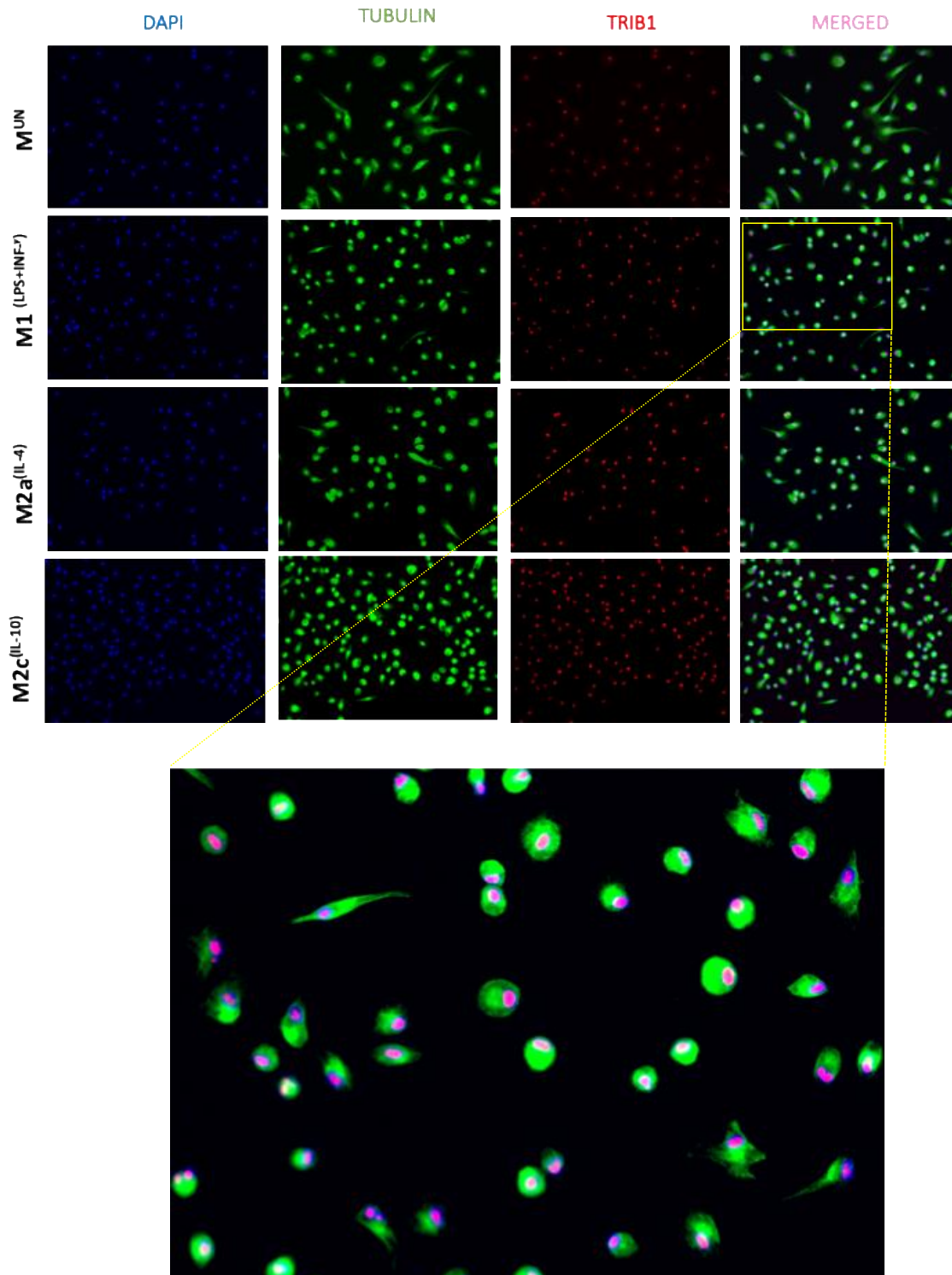


Figure 3.4. Representative immunofluorescence images

Representative immunofluorescence images for Donor B showing polarised MDMs stained for dapi (blue) tubulin (green), TRIB1 (red); merged channels are also shown in the last panel. Images were acquired using a 20x objective magnification. Integrated density analysis was performed in Fiji/ImageJ.

3.3.2. TRIB1 overexpression in human macrophages

Our lab previously investigated the role of Trib1 manipulation in tissue-resident macrophages with focus on metabolic tissues (liver and adipose). By using Trib1 knockout and transgenic mice, we observed that Trib1 does not alter macrophage number but changes their phenotype. Specifically, Trib1^{KO} mice exhibit more pro-inflammatory cells, compared to Trib1^{WT}; conversely, macrophages from Trib1^{Tg} mice show an anti-inflammatory phenotype (data not shown, manuscript in preparation). A recent study performed on murine bone-marrow derived macrophages (BMDMs) has also shown that Trib1 alters macrophage phagocytosis, migration and polarisation (Arndt *et al.*, 2018). However, no data is available about the role of TRIB1 in human primary macrophages. Therefore, we carried out a TRIB1 plasmid overexpression in unpolarised MDMs and checked the gene expression of macrophage markers and pro-inflammatory cytokines. First, we confirmed the overexpression of TRIB1 RNA by using RT-qPCR (**Figure 3.5.**), which is highly variable, probably due to different transfection efficiency as well as different endogenous levels of TRIB1 transcript in different individuals. We found that when TRIB1 is upregulated, there is a significant increase in anti-inflammatory macrophage markers (MSR-1, CD163 and IL-4) at the RNA level (**Figure 3.6. A-C**) and a decrease in the pro-inflammatory IL-6 and IL-8 RNA expression (**Figure 3.6. D-E**). We also measured IL-8 protein secretion by performing ELISA on supernatants and found that it is significantly decreased and this was consistent with the RNA data (**Figure 3.6. F**). This was in line with what was reported by Arndt and colleagues who showed that BMDMs from Trib1 deficient mice are pro-inflammatory (Arndt *et al.*, 2018).

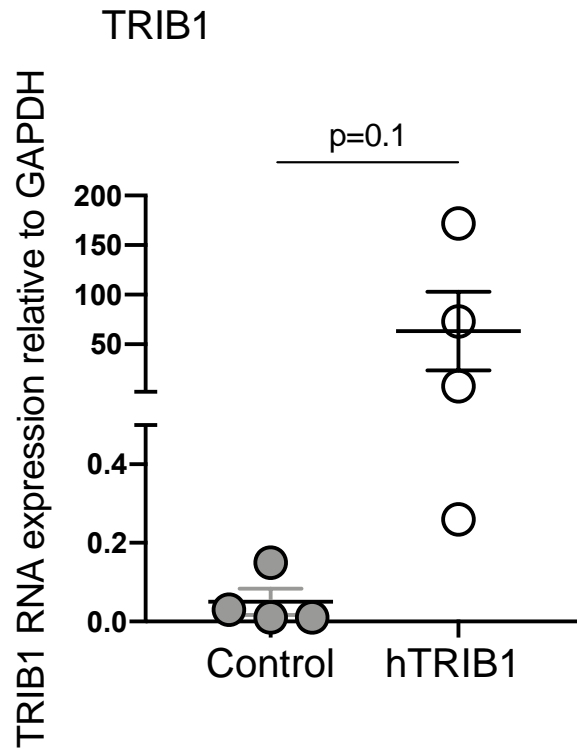


Figure 3.5. Assessment of TRIB1 overexpression in MDMs by RT-qPCR

Relative TRIB1 RNA expression normalised to the housekeeping GAPDH in MDMs transfected with a control plasmid (GFP) and a TRIB1 overexpression plasmid (24 hours transfection); total DNA transfected was 2500ng/well in a 6 well plate. Data are presented as mean \pm SEM (n = 4, paired t-test, ns $p \geq 0.05$).

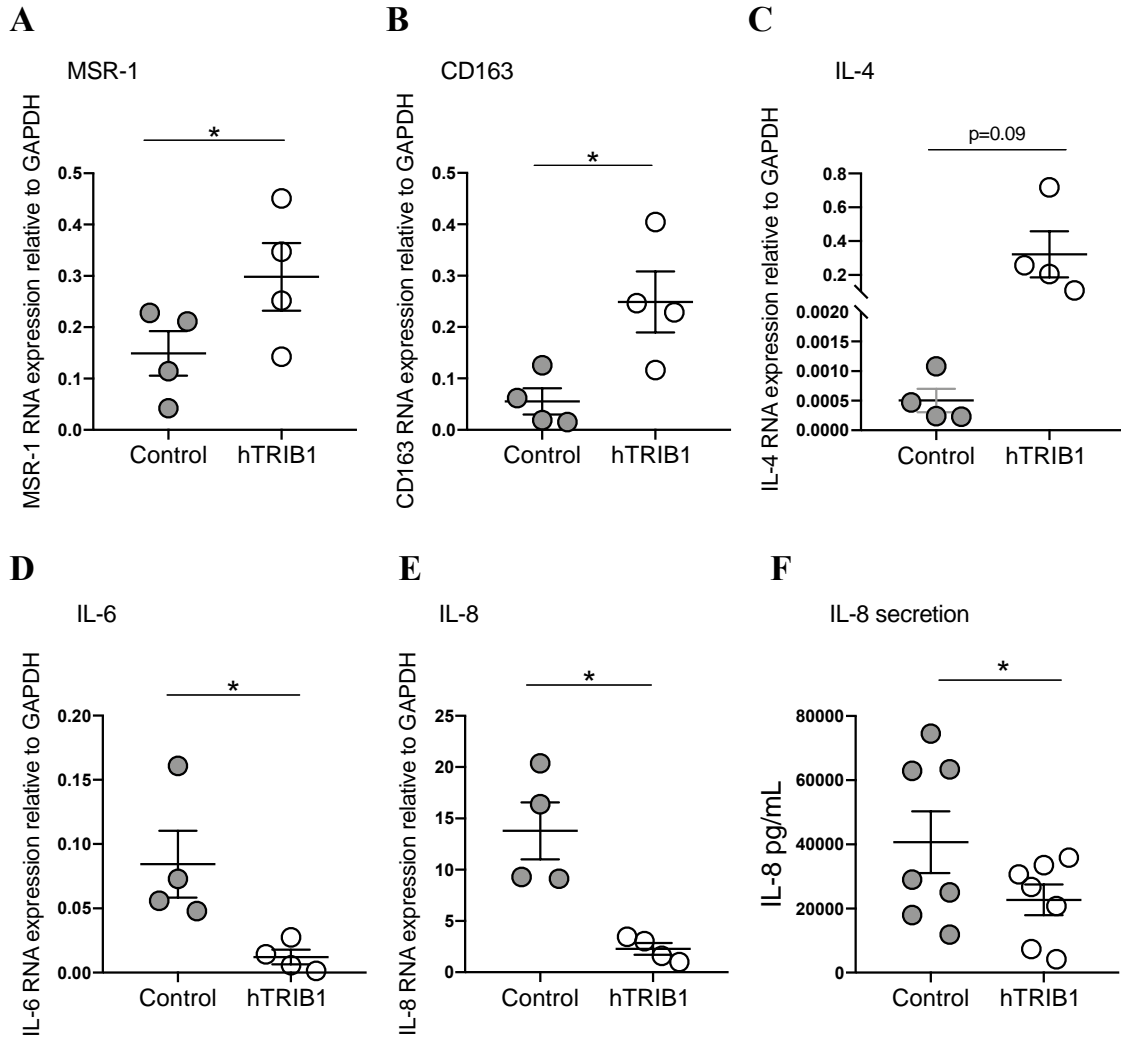


Figure 3.6. Impact of TRIB1 overexpression on MDMs phenotype

Relative RNA expression of MSR-1 (A), CD163 (B), IL-4 (C), IL-6 (D) and IL-8 (E) normalised to the housekeeping GAPDH in MDMs transfected with a plasmid control (GFP) and TRIB1 overexpression plasmid (24 hours transfection); total DNA transfected was 2500ng/well in a 6 well plate. IL-8 protein levels measured by using ELISA in supernatants collected after 24 hours MDMs transfection (F) (n =4-7, paired t-test, * p<0.05, ns p≥0.05).

3.3.3. Post-transcriptional regulation of TRIB1: impact of the 3'UTR

It has been reported that TRIB1 exhibits an mRNA half-life shorter than 1 hour (*Sharova et al., 2009*) and it is likely to be post-transcriptionally regulated by either proteasomal or non-proteasomal mechanisms (*Soubeyrand et al., 2016*). Therefore, we investigated the role of the 3'UTR in the post-transcriptional regulation of TRIB1. We cloned the full-length sequence of the 3'UTR of TRIB1 downstream of a renilla luciferase gene and evaluated the impact of this region on the enzyme activity, by using a dual luciferase reporter assay. We observed a robust reduction of the enzymatic activity (> 40% reduction, $p < 0.0001$), suggesting that this region contributes to the post-transcriptional regulation of TRIB1 (**Figure 3.7.**). In fact, the 3'UTR of coding genes is the main target of miRNAs (*Bartel et al., 2009*). To investigate whether TRIB1 might be regulated by miRNAs, we performed a transient knock-down of DICER1 and AGO2, both key regulators of miRNA biogenesis and function (*O'Brien et al., 2018*) and checked TRIB1 mRNA and protein levels. **Figure 3.8.** shows the confirmation of efficient DICER1 and AGO2 enzyme knock-down in MDMs by RT-qPCR (DICER1 70% knock-down, $p = 0.001$; AGO2 80% knock-down, $p = 0.02$). In both conditions, TRIB1 mRNA levels tended to increase but with high variability and not in all the individuals and the change was not statistically significant (siDICER1, 1.3-fold-change, $p = 0.069$; siAGO2 1.6-fold-change, $p = 0.36$) (**Figure 3.9.**). Similarly, TRIB1 protein in siDICER1 samples tended to increase but the change was not statistically significant (1.6-fold-change, $p = 0.23$) (**Figure 3.10.**). In fact, by genetically impairing the biogenesis and the activity of miRNAs we are likely perturbing multiple genes, that can indirectly have an effect on TRIB1.

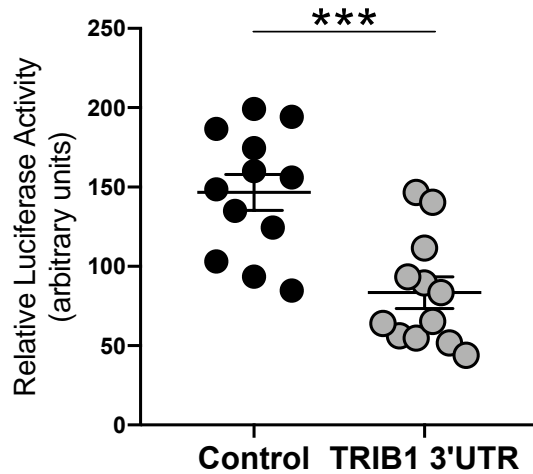


Figure 3.7. Impact of the 3'UTR of TRIB1 on gene reporter activity

Relative luciferase activity measured in HEK293T cell line after 24 hours co-transfection of a renilla luciferase reporter (control plasmid, no UTR) and a TRIB1 3'UTR reporter with a firefly luciferase control (required for normalisation). Total DNA transfected 100 ng/well (96-well plate). Data are presented as mean \pm SEM (unpaired t-test, $n = 12$, *** $p < 0.001$).

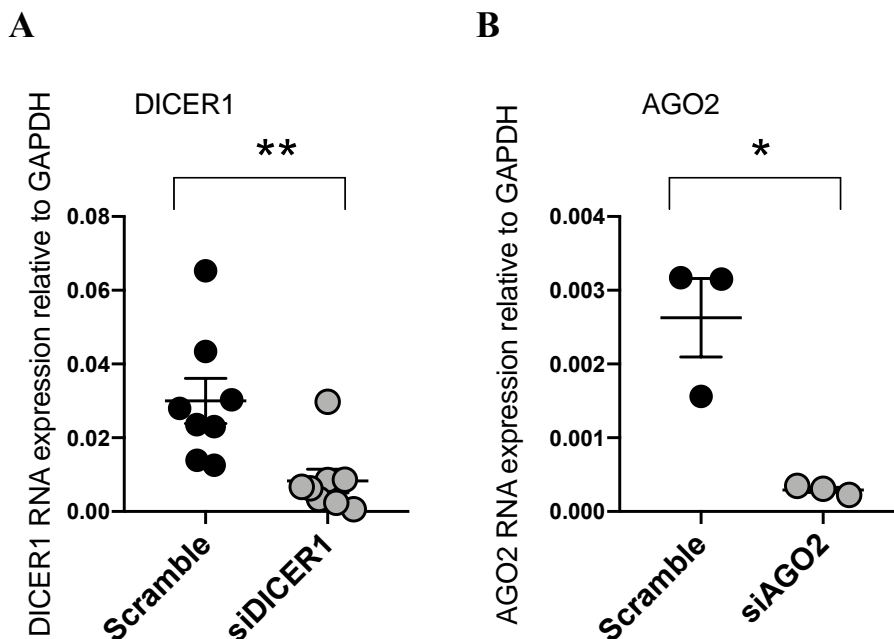


Figure 3.8. Confirmation of DICER1 and AGO2 knock-down by RT-qPCR

Relative RNA expression of DICER1 and AGO2 normalised to the housekeeping GAPDH in MDMs transfected with DICER1 siRNA (A) and AGO2 siRNA (B) (48 hours transfection); total RNA transfected was 50nM in a 6 well plate. Data are presented as mean \pm SEM ($n=3-8$, paired t-test, *** $p < 0.001$, * $p < 0.05$).

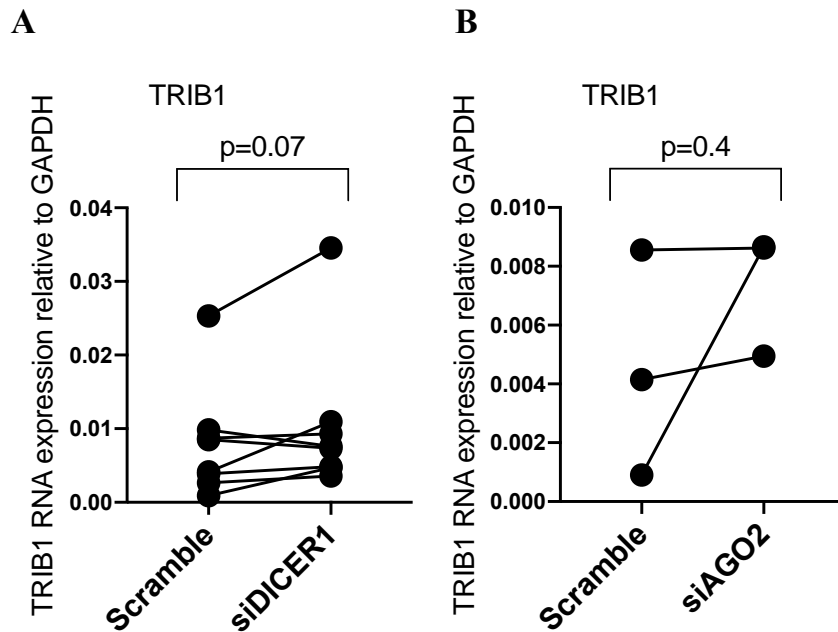


Figure 3.9. Effect of DICER1 and AGO2 knock-down on TRIB1 mRNA expression

Relative RNA expression of TRIB1 normalised to the housekeeping GAPDH in MDMs transfected with DICER1 siRNA (**A**) and AGO2 siRNA (**B**) (48 hours transfection); total RNA transfected was 50nM in a 6 well plate. Data are presented as individual points (n=3-8, paired t-test, ns $p \geq 0.05$).

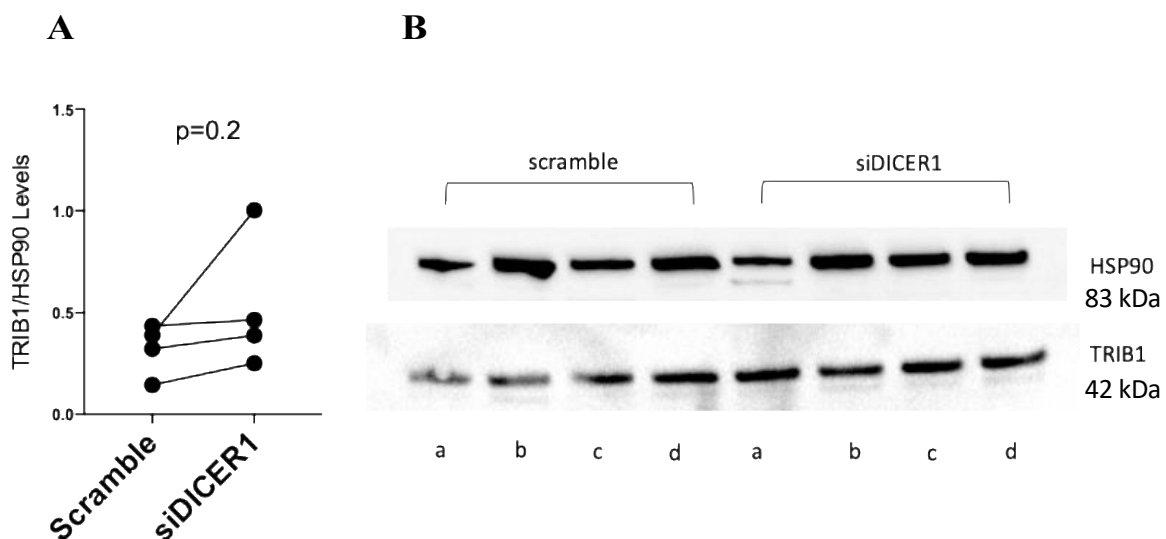


Figure 3.10. Effect of DICER1 knock-down on TRIB1 protein expression

Relative TRIB1 protein expression normalised to the housekeeping HSP90 in MDMs transfected with DICER1 siRNA/scramble (**A**) (48 hours transfection); total RNA transfected was 50nM in a 6 well plate; western blot representative picture (**B**); letters (a, b, c, d) refer to 4 different individuals. Data are presented as individual points (n=4, paired t-test, ns $p \geq 0.05$).

3.3.4. Identification of miRNAs potentially targeting TRIB1

Our previous findings suggest that TRIB1 might be subject to post-transcriptional regulation by miRNAs, so our next aim was to *in silico* identify potential regulators of the pseudo-kinase. We performed a comprehensive miRNA-target prediction analysis taking advantage of multiple web-based tools and algorithms, as described in Chapter 2. **Table 3.1.** lists the predicted number of miRNAs targeting the 3'UTR of TRIB1, according to 7 different prediction tools. We identified a total of 1237 miRNAs predicted to target TRIB1: the list was further narrowed down by selecting high-confidence miRNAs and those predicted by at least 3 databases. Next, we selected miR-101-3p, miR-132-3p and miR-214-5p for experimental validation, according to the following criteria:

- miR-101-3p is known to regulate macrophage function (*Wei et al., 2015, Zhang et al., 2015, Huang et al., 2020*); it is a high-confidence annotated miRNA and the predicted interaction, detected in ≥ 3 databases, is well conserved among different species;
- miR-132-3p is also established to regulate inflammatory responses in different contexts (*Shaked et al., 2009, Liu et al., 2014, Leinders et al., 2016*) and it is a high confidence miRNA, detected in ≥ 3 databases; however, the 2 binding sites on the 3'UTR of TRIB1 are poorly conserved among different species;
- miR-214-5p is not listed among the high-confidence miRNAs, but it has been previously associated with inflammation (*Iizuka et al., 2012, Yang et al., 2019*); the 2 predicted binding sites are poorly conserved, but the interaction was predicted by ≥ 3 databases.

Moreover, we also considered that all the predicted interactions are characterised by a canonical seed region (7mers). The characteristics of miR-101-3p, miR-132-3p and miR-214-5p are summarised in **Table 3.2.**; binding site position, seed region types and phylogenetic conservation were taken from TargetScan, while high confidence miRNAs were taken from miRbase. Next, we checked the expression of these miRNAs in polarised MDMs, by using a small non-coding RNA-seq, performed on M0 and M1 macrophages (sequencing experiment is explained in Chapter 4). **Figure 3.11.** shows the counts per million values (CPM) of the candidate miRNAs in M0 and M1 macrophages. None of the miRNAs was differentially

expressed between the two groups. However, considering that the highest CPM value among the small RNA sequenced was 17 and the lowest was -2, we can conclude that miR-101-3p and miR-132-3p were abundant in both M0 and M1 macrophages (miR-101-3p average CPM M0=7, average CPM M1=7.3; miR-132-3p average CPM M0=7.6 average CPM M1=7.8), whilst miR-214-5p was the least expressed (average CPM M0= -0.4, average CPM M1= -0.8). To investigate whether these miRNAs are able to modulate TRIB1 expression, we transiently transfected miRNA mimics in unpolarised MDMs and iBMDMs and performed RT-qPCR on both human and murine TRIB1. We first evaluated that the overexpression of miRNAs by transfection of mimics in MDMs was successful (**Figure 3.12.**) and then we determined the downstream effect on TRIB1 RNA. MiR-101-3p, miR-132-3p and miR-214-5p significantly impaired TRIB1 expression in human macrophages, causing a ~40% reduction (**Figure 3.13. A-C**); similarly, in murine macrophages, Trib1 expression was negatively modulated by the mimics (~30% decrease). However, the change induced by miR-214-5p was not statistically significant (p=0.1) (**Figure 3.14.**). This may be due to the high variability of the negative control in transfected iBMDMs. Lastly, we performed a pathway enrichment analysis of all predicted target genes of candidate miRNAs by using Reactome (<https://reactome.org/>) (p-value cut off 0.05). The list of target genes of each miRNA was downloaded from TargetScan. **Table 3.3.** lists the top 10 significant pathways for miRNAs target genes. The majority of miR-101-3p target genes appear to be involved in chromatin organization and oestrogen-mediated signalling pathways; miR-132-3p target genes seem to be transcription factors, regulating AKT and PTEN signalling pathways, while genes targeted by miR-214-5p are involved in development and axon guidance. We then filtered the list of target genes, selecting only those differentially expressed by human polarised macrophages (M0 vs M1), by using an RNA-seq dataset, previously generated in our lab (DOI: 10.17632/j2hmt7k9fh.1). We performed a KEGG pathway enrichment analysis using GOSep R package (cut off p value 0.05). **Figure 3.15.** shows the results for miR-101-3p and miR-132-3p; unfortunately, miR-214-5p did not show any significant enrichment. Interestingly, among the most significant enriched pathways for miR-101-3p we observed MAPK signalling pathway, which is a master regulator of inflammation, and chemokine signalling pathway, while for miR-132-3p was either WNT-signalling pathway or actin regulation. We then decided to go on with the full validation of miR-101-3p/TRIB1 interaction, as it appears more biologically relevant in macrophages.

Table 3.1. miRNA-TRIB1 target prediction analysis

The table lists the number of miRNAs predicted to target the 3'UTR of TRIB1 according to 7 different prediction tools; the total number of predicted miRNAs is the result of each tools, without duplicates.

Prediction tool	Target	Number of predicted miRNAs	Total number of predicted miRNAs
miRanda	TRIB1 3'UTR	681	1237
TargetScan	TRIB1 3'UTR	673	
StarBase	TRIB1 3'UTR	194	
miRWalk	TRIB1 3'UTR	406	
MicroT-CDS	TRIB1 3'UTR	140	
TaRbase	TRIB1 3'UTR	147	
miRDB	TRIB1 3'UTR	149	

Table 3.2. Characteristics of candidate miRNAs

The table summarises the characteristics of miR-101-3p, miR-132-3p and miR-214 binding sites on TRIB1. Target sites positions, seed region type and phylogenetic conservation were taken from TargetScan; high-confidence miRNAs were taken from miRbase.

Candidate miRNA	High confidence	Target sites position and seed region type	Phylogenetic conservation	Number of prediction tools	Relevant publications
miR-101-3p	Yes	Position 1526-1532, 7mer m8	++++	7	Wei et al., 2015, Zhang et al., 2015, Huang et al., 2020
		Position 1424-1430, 7mer A1	+	2	
miR-132-3p	Yes	Position 554-560, 7mer m8	+	3	Shaked et al., 2009, Liu et al., 2014, Leinders et al., 2016
		Position 1763-1769, 7mer m8	+	6	
miR-214-5p	No	Position 61-67, 7mer m8	++	5	Iizuka et al., 2012
		Position 1451-1457, 7mer A1	++	2	

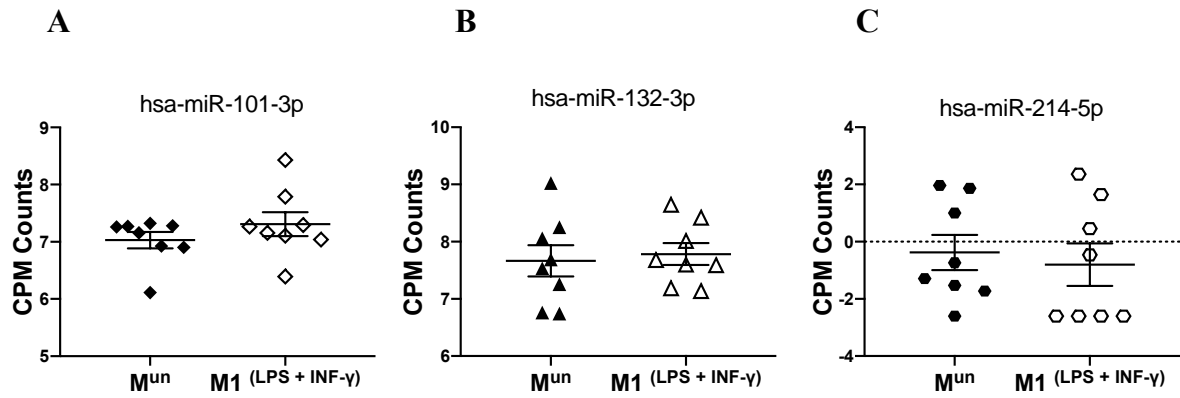


Figure 3.11. Endogenous expression of candidate miRNAs in human polarised MDMs: small RNA-seq

miR-101-3p (A), miR-132-3p (B) and miR-214-5p (C) abundance in M0 and M1 macrophages, expressed as counts per million values ($\log_2 \text{CPM} + 1$), from small RNA sequencing analysis. No statistical analysis was performed.

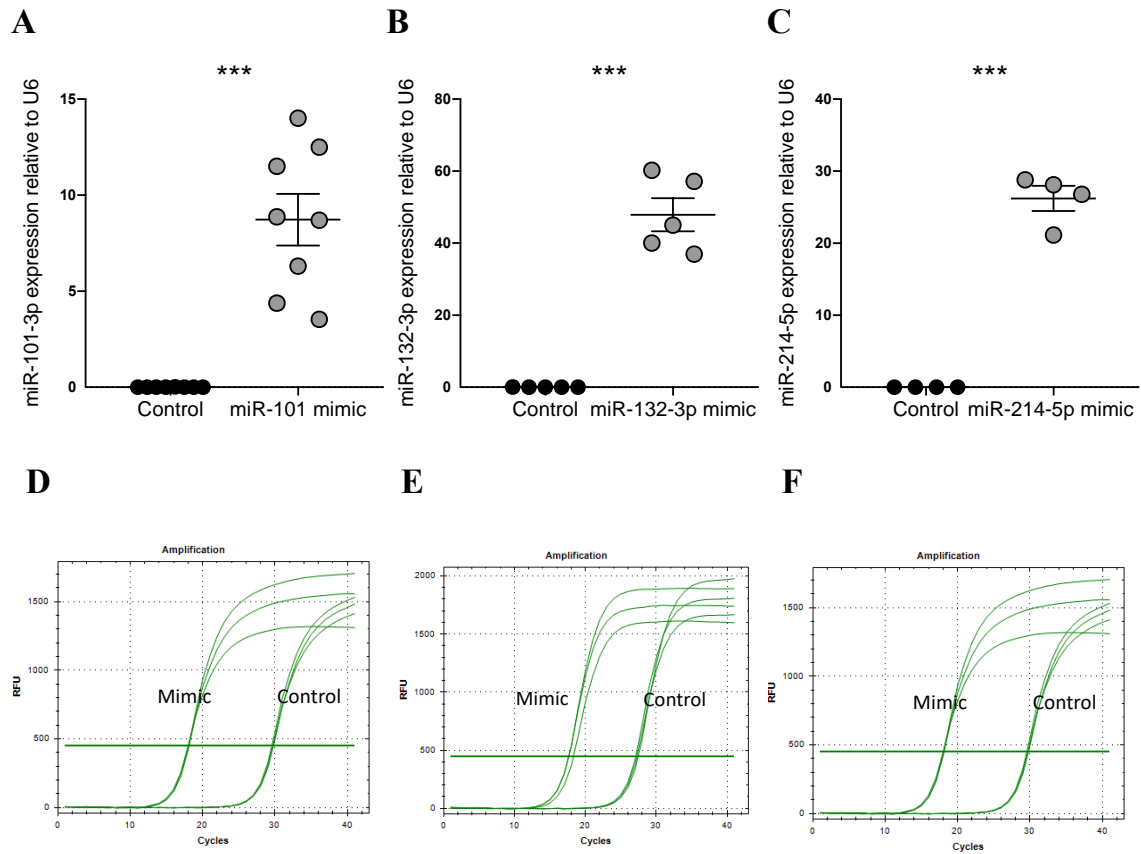


Figure 3.12. Confirmation of miRNAs overexpression in MDMs by RT-qPCR

Relative expression of miR-101-3p (**A**), miR-132-3p (**B**) and miR-214-5p (**C**) normalised to the housekeeping U6 in samples transfected with miRNA mimics (24 hours transfection). Total RNA transfected was 50nM per well in a 6 well plate. Data are presented as mean \pm SEM (n = 4-8, paired t-test, *** p<0.001). Plots showing PCR amplification of a representative sample for miR-101-3p/control (**D**), miR-132-3p/control (**E**) and miR-214-5p/control (**F**).

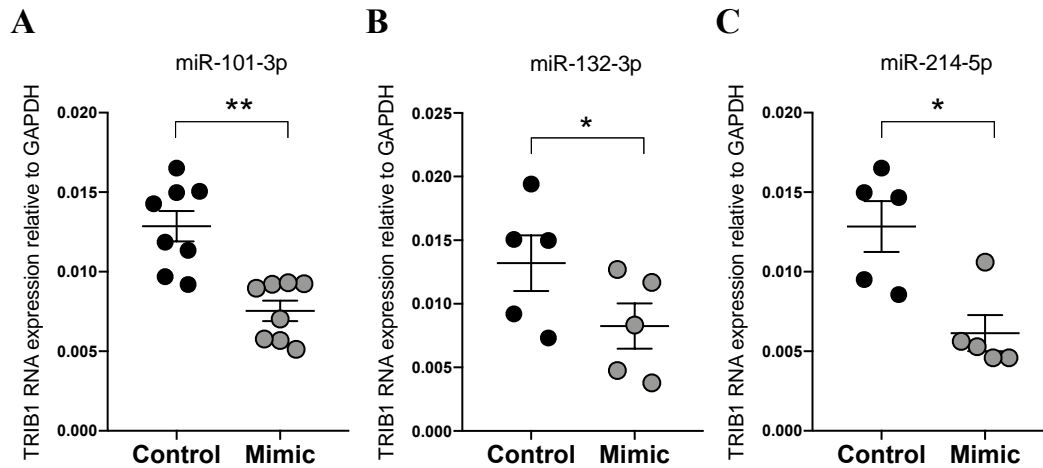


Figure 3.13. Assessment of TRIB1 endogenous expression in transfected MDMs by RT-qPCR

Relative TRIB1 RNA expression normalised to the housekeeping GAPDH in MDMs treated with miR-101-3p mimic (A), miR-132-3p mimic (B) and miR-214-5p mimic (C) and a negative control (24 hours transfection). Total RNA transfected was 50nM per well in a 6 well plate. Data are presented as mean \pm SEM (n = 5-8, paired t-test, ** p<0.01, * p<0.05).

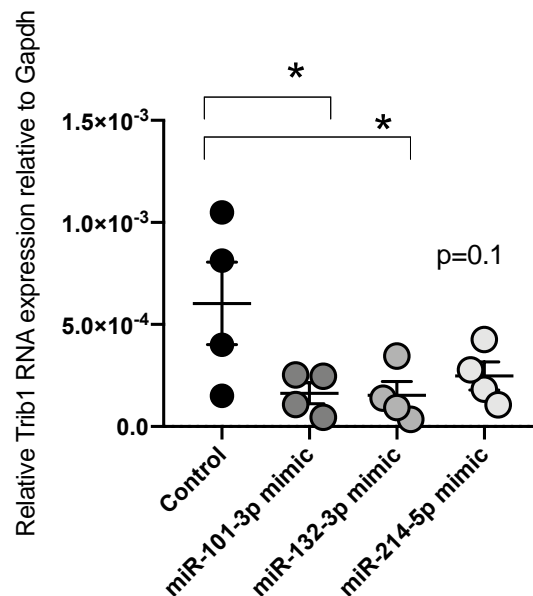


Figure 3.14. Assessment of mTrib1 endogenous expression in transfected iBMDMs by RT-qPCR

Relative Trib1 RNA expression normalised to the housekeeping Gapdh in iBMDMs treated with miRNA mimics and negative control (24 hours transfection). Total RNA transfected was 50nM per well in a 6 well plate. Data are presented as mean \pm SEM (n = 4, ordinary one-way ANOVA with Dunnett's post-test, * p<0.05, ns p \geq 0.05).

Table 3.3. Reactome pathway analysis of candidate miRNAs target genes

Top 10 significant enriched pathways of miR-101-3p, miR-132-3p and miR-214-5p target genes, downloaded from TargetScan. Reactome was used online and results were downloaded as tables (p-value cut off 0.05).

#Entities found refer to the number of input genes found in each specific pathway overlapping with the total genes involved in the pathway.

#Entities total refer to the total number of genes involved in each specific pathway.

Entities ratio refers to the ratio of reactions from each pathway that contain the input genes.

Entities p value refers to the result of statistical test.

Reactome pathway analysis

miR-101-3p	Pathway name	#Entities found	#Entities total	Entities ratio	Entities pValue
	Chromatin organization	38	256	1.76E-02	1.07E-04
	Chromatin modifying enzymes	38	256	1.76E-02	1.07E-04
	Transcriptional Regulation by MECP2	20	100	6.89E-03	1.21E-04
	Estrogen-dependent gene expression	26	154	1.06E-02	1.91E-04
	Regulation of MECP2 expression and activity	11	39	2.69E-03	2.55E-04
	PKMTs methylate histone lysines	12	49	3.38E-03	4.79E-04
	MET activates RAP1 and RAC1	6	13	8.96E-04	5.50E-04
	ESR-mediated signaling	35	256	1.76E-02	8.34E-04
	MECP2 regulates neuronal receptors and channels	9	32	2.20E-03	9.22E-04
	HDMs demethylate histones	8	31	2.14E-03	2.94E-03

miR-132-3p	Pathway name	#Entities found	#Entities total	Entities ratio	Entities pValue
	PIP3 activates AKT signaling	32	316	2.18E-02	9.62E-07
	Intracellular signaling by second messengers	33	363	2.50E-02	6.22E-06
	FOXO-mediated transcription	15	110	7.58E-03	3.11E-05
	PTEN Regulation	18	171	1.18E-02	1.42E-04
	Diseases of signal transduction by growth factor receptors and second messengers	36	484	3.33E-02	1.47E-04
	Regulation of MECP2 expression and activity	8	39	2.69E-03	1.56E-04
	Transcriptional Regulation by MECP2	13	100	6.89E-03	1.64E-04
	Gene expression (Transcription)	100	1850	1.27E-01	2.22E-04
	FOXO-mediated transcription of cell death genes	6	23	1.58E-03	2.96E-04
	MECP2 regulates transcription factors	4	10	6.89E-04	6.47E-04

miR-214-5p	Pathway name	#Entities found	#Entities total	Entities ratio	Entities pValue
	Transcriptional Regulation by E2F6	5	46	3.17E-03	1.06E-03
	Oxidative Stress Induced Senescence	7	114	7.85E-03	3.01E-03
	Nuclear Receptor transcription pathway	6	86	5.93E-03	3.20E-03
	Axon guidance	19	584	4.02E-02	3.84E-03
	POU5F1 (OCT4), SOX2, NANOG activate genes related to proliferation	3	21	1.45E-03	5.22E-03
	Cellular Senescence	9	199	1.37E-02	6.06E-03
	Post-transcriptional silencing by small RNAs	2	7	4.82E-04	6.08E-03
	Transcriptional regulation of pluripotent stem cells	4	45	3.10E-03	6.79E-03
	Nervous system development	19	620	4.27E-02	7.14E-03
	Developmental Biology	32	1241	8.55E-02	7.37E-03

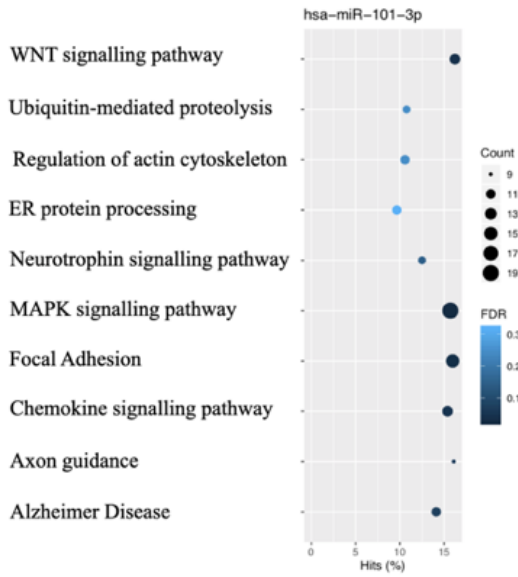
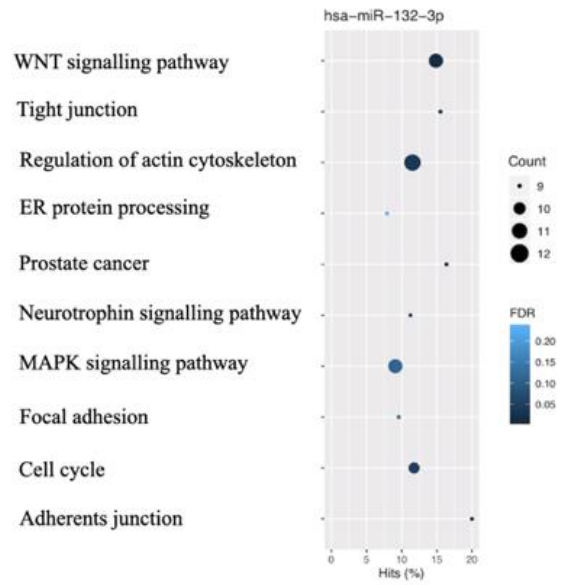
A**B**

Figure 3.15. KEGG enrichment pathway analysis of macrophage-specific genes targeted by miR-101-3p and miR-132-3p

Top 10 significant enriched pathways of miR-101-3p (**A**) and miR-132-3p (**B**) macrophage-specific target genes. miRNA-target prediction analysis was performed using TargetScan; the list of target genes was filtering selecting only genes differentially expressed in macrophages (M0 vs M1) from RNA-seq dataset (DOI: 10.17632/j2hmt7k9fh.1). KEGG analysis was done by using GOSep and the plots were generated in R (p value < 0.05).

3.3.5. Experimental validation of miR-101-3p/TRIB1 interaction

miR-101-3p, a miRNA well known to regulate inflammatory responses in monocyte/macrophages (Wei *et al.*, 2015, Zhang *et al.*, 2015, Huang *et al.*, 2020), is predicted to bind to the 3'UTR of TRIB1 between positions 1526-1532 (**Figure 3.16. A**). The interaction is characterised by one of the most effective canonical seed region type (7mer-m8 site), an exact match to position 2-8 of the mature miRNA, which is known to strongly correlate with targeting efficiency (Friedman *et al.*, 2009, Agarwal *et al.*, 2015). As mentioned earlier, the binding site is highly conserved among different animal species (**Figure 3.17.**) and this is a strong factor, associated with biological relevance (Agarwal *et al.*, 2015). Then, to confirm the direct interaction between miR-101-3p and TRIB1 3'UTR, we co-transfected the TRIB1 3'UTR reporter plasmid and 50nM of miR-101-3p mimic/ negative control in HEK293T cells and carried out a dual luciferase reporter assay. Overexpression of miR-101-3p led to a significant reduction of the reporter activity compared to control (~50% reduction, $p=0.006$) (**Figure 3.16. B**). In contrast, when we used the TRIB1 3'UTR mutant, lacking the 7 nucleotides complementary to the miR-101-3p seed region (**Figure 3.18. A**) there was no effect on TRIB1 3'UTR reporter activity ($p=0.8$) (**Figure 3.18. B**). This confirms the specificity of the miR-101-3p mimic. Mutagenesis was confirmed by Sanger sequencing (**Figure 3.19.**). However, we did not generate a mutant for the second binding site in position 1424-1430, which is not well conserved and despite it being characterised by a canonical, strong seed region, was not predicted by all the 7 tools we used. Our data suggest that the activity of miR-101-3p is mainly exerted via the binding site in position 1526-1532. We also tested the impact of an inhibitor, which is designed to antagonise the activity of the endogenous miR-101-3p. This led to a significant rescue of the TRIB1 3'UTR reporter activity (~16% increase, $p=0.005$) and had no effect when co-transfected together with a control plasmid, without the 3'UTR of TRIB1 ($p=0.4$) (**Figure 3.20.**). Next, we evaluated the effect of miR-101-3p mimic on TRIB1 protein levels in transfected human MDMs, as we previously showed that the mRNA of both human and murine TRIB1 is negatively modulated (**Figure 3.13. A**). TRIB1 protein was reduced by approximately 60% which was statistically significant when compared to control ($p=0.03$) (**Figure 3.21.**). Lastly, we investigated whether or not the activity of miR-101-3p on endogenous TRIB1 mRNA and protein levels in macrophages is directly due to their physical interaction. To this aim, we transiently transfected MDMs with 50nM of a miR-101/TRIB1 Target Site Blocker (TSB), an antisense oligonucleotide designed to selectively compete with miR-101-3p for binding the TRIB1 3'UTR. The TSB does not activate the RISC complex but

prevents the access of a miRNA to a given target gene. This enables the study of a single miRNA in the context of a single gene. The TSB treatment caused a significant increase of both TRIB1 mRNA (1.3-fold change, $p=0.004$) and protein levels (~76%, $p=0.04$), compared to controls (**Figure 3.22.**). Taken together, these data indicate that miR-101-3p is a negative regulator of TRIB1 in macrophages.

A

5'...CCGUGUAUACCCUCAGUACUGUG...3' TRIB1 3'UTR 1526-1532
 |||||
 3' AAGUCAAUAGUGUCAUGACAU 5' miR-101-3p

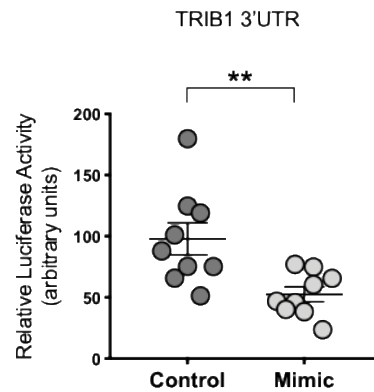
B

Figure 3.16. Impact of miR-101-3p on gene reporter activity

Nucleotide alignment between miR-101-3p and TRIB1 3'UTR (**A**); relative luciferase activity measured in HEK293T cells after 24 hours co-transfection of TRIB1 3'UTR reporter, firefly luciferase reporter (required for data normalisation) and 50nM of miR-101-3p mimic or negative control. Total DNA transfected 100 ng/well (96-well plate). Data are presented as mean \pm SEM (unpaired t-test, n = 9, ** p<0.01) (**B**).

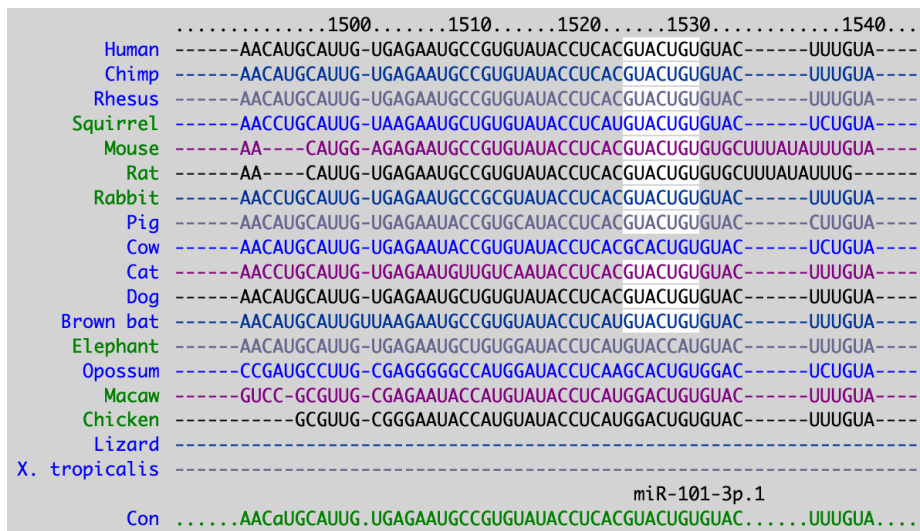


Figure 3.17. Phylogenetic conservation of miR-101-3p binding site on the 3'UTR of TRIB1

The figure, taken from TargetScan, shows that miR-101-3p binding site on TRIB1 is highly conserved.

A

5'...CCGUGUAUACCUCA ----- G...3' TRIB1 3'UTR mutant
3' AAGUCAAUAGUGUCAUGACAU 5' miR-101-3p

B

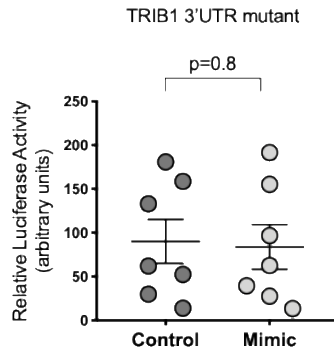


Figure 3.18. Impact of miR-101-3p on TRIB1 3'UTR mutant

Nucleotide alignment between miR-101-3p and TRIB1 3'UTR mutant lacking the 7 bases complementary to the seed-region of the miRNA (A); relative luciferase activity measured in HEK293T cells after 24 hours co-transfection of TRIB1 3'UTR mutant, firefly luciferase reporter (required for data normalisation) and 50nM of miR-101-3p mimic or negative control. Total DNA transfected 100 ng/well (96-well plate). Data are presented as mean \pm SEM (unpaired t-test, n = 7, ns $p \geq 0.05$) (B).

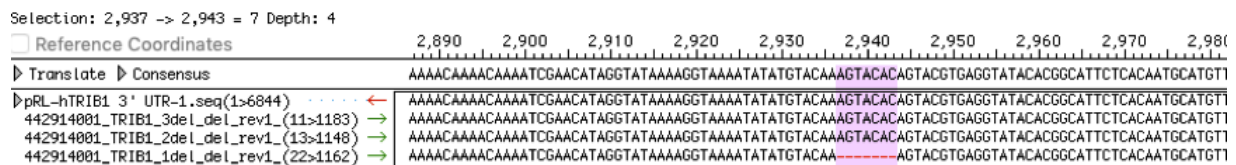


Figure 3.19. Confirmation of site-directed mutagenesis: miR-101-3p binding site deletion

TRIB1 3'UTR mutagenesis to generate was confirmed by reverse Sanger sequencing: 1 out of 3 plasmids had the 7-nucleotides deletion (screenshot taken from SeqMan Pro alignment software, DNASTar).

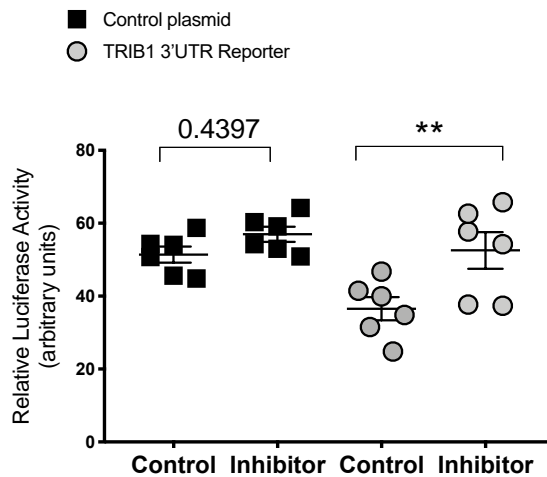


Figure 3.20. Impact of miR-101-3p inhibitor on *TRIB1* gene reporter activity

Relative luciferase activity measured in HEK293T cells after 24 hours co-transfection of renilla control reporter (control plasmid) and *TRIB1* 3'UTR reporter with firefly reporter (required for data normalisation) and 25nM of miR-101-3p inhibitor or negative control. Data are presented as mean \pm SEM (ordinary one-way ANOVA with Sidak's post-test, n = 6, ** p<0.01, ns p \geq 0.05).

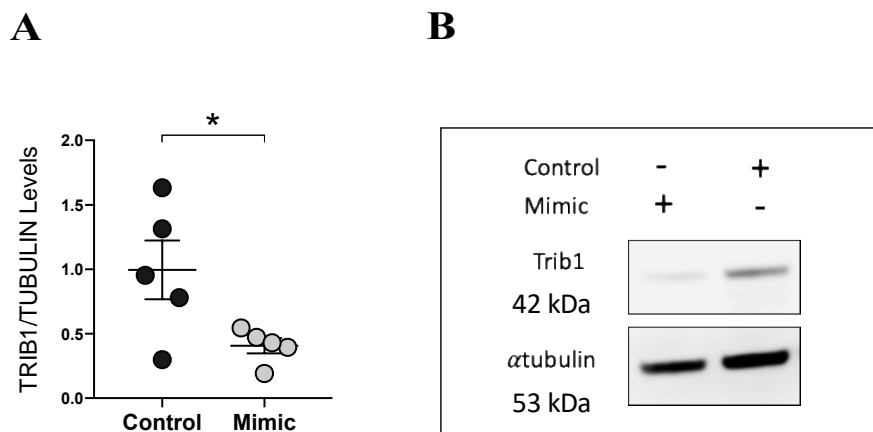


Figure 3.21. Effect of miR-101-3p mimic on Trib1 protein expression

Relative Trib1 protein expression normalised to the housekeeping alpha-tubulin in human MDMs transfected with 50nM of miR-101-3p mimic/negative control (24 hours transfection); data are presented as mean \pm SEM (n = 5, paired t-test, * p<0.05) (A); western blot membrane of a representative sample, showing bands for Trib1 and alpha-tubulin (B).

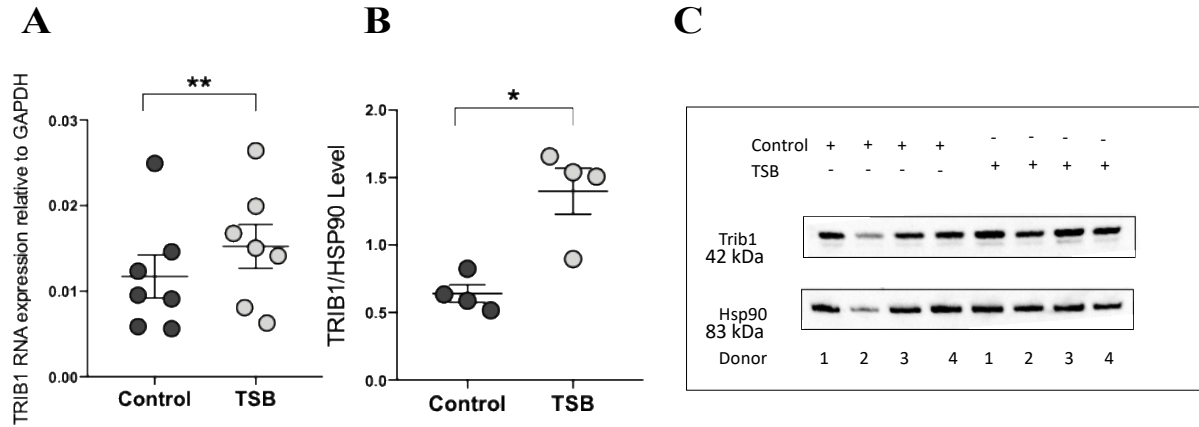


Figure 3.22. Assessment of miR-101-3p specificity: miR-101/TRIB1 target site blocker

Relative TRIB1 RNA level normalised to the housekeeping GAPDH in MDMs transfected with 50nM of TSB/Negative Control for 24 hours (**A**); relative Trib1 protein expression normalised to the housekeeping Hsp90 in MDMs transfected with 50nM of TSB/Negative Control for 24 hours (**B**); representative western blot membrane showing band intensities for Trib1 and Hsp90 (**C**). Data are presented as mean \pm SEM (n=4-7, paired t-test, ** p<0.01, * p<0.05).

3.3.6. Impact of miR-101-3p on human macrophages

Our previous results demonstrated that miR-101-3p is a negative regulator of TRIB1 expression by direct interaction. Next, we evaluated the effect of these miRNAs on DUSP1 and ABCA1, which have been previously identified and experimentally validated as miR-101-3p target genes in macrophages (Wei *et al.*, 2015, Zhang *et al.*, 2015). DUSP1, dual specificity phosphatase, interacts with MAPK proteins as a negative regulator, limiting inflammatory responses (Abraham *et al.*, 2006). ABCA1, ATP-binding cassette transporter A1, is responsible for cholesterol efflux from macrophages to lipid-free apoA-I, the main component of HDL (Zhao *et al.*, 2012). The binding site of miR-101-3p on the 3'UTR of DUSP1 and ABCA1 is characterised by canonical seed regions (8mer and 7mer A1, respectively) and they are both well conserved among different species (from TargetScan). Accordingly, in response to miR-101-3p mimic, both genes were significantly downregulated at the mRNA levels (**Figure 3.23. A, B**). We evaluated also the effect of miR-101-3p mimic and inhibitor on cholesterol efflux in transfected MDMs and found that in the presence of the mimic the % of total cholesterol efflux from macrophages to HDL was reduced by ~20% ($p=0.008$). Similarly, when we used the inhibitor we observed an increase of ~20% ($p=0.003$) (**Figure 3.23. C**). Despite the significance, the effect of miR-101-3p on cholesterol efflux was quite small, but this is likely due to the assay itself, requiring frequent media changes and testing 2 days post-transfection. However, this effect of miR-101-3p is not TRIB1-dependent. Therefore, we investigated the expression of IL-6 and IL-8 genes, which were significantly impaired in response to TRIB1 overexpression in MDMs (see **Figure 3.6**). Macrophages transfected with miR-101-3p mimic showed a significant increase of both IL-6 and IL-8 mRNA levels, compared to control ($p=0.03$, $p=0.04$, respectively) (**Figure 3.24. A, B**). We also measured IL-8 protein through ELISA and observed that there was a significant increase in response to miR-101-3p mimic ($p=0.007$) (**Figure 3.24. C**). IL-6 ELISA did not show any differences among conditions, as levels measured were below the threshold of detection (data not shown). To understand whether the effect on IL-8 is TRIB1-dependent, we performed IL-8 ELISA in MDMs transfected with the TSB. The TSB led to a small but significant decrease of IL-8 protein ($p=0.01$) (**Figure 3.24. D**). This suggests that TRIB1 might be an upstream regulator of IL-8 gene, by either direct or indirect regulation. M1-like macrophages, challenged with LPS and INF- γ , are also characterised by an increase in IL-8 production, compared to unpolarised cells (**Figure 3.24. E**). Lastly, we looked at the gene expression of other macrophage polarisation markers: miR-101-3p increased the expression of the M1 markers CD80 ($p=0.04$), CD86

($p=0.02$), $\text{TNF-}\alpha$ ($p=0.04$) and FAM26F ($p=0.01$) (**Figure 3.25.**). The latter was characterised in our lab as M1 macrophage marker and it is strongly induced by LPS and $\text{INF-}\gamma$ (manuscript in submission). However, we did not observe any miR-101-3p mediated changes in M2 markers IL-4 ($p=0.5$), IL-10 ($p=0.7$), CD36 ($p=0.3$) and CD163 ($p=0.4$) (**Figure 3.26.**). Overall, we can conclude that miR-101-3p induces an M1-like phenotype in human macrophages, partially by directly targeting TRIB1 , which, as mentioned earlier, is a positive regulator of M2 macrophages, acting as anti-inflammatory gene.

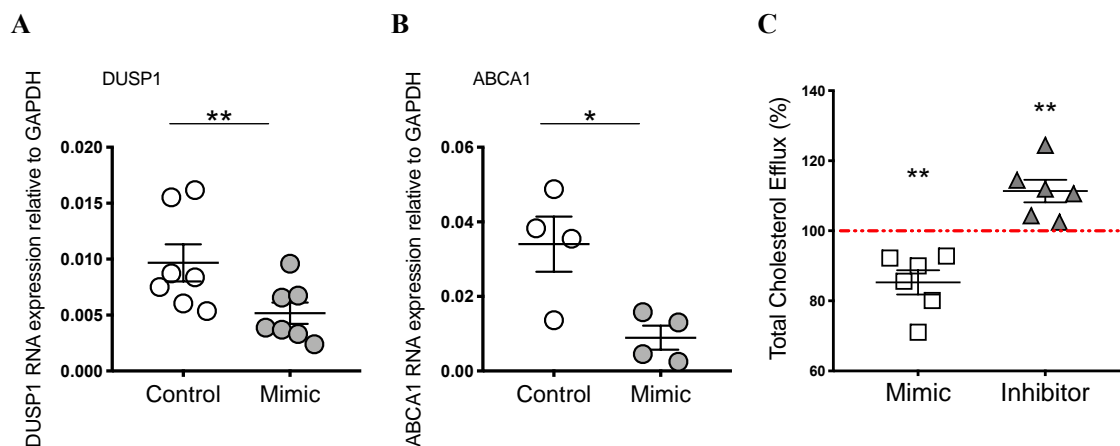


Figure 3.23. Impact of miR-101-3p mimic on DUSP1 and ABCA1 genes in human macrophages

Relative RNA expression of DUSP1 (A) and ABCA1 (B) normalised to the housekeeping GAPDH in MDMs transfected with miR-101-3p mimic/control (50nM, 24 hours transfection). Percentage of total cholesterol efflux to HDL measured on MDMs transfected with miR-101-3p mimic/control (50nM) and miR-101-3p inhibitor/control (25nM) (C). Data are presented as mean \pm SEM ($n=4-7$, paired t-test, ** $p<0.01$, * $p<0.05$).

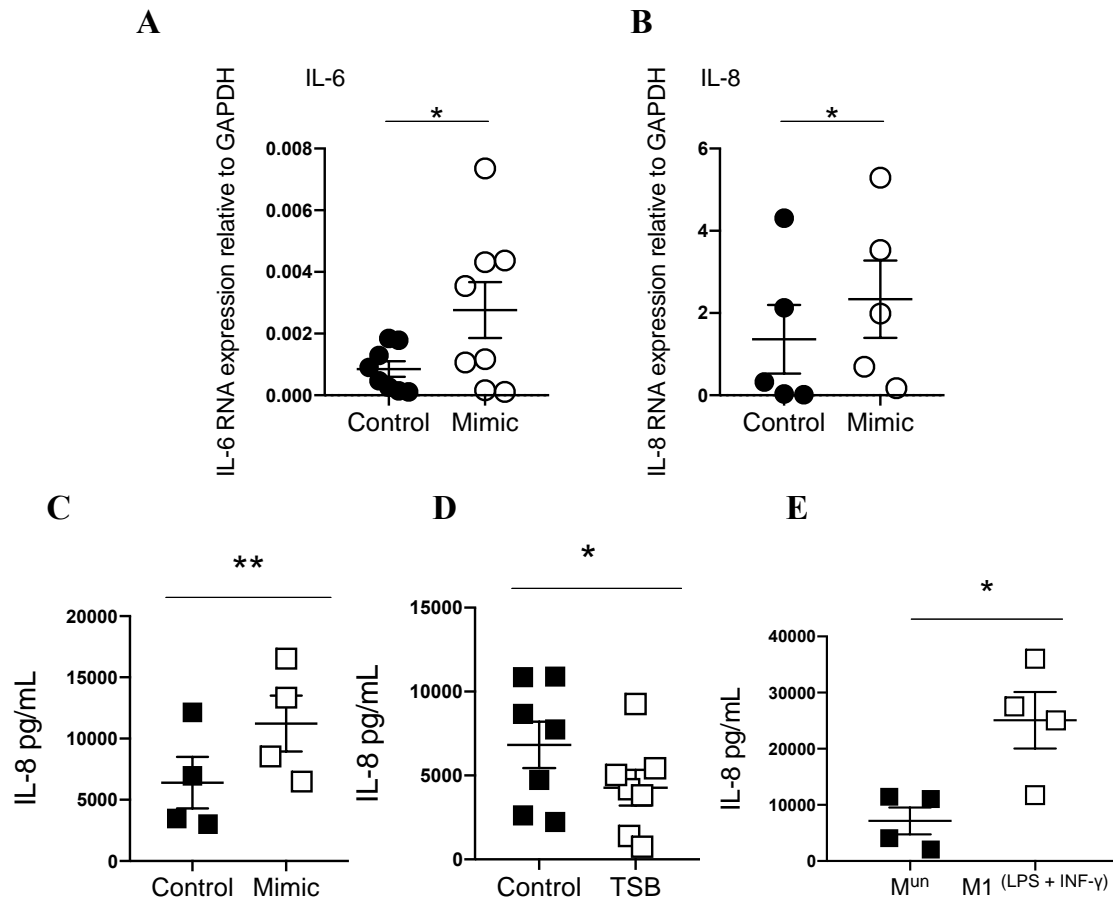


Figure 3.24. miR-101-3p effect on pro-inflammatory IL-6 and IL-8

Relative RNA expression of IL-6 (A) and IL-8 (B) normalised to the housekeeping GAPDH in MDMs transfected with miR-101-3p mimic/control (24 hours transfection). IL-8 protein levels measured by using ELISA in supernatants collected after 24 hours MDMs transfection with miR-101-3p mimic/control (C), TSB/control (D) and 24 hours MDMs polarisation (E). Total RNA transfected was 50nM per well in a 6 well plate. Data are presented as mean \pm SEM (n=4-8, paired t-test, ** p<0.01, * p<0.05).

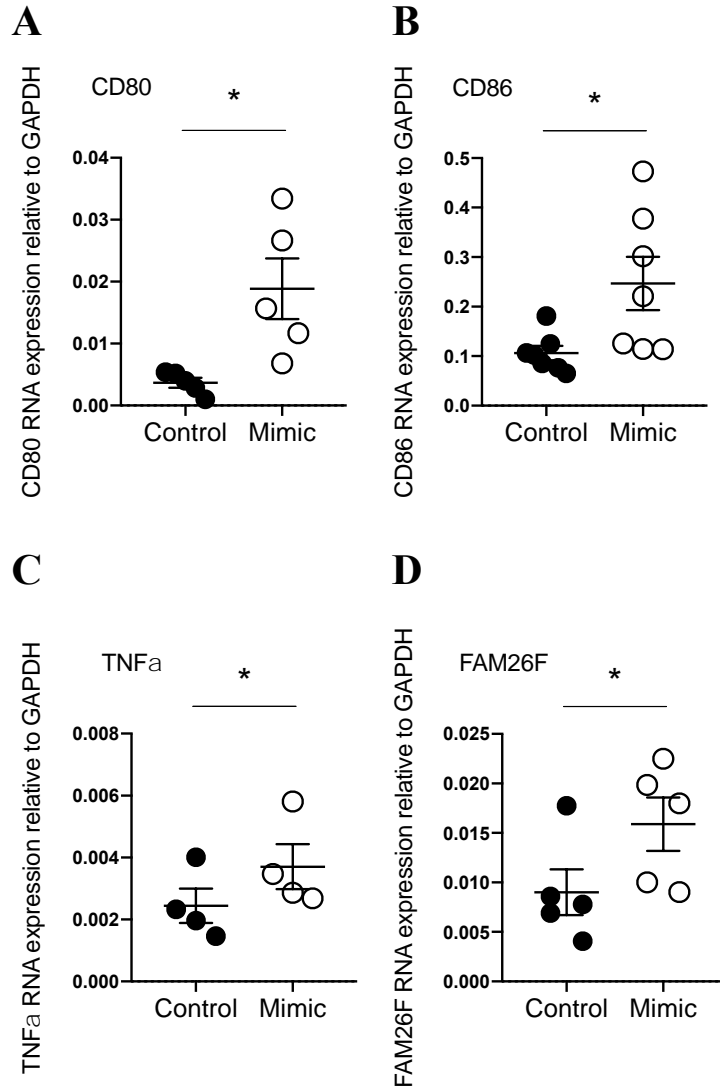


Figure 3.25. miR-101-3p impact on M1 polarisation markers expression by RT-qPCR

Relative RNA expression of CD80 (**A**), CD86 (**B**), TNFα (**C**) and FAM26F (**D**) normalised to the housekeeping GAPDH in MDMs transfected with miR-101-3p/control (50nM, 24 hours transfection). Data are presented as mean ±SEM (n=4-7, paired t-test, * p<0.05).

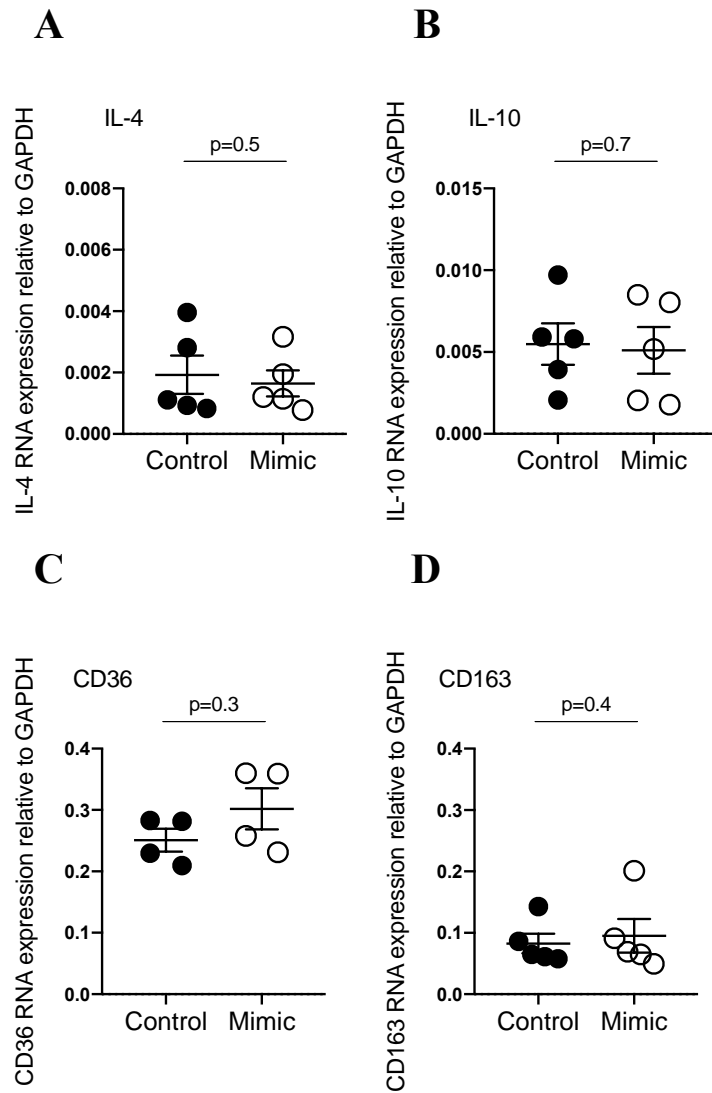


Figure 3.26. miR-101-3p impact on M2 polarisation markers expression by RT-qPCR

Relative RNA expression of IL-4 (**A**), IL-10 (**B**), CD36 (**C**) and CD163 (**D**) normalised to the housekeeping GAPDH in MDMs transfected with miR-101-3p/control (50nM, 24 hours transfection). Data are presented as mean \pm SEM (n=4-5, paired t-test, ns $p \geq 0.05$).

3.4. Summary

To date, multiple *in vivo* and *in vitro* studies highlighted the critical role of TRIB1 in the function and polarisation of macrophages, in both physiological and pathological contexts (Sato *et al.*, 2013, Akira *et al.*, 2013). TRIB1, along with its family members TRIB2 and TRIB3, are considered master regulators of inflammation, metabolism and cancer, given their ability to interact with proteins such as MAPK, AKT and COP1 (Dugast *et al.*, 2013, Johnston *et al.*, 2015, Evers *et al.*, 2017).

It is well appreciated that TRIB1 can have a context-dependent function, acting as either activator or inhibitor of inflammation in different tissues (Ostertag *et al.*, 2010, Akira *et al.*, 2013). In addition, TRIB1 is characterised by an unstable transcript and it was ranked among the top 50 most unstable genes, with a mRNA half-life shorter than 1 hour (Sharova *et al.*, 2009). It has been estimated that more than half of the protein-coding genes in the human genome are post-transcriptionally repressed by miRNAs (Friedman *et al.*, 2009).

In the present work, we aimed to investigate the post-transcriptional regulation of TRIB1 mRNA, focussing on miRNA-mediated gene regulation in human macrophages. We investigated the expression of TRIB1 mRNA in human polarised macrophages and showed that it significantly increases in response to LPS and INF- γ (M1 stimuli), as well as IL-4 (M2a stimulus). Immunofluorescence staining of MDMs highlighted that Trib1 protein is mainly located in the nucleus, where it ultimately acts as a transcription factor. Indeed, the overexpression of the pseudo-kinase in MDMs resulted in increased M2 markers (MSR-1, CD163 and IL-4) and decreased M1 markers (IL-6, IL-8). However, this was not consistent with what Arndt and colleagues found in murine BMDMs, where Trib1 deficiency resulted in the impairment of both M1 and M2 genes, including Il6 (Arndt *et al.*, 2018). However, it is well known that genetic manipulation in animals is often associated with gene compensatory events and it is not equally comparable to *in vitro* settings (El-Brolosy *et al.*, 2017).

To determine whether TRIB1 is post-transcriptionally regulated by miRNAs, we took advantage of bioinformatics analysis and experimental approaches. For the first time, we demonstrated that the 3'UTR of TRIB1 exerts a robust, negative effect on gene regulation and it is enriched in miRNA-binding sites, some of them highly conserved among different species. We identified a total of 1237 potential regulators of TRIB1 using 7 different miRNA-target prediction tools, but we narrowed down the list, selecting high-confidence miRNAs and miRNAs predicted by ≥ 3 tools. We showed that miR-101-3p, miR-132-3p and miR-214-5p are expressed in human macrophages and they are able to negatively modulate TRIB1

transcript in both human and murine macrophages. However, we decided to focus on miR-101-3p: as suggested by previous studies, miR-101-3p targets key genes regulating inflammatory and metabolic outcomes in macrophages, such as DUSP1 and ABCA1 (Wei *et al.*, 2015, Zhang *et al.*, 2015). In addition, our enrichment analysis suggested that the target genes of miR-101-3p, specifically expressed by human macrophages, are involved in inflammatory signalling pathways (i.e. MAPK pathway, chemokines pathway). By using a dual luciferase reporter assay in HEK293T cell line, we fully validated the interaction between miR-101-3p and TRIB1. Site-directed mutagenesis experiment confirmed that the binding site in position 1526-1532 on the 3'UTR of TRIB1 is functional. To substantiate further our findings, we employed a novel approach: the use of a target-site blocker. Target site blockers (TSB) are antisense oligonucleotides (18-20 nucleotides long), designed to bind selectively to the miRNA target site within a mRNA, competing with the endogenous miRNA and without activating the RNA interference mechanism (RISC complex). By using this approach, we could evaluate the impact of miR-101-3p inhibition on TRIB1 without using an inhibitor. In fact, the use of inhibitors is associated with changes in multiple genes, as a single miRNA can target hundreds of different genes simultaneously. When we transfected the TSB in MDMs, we observed a small but significant increase in TRIB1 at both mRNA and protein level. This suggests that miR-101-3p/TRIB1 interaction is biologically relevant in macrophages. Finally, we observed that miR-101-3p induced an M1-like phenotype in macrophages, partially due to TRIB1 downregulation. Particularly, the pro-inflammatory IL-8 was downregulated in TRIB1 overexpressing cells and upregulated in cells treated with miR-101-3p mimic. Notably, IL-8 significantly increased in response to the TSB treatment, hinting that TRIB1 is an upstream negative regulator of IL-8 transcription. However, this should be investigated further.

In conclusion, our data suggest that TRIB1 undergoes miRNAs-mediated regulation. MiR-101-3p is a direct regulator of TRIB1 expression in human macrophages. As it also controls the expression of DUSP1 and ABCA1 genes, miR-101-3p offers an interesting, potential target to antagonise inflammation and improve cholesterol metabolism. Future efforts are needed to investigate this interaction in *in vivo* environments and in the context of human disease, in which both TRIB1 and macrophages are dysregulated, including atherosclerosis.

Chapter 4. Integrated transcriptome analysis of small non-coding RNAs and mRNAs in pro-inflammatory macrophages

Declaration

This part of my thesis is intended to be published along with additional data produced by collaborators, thus not shown here (manuscript in preparation). All the experiments have been performed by myself. The RNA-seq and downstream bioinformatics analyses have been carried out entirely by Sumeet Deshmukh, under the supervision of Dr Ian Sudbery.

We declare no conflicts of interest.

Abstract

Macrophage polarisation is a crucial process through which macrophages respond to environmental signals, adapting and integrating multiple clues from damaged and healthy tissues. This process is highly dynamic and it is regulated by complex signalling networks, including miRNA-mediated regulation of gene expression. However, studies that correlate miRNAs and target gene expression in polarised macrophages are missing. Here, we investigated the expression of miRNAs and their target genes in human polarised macrophages by using an integrative approach and multiple RNA-seq experiments. We found that 73 miRNAs were differentially expressed between M0 and M1-polarised macrophages: 47 were downregulated and 26 upregulated. By using TargetScan we predicted their target genes and investigated their expression by using data from a second M0/M1 RNA-seq experiment. Interestingly, we observed that 1573 upregulated genes in M1 macrophages are predicted to be targets of 44 downregulated miRNAs; the M1 polarising stimuli led to the increased expression of genes involved in immune responses and inflammation. Similarly, 1790 downregulated genes are potential targets of 26 upregulated miRNAs. Significantly, enriched terms in a KEGG analysis for downregulated genes included cell cycle and proliferation. We identified 9 differentially expressed miRNAs (miR-7-5p, miR-125a-3p, miR-3614-5p, miR-4773, miR-186-5p, miR-4709-3p, miR-1343-3p, miR-766-3p, miR-335-3p) which were predicted to target more than 500 different genes and named them “super regulators”. We evaluated the direct impact of some of these on M0 macrophage transcriptome, by employing the transient transfection of miRNA mimics followed by RNA-seq and observed altered gene expression that recapitulate those seen in M1-like phenotype. Our results demonstrate the existence of a

macrophage-specific targetome that underpin many of the critical biological pathways involved in inflammation.

4.1. Introduction

Macrophages are the most plastic cell type of the haematopoietic system, playing a crucial role in maintaining all tissues in a physiological state and influencing disease development and progression. This is due to their ability to sense microenvironmental signals, adopting different phenotypes in a process named “polarisation” (*Mills et al., 2012*). Macrophage polarisation has been extensively studied in both *in vitro* and *in vivo* models: it is not a fixed event and can be triggered by a multitude of biological and mechanical events, such as infection, tissue injury and carcinogenesis (*Murray et al., 2017*). Polarisation is often simplified into two main phenotypes: pro-inflammatory M1 macrophages and anti-inflammatory M2 macrophages. However, this definition finds significant limitations in *in vivo* contexts, where classifying macrophages remains a big challenge, due to their high plasticity and the existence of mixed phenotypes (*Martinez et al., 2014*).

One of the major mechanisms controlling macrophage polarisation is transcriptional regulation of gene expression. Macrophage polarisation results in distinct genetic signatures that recapitulate their phenotype and function (*Martinez et al., 2006*). It has been shown that the main gene networks involved in M1/M2 polarisation are those related to membrane receptor signalling pathways, cytokine and chemokine release, lipid metabolism and apoptosis (*Martinez et al., 2006*). Key transcription factors involved in macrophage activation are STATs (Signal Transducers and Activators of Transcription), PPARs (Peroxisome Proliferator Activated Receptors), IRFs (Interferon Regulatory Factors), NF κ B (Nuclear Factor κ B), GRs (glucocorticoid receptors), HIFs (Hypoxia-Inducible Factors) and KLFs (Krüppel-Like Factors) (*Tugal et al., 2013*). Transcriptional changes behind macrophage polarisation are also affected by the activity of endogenous miRNAs (*Essandoh et al., 2016, Curtale et al., 2019*). miRNAs are a class of small non-coding RNAs that negatively regulate gene expression via binding to complementary sequences located on the 3'UTR of target mRNAs (*Bartel et al., 2004*). To date, numerous studies highlight the potential of miRNAs in regulating macrophage activation by direct interaction with multiple genes: this has been particularly studied in the context of cancer and metabolic diseases (*Fernández-Hernando et al., 2013, Deiuliis et al., 2016, Essandoh et al., 2016*). However, the extent of the association between miRNAs and

their target genes during macrophage polarisation has not been investigated in a systematic manner.

In the present work, we aimed to address the differential expression between miRNAs and their putative target genes in human macrophages challenged with LPS and INF- γ (M1-like cells), by using an integrative approach. We identified 73 differentially expressed miRNAs during M1-polarisation which could lead to the dysregulation of 3363 genes. We identified 9 distinct miRNAs, each predicted to target more than 500 genes in macrophages, and named them “super regulators”. Gene Ontology and KEGG pathway enrichment analysis indicate that these miRNAs are key regulators of innate immune responses and cell division, thus contributing to the transcriptional changes underlying the M1-like phenotype. Further research is needed to experimentally validate miRNA-target gene networks and determine functional outcomes by dedicated *in vitro* assays.

4.2. Hypothesis and aims

We hypothesised that the transcriptional changes induced in M1 polarised macrophages are due to the activity of miRNAs. Therefore, we aimed to:

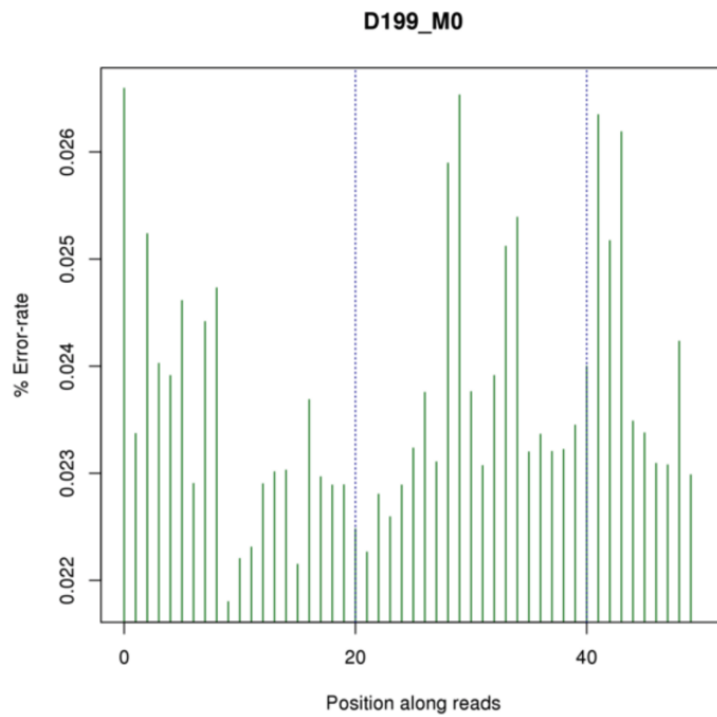
- identify differentially expressed miRNAs between M0 and M1 macrophages;
- investigate their association with differentially expressed genes;
- address the extent of this association;
- determine the functional category of miRNA targetome.

4.3. Results

4.3.1. Small RNA sequencing data quality and analysis strategy

To investigate the expression of miRNAs in human macrophages, we performed a small non-coding RNA sequencing on unpolarised (M^{un} or $M0$) and polarised ($M1^{LPS+INF-\gamma}$ or $M1$) monocyte-derived macrophages (MDMs), isolated from 8 healthy volunteers. The sequencing was performed with an Illumina platform by the genome sequencing company Novogene. Illumina technology uses a “sequencing by synthesis” approach and it is usually associated with an error rate of 0.1% per nucleotide (Pfeiffer *et al.*, 2018). Errors are due to either the consumption of the sequencing reagents or the imperfect binding of the primers to the template (Erlich and Mitra, 2008, Jiang *et al.* 2011). In our cases, the error rate was very low ($>0.03\%$ per nucleotide) for all the samples (representative sample is shown in **Figure 4.1.**). The recommended sequencing depth for small RNAs is $> 10,000,000$ raw reads; the depth of our sequencing ranged from 18,959,214 to 24,618,695. **Table 4.1.** shows the data quality summary provided by the company. The raw data were further processed by the company in order to eliminate some contaminants and to obtain the final clean reads. The data filtering is summarised in **Table 4.2.** Specifically, they eliminated reads of which more than 50% bases show a base quality score ≤ 5 , reads containing more than 10% of unsolved bases (“N”), reads with 5’ primer contaminants, reads without 3’ primer and without the insert tag and reads with poly A/T/G/C. However, the percentage of these contaminants was very low. After performing the quality check, the company sent us fastq files. The fastq files were analysed as described in Chapter 2 (**Section 2.2.1.**). For the mapping phase, we did not use the reference human genome, but sequences downloaded from RNA Central, a comprehensive database containing sequences of all type of non-coding RNAs (RNAcentral Consortium, 2017). We observed a strong signal for a sequence of 23 nucleotides corresponding to hsa-miR-21 (UAGCUUAUCAGACUGAUGUUGAC), therefore we decided to exclude it from the analysis to avoid biased results. This sequence was over represented in all the samples (30-50%, shown in Chapter 8, Appendix III). When we performed the analysis considering miR-21, gene differential expression was not statistically significant, but removing this sequence improved the results. In fact, miR-21 is known to be one of the most abundant miRNAs in macrophages with roles in both inflammatory and anti-inflammatory mechanisms (Sheedy 2015). The overview of the analysis described in this chapter is briefly illustrated in **Figure 4.2.** and each step is specified in the following result sections.

A



B

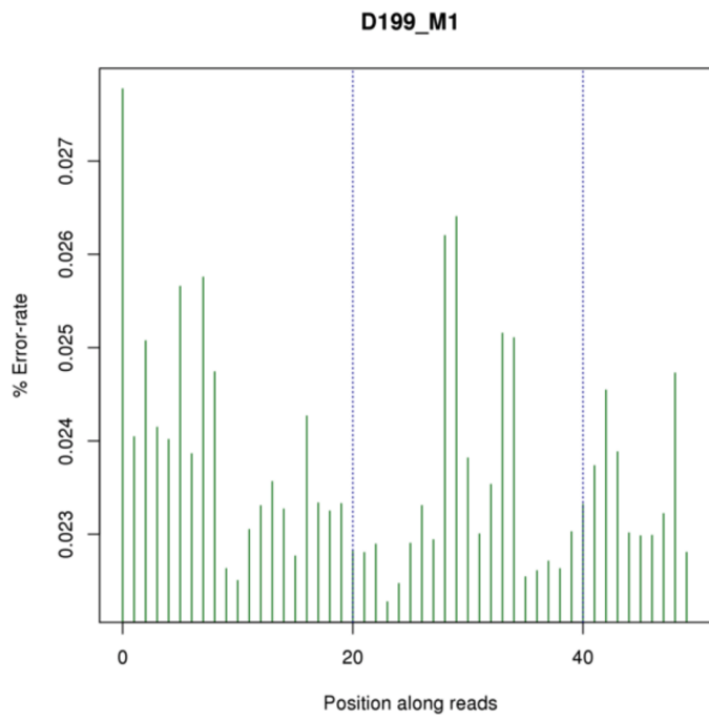


Figure 4.1. Sequencing error distribution rate

Sequencing error distribution rates of two representative samples. The horizontal axis shows the reads position, the vertical axis shows the percentage of single base error rate. Graphs were provided by Novogene company.

Table 4.1. Data quality summary

The table summarises our sequencing data quality and it was provided by the company. Sample: sample ID; raw reads: four rows as a unit to calculate the sequence number of each raw data file. Clean reads: calculated as raw reads, statistics object is clean data file. The subsequent analyses are all based on clean reads: raw bases= (Number of sequences) * (sequence length), use G for unit. Clean bases= (Number of sequences) * (sequence length), use G for unit. Error rate: base error rate. Q20, Q30= (Base number of Phred value > 20(> 30)) / (Total base number). GC content: (G&C base number) / (Total base number). Description provided by Novogene.

Sample	Raw Reads	Clean Reads	Raw Bases(G)	Clean Bases(G)	Error rate(%)	Q20(%)	Q30	GC content(%)
D199_M0	20665801	20665682	1.033	1.033	0.01	98.42	95.66	47.27
D199_M1	20536744	20536643	1.027	1.027	0.01	98.42	95.66	48.02
D204_M0	24266598	24266499	1.213	1.213	0.01	98.45	95.91	47.41
D204_M1	20581158	20581061	1.029	1.029	0.01	98.39	95.54	47.45
D179_M0	24417998	24417855	1.221	1.221	0.01	98.49	95.87	46.91
D179_M1	18959214	18959113	0.948	0.948	0.01	98.34	95.62	46.84
D194_M0	22670952	22670839	1.134	1.134	0.01	98.31	95.56	47.87
D194_M1	21464756	21464646	1.073	1.073	0.01	98.44	95.75	47.19
D206_M0	24618695	24618559	1.231	1.231	0.01	98.50	96.05	46.44
D206_M1	20304336	20304235	1.015	1.015	0.01	98.47	95.84	47.09
D221_M0	23995072	23994973	1.200	1.200	0.01	98.43	95.68	47.48
D221_M1	20639156	20639049	1.032	1.032	0.01	98.42	95.67	48.49
D223_M0	24130715	24130600	1.207	1.207	0.01	98.43	95.67	47.39
D223_M1	23468860	23468724	1.173	1.173	0.01	98.40	95.57	48.12
D225_M0	24096600	24096468	1.205	1.205	0.01	98.46	95.82	47.55
D225_M1	21805125	21805021	1.090	1.090	0.01	98.25	95.53	47.08

Table 4.2. Data filtering summary

The table contains a summary of data filtering and it was provided by the company. Sample: Sample id; total_reads: total sequenced reads; N% > 10%: Percentage of reads with N > 10%; low quality: percentage of low quality reads; 5_adapter_contaminate: Percentage of reads with 5'adapter contamination; 3_adapter_null or insert_null: Percentage of reads with 3'adapter null or insert null; with polyA/T/G/C: Percentage of reads with polyA/T/G/C; clean reads: total clean reads and its percentage accounted for raw reads. Description provided by Novogene.

Sample	total_reads	N% > 10%	low quality	5_adapter_contaminate	3_adapter_null or insert_null	with polyA/T/G/C	clean reads
D199_M0	20665801 (100.00%)	119 (0.00%)	0 (0.00%)	9087 (0.04%)	1480403 (7.16%)	9674 (0.05%)	19166518 (92.75%)
D199_M1	20536744 (100.00%)	101 (0.00%)	0 (0.00%)	17525 (0.09%)	1481878 (7.22%)	7510 (0.04%)	19029730 (92.66%)
D204_M0	24266598 (100.00%)	99 (0.00%)	0 (0.00%)	24416 (0.10%)	2309753 (9.52%)	12032 (0.05%)	21920298 (90.33%)
D204_M1	20581158 (100.00%)	97 (0.00%)	0 (0.00%)	17175 (0.08%)	1800058 (8.75%)	13117 (0.06%)	18750711 (91.11%)
D179_M0	24417998 (100.00%)	143 (0.00%)	0 (0.00%)	6906 (0.03%)	1502087 (6.15%)	21407 (0.09%)	22887455 (93.73%)
D179_M1	18959214 (100.00%)	101 (0.00%)	0 (0.00%)	4711 (0.02%)	1276694 (6.73%)	9713 (0.05%)	17667995 (93.19%)
D194_M0	22670952 (100.00%)	113 (0.00%)	0 (0.00%)	26875 (0.12%)	2343525 (10.34%)	18474 (0.08%)	20281965 (89.46%)
D194_M1	21464756 (100.00%)	110 (0.00%)	0 (0.00%)	7938 (0.04%)	1534902 (7.15%)	29600 (0.14%)	19892206 (92.67%)
D206_M0	24618695 (100.00%)	136 (0.00%)	0 (0.00%)	5514 (0.02%)	1643806 (6.68%)	20897 (0.08%)	22948342 (93.22%)
D206_M1	20304336 (100.00%)	101 (0.00%)	0 (0.00%)	8740 (0.04%)	1420593 (7.00%)	15007 (0.07%)	18859895 (92.89%)
D221_M0	23995072 (100.00%)	99 (0.00%)	0 (0.00%)	24143 (0.10%)	2498826 (10.41%)	12302 (0.05%)	21459702 (89.43%)
D221_M1	20639156 (100.00%)	107 (0.00%)	0 (0.00%)	19980 (0.10%)	1909131 (9.25%)	17067 (0.08%)	18692871 (90.57%)
D223_M0	24130715 (100.00%)	115 (0.00%)	0 (0.00%)	13828 (0.06%)	1769383 (7.33%)	18777 (0.08%)	22328612 (92.53%)
D223_M1	23468860 (100.00%)	136 (0.00%)	0 (0.00%)	24602 (0.10%)	1704725 (7.26%)	17773 (0.08%)	21721624 (92.56%)
D225_M0	24096600 (100.00%)	132 (0.00%)	0 (0.00%)	18034 (0.07%)	2033805 (8.44%)	18899 (0.08%)	22025730 (91.41%)
D225_M1	21805125 (100.00%)	104 (0.00%)	0 (0.00%)	9106 (0.04%)	1827568 (8.38%)	12903 (0.06%)	19955444 (91.52%)

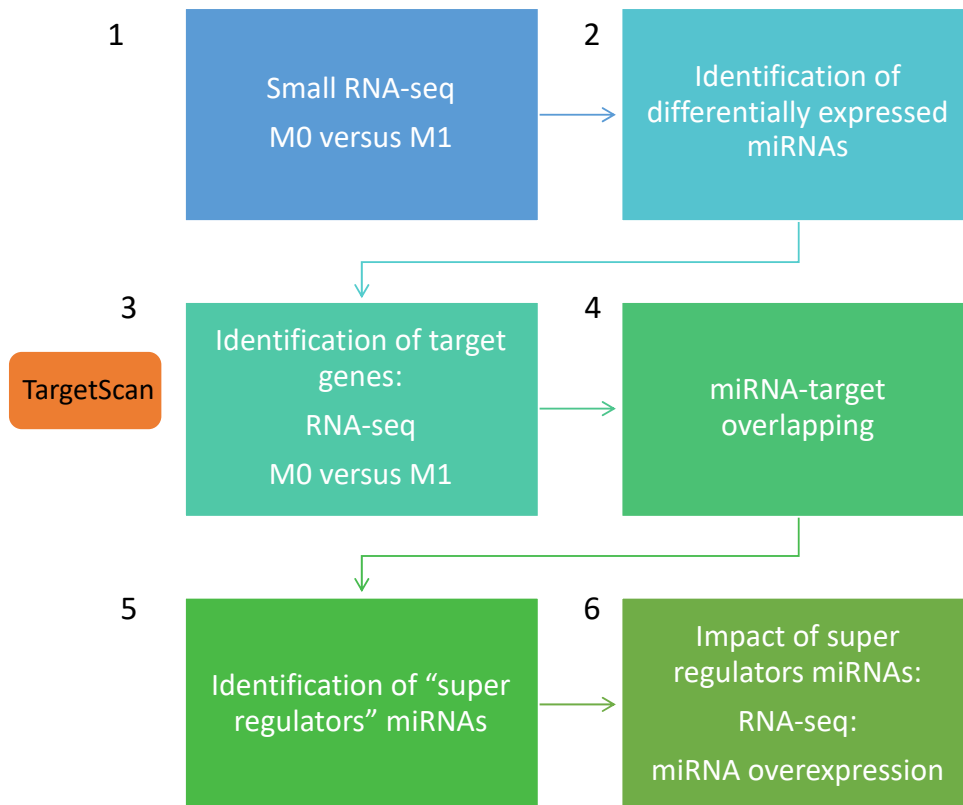


Figure 4.2. Overview of analysis strategy

RNA isolated from polarised macrophages (M0, M1) was sequenced (1) and analysed for the identification of differentially expressed small non-coding RNAs (i.e. microRNAs) (2). A microRNA-target prediction analysis was performed to identify the predicted target genes of the differentially expressed microRNA, which were detected using TargetScan and then evaluated their expression using a macrophage RNA-seq dataset (DOI: 10.17632/j2hmt7k9fh.1) (3,4); differentially expressed miRNAs with more than 500 predicted target genes were named “super regulators” (5). We selected three of them and evaluate their impact in samples transiently transfected with miRNA mimics and sent for RNA sequencing (6).

4.3.2. Differential expression of miRNAs in response to LPS and INF- γ in human primary macrophages

The majority of small RNAs sequenced consisted of miRNAs (~80%), but also other types, including piwi-interacting RNAs (piR), ribosomal RNAs, transfer RNAs (tRNA) and Y RNAs were found in our sequencing (~20%) (**Figure 4.3.**). The Principal Component Analysis (PCA), displayed as two-dimensional plot in **Figure 4.4.**, shows the distance between the two groups of samples. We observed that the majority of samples cluster according to the treatment (M0 and M1). The heatmap (**Figure 4.5. A**) highlights the differential expression of small RNAs across the samples. The volcano plot (**Figure 4.5. B**), showing the statistical significance (y axis) versus the magnitude of the fold change (x axis), highlights upregulated and downregulated small RNAs (green), as well as small RNAs passing the threshold of our analysis (orange and red) (adjusted p value 0.05, fold change 1). A total of 272 small non-coding RNAs were differentially expressed between the two groups; among them, 73 were miRNAs: 47 were downregulated and 26 were upregulated in M1 macrophages, compared to unpolarised cells. A previous study performed on murine BMDMs by using a miRNA-microarray, detected a total of 120 miRNAs differentially expressed between M0 and M1 polarised cells, but with only 1 miRNA downregulated (*Zhang et al. 2013*). In our analysis, the majority of differentially expressed miRNAs were downregulated in M1 cells. Cobos Jimenez and colleagues also identified a total of 303 differentially expressed miRNAs across human monocytes and polarised macrophages by using SOLID sequencing and RT-qPCR (*Cobos Jimenez et al. 2013*). Among the differentially expressed miRNAs we observed miR-155-5p (up), miR-125a-3p (up), miR-149-5p (down) and miR-191-3p (down). These miRNAs have all been reported to control macrophage M1/M2 polarisation and response to infection (*Curtale et al., 2019*). Differentially expressed miRNAs are listed in **Table 4.3.** and **Table 4.4.**, while the complete list of differentially expressed small RNAs is provided in Chapter 8 (Appendix III), along with expression and p-values. However, small RNAs other than miRNAs were not further investigated in this thesis.

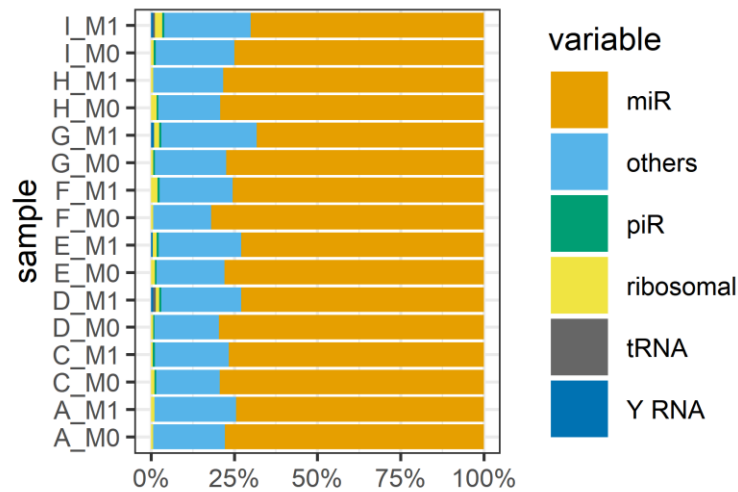


Figure 4.3. Percentage of RNA types sequenced

Bar chart graph showing the % of RNA classes sequenced in our small non-coding sequencing (figure made in R). miR= microRNA; piR= piwi-interacting RNA; tRNA=transfer RNA; letters refer to different individuals; M1 and M0 refer to polarised (LPS+INF- γ) and unpolarised (untreated) macrophages.

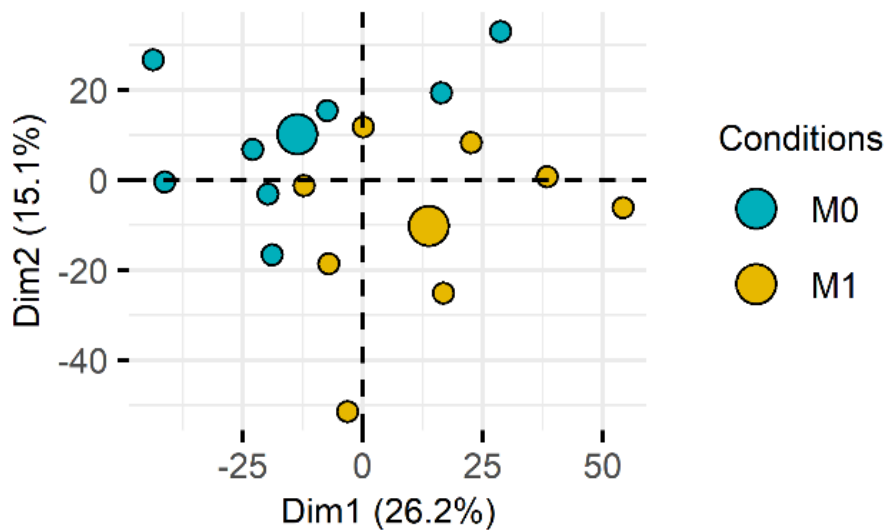


Figure 4.4. PCA plot of small RNA-seq

PCA plot of small non-coding RNA-seq data showing the clustering of the samples according to their gene expression. Dots represent different samples; larger dots represent the class-centroid. Figure was made in R from CPM values.

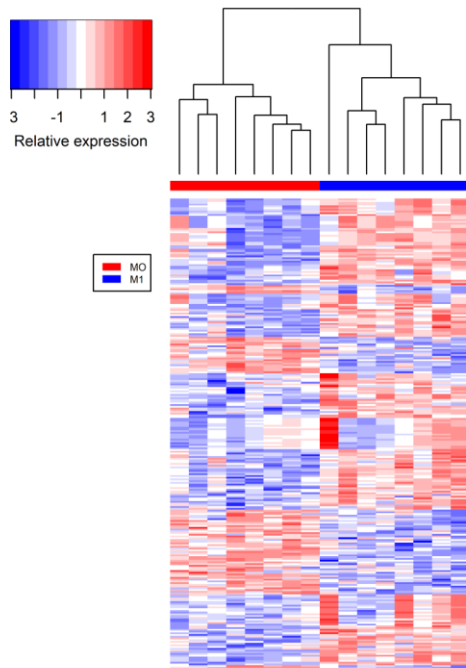
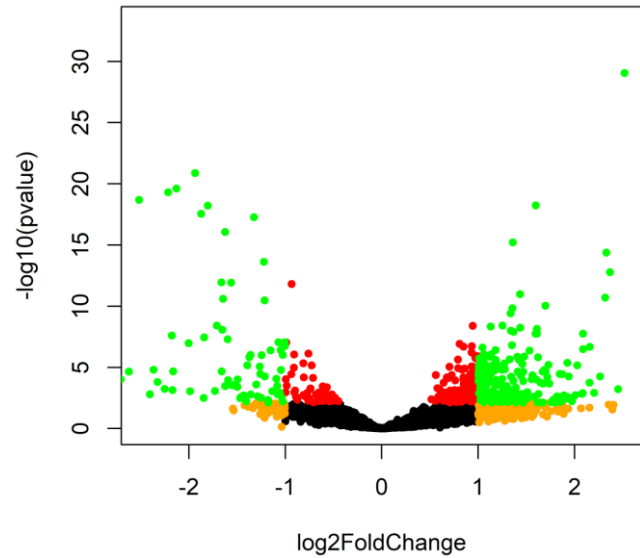
A**B**

Figure 4.5. Differential expression of small RNAs in pro-inflammatory M1 macrophages

Heatmap of small non-coding RNA sequencing showing the differential expression of small RNAs across the two groups of samples (heatmap generated in R) (**A**); volcano plot showing small RNAs passing cut off of adjusted p value 0.05 (red), small RNAs passing threshold of log fold change 0 (orange); significant small RNAs with cut off of adjusted p-value 0.05 and log fold change 1 (green); not statistically significant small RNAs (black) (**B**).

Table 4.3. List of upregulated miRNAs

The table lists the miRNAs significantly upregulated in M1 macrophages, compared to M0 cells; baseMean is the average of the normalised count values; log2FoldChange represents the effect size estimate: how much the expression of a gene changed due to the treatment (M0 vs M1); lfcSE is the standard error estimate for the log2FoldChange; stat represents the wald statistics; pvalue is attained by the wald test; padj is the pvalue corrected for multiple testing using the Benjamini and Hochberg method.

rnacentral_id	description	baseMean	log2FoldChange	lfcSE	stat	pvalue	padj
URS0000D54CAD	hsa-miR-155-5p	211862.08	2.83	0.23	12.05	1.89E-33	3.67E-31
URS00004208C5	hsa-miR-9-5p	1644.39	1.60	0.18	8.89	5.88E-19	3.36E-17
URS00003D4175	hsa-miR-3614-5p	66.96	3.59	0.44	8.17	3.01E-16	1.17E-14
URS000040DCFF	hsa-miR-186-5p	1826.38	1.36	0.17	8.09	6.10E-16	2.15E-14
URS0000410073	hsa-miR-4773	11.84	6.73	0.86	7.82	5.47E-15	1.63E-13
URS0000424278	hsa-miR-147b	300.29	2.37	0.32	7.37	1.69E-13	3.87E-12
URS0000591950	hsa-miR-7-5p	298.69	1.44	0.21	6.80	1.07E-11	1.98E-10
URS00001F0C23	hsa-miR-125a-3p	55.30	2.32	0.35	6.70	2.05E-11	3.61E-10
URS00002DABEA	hsa-miR-125b-1-3p	13.47	4.97	0.74	6.67	2.56E-11	4.33E-10
URS00002198F3	hsa-miR-449c-5p	16.15	2.95	0.45	6.58	4.59E-11	7.13E-10
URS0000593537	hsa-miR-221-5p	178.13	1.70	0.26	6.48	9.34E-11	1.39E-09
URS000061B694	hsa-miR-146b-5p	12821.77	1.13	0.19	5.86	4.72E-09	6.54E-08
URS00003496BE	hsa-miR-9-3p	71.05	1.44	0.25	5.82	5.88E-09	7.86E-08
URS000075BEBE	hsa-miR-324-5p	35.93	2.09	0.37	5.64	1.75E-08	2.19E-07
URS00001F5B39	hsa-miR-449a	15.61	2.16	0.42	5.18	2.17E-07	2.10E-06
URS00000FC8EB	hsa-miR-1301-3p	1694.09	1.06	0.22	4.84	1.32E-06	1.13E-05
URS00004B1671	hsa-miR-1307-3p	1602.06	1.48	0.31	4.83	1.34E-06	1.13E-05
URS000001C659	hsa-miR-135b-5p	7.14	4.50	0.93	4.83	1.40E-06	1.16E-05
URS00001C308D	hsa-miR-99b-3p	1258.45	1.28	0.29	4.34	1.44E-05	1.01E-04
URS00001123BD	hsa-miR-29b-1-5p	24.72	1.41	0.33	4.24	2.20E-05	1.50E-04
URS000031B6ED	hsa-miR-365a-5p	8.28	1.87	0.45	4.13	3.58E-05	2.28E-04
URS000043D1A9	hsa-miR-30a-5p	93.87	1.03	0.27	3.84	1.23E-04	6.63E-04
URS000034309A	hsa-miR-155-3p	8.34	3.31	0.87	3.79	1.54E-04	8.05E-04
URS00000AA464	hsa-miR-193b-3p	22.03	1.39	0.40	3.50	4.59E-04	2.09E-03
URS0000381B86	hsa-miR-3200-3p	5.17	1.82	0.60	3.05	2.32E-03	8.80E-03
URS0000244A71	hsa-miR-181c-3p	5.05	1.47	0.55	2.67	7.57E-03	2.41E-02

Table 4.4. List of downregulated miRNAs

The table lists the miRNAs significantly downregulated in M1 macrophages, compared to M0 cells; baseMean is the average of the normalised count values; log2FoldChange represents the effect size estimate: how much the expression of a gene changed due to the treatment (M0 vs M1); lfcSE is the standard error estimate for the log2FoldChange; stat represents the wald statistics; pvalue is attained by the wald test; padj is the pvalue corrected for multiple testing using the Benjamini and Hochberg method.

rnacentral_id	description	baseMean	log2FoldChange	lfcSE	stat	pvalue	padj
URS000056B04E	hsa-miR-425-3p	240.87	-3.61	0.3	-1.21E+01	7.05E-34	2.73E-31
URS000005D4F5	hsa-miR-345-5p	407.73	-2.21	0.24	-9.16E+00	5.00E-20	4.85E-18
URS0000237FB8	hsa-miR-30c-1-3p	64.7	-2.52	0.28	-9.01E+00	2.06E-19	1.60E-17
URS0000045DBD	hsa-miR-3613-5p	163.6	-1.8	0.2	-8.89E+00	6.07E-19	3.36E-17
URS00002CBC6D	hsa-miR-4787-3p	280.84	-1.87	0.21	-8.72E+00	2.78E-18	1.35E-16
URS0000080D0A	hsa-miR-5480-3p	809.22	-1.63	0.2	-8.32E+00	8.94E-17	3.85E-15
URS00002B2B5C	hsa-miR-191-3p	15.6	-4.75	0.61	-7.85E+00	4.02E-15	1.30E-13
URS000060AABB	hsa-miR-1249-3p	428.54	-1.22	0.16	-7.63E+00	2.36E-14	6.55E-13
URS000075E96D	hsa-miR-7974	35.02	-2.97	0.39	-7.62E+00	2.60E-14	6.73E-13
URS00001C770D	hsa-miR-149-5p	15.83	-3.04	0.41	-7.47E+00	8.12E-14	1.97E-12
URS000002103A	hsa-miR-1296-5p	11.92	-4.6	0.63	-7.33E+00	2.22E-13	4.78E-12
URS00001012BC	hsa-miR-766-3p	58.79	-1.56	0.22	-7.11E+00	1.19E-12	2.30E-11
URS00004E57E7	hsa-miR-23b-3p	65.82	-1.66	0.23	-7.11E+00	1.16E-12	2.30E-11
URS00000CF1D2	hsa-miR-361-5p	827.74	-1.22	0.18	-6.63E+00	3.38E-11	5.47E-10
URS000075C34D	hsa-miR-1273h-3p	288.28	-1.71	0.29	-5.89E+00	3.97E-09	5.71E-08
URS0000241987	hsa-miR-181a-2-3p	172.07	-1.65	0.29	-5.76E+00	8.52E-09	1.10E-07
URS00001597DC	hsa-miR-331-5p	11.68	-2.18	0.39	-5.57E+00	2.56E-08	3.10E-07
URS00003FFA6C	hsa-miR-550a-5p	20.68	-1.84	0.33	-5.51E+00	3.51E-08	4.12E-07
URS0000384021	hsa-miR-106b-3p	23.54	-1.6	0.29	-5.45E+00	5.04E-08	5.75E-07
URS000003F252	hsa-miR-181a-3p	1081.27	-1.07	0.2	-5.35E+00	8.95E-08	9.92E-07
URS00000DA3DF	hsa-miR-1343-3p	8.82	-4.13	0.79	-5.24E+00	1.65E-07	1.73E-06
URS000050E4BA	hsa-miR-941	1798.91	-1	0.19	-5.22E+00	1.81E-07	1.84E-06
URS00000451A1	hsa-miR-378a-3p	131428.28	-1.05	0.21	-5.07E+00	3.93E-07	3.72E-06
URS00003E16E5	hsa-miR-148a-5p	140.82	-1.15	0.23	-5.07E+00	4.08E-07	3.77E-06
URS0000079D48	hsa-miR-1180-3p	196.05	-1.36	0.28	-4.90E+00	9.73E-07	8.58E-06
URS00004B2A47	hsa-miR-30d-3p	49.73	-1.37	0.29	-4.81E+00	1.51E-06	1.22E-05
URS000015D23B	hsa-miR-26a-2-3p	22.22	-1.39	0.31	-4.50E+00	6.96E-06	5.40E-05
URS00004FCB5F	hsa-mir-RG-126 varia	6.12	-3.24	0.72	-4.48E+00	7.60E-06	5.78E-05
URS00004C9052	hsa-miR-133a-3p	100.63	-1.26	0.28	-4.45E+00	8.43E-06	6.29E-05
URS000003ABC4	hsa-miR-26b-3p	22.32	-2.37	0.55	-4.32E+00	1.56E-05	1.08E-04
URS000023BE29	hsa-miR-139-3p	154.63	-1.26	0.3	-4.14E+00	3.41E-05	2.24E-04
URS0000554A4F	hsa-miR-199a-5p	33.16	-1.09	0.28	-3.93E+00	8.49E-05	4.92E-04
URS000052AB63	hsa-miR-4684-3p	14.5	-1.49	0.38	-3.90E+00	9.82E-05	5.52E-04
URS00005092C2	hsa-miR-335-3p	8.62	-1.59	0.41	-3.86E+00	1.12E-04	6.22E-04
URS00000BD1DE	hsa-miR-219a-1-3p	24.48	-1.3	0.36	-3.66E+00	2.54E-04	1.28E-03
URS0000065D58	hsa-miR-30a-3p	18.51	-1.52	0.42	-3.60E+00	3.18E-04	1.58E-03
URS00002F8148	hsa-let-7f-1-3p	9.54	-1.62	0.45	-3.58E+00	3.43E-04	1.66E-03
URS0000D55DFB	hsa-miR-224-5p	14.74	-1.73	0.52	-3.33E+00	8.53E-04	3.76E-03
URS0000246356	hsa-miR-885-5p	23.42	-1.14	0.34	-3.32E+00	8.91E-04	3.88E-03
URS000075AEBC	hsa-miR-6813-5p	5.52	-1.99	0.6	-3.32E+00	9.02E-04	3.89E-03
URS000023133F	hsa-miR-4709-3p	31.81	-1.08	0.34	-3.16E+00	1.58E-03	6.32E-03
URS00001C85C7	hsa-miR-1294	12.23	-1.29	0.42	-3.04E+00	2.34E-03	8.80E-03
URS0000156390	hsa-miR-4746-5p	43.49	-1.04	0.35	-2.99E+00	2.80E-03	1.02E-02
URS000044EF2B	hsa-miR-4664-3p	29.8	-1.25	0.42	-2.96E+00	3.05E-03	1.09E-02
URS0000383E7F	hsa-miR-133a-5p	9.07	-1.18	0.44	-2.68E+00	7.44E-03	2.39E-02
URS00005918D5	hsa-let-7b-3p	8.67	-1.1	0.42	-2.61E+00	9.11E-03	2.83E-02
URS000030C9DE	hsa-miR-652-5p	10.6	-1.15	0.46	-2.52E+00	1.17E-02	3.54E-02

4.3.3. Identification of “super regulator” miRNAs: miRNA-target prediction analysis and datasets overlapping

miRNAs regulate gene expression through physically targeting the mRNA of protein-coding genes, therefore once we identified candidate miRNAs differentially expressed between M0 and M1 macrophages, we performed a target prediction analysis by using TargetScan (http://www.targetscan.org/vert_72/). We downloaded the predicted target genes of both upregulated and downregulated miRNAs and carried out a Gene Ontology and KEGG Pathway Enrichment analysis by using GOSeq. However, among the putative target genes, we only considered those differentially expressed in human polarised macrophages. To this aim, we used an RNA-seq dataset previously generated in our lab (DOI: 10.17632/j2hmt7k9fh.1) and performed an overlaying between DE miRNAs and DE target genes. We chose this dataset as it was carried out following the same cell isolation and polarisation protocol (M^{un} and M1^{LPS+INF- γ}) and it was done using the same number of donors (n=8 per group). The method used to analyse the RNA-seq dataset is described in detail Chapter 2 (Section 2.2.). The PCA of the RNA-seq is shown in **Figure 4.6**. We observed two distinct groups of samples suggesting that the M1-polarising stimuli caused a robust gene expression profile change, consistent in all samples. The volcano plot shows that 5681 genes are significantly differentially expressed: 2728 genes are upregulated, 2953 are downregulated (**Figure 4.7**). We found that 1573 upregulated genes are predicted targets of 44 downregulated miRNAs (**Table 4.5**). Similarly, 1790 downregulated genes are potential targets of 26 upregulated miRNAs (**Table 4.6**). Distinct miRNAs are also predicted to have common target genes. When we counted the number of predicted target genes of each DE miRNA it ranged from 9 to 740 (**Figure 4.8**): we selected those targeting more than 500 genes and named them “super regulators” (**Table 4.7**). Next, we assessed the expression of selected super regulators by using RT-qPCR. For the upregulated miRNAs, we also chose to include miR-155-5p which has less than 500 target genes but it is a well characterized miRNA in pro-inflammatory macrophages (*Jablonski et al., 2016, Curtale et al., 2019*). Therefore, we used it as a “positive control” in the further analysis. Similarly, for the downregulated miRNAs, we included miR-149-5p as it is negatively modulated in response to inflammatory stimuli (*Xu et al., 2014*). We measured the expression of the upregulated miRNAs in polarised MDMs from 9 different donors: miR-155-5p and miR-125a-3p were significantly upregulated in M1 macrophages, compared to unpolarised cells (p<0.0001, p=0.003, respectively) (**Figure 4.9. A, B**); miR-186-5p expression was also increased but the change was not statistically significant (p=0.07) (**Figure 4.9. C**).

However, the expression of the downregulated miRNAs, measured in 5 donors, was highly variable and in some samples was increased in M1, compared to M0 and miR-149-5p was expression was not detected in samples from 2 different donors (**Figure 4.9. D-F**). This could be explained by the very low expression levels of these miRNAs: the Ct values generated in the RT-qPCR were very high, compared to the housekeeping gene (average Ct values for the housekeeping U6 was 20, average Ct values for miR-766-3p, miR-149-5p and miR-1343-3p was > 33). KEGG pathway enrichment analysis (**Figure 4.10. A**) highlights that the target genes of downregulated miRNAs are involved in cytokine and chemokine signalling pathways, antigen presentation, T cell receptor signalling pathway, apoptosis and MAPK signalling pathway, while the target genes of upregulated miRNAs seem to participate in cell cycle and DNA replication mechanisms. Similarly, the gene ontology terms (**Figure 4.10. B**), divided into biological process, cellular component and molecular function, show that the target genes of downregulated miRNAs are involved in innate immune and cytokine-mediated cellular responses: they localise in the plasma membrane or cell surface, regulating chemokine/cytokine receptor and ligand activity. Conversely, when we looked at genes potentially targeted by upregulated miRNAs, we observed that they act as regulators of mitosis and cell cycle and localise intracellularly. In fact, M1-like macrophages and macrophages activated with LPS and INF- γ are highly cytotoxic and less viable, compared to M2 cells (*Martinez et al., 2008*). We also performed a gene enrichment component analysis on the potential targets of super regulator miRNAs: the most significant enriched terms for the genes targeted by upregulated miRNAs were chromosome assembly and condensation (**Figure 4.11. A**), while for the genes targeted by downregulated miRNAs, which are overexpressed in M1 macrophages, significant enriched terms were responses to the cytokine INF- γ (**Figure 4.11. B**). This suggests that super regulators also have common target genes and it is particularly evident for the targets of downregulated miRNAs. In fact, we can observe that INF- γ signalling pathway is not only the most significant ($-\log_{10} \text{FDR} > 4$), but it is also common between 3 super regulators. To substantiate this, we calculated the overlap between super regulator target genes, by using Jaccard Index analysis. The Jaccard index of two or more gene lists counts the number of genes in the intersection divided by the number of genes in the union of the gene lists and it is a number between 0 and 1: the higher the index, the higher the overlap (*Bass et al., 2013*). We found that there is an overlap of 19% to 33% between upregulated miRNAs target genes (**Figure 4.12. A**) and of 29% to 39% between downregulated target genes (**Figure 4.12. B**). The highest % was for miR-1343-3p and miR-766-3p pair (39% genes overlapping).

Interestingly, miR-1343-3p was also one of the most downregulated by M1-polarising stimuli, as it shows a log₂ fold change of -4.13 (see **Table 4.4.**), suggesting it might have a big impact on gene expression. So far, this miRNA has not been investigated in the literature.

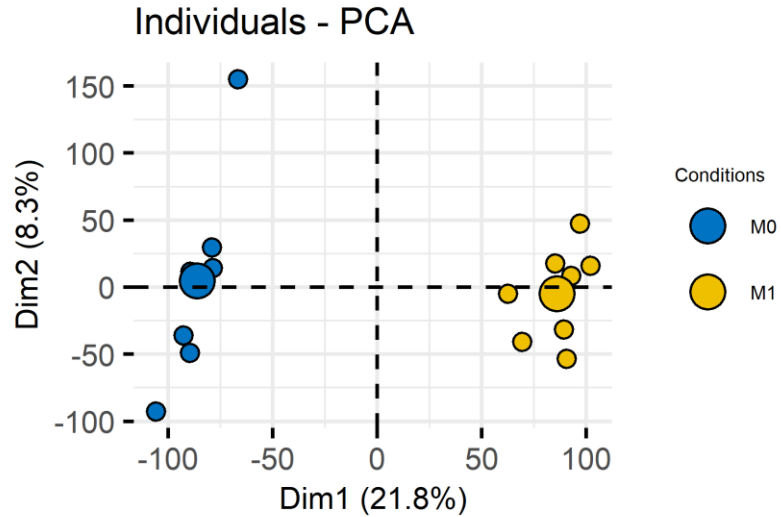


Figure 4.6. PCA plot of RNA-seq data

PCA plot of RNA-seq data showing the clustering of the samples according to their gene expression. Dots represent different samples; larger dots are the class-centroids. Plots were made in R from CPM values.

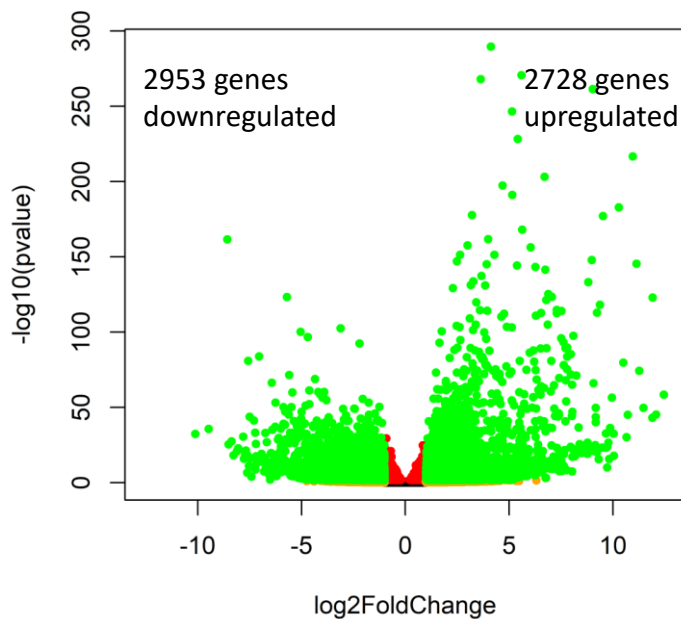


Figure 4.7. Volcano plot of RNA-seq data

Volcano plot of RNA-seq data showing genes passing cut-off of adjusted p value 0.05 (red), genes passing threshold of Log fold change 1 (orange); significant genes with cut-off of adjusted p-value 0.05 and log fold change 1 (green). Plot made in R.

Table 4.5. Number of target genes of upregulated miRNAs

	small RNA seq		RNA seq
miRNA	M1 expression	Target genes	M1 expression
hsa-miR-193b-3p	Upregulated	26	Downregulated
hsa-miR-135b-5p	Upregulated	42	Downregulated
hsa-miR-449a	Upregulated	55	Downregulated
hsa-miR-146b-5p	Upregulated	56	Downregulated
hsa-miR-99b-3p	Upregulated	58	Downregulated
hsa-miR-125b-1-3p	Upregulated	59	Downregulated
hsa-miR-147b	Upregulated	95	Downregulated
hsa-miR-181c-3p	Upregulated	175	Downregulated
hsa-miR-30a-5p	Upregulated	185	Downregulated
hsa-miR-449c-5p	Upregulated	193	Downregulated
hsa-miR-1307-3p	Upregulated	212	Downregulated
hsa-miR-3200-3p	Upregulated	258	Downregulated
hsa-miR-324-5p	Upregulated	324	Downregulated
hsa-miR-155-3p	Upregulated	333	Downregulated
hsa-miR-155-5p	Upregulated	362	Downregulated
hsa-miR-365a-5p	Upregulated	401	Downregulated
hsa-miR-221-5p	Upregulated	430	Downregulated
hsa-miR-9-3p	Upregulated	471	Downregulated
hsa-miR-1301-3p	Upregulated	480	Downregulated
hsa-miR-9-5p	Upregulated	481	Downregulated
hsa-miR-29b-1-5p	Upregulated	490	Downregulated
hsa-miR-7-5p	Upregulated	533	Downregulated
hsa-miR-125a-3p	Upregulated	555	Downregulated
hsa-miR-3614-5p	Upregulated	566	Downregulated
hsa-miR-4773	Upregulated	617	Downregulated
hsa-miR-186-5p	Upregulated	739	Downregulated

Table 4.6. Number of target genes of downregulated miRNAs

	small RNA seq		RNA seq
miRNA	M1 expression	Target genes	M1 expression
hsa-miR-550a-5p	Downregulated	9	Upregulated
hsa-miR-23b-3p	Downregulated	38	Upregulated
hsa-let-7b-3p	Downregulated	39	Upregulated
hsa-miR-4787-3p	Downregulated	48	Upregulated
hsa-miR-30d-3p	Downregulated	53	Upregulated
hsa-miR-181a-3p	Downregulated	54	Upregulated
hsa-miR-26a-2-3p	Downregulated	59	Upregulated
hsa-miR-1180-3p	Downregulated	62	Upregulated
hsa-miR-4664-3p	Downregulated	65	Upregulated
hsa-miR-106b-3p	Downregulated	66	Upregulated
hsa-miR-191-3p	Downregulated	71	Upregulated
hsa-miR-1249-3p	Downregulated	72	Upregulated
hsa-miR-425-3p	Downregulated	92	Upregulated
hsa-miR-4746-5p	Downregulated	92	Upregulated
hsa-miR-6813-5p	Downregulated	100	Upregulated
hsa-miR-941	Downregulated	105	Upregulated
hsa-let-7f-1-3p	Downregulated	143	Upregulated
hsa-miR-1296-5p	Downregulated	208	Upregulated
hsa-miR-30c-1-3p	Downregulated	210	Upregulated
hsa-miR-3613-5p	Downregulated	243	Upregulated
hsa-miR-652-5p	Downregulated	257	Upregulated
hsa-miR-331-5p	Downregulated	266	Upregulated
hsa-miR-885-5p	Downregulated	297	Upregulated
hsa-miR-4684-3p	Downregulated	310	Upregulated
hsa-miR-219a-1-3p	Downregulated	321	Upregulated
hsa-miR-139-3p	Downregulated	327	Upregulated
hsa-miR-361-5p	Downregulated	347	Upregulated
hsa-miR-133a-5p	Downregulated	351	Upregulated
hsa-miR-378a-3p	Downregulated	363	Upregulated
hsa-miR-1294	Downregulated	374	Upregulated
hsa-miR-199a-5p	Downregulated	376	Upregulated
hsa-miR-148a-5p	Downregulated	389	Upregulated
hsa-miR-345-5p	Downregulated	402	Upregulated
hsa-miR-1273h-3p	Downregulated	418	Upregulated
hsa-miR-224-5p	Downregulated	444	Upregulated
hsa-miR-26b-3p	Downregulated	447	Upregulated
hsa-miR-7974	Downregulated	460	Upregulated
hsa-miR-181a-2-3p	Downregulated	468	Upregulated
hsa-miR-30a-3p	Downregulated	494	Upregulated
hsa-miR-149-5p	Downregulated	497	Upregulated
hsa-miR-4709-3p	Downregulated	506	Upregulated
hsa-miR-1343-3p	Downregulated	620	Upregulated
hsa-miR-766-3p	Downregulated	653	Upregulated
hsa-miR-335-3p	Downregulated	734	Upregulated

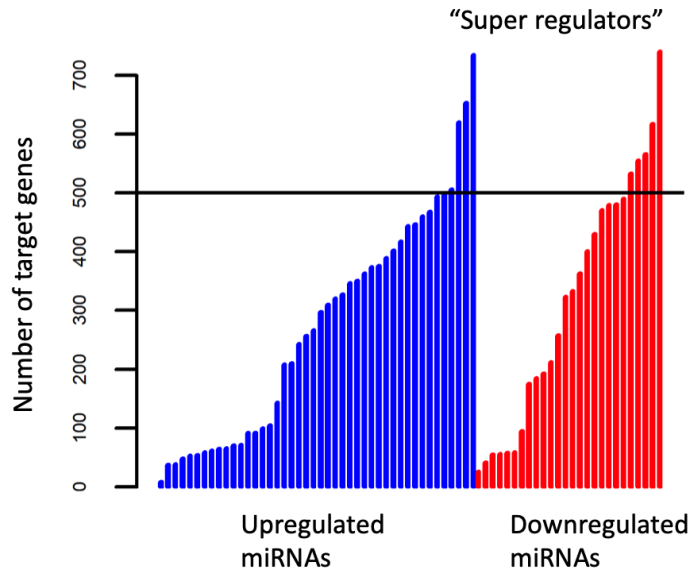


Figure 4.8. Number of differentially expressed miRNA-target genes

The graph shows the number of predicted target genes (y axis) of differentially expressed miRNAs (x axis); downregulated miRNAs are shown in red, upregulated miRNAs are shown in blue. miRNA-target prediction analysis was done by using TargetScan. The list of the target genes was then filtered using only genes differentially expressed in the macrophage RNA-seq (DOI: 10.17632/j2hmt7k9fh.1).

Table 4.7. List of “super regulator” miRNAs with more than 500 target genes in macrophages

The table lists the number of target genes of differentially expressed miRNAs in human macrophage (M1^{LPS+INF γ}), predicted by the algorithm TargeScan. Genes were filtered selecting only those differentially expressed by human macrophages, according to the dataset DOI: 10.17632/j2hmt7k9fh.1.

miRNAs	Expression M0 vs M1	Number of target genes
hsa-miR-7-5p	Upregulated	533
hsa-miR-125a-3p	Upregulated	555
hsa-miR-3614-5p	Upregulated	566
hsa-miR-4773	Upregulated	617
hsa-miR-186-5p	Upregulated	739
has-miR-155-5p	Upregulated	362
hsa-miR-4709-3p	Downregulated	506
hsa-miR-1343-3p	Downregulated	620
hsa-miR-766-3p	Downregulated	653
hsa-miR-335-3p	Downregulated	734

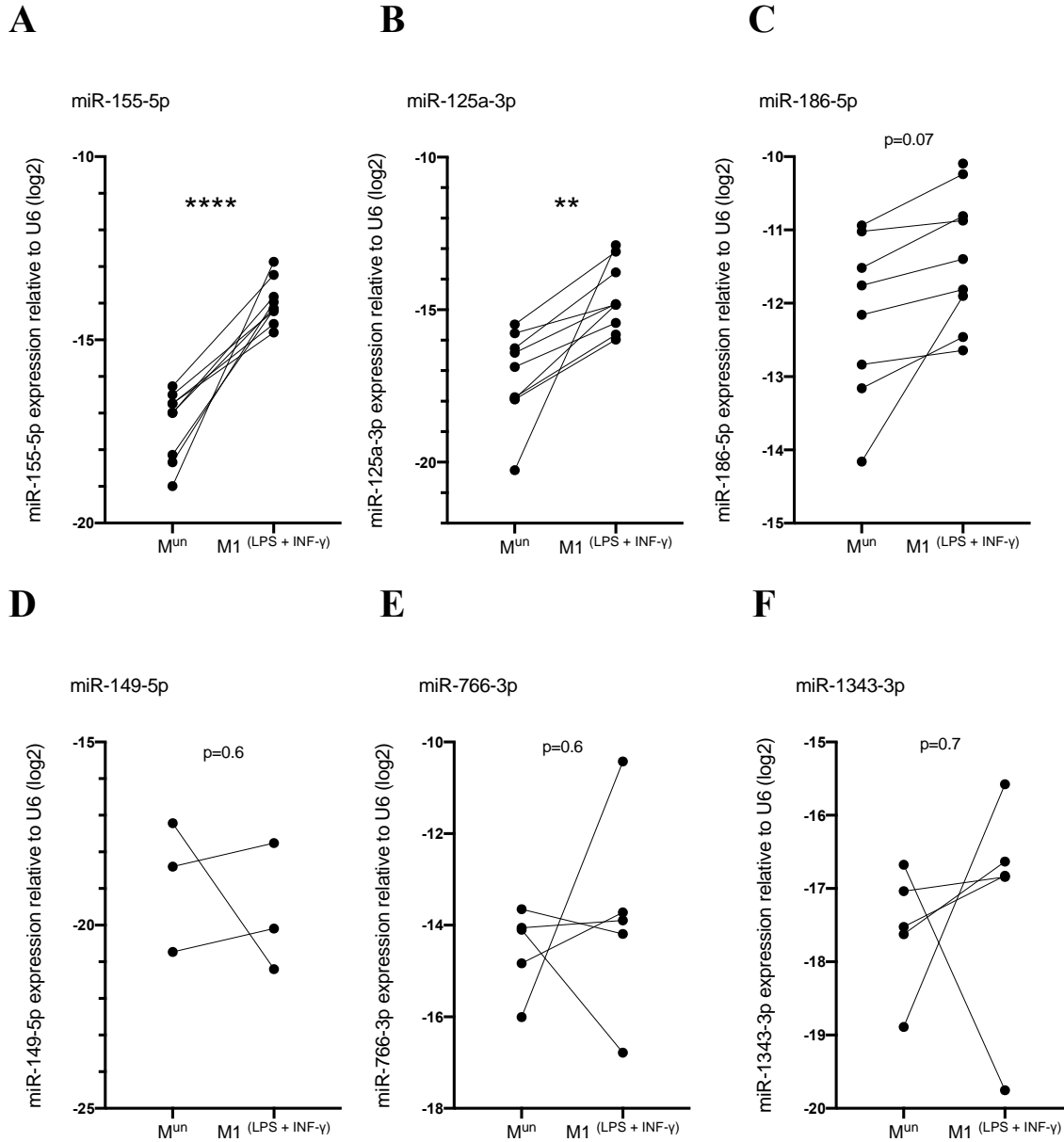


Figure 4.9. Assessment of “super regulator” miRNAs by RT-qPCR

Relative abundance of miR-155-5p (**A**), miR-125a-3p (**B**) and miR-186-5p (**C**) normalised to the housekeeping U6 (upregulated miRNAs); relative abundance of miR-149-5p (**D**), miR-766-3p (**E**) and miR-1343-3p (**F**) normalised to the housekeeping U6 (downregulated miRNAs). Data were analysed using the log2 transformed 2-DCT values and presented as individual points (n = 3-9, paired t-test, **** p < 0.0001, ** p < 0.01, ns p ≥ 0.05).

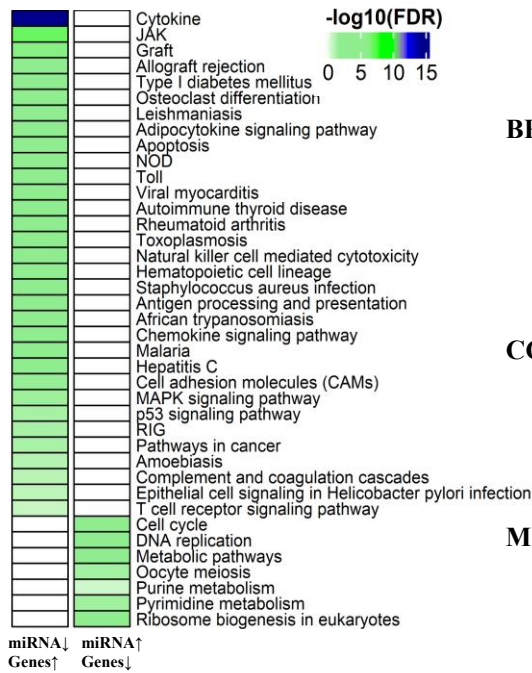
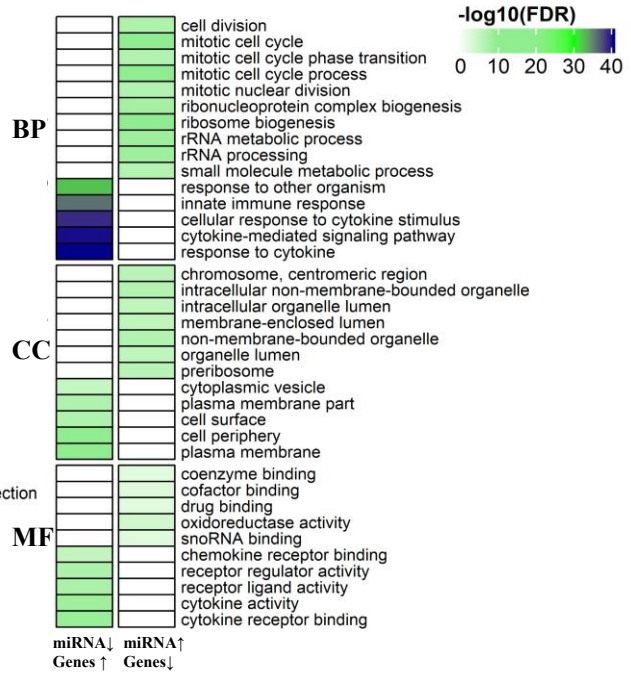
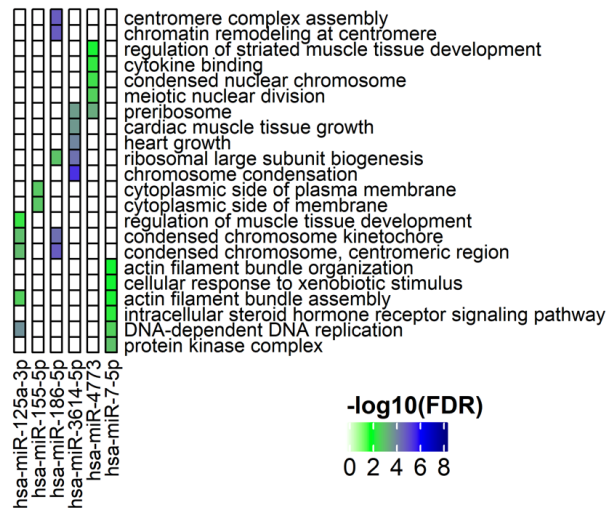
A**B**

Figure 4.10. Gene Ontology and KEGG Pathway Enrichment analysis of DE miRNAs target genes

KEGG Pathway enrichment analysis (A) and Gene Ontology terms (B) of macrophage-specific genes, predicted to be regulated by differentially expressed miRNAs. First column shows the condition in which miRNAs are downregulated and their target genes are upregulated; the second column shows the opposite, downregulated genes and upregulated miRNAs. BP= biological process, CC= cellular component, MF= molecular function. Analysis was performed using GOSeq, heatmaps were generated in R.

A Target genes of upregulated miRNAs



B Target genes of downregulated miRNAs

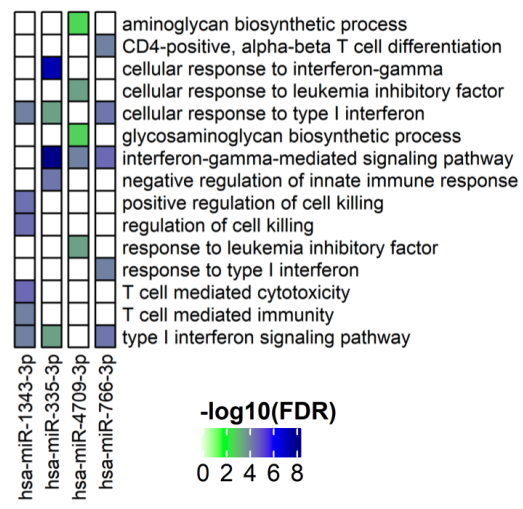
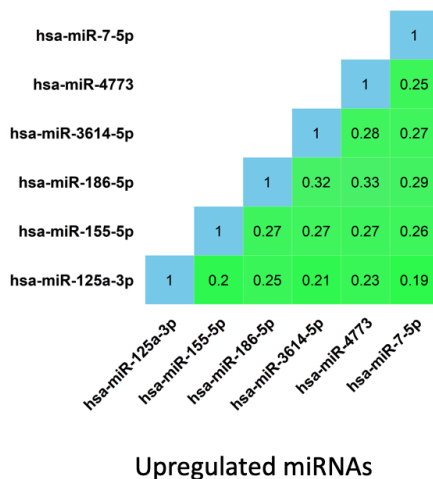


Figure 4.11. Gene Ontology terms of target genes of “super regulator” miRNAs

Gene Ontology terms of genes targeted by upregulated miRNAs (A) and downregulated miRNAs (B). Analysis was done by using GOSeq. Heatmaps were generated in R.

A



B

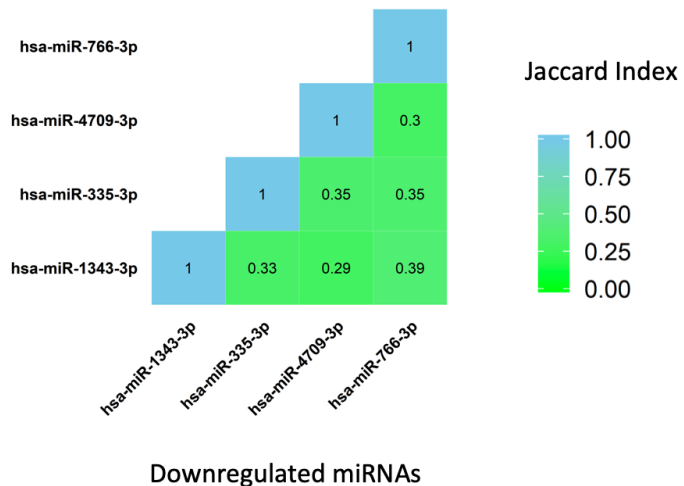


Figure 4.12. Target genes overlapping: Jaccard Index

Target gene overlapping analysis using Jaccard Index: overlapping between upregulated (A) and downregulated (B) miRNAs target genes. Diagrams were generated in R.

4.3.4. Impact of “super regulator” miRNAs on macrophage transcriptome

To substantiate the role of “super regulator” miRNAs in macrophages, we performed an RNA-seq on MDMs, transfected with mimics of selected miRNAs. Our previous RNA-seq on polarised macrophages showed that M1-polarising stimuli led to more gene downregulation, compared to upregulation (2953 were downregulated, 2728 genes were upregulated). Although the difference in the number of genes down- and up-regulated is small (only 225 genes), we decided to focus on the activity of upregulated miRNAs, which in turn could contribute to the downregulation of these genes and to the M1 phenotype. We transiently overexpressed miR-155-5p, miR-125a-3p and miR-186-5p in MDMs by using miRNA mimics and analysed their impact on gene expression. miRNA-155-5p is not a super regulator by our definition, but we included it as a positive control, due to its well characterised biological function in macrophage polarisation. We used MDMs isolated from 6 different individuals and transfected them for 24 hours with 50nM of miRNA mimics or negative control. Prior to the RNA-seq we confirmed the overexpression of the 3 miRNAs by using RT-qPCR (**Figure 4.13.**). The sequencing was carried out by the company Novogene using Illumina technology. We performed 3 simultaneous paired-analysis: each miRNA mimic versus the negative control. Unfortunately, the PCA plots (**Figure 4.14.**) did not show defined clusters between conditions. This can be explained by several reasons: miRNAs endogenous expression is highly variable among different individuals and this can have a different impact on the overexpression experiment (as shown by RT-qPCR data), primary cells isolated from different donors might also respond differently to transient transfection. Results described in Chapter 3 are also affected by high variability, as macrophages are extremely sensitive and being cells of the innate immune system can be easily activated by *in vitro* procedures. Moreover, in this experiment, we used cells isolated from 3 male individuals and 3 female individuals, aged 23 to 28 and with different ethnicity. It is well appreciated that miRNAs expression can be different between males and females, as some studies have reported (*Dai et al., 2014, Cui et al., 2018*). Interestingly, the global PCA, plotted on the 3 overexpression experiments (miR-155-5p, miR-125a-3p, miR-186-5p vs negative control) (showed in **Figure 4.15.**) suggests that there is a clustering according to the gender of the donors. However, this was not further investigated in the present analysis due to the low number of individuals.

When we performed the differential expression analysis (each miRNA versus the negative control), we found only few significant differentially expressed genes (adjusted p value ≤ 0.05). Specifically, we found 158, 4 and 1 DE genes, for miR-155-5p, miR-125a-3p and miR-186-5p

respectively (list of significant DE genes is provided in Chapter 8, Appendix III). This was not surprising, as it is believed that the effect of miRNAs on gene expression is small and overexpressing a single miRNA not always leads to the downregulation of target genes, which is also seed region type- and context-dependent (*Liu et al., 2019*). Nevertheless, we carried on with the downstream analysis, considering the directional changes of the genes, rather than the p-values. The volcano plots on the DE analysis for each overexpressed miRNA are shown in **Figure 4.16**. The dots in green represent genes with an FDR ≤ 0.05 , including those with adjusted p values ≤ 0.05 . For miR-155-5p-overexpressing cells (**Figure 4.16. A**) there are more dysregulated genes passing the FDR threshold, both up- and downregulated, in comparison to miR-125a-3p and miR-186-5p overexpressing cells (**Figure 4.16. B, C**). When we compared the DE genes in each miRNA overexpression condition with DE genes between M0 and M1, we observed an interesting overlap (**Figure 4.17.**):

1. miR-155-5p: 362 target genes, previously identified as downregulated in M1 macrophages, 82 were upregulated and 280 were downregulated;
2. miR-125a-3p: among its 555 target genes, previously identified as downregulated in M1 macrophages, 336 were upregulated and 219 were downregulated;
3. miR-186-5p: among its 739 target genes, previously identified as downregulated in M1 macrophages, 326 were upregulated and 413 were downregulated.

Despite it being well established that miRNAs work by repressing the expression of target genes, the presence of upregulated transcripts is not surprising, even among their potential target genes. Overexpressing a miRNA by cell transient transfection leads to a massive perturbation of gene expression, by either direct or indirect activity (*Khan et al., 2009*). However, when we looked at the gene ontology terms of downregulated genes we found results consistent with the M1-like phenotype (**Figure 4.18.**): enrichment of genes involved in mitosis, cell cycle, DNA replication and chromosome condensation/segregation. The enriched terms for each miRNA overexpression experiment are specified below.

1. miR-155-5p: downregulation of genes related to DNA replication, mitosis and cell cycle; upregulation of genes involved in B cells activation and proliferation as well as chemokine signalling pathway;

2. miR-125a-3p: downregulation of genes involved in chromosome segregation and condensation; upregulation of genes related to inositol phosphate metabolism;
3. miR-186-5p: downregulation of genes related to chromosome and DNA package; upregulation of genes involved in mitosis and chromosome segregation.

The latter was not consistent with miR-155-5p and miR-125a-3p, as it shows similar enrichment for both down- and up-regulated genes. In fact, miR-186-5p has been well characterised in cancer, where it acts as either oncogene (inducing proliferation) or onco-suppressor (inducing apoptosis), depending on the tissue (*Wang et al., 2019*). Overall, this data suggests that the overexpression of these miRNAs affect DNA replication and mitosis. Therefore, we evaluated the effect of miRNA mimics on cells viability, using an MTT assay. This assay measures cells viability through a substrate that is reduced only by live and metabolically active cells. The assay did not show any significant difference (**Figure 4.19.**), likely due to either individuals or transfection variability, as well as the low n number. However, we can observe that samples transfected with the mimics tend to be less metabolically active, compared to the negative control.

Lastly, we looked at the identity of the genes showing the same direction in fold change of those differentially expressed in M1 macrophages. **Table 4.8.** lists the top 10 genes selected according to adjusted p values, while **Table 4.9.** shows those filtered according to the fold change. For the latter we prioritised downregulation. We observed that not all the genes show the same expression status in M1 macrophages and only some of them are predicted targets of the miRNAs. Among the downregulated genes in both miRNA overexpression and M1 macrophages we observed:

- E2F2 (miR-155-5p target), a transcription factor regulating inflammation (*Wang et al., 2018*);
- DUSP1 (miR-125a-3p target), negative regulator of MAPK signalling pathway;
- CCL1 (miR-214-5p target), ligand of the chemokine receptor CCR8, driving inflammation (*Kishi et al., 2016*).

Taken together, our results suggest that these miRNAs, strongly induced by LPS and INF- γ , contribute to the transcriptomic profile of human pro-inflammatory macrophages.

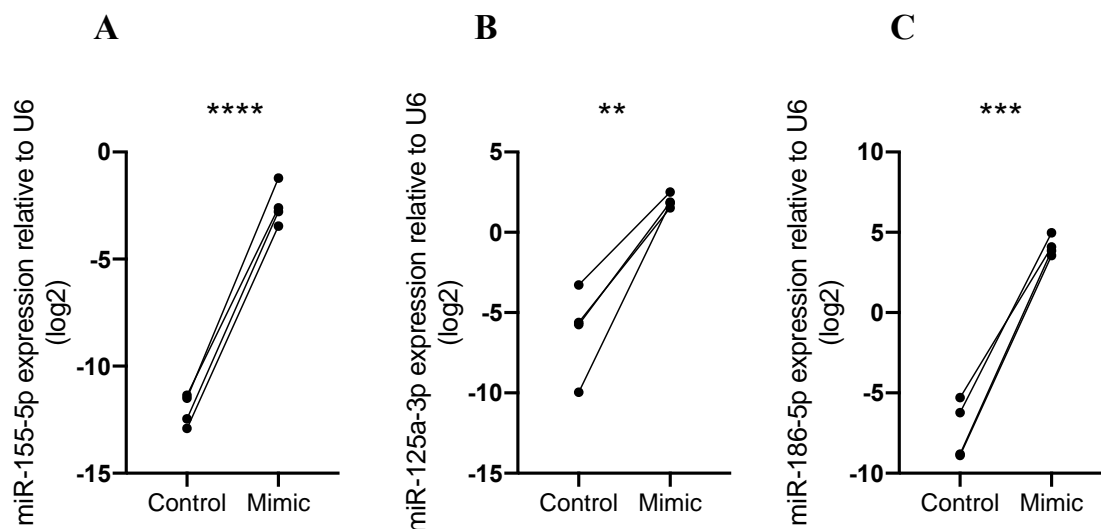


Figure 4.13. Confirmation of miRNAs overexpression in transfected MDMs by RT-qPCR

Relative abundance of miR-155-5p (A), miR-125a-3p (B) and miR-186-5p (C) normalised to the housekeeping U6 in MDMs transiently transfected with miRNA mimics or negative control. Total RNA transfected was 50nM per well, in a 6 well plate. Data were analysed using the log2 transformed 2-DCT values and presented as individual points (n =4, paired t-test, **** p<0.0001, *** p<0.001, ** p<0.01).

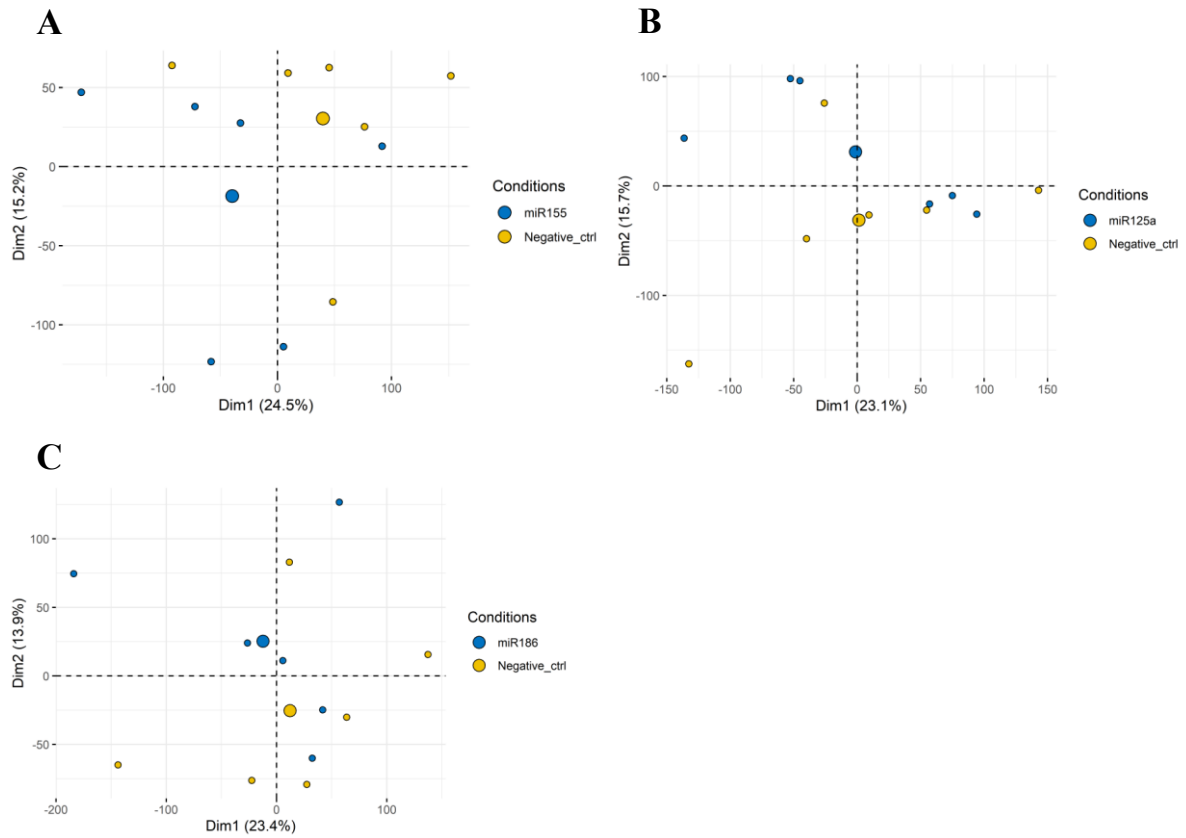


Figure 4.14. Single PCA plots of RNA-seq data: super regulator miRNAs overexpression

PCA plots of paired RNA-seq analysis showing miR-155-5p/control (A), miR-125a-3p/control (B) and miR-186-5p/control (C) overexpression experiments in MDMs isolated from 6 individuals. Dots represent different samples; larger dots are the class-centroids. Plots were made in R.

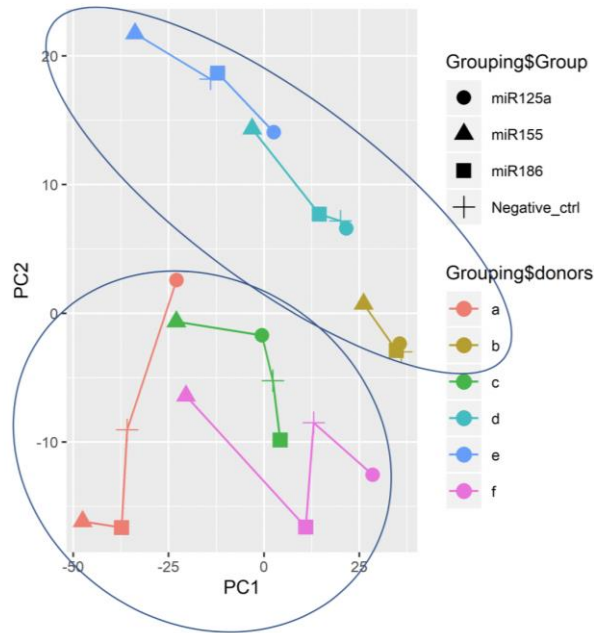


Figure 4.15. Global PCA plot of RNA-seq data: gender-dependent clustering?

Global PCA plot of super regulators overexpression RNA-seq analysis showing a potential clustering of the samples, according to gender, highlighted by blue circles. Plot was generated in R, using CPM values.

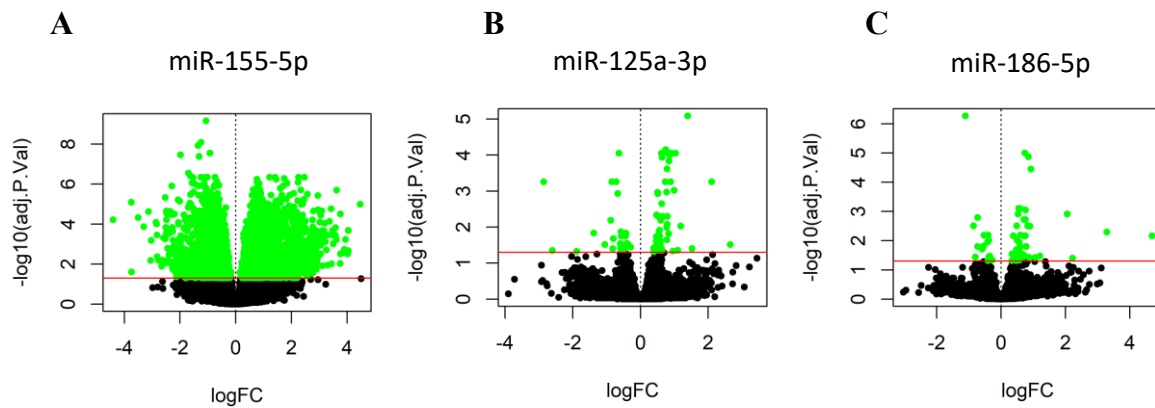


Figure 4.16. Volcano plots of RNA-seq data: super regulators overexpression

Volcano plot showing the log2fold change vs the log adjusted p value of macrophage genes in response to miR-155-5p mimic (A), miR-125a-3p mimic (B) and miR-186-5p mimic (C). None of the genes is significantly differentially expressed (fold change threshold 0; FDR cut off 0.05; genes passing FDR cut off are shown in green).

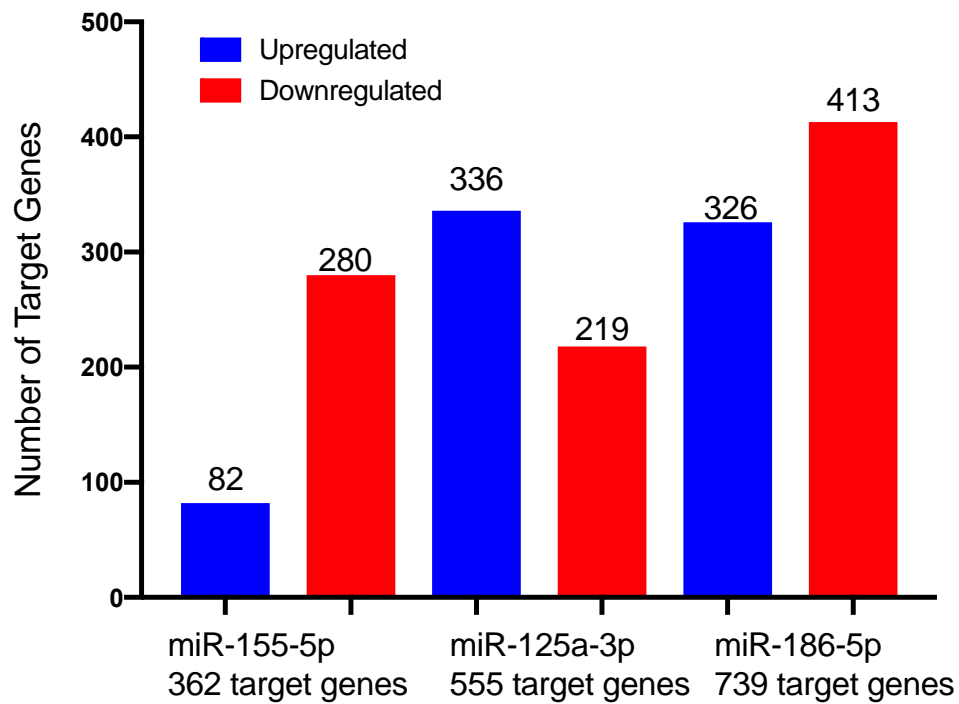


Figure 4.17. Number of target genes up- and downregulated in response to miRNA overexpression

The bar graph shows the number of up- and downregulated genes in response to miR-155-5p, miR-125a-3p and miR-186-5p overexpression. These genes were previously identified as downregulated in response to M1 polarising stimuli (RNA-seq, DOI:10.17632/j2hmt7k9fh.1).

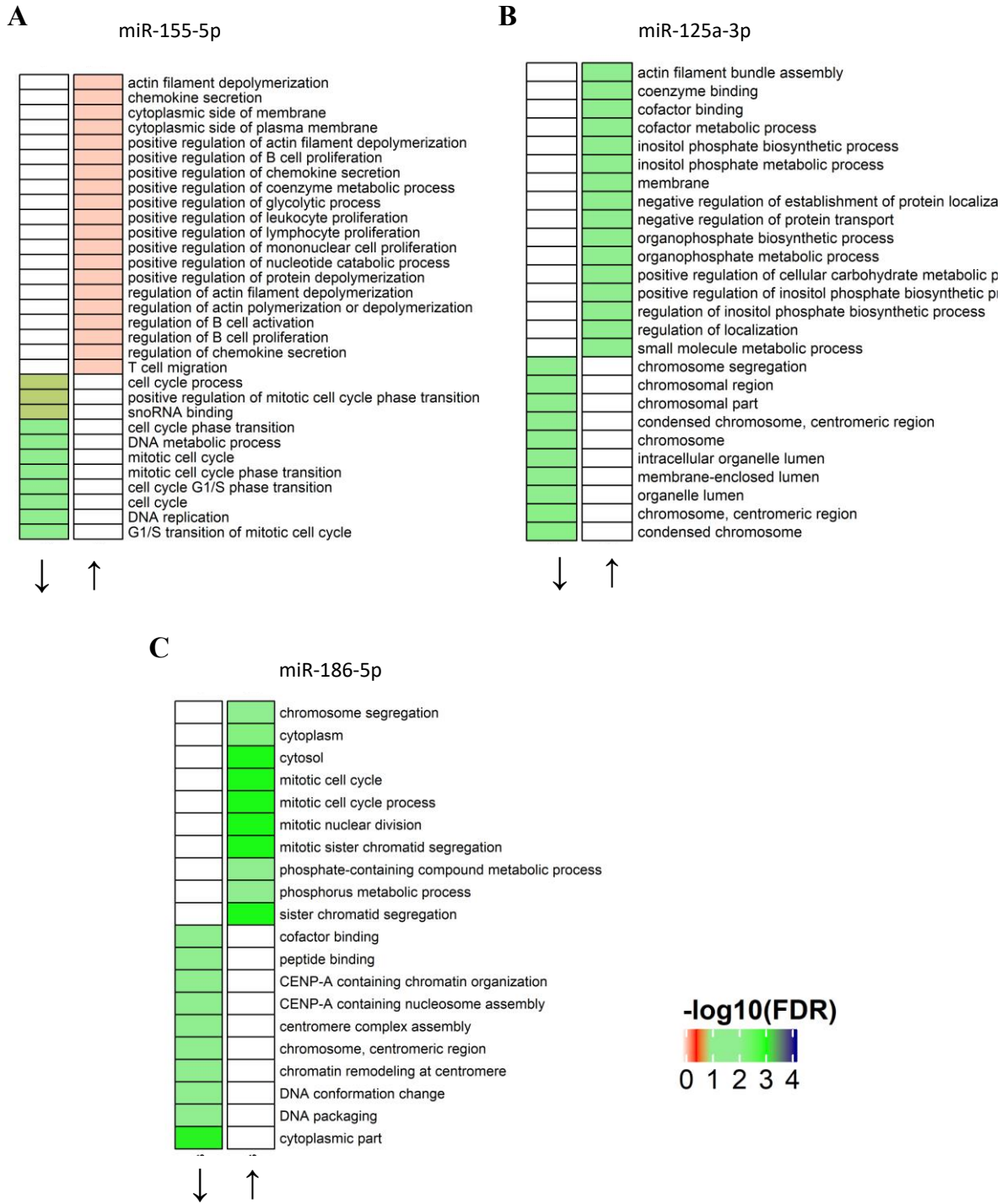


Figure 4.18. Gene ontology terms of genes differentially expressed in response to miRNA mimics

Gene ontology terms of downregulated (left panel) and upregulated (right panel) genes in response to miR-155-5p (A), miR-125a-3p (B) and miR-186-5p (C) overexpression in MDMs (FDR cut off 0.05). GO analysis was made by using GOSeq. Heatmaps generated in R.

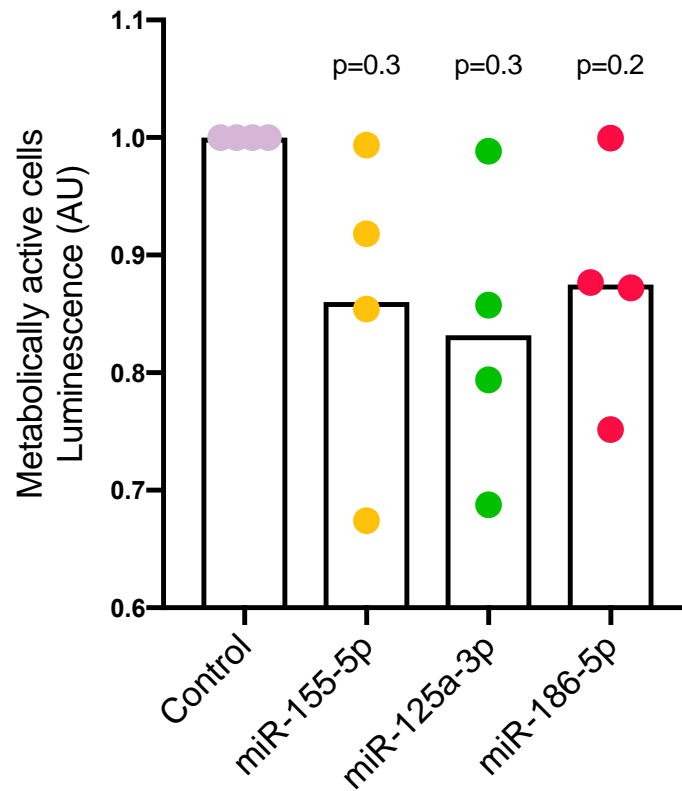


Figure 4.19. MTT assay on MDMs transfected with miRNAs mimics

MTT assay on MDMs transfected with 50nM of miRNA mimics/control (24 hours transfection). Cells viability is normalised to the control. Dots represent different donors (n=4, RM One-way ANOVA with Dunnett's post-test, ns p<0.05).

Table 4.8. Adjusted p-values-filtered differentially expressed genes

Table listing the DE genes in response to miRNAs overexpression filtered according to adjusted p values; only those highlighted in red are statistically significant; last column shows the expression status of the same genes in M1 macrophages, according to the RNA-seq DOI:10.17632/j2hmt7k9fh.1. Target prediction analysis was done by using TargetScan.

Gene	Control vs miR-155-5p	miR-155-5p target gene	M0 vs M1
SLC1A3	Upregulated	No	Downregulated
ARHGAP18	Downregulated	No	Downregulated
CSF1R	Downregulated	Yes	Downregulated
MOCS2	Downregulated	No	Downregulated
MPEG1	Downregulated	Yes	Downregulated
MARCHF1	Upregulated	No	Downregulated
PICALM	Upregulated	Yes	Downregulated
ANXA2	Downregulated	No	Downregulated
PTPN22	Downregulated	No	Downregulated
SPRED1	Downregulated	Yes	Downregulated
Gene	Control vs miR-125a-3p	miR-125a-3p target gene	M0 vs M1
DTX4	Downregulated	Yes	Downregulated
DUSP1	Downregulated	Yes	Upregulated
INF2	Downregulated	Yes	Downregulated
EHD1	Downregulated	Yes	Upregulated
TP53INP2	Downregulated	Yes	Upregulated
TRAF1	Downregulated	Yes	Upregulated
BCAT2	Downregulated	Yes	Downregulated
NFKBIA	Downregulated	Yes	Upregulated
BBS5	Downregulated	Yes	Downregulated
SLC43A2	Downregulated	Yes	Upregulated
Gene	Control vs miR-186-5p	miR-186-5p target gene	M0 vs M1
CRTAP	Downregulated	No	Downregulated
PDIA4	Downregulated	No	Downregulated
BLMH	Downregulated	Yes	Downregulated
GINM1	Downregulated	Yes	Upregulated
OAZ2	Downregulated	No	Upregulated
DENND10	Downregulated	No	Upregulated
UBQLN2	Downregulated	Yes	Upregulated
ASIC1	Downregulated	No	Downregulated
PSAT1	Downregulated	No	Upregulated
PUDP	Downregulated	No	Downregulated

Table 4.9. Log fold change values-filtered differentially expressed genes

Table listing the DE genes in response to miRNAs overexpression filtered according to log fold change values; only those highlighted in red are statistically significant; last column shows the expression status of the same genes in M1 macrophages, according to the RNA-seq DOI:10.17632/j2hmt7k9fh.1. Target prediction analysis was done by using TargetScan.

Gene	Control vs miR-155-5p	miR-155-5p target gene	M0 vs M1
LIN7A	Downregulated	No	Downregulated
LGI2	Downregulated	No	Downregulated
S1PR3	Downregulated	No	Downregulated
CDC25A	Downregulated	No	Downregulated
SYT1	Downregulated	Yes	Downregulated
RGS18	Downregulated	No	Downregulated
E2F2	Downregulated	Yes	Downregulated
FGD5	Downregulated	No	Downregulated
MPEG1	Downregulated	Yes	Downregulated
ANTXR1	Downregulated	No	Downregulated
Gene	Control vs miR-125a-3p	miR-125a-3p target gene	M0 vs M1
SLCO5A1	Downregulated	Yes	Upregulated
CCL1	Downregulated	Yes	Upregulated
UBD	Downregulated	Yes	Upregulated
CHST3	Downregulated	Yes	Upregulated
CCR7	Downregulated	Yes	Upregulated
ACOD1	Downregulated	No	Upregulated
PTGS2	Downregulated	Yes	Upregulated
TRAF1	Downregulated	Yes	Upregulated
DYRK1A	Downregulated	Yes	Upregulated
GUCY1A1	Downregulated	No	Upregulated
Gene	Control vs miR-186-5p	miR-186-5p target gene	M0 vs M1
SPIN3	Downregulated	No	Downregulated
EDNRB	Downregulated	No	Downregulated
MRO	Downregulated	No	Downregulated
FAM124B	Downregulated	Yes	Downregulated
GPC5	Downregulated	No	Upregulated
C15orf41	Downregulated	No	Downregulated
AL139260.3	Downregulated	No	Upregulated
ASIC1	Downregulated	No	Downregulated
DLG2	Downregulated	No	Upregulated
LOXL4	Downregulated	No	Upregulated

4.4. Summary

Macrophages are involved in a multitude of physiological and pathological conditions. Hence, understanding the mechanisms behind their activation can lead to the identification of novel therapeutic targets. It has been reported that one of the major mechanisms regulating macrophages polarisation towards different phenotypes is transcriptional regulation (*Martinez et al., 2006, Tugal et al., 2013*). To date, a significant number of studies pointed out the potential role of miRNAs (*Jablonski et al., 2016, Li et al., 2018, Curtale et al., 2019*). However, the association of miRNA and their target genes in macrophages remains elusive, due to the lack of integrated and systematic studies.

The work described in this chapter was designed to address the transcriptional changes induced by inflammatory stimuli, with a focus on miRNAs targetome. We investigated the gene expression profile of human macrophages challenged with LPS and INF- γ , taking advantage of computational tools and 3 RNA-seq experiments. We performed a small non-coding RNA-seq on polarised MDMs and identified 73 miRNAs differentially expressed in M1 macrophages, 44 were downregulated and 26 upregulated. Among them, we found miR-155-5p which is on the most characterised in the context of pro-inflammatory macrophages and it was previously shown to control multiple genes (*Jablonski et al., 2016*). By using TargetScan we identified the potential target genes of differentially expressed miRNAs. We used TargetScan as its prediction is strongly based on phylogenetic conservation of miRNA-binding sites, which in turn can be predictive of biological relevance (*Agarwal et al., 2015*). We determined the expression of potential target genes using a second RNA-seq experiment, carried out on the same number of samples and experimental conditions. The differentially expressed genes between M0 and M1 macrophages were 5681. We observed that 1573 upregulated genes are predicted targets of 44 downregulated miRNAs. Similarly, 1790 downregulated genes are potential targets of 26 upregulated miRNAs. This is suggesting that more than 50% of the macrophage transcriptome could be controlled by miRNAs, during polarisation. However, we did not validate any of the interactions, therefore we are not sure whether all the predictions occur in our model. Gene ontology and KEGG pathway enrichment analysis indicate that the target genes of downregulated miRNAs are related to innate immune responses, while those targeted by upregulated miRNAs have a role in cell cycle regulation. Our enrichment analysis was consistent with what Jiang and colleagues reported in murine polarised macrophages (*Jiang et al., 2017*). In addition, we identified 9 “super regulators” miRNAs (miR-7-5p, miR-125a-3p, miR-3614-5p, miR-4773, miR-186-5p, miR-4709-3p,

miR-1343-3p, miR-766-3p, miR-335-3p) predicted to target more than 500 genes. In fact, the potential of miRNAs relies on their ability to simultaneously target multiple genes and the same gene can be regulated by multiple miRNAs at the same time (*Bartel et al., 2009*). In light of this, we determined the impact of two super regulators (miR-125a-3p and miR-186-5p) and miR-155-5p as positive control on unpolarised macrophage transcriptome. To this aim we employed the RNA-seq of samples transfected with miRNA mimics and a non-targeting control. As expected we did not find many statistically significant differentially expressed genes, due to either the variability among the individuals or the difference in transfection efficiency. Moreover, it is recognised that despite miRNAs are master regulators of gene expression, their individual effect on target genes is likely to be small (*Liu et al., 2019*). This is particularly evident if we compare it with the effect induced by M1 polarising stimuli after 24 hours, which was strong and robust as shown by the PCA analysis. The mimics transfection was also carried on for 24 hours, as it was found efficient, for example, in causing the repression miR-101-3p target genes (TRIB1, DUSP1 and ABCA1), described in Chapter 3. Nevertheless, among the two datasets (M0/M1 RNA-seq and miRNA/control RNA-seq) we did find gene overlapping and the same directional changes in expression.

Overall our findings indicate the existence of a gene network controlled by multiple miRNAs, which account for the regulation of the most relevant biological pathways activated or repressed during M1 macrophage polarisation. Further work is needed to validate miRNA target interactions and perform dedicated assay to evaluate the biological impact of super regulators miRNAs.

Chapter 5. miRNAs targeting TRIB1 non-coding variants and identification of two novel eQTLs

Declaration

The work and the experiments described in this chapter have been performed by myself. I received great help and support from Dr Oscar Villacanas Perez, Dr Ignasi Gomez and Juan Salamanca Vilorio in the development of the bioinformatics pipeline and in the use of miRanda, MySQL and Python. Help from Veronika Kiss-Toth in the preparation of the mutants was also greatly appreciated. Sumeet Deshmukh contributed to this work by providing me with the bioinformatics analysis of a publicly available transcriptomic dataset. Finally, a huge thanks to Dr Stephen Hamby (University of Leicester) who provided me with the analysis of a monocyte/macrophage RNA microarray dataset, used for the identification of eQTLs.

Abstract

Non-coding single nucleotide polymorphisms (SNPs) are the most common variation in the human genome, affecting mRNA stability and disease susceptibility. SNPs in regulatory regions of the genome, can alter gene expression in a tissue-specific manner, acting as Expression Quantitative Trait Loci (eQTLs). The TRIB1 gene, a key regulator of cancer, inflammation and lipid metabolism, is characterised by a highly unstable transcript, it is enriched in non-coding variants and it is subject to post-transcriptional regulation with a context-dependent function. However, the role of non-coding SNPs in the post-transcriptional regulation of TRIB1 has not been investigated. We hypothesised that an association between TRIB1 non-coding variants and miRNA-binding sites exists as a mechanism of gene expression regulation. To investigate this, we took advantage of both computational and experimental approaches. In this chapter, we showed that TRIB1 genetic variants affect miRNA-target sites, by creating new binding sites. When tested *in vitro*, rs62521034 and rs56395423 significantly impaired TRIB1 gene stability ($p=0.002$, $p=0.01$) and rs62521034, but not the reference allele, was able to bind to miR-29a-3p ($p=0.03$), a miRNA implicated in cancer, inflammation and cardiovascular disease. By using an RNA microarray dataset generated within the Cardiogenics Consortium, we found that rs3201475 and rs62521034, located in the 5'UTR and 3'UTR of TRIB1, respectively, are associated with a significant reduction in the expression of distant genes (NLRC4, $p=1.34E-07$ and MRPS21, $p=3.70E-06$),

acting as trans-eQTLs. Although we demonstrated that TRIB1 non-coding SNPs have an effect on post-transcriptional regulation of TRIB1 itself and other genes, additional work is needed to investigate the impact of TRIB1 SNPs particularly in the context of disease.

5.1. Introduction

Single-Nucleotide Polymorphisms (SNPs) represent the most abundant genetic variation in the human genome, responsible for the diversity among individuals, such as differences in response to drugs, microorganisms, vaccines and other agents, as well as disease susceptibility and outcome. For this reason, SNPs are subject of intense genetic investigations for the development of personalised medicine (*Laing et al., 2011*). By definition, SNPs are substitutions of a single nucleotide in specific positions of the genome, estimated to occur approximately every 100-300 bases and present in more than 1% of the population; small insertions and deletions (INDELs) are also classified as SNPs (*Brookes et al., 1999, Orr and Chanock, 2008*). It has been reported that the majority of SNPs occur in non-coding regions of the genome. The main function of these non-coding variants is to regulate gene expression (*Ward et al., 2012, Tak et al., 2015*). Several studies reported that genetic variants in the 5' untranslated region (5'UTR) of protein-coding genes affect translation. For example, Khan and colleagues found that a SNP in the 5'UTR of p53, the “guardian” of the genome, impairs translation by compromising internal ribosome entry sites (IRES) and ribosomal assembly (*Khan et al., 2013*). A number of SNPs have been also identified to affect the Kozak consensus sequence (containing the initiation codon required for translation) and impair translational outputs (*Xu et al., 2010*). Moreover, it is well established that regulatory SNPs can account for tissue-specific differential gene expression: these are named Expression Quantitative Trait Loci (eQTLs). By definition, eQTLs are genetic variants affecting local (cis-acting) and distal (trans-acting) gene expression by mechanisms that are still not fully understood (*Gilad et al., 2008, The GTEx Consortium, 2013*). To date, multiple cis- and trans-eQTLs have been discovered: for example, the intronic SNP rs3129934, associated with an increased risk of multiple sclerosis (*Comabella et al., 2008*), is a cis-eQTL for several HLA transcripts (*Wellcome Trust Case Control Consortium, 2007*). Mangravite and colleagues identified the SNP rs9806699 as cis-eQTL for the gene glycine amidinotransferase (GATM) and they observed that there is an association with statin exposure and the risk of statin-induced myopathy (*Mangravite et al., 2013*). Interestingly, the variation in gene expression mediated by SNPs is often due to the activity of endogenous microRNAs (miRNAs). miRNAs are abundant and critical in

maintaining the transcriptional profile of all tissues, therefore SNPs affecting miRNA-target sequences can perturbate gene expression and lead to disease traits (*Sethupathy et al., 2008*). For example, a SNP found in the oncogene MDM4 (rs4245739) creates new binding sites for miR-191 and miR-887-3p and this has been associated with decreased viability and proliferation of prostate cancer cells *in vitro* (*Stegeman et al., 2015*). Similarly, a SNP found in the 3'UTR of apolipoprotein C-III (APOC3) has been shown to create a binding site for miR-4271, increasing the risk of hypertriglyceridemia and coronary heart disease (CHD), due to APOC3 accumulation (*Hu et al., 2016*). SNPs can also abolish miRNA-binding sites: for instance, a single nucleotide substitution found in the 3'UTR of the heparin binding epidermal growth factor (HBEGF) has been shown to destroy the binding site for miR-1207-5p, leading to HBEGF dysregulation, which in turn aggravates C3-glomerulopathy (*Papagregoriou et al., 2012*). Besides these, many other SNP/miRNA axes have been characterized, particularly in cancer (*Wilk et al., 2018*).

The TRIB1 gene is a regulator of inflammation, metabolism and cancer and its function has been intensively investigated in the context of myeloid disorders and metabolic diseases (*Satoh et al., 2013, Eyers et al., 2017*). Multiple studies have reported that TRIB1 is characterized by a highly unstable transcript and a context-dependent expression (*Sharova et al., 2009, Soubeyrand et al., 2016*). Previously, we have shown that TRIB1 undergoes miRNA-mediated post-transcriptional regulation. According to different miRNA-target prediction tools, TRIB1 is a potential target of multiple miRNAs; by knocking down DICER1 and blocking miRNA biogenesis in human macrophages, we observed that TRIB1 RNA expression tends to increase (see Chapter 3). Interestingly, genome-wide association studies (GWAS) have identified several SNPs in the TRIB1 gene linked to high plasma lipids, high cholesterol and triglycerides and the risk of cardiovascular disease (*Kathiresan et al., 2008, Aulchenko et al., 2009, Wang et al., 2015*). However, to date there is no information about the role of non-coding SNPs in the post-transcriptional regulation of TRIB1, as well as their impact on miRNA-binding sites and disease traits. Therefore, we investigated the association between 3'UTR SNPs and miRNAs, as well as the existence of regulatory eQTLs, employing both bioinformatics and experimental tools. We showed, for the first time, that TRIB1 non-coding variants influence miRNA-mediated gene regulation, by creating multiple 3'UTR binding sites. We experimentally validated a non-canonical miRNA-target interaction (offset seed, 3-9) between a 3'UTR SNP (rs62521034) and miR-29a-3p. Also, we identified cis- and trans-eQTLs that have not been reported before. Overall, our results provide new insights into TRIB1 post-transcriptional regulation, suggesting that both SNPs and miRNAs play a role; however, due to the limitations

of this study, more experimental validation is needed (see Section 5.4. Limitations of this study).

5.2. Hypothesis and aim of this study

We hypothesised that an association between TRIB1 non-coding variants and miRNAs exists as a mechanism of gene expression regulation. Therefore, the aim of this study was to identify SNPs affecting miRNA-binding sites and investigate whether they associate with gene expression regulation by using target prediction tools and existing transcriptomic datasets.

5.3. Results

5.3.1. Impact of the 3'UTR of TRIB1 on mRNA stability

We first evaluated the impact of the 3'UTR of TRIB1 on mRNA stability, by using a dual luciferase reporter assay. We used two renilla luciferase reporter plasmids: a control plasmid with the renilla luciferase gene and a TRIB1 3'UTR reporter (consisting of the same plasmid with the 3'UTR of TRIB1 cloned downstream of the renilla luciferase gene). These were co-transfected in HEK293T cell line in combination with a firefly luciferase reporter, used as internal control for data normalisation. The result is shown in **Figure 5.1**: the presence of the 3'UTR of TRIB1 significantly impaired ($p = 0.0004$) the gene reporter activity, causing a 42% reduction; this suggests that the 3'UTR of TRIB1, downstream of the renilla gene, exert a negative translational effect. We are not sure whether this is due to post-transcriptional regulation of TRIB1 by endogenous miRNAs expressed by HEK293T cells. However, we have previously showed that the 3'UTR of TRIB1 is enriched in miRNA-binding sites and inhibiting DICER1 in human macrophages resulted in the increase of TRIB1 mRNA and protein levels (see Chapter 3). Therefore, we do not exclude that the reduction of the reporter activity is due to the presence of endogenous miRNAs in HEK293T cells.

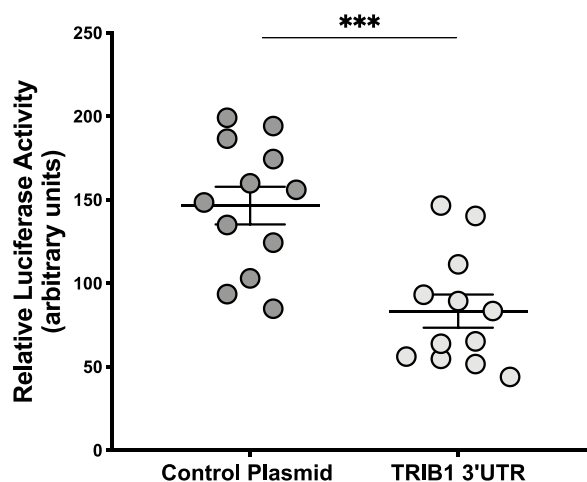


Figure 5.1. Impact of the 3'UTR of TRIB1 on mRNA stability

Relative luciferase activity measured in HEK293T cell line after 24 hours co-transfection of a renilla luciferase reporter (control plasmid, no UTR) and a TRIB1 3'UTR reporter with a firefly luciferase control (required for normalisation). Total DNA transfected 100 ng/well (96-well plate). Data are presented as mean \pm SEM (unpaired t-test, $n = 12$, *** $p < 0.001$).

5.3.2. Identification of TRIB1 non-coding variants affecting miRNA-binding sites

To determine whether TRIB1 3'UTR variants have an impact on miRNA-binding sites, we used the miRNA-target prediction algorithm miRanda to align human mature miRNA sequences with TRIB1 non-coding variants. The algorithm was downloaded and used as an independent script (<http://microrna.org>, August 2010 release). We applied a score cutoff of ≥ 140 and a free energy threshold of 1 kcal/mol (default settings). These are considered non-stringent parameters (Marin *et al.*, 2011). As input files for the algorithm, we used TRIB1 reference sequence (transcript variant 1, NM_025195.4) and 90 variants affecting the 3'UTR of TRIB1, downloaded from NCBI database (<https://www.ncbi.nlm.nih.gov/snp>). The TRIB1 SNPs were downloaded as short sequences containing IUPAC ambiguity codes, therefore we pre-processed them using Python (Python v3.6.2/BioPython v1.70) to generate the full-length 3'UTR sequences carrying each SNP (see Chapter 8, Appendix IV). An example of a SNP before and after the processing in Python is shown in **Figure 5.2.**, while the complete list of TRIB1 variants is provided in Chapter 8 (Appendix IV). After executing miRanda, we used Python to organise the output file into tables. We created a table for the reference transcript and a table for all the SNPs; we then imported the tables in MySQL (pgAdmin tools version 4) and used structural queries to intersect each dataset and find, for example, common interactions and non-common interactions. By using this approach, we found that 62 of 90 3'UTR variants create new miRNA-binding sites for 135 distinct miRNAs which have not been detected for the reference allele (**Table 5.1.**); most of these variants are associated with a minor allele frequency (MAF) of less than 1% and only 6 SNPs are present in more than 1% of the population. We did not find any abolished interaction but we found that a number of SNPs modify the alignment score and the free energy values for multiple miRNAs, compared to the reference transcript. Possibly, those SNPs are predicted to modify the affinity of miRNAs for the 3'UTR of TRIB1, by either enhancing or weakening the interaction. However, as mentioned earlier, we used miRanda algorithm relying on relaxed parameters, therefore we do not exclude the possibility of abolished interactions. Next, we compared our output with the output generated by PolymiRTS (Version 3.0, <http://compbio.uthsc.edu/miRSNP/>) an online database, based on the miRNA-target prediction algorithm TargetScan (Bhattacharya *et al.*, 2014). The output from PolymiRTS is shown in **Table 5.2.**: 13 distinct 3'UTR SNPs create new binding sites for 29 miRNAs; the SNPs and miRNAs highlighted in yellow are those which are overlapping with our analysis. TargetScan is usually more stringent than miRanda

and it also considers the phylogenetic conservation of miRNA-target interaction. Therefore, it is not surprising that, using miRanda, we found a greater number of SNPs creating novel target sites. However, miRanda allowed us to detect also non-canonical binding sites which are discussed further in the next sections.

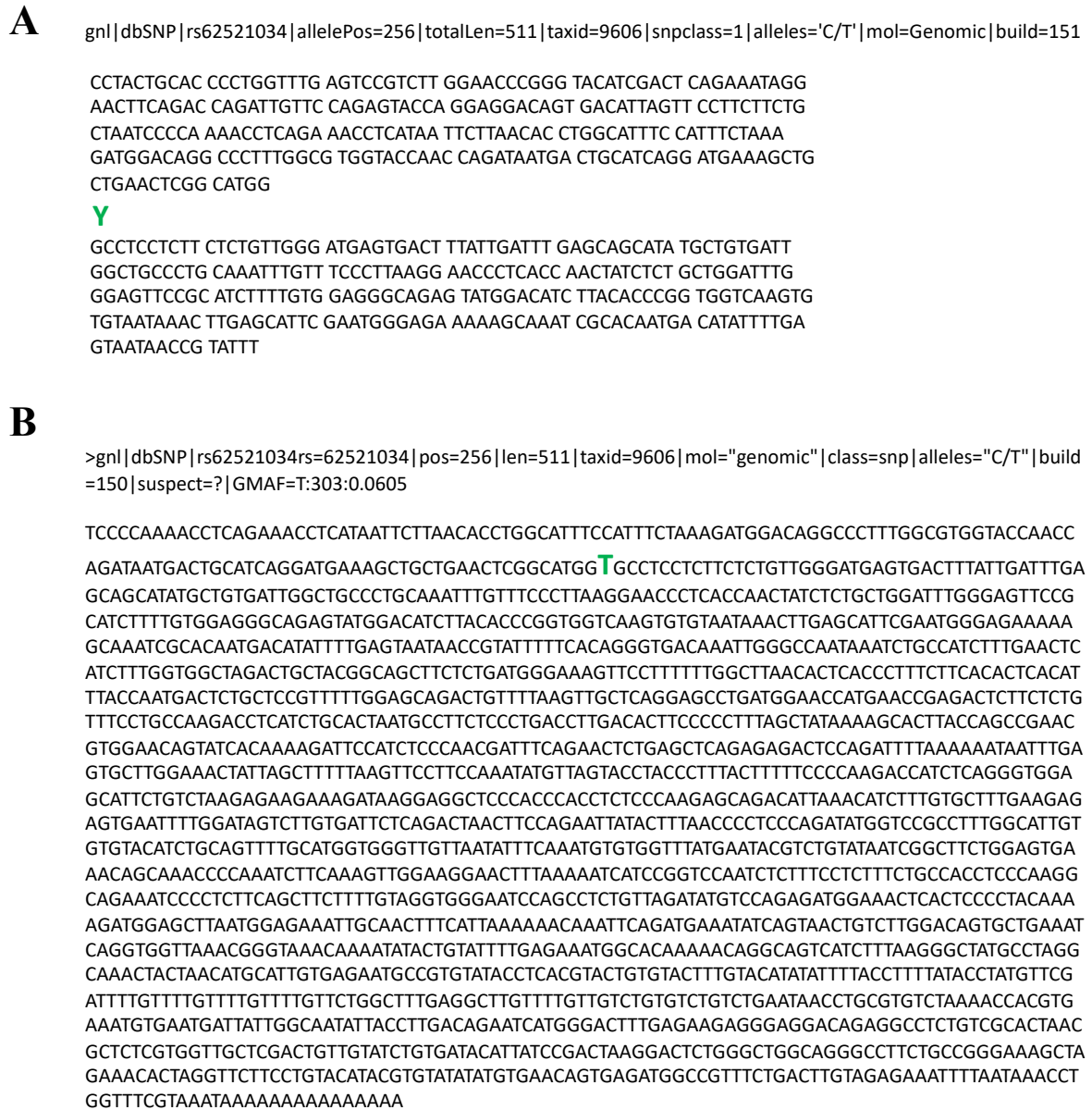


Figure 5.2. Example of SNP sequence before and after Python processing

SNP in TRIB1 downloaded as IUPAC ambiguity code (Y, C>T) flanked by two small sequences (**A**) was pre-processed in Python before the use of miRanda algorithm in order to generate the 3'UTR full-sequence containing the SNP (**B**).

Table 5.1. List of TRIB1 3'UTR SNPs creating new miRNA-binding sites

List of TRIB1 non-coding SNPs creating new miRNA-binding sites, not detected for the reference allele. Highest population MAF refers to the highest Minor Allele Frequency observed in a population, taken from Ensembl database (<https://www.ensembl.org>). The prediction analysis was carried out using the algorithm miRanda (<http://www.microna.org/microna/home.do>); score cut off ≥ 140 ; free energy threshold 1 kcal/mol.

SNP ID	Allele	Highest MAF	Associated miRNAs
rs751789944	C/-	<1%	miR-6508-5p, miR-8067, miR-4683
rs754065243	A>T	<1%	miR-452-5p, miR-4719
rs755860381	C>G	<1%	miR-6721-5p, miR-3126-3p, miR-4776-5p
rs756175087	-/G	<1%	miR-652-3p, miR-6847-5p
rs756397904	T>C	<1%	miR-3944-3p
rs757344260	G>A	<1%	miR-7159-3p
rs758576660	C/A/G	<1%	miR-544b
rs758819773	A>G	<1%	miR-4685-3p, miR-4755-5p, miR-4287
rs367637074	C>T	< 1%	miR-487a-3p, miR-3678-5p
rs372324007	C>T	< 1%	miR-4477b
rs375565353	A>G	< 1%	miR-4477b
rs530681133	C>T	< 1%	miR-6508-3p
rs533208547	C>G	< 1%	miR-6504-3p
rs546479447	C>T	< 1%	miR-6797-5p, miR-4428, miR-4726-5p, miR-4776-5p
rs550939781	C>T	< 1%	miR-130a-3p, miR-130b-3p, miR-301b-3p, miR-3666, miR-4295, miR-454-3p
rs557685029	G>A>C	< 1%	miR-659-3p
rs560408937	C>T	< 1%	miR-6861-5p, miR-1229-5p, miR-3140-3p
rs564442600	C>G	< 1%	miR-6841-5p
rs72647345	C>T	< 1%	miR-454-3p
rs72647346	C>G	< 1%	miR-4491, miR-4657
rs72647347	G>A	< 1%	miR-145-3p
rs759347835	C>G>T	< 1%	miR-190a-3p, miR-466, miR-500a-3p, miR-502-3p, miR-5580-3p
rs761444485	G>A	< 1%	miR-6886-3p
rs762994344	T>C	< 1%	miR-184
rs764779399	T>A	< 1%	miR-211-5p, miR-4287, miR-4685-3p
rs765360657	T>C	< 1%	miR-629-5p
rs767431696	C>T	< 1%	miR-3121-3p
rs768403240	G>A	< 1%	miR-4729, miR-181c-5p
rs770137661	A>G>T	< 1%	miR-4653-3p, miR-3159
rs772580999	C>G	< 1%	miR-4520-5p

rs775724040	C>T	< 1%	miR-4477a
rs776325924	C>T	< 1%	miR-7153-5p
rs776449618	G>A	< 1%	miR-4784, miR-1262, miR-1269, miR-4428, miR-4515, miR-4529-3p
rs777539484	TGTGAATGATTATTG/TG	< 1%	miR-4776-3p
rs777776886	C>T	< 1%	miR-19b-5p, miR-620
rs780519373	C>T	< 1%	miR-655-5p
rs140952648	A>G	1%	miR-8070
rs145449131	C>T	1%	miR-6768-5p
rs149107463	C>A>T	1%	miR-125b-3p, miR-4738-3p, miR-4769-3p, miR-548g-3p, miR-6801-5p, miR-6817-5p
rs529289692	G>A	1%	miR-452-5p
rs530790403	T>C	1%	miR-3686
rs539767360	G>T	1%	miR-942-3p, miR-98-3p, let-7a-3p, let-7b-3p, let-7f-1-3p, miR-300, miR-3616-3p, miR-381-3p, miR-4761-3p, miR-493-5p, miR-624-3p
rs540547779	C>T	1%	miR-335-5p
rs544175527	G>A	1%	miR-607
rs544226392	G>A	1%	miR-6888-3p, miR-5699-3p
rs546022723	A>T	1%	miR-875-3p, miR-18a-5p, miR-3978, miR-519d-3p, miR-520g-3p, miR-526b-3p
rs546842228	C>T	1%	miR-6736-5p, miR-1262, miR-4701-3p
rs552692797	C>T	1%	miR-3928-5p, miR-6806-3p
rs554138846	T/TT	1%	miR-488-5p, miR-597-5p
rs555208281	A>G	1%	miR-148a-5p
rs555485182	A>G	1%	miR-429, miR-1278, miR-200b-3p, miR-200c-3p
rs568362286	C>T	1%	miR-4744
rs568453644	T>A	1%	miR-21-5p
rs568845890	G >A	1%	miR-542-3p
rs575198443	C>T	1%	miR-148a-5p
rs577356981	A>G	1%	miR-518c-3p, miR-518e-3p
rs548386397	G>C	2%	miR-6516-3p, miR-4666a-5p
rs80023284	G>A	6%	miR-3920, miR-3929
rs74486799	A>G	7%	miR-4523, miR-4740-3p
rs56395423	A>C>G	9%	miR-4464, miR-4525, miR-4748, miR-5705, miR-6740-5p
rs62521034	C>T	22%	miR-593-5p, miR-29a-3p, miR-29b-3p, miR-506-3p, miR-767-5p
rs2235108	G>A	41%	miR-4659b-5p

Table 5.2. Output generated by PolymiRTS database 3.0

List of TRIB1 non-coding SNPs creating new miRNA-binding sites according to PolymiRTS database (version 3.0). Function class C=created, D=deleted (deleted binding sites are shown only for the ancestral allele, so no SNPs is found to abolish miRNA-binding sites).

dbSNP ID	Variant type	Ancestral Allele	Allele	miR ID	miRSite	Function Class			
rs2235108	SNP	G	A	hsa-miR-6872-3p hsa-miR-7153-3p	tttGGC A TGGTtac tttgg C ATGGTAc	C C			
rs62521034	SNP	C	C	hsa-miR-3197	gcatg G CGCCTCc	D			
			T	hsa-miR-3612	gcatgg T GCCTCC	C			
				hsa-miR-593-5p	gca TGG TGCCtcc	C			
				hsa-miR-650 hsa-miR-767-5p	gcatgg T GCCTCC gc ATGG TGCtcc	C C			
rs72647345	SNP	C	C	hsa-miR-147b hsa-miR-210-3p	gcaaat C GCACAA gcaaat C GCACAA	D D			
			T	hsa-miR-19a-3p hsa-miR-19b-3p	gcaaa T GCACAa gcaaa T GCACAa	C C			
rs140952648	SNP	G	G	hsa-miR-147b hsa-miR-210-3p	caaat C GCACAAt caaat C GCACAAt	D D			
			A	hsa-miR-147a hsa-miR-6818-5p hsa-miR-8070	caaat C ACACAAt caaa T CACACAAt ca AATC ACacaat	C C C			
				G	hsa-miR-4668-3p hsa-miR-516b-5p	actcca G ATTTTA aCTCCAGAtttta	D D		
rs72647346	SNP	G	C	hsa-miR-3662 hsa-miR-4491 hsa-miR-4657 hsa-miR-7847-3p	actcca C ATTTTA ac TCC ACATtta ac TCC ACATtta aCTCCACAtttta	C C C C			
			A	hsa-miR-125a-5p hsa-miR-125b-5p hsa-miR-1273f hsa-miR-143-3p hsa-miR-3620-3p hsa-miR-4319 hsa-miR-4324 hsa-miR-4708-5p hsa-miR-4770 hsa-miR-6088	catCTC A GGGtgg catCTC A GGGtgg CATCTC A gggtgg CATCTC A gggtgg catct C AGGGTg catCTC A GGGtgg caTCTC A GGgtgg CATCTC A gggtgg CATCTC A gggtgg CATCTC A gggtgg	D D D D D D D D D D			
G	hsa-miR-4740-3p	caTCTC G GGtgg		C					
rs80023284	SNP	G		A	hsa-miR-3920	aTAATC A Gcttct	C		
rs76707681	SNP	A		A	hsa-miR-4709-3p	TCTTCA A agttgg	D		
				G	hsa-miR-146a-3p hsa-miR-4714-5p	tcTTCA A AGtgg tctTCAG A GTtgg	C C		
rs72647347	SNP	G		G	hsa-miR-1224-3p hsa-miR-1260a hsa-miR-1260b hsa-miR-188-3p hsa-miR-3156-3p	gtAGGT G GGAAtc gtaGG T GGGAAtc gtaGG T GGGAAtc gtagGT G GGAAtc gtagGT G GGAAtc	D D D D D		
					A	hsa-miR-145-3p hsa-miR-155-3p hsa-miR-3685	gtaggt A GGAAATC gtagGT A GGAAAtc gtagGT A GGAAAtc	C C C	
						C	hsa-miR-135b-3p hsa-miR-3674	cCCCTA C AAaaga cccCTA C AAaaga	D D
							A	hsa-miR-2909 hsa-miR-4278 hsa-miR-6789-5p hsa-miR-6824-5p	cCCCTA A Aaaaga CCCCTA A aaaaga CCCCTA A aaaaga CCCCTA A aaaaga
				rs72647349	SNP	G	G	hsa-miR-205-3p hsa-miR-452-3p	tcaga T GAAATAt tCAGAT G AAaatat
A	hsa-miR-3200-5p	TCAGAT A aaaatat	C						
rs201361138	SNP	G	G	hsa-miR-3065-5p hsa-miR-3529-3p	tgtTT T GTTGtct tgttTT G TTGTct	D D			
			T	hsa-miR-3613-3p	tgtTT T TTGtct	C			
rs145449131	SNP	C	C	hsa-miR-657	AACCT G Cgtgtct	D			
			T	hsa-miR-6768-5p	aaCCT G TGTgtct	C			

5.3.3. Effect of TRIB1 3'UTR SNPs on gene reporter activity

For experimental validation, we selected the two SNPs listed in **Table 5.3.** that we have generated *in vitro* through site-directed mutagenesis. **Figure 5.3.** shows the confirmation of 3'UTR mutants by Sanger sequencing. We have chosen a triallelic (rs56395423) and a biallelic (rs62521034) SNP with a population frequency higher than 1% and associated with more than one miRNA. Moreover, both SNPs have not been linked to any clinical trait or disease susceptibility and they have not been investigated in the context of miRNA-mediated gene regulation. Therefore, we tested the impact of these two SNPs on the regulatory function of the 3'UTR, using the reporter assay. We found that both rs56395423 and rs62521034 caused a small, significant reduction in the luciferase activity (17% reduction, $p=0.01$ and 20% reduction, $p=0.002$, respectively) (**Figure 5.4.**). However, for the triallelic SNP rs56395423 only one allele (C), the less frequent in the population, had a negative effect on TRIB1 mRNA, while the other one (G) did not show any significant effect, compared to the reference sequence. In fact, the minor allele C is associated with 5 new miRNAs, whereas the allele G is predicted to create only 1 novel miRNA binding site. However, we cannot conclude that the negative impact of rs56395423 and rs62521034 is specifically due to the activity of endogenous miRNAs, because of the lack of experimental evidence. As they caused a reduction in the gene reporter activity and then in TRIB1 expression itself, rs56395423 (A>C) and rs62521034 (C>T) are likely to be cis-eQTLs, which are tissue-dependent. This suggests that the assay could give different results in a different cell line/environment.

Table 5.3. TRIB1 non-coding variants selected for experimental validation

Triallelic and biallelic SNPs in TRIB1 3'UTR predicted to create new miRNA-binding sites and selected for experimental validation.

SNP ID	Allele	Highest MAF	Associated miRNAs
rs56395423	A>C	<1%	miR-4464, miR-4525, miR-4748, miR-5705, miR-6740-5p
rs56395423	A>G	9%	miR-5705
rs62521034	C>T	22%	miR-506-3p, miR-29a-3p, miR-29b-3p, miR-593-5p, miR-3612, miR-650, miR-767-5p

A

rs62521034

ATGAAAGCTGCTGAACTCGGCATGG[C/T]GCCTCCTCTTCTGTGGGATGAG

▷pRL-hTRIB1 3' UTR-1.seq(1>6842)	→	ctcggcatggcgcctc
444571601_1-1_fw3_H02.seq(12>906)	→	CTCGGCATGGTGCCTC
444571601_1-2_fw3_G02.seq(14>626)	→	CTCGGCATGGTGCCTC

B

rs56395423

TCCCC[A/C/G]AAACCTCAGAAACCTCATAATTCTT

▷pRL-hTRIB1 3' UTR-13.seq(1>6842)	→	CCTTcacctccccaaacc
444166701_2_1_FW_2_E04.seq(9>1252)	→	CCTTCACCTCCCCAAACC
444166701_2_2_FW_2_F04.2.seq(13>1206)	→	CCTTCACCTCCCCAAACC

▷pRL-hTRIB1 3' UTR-1.seq(1>6842)	→	cctccccaaacct
444166701_3_1_FW_2_G04.seq(10>1218)	→	CCTCCCCGAAACCTI
444166701_3_2_FW_2_H04.seq(12>1286)	→	CCTCCCCAAACCTI

Figure 5.3. Confirmation of TRIB1 3'UTR mutants: Sanger sequencing results

TRIB1 3'UTR mutagenesis to generate rs62521034 (**A**) and rs56395423 (**B**) was confirmed by forward Sanger sequencing (screenshots taken from SeqMan Pro alignment software, DNASTar).

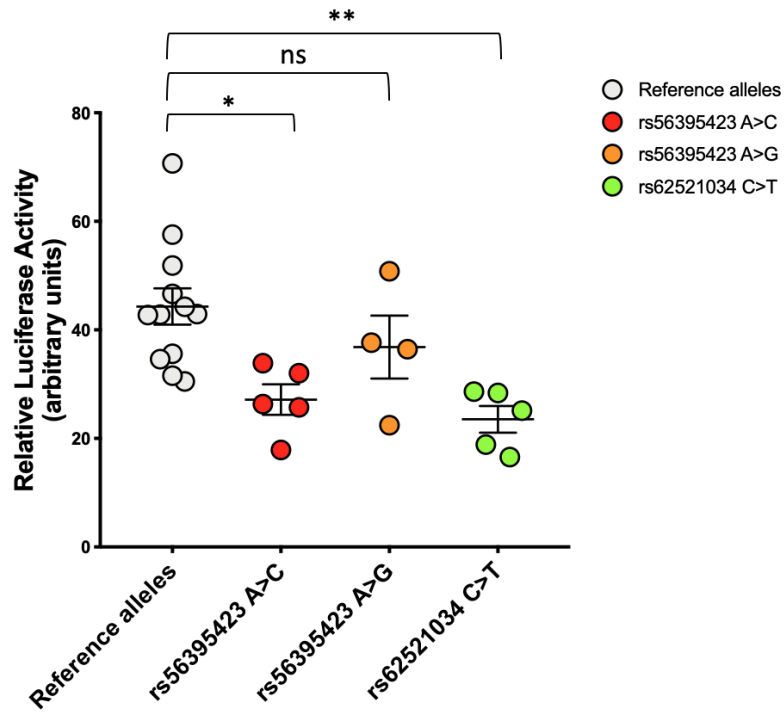


Figure 5.4. Effect of TRIB1 non-coding SNPs on gene reporter activity

Relative luciferase activity measured in HEK293T cell line after 24 hours co-transfection of TRIB1 3'UTR reporter (reference allele and 3 minor alleles) with a firefly luciferase control (required for normalisation). Total DNA transfected 100 ng/well (96-well plate). Data are presented as mean \pm SEM (One Way ANOVA with Dunnett's multiple comparison test $n = 4-12$, ** $p < 0.002$, * $p < 0.05$, ns $p > 0.05$).

5.3.4. Experimental validation of rs62521034/miR-29a-3p interaction

For the experimental validation of SNP/miRNA interaction, we selected rs62521034, as it is the SNP with the biggest impact on the luciferase reporter activity. According to our *in-silico* analysis, rs62521034 creates novel binding sites for miR-29a-3p, miR-29b-3p, miR-506-3p, miR-593-5p, miR-3612, miR-650, miR-767-5p. The alignment of these miRNAs with the SNP and the reference transcript are shown in **Figure 5.5**, along with the algorithm score, free-energy values and seed-region type. Despite the fact we used the algorithm applying non-stringent parameters (score threshold ≥ 140 , free-energy threshold 1 kcal/mol), the predicted interactions between rs62521034 and miRNAs show an optimal alignment score (>140) and free energy (≤ -15). Interestingly, the seed region pairs for miR-29a/b-3p and miR-593-5p are non-canonical matches, as they start from the 3rd miRNA nucleotide and end with the 9th (“offset” 7-mer, 3-9). This seed region type is not widespread and it has not been investigated. However, there are a few studies showing that offset seed matches are functional in repressing the expression of target genes (*Manzano et al., 2015, Broughton et al., 2016*). Therefore, we experimentally validated the non-canonical interaction between rs62521034 and miR-29a-3p/miR-29b-3p which belong to the same miRNA family and have the same seed region, despite small changes in the sequence. We performed a luciferase reporter assay and we used miR-29a-3p mimic in combination with the reporter plasmids, thus causing an overexpression of the miRNA within the host cell line. In line with our prediction, miR-29a-3p caused a small, significant reduction (15%, $p=0.03$) of the luciferase activity only when co-transfected with the rs62521034 reporter plasmid. No effect was observed for the reference allele ($p=0.7$) (**Figure 5.6**). This confirms that off-set 3-9 non-canonical binding sites are functional. By using published literature, we identified some biological conditions in which both miR-29 and TRIB1 are active players, often with opposing roles (**Table 5.4**). In fact, miR-29a/b is an established tumour suppressor, while TRIB1 is known to be overexpressed in cancer, acting as an oncogene. Moreover, both miR-29 and TRIB1 have been implicated in hepatic lipid metabolism and cardiovascular disease. Therefore, the interaction between miR-29 and the TRIB1 SNP rs62521034 could be further investigated in the context of these diseases.



Figure 5.5. miRNA-target alignment calculated by the algorithm miRanda

The figure shows the alignment of rs62521034 and TRIB1 reference transcript with miR-29a-3p, miR-29b-3p, miR-593-5p, miR-506-3p and miR-767-5p along with the score and free energy predicted by miRanda and seed-region type (seed region classification according to *Bartel et al., 2009, Seok et al, 2016*). miRanda algorithm was used with relaxed parameters (score threshold ≥ 140 ; free-energy threshold 1 kcal/mol).

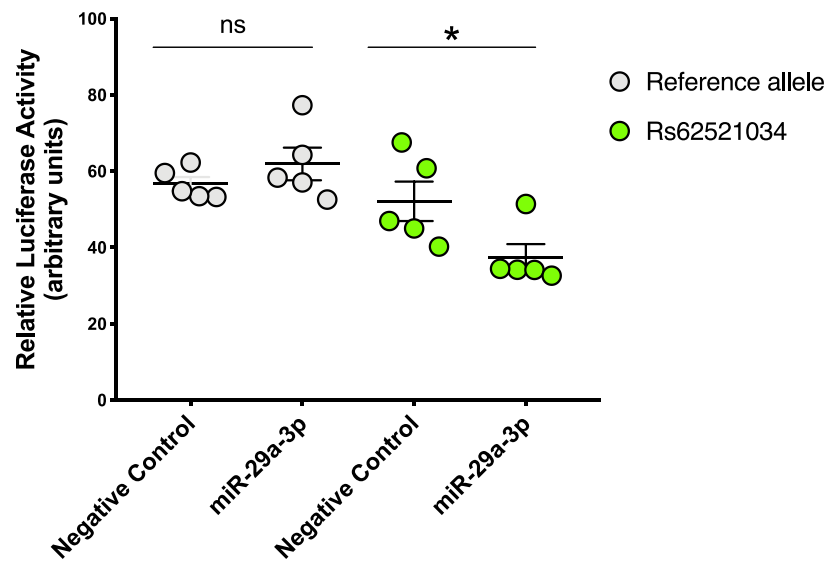


Figure 5.6. Experimental validation of rs62521034/miR-29a-3p interaction

Relative luciferase activity measured in HEK293T cell line after 24 hours co-transfection of TRIB1 3'UTR reporter (reference allele and rs62521034) with a firefly luciferase control (required for normalisation) and miR-29a-3p mimic/negative control. Total DNA transfected was 100 ng/well, total RNA transfected was 50 nM/well (96-well plate). Data are presented as mean \pm SEM (One Way ANOVA with Bonferroni's multiple comparison test $n = 5$, * $p < 0.05$, ns $p > 0.05$).

Table 5.4. miR-29a/b and TRIB1 involvement in cancer and metabolism

The table lists some of the biological processes and diseases in which both miR-29a/b and TRIB1 are actively involved, often with opposing roles.

miR-29a/b-3p		TRIB1	
Biological Process/Disease	Status/Effect	Biological Process/Disease	Status/Effect
Acute myeloid leukemia (Wang et al., 2012)	Downregulated	Acute myeloid leukemia (Röthlisberger et al., 2007)	Upregulated
Prostate cancer (Ru et al., 2012, Zhu et al., 2018)	Downregulated	Prostate Cancer (Mashima et al., 2014, Moya et al., 2018)	Upregulated
Hepatocellular carcinoma (Wang et al., 2017)	Downregulated	Hepatocellular carcinoma (Ye et al., 2017)	Upregulated
Lung cancer (Liu et al., 2018)	Downregulated	Lung cancer (Wang et al., 2017)	Upregulated
Hepatic lipogenesis (Kurtz et al., 2015)	Increased lipogenesis	Hepatic lipogenesis (Bauer et al., 2015)	Decreased lipogenesis
Atherosclerosis (Chen et al., 2011, Huang et al., 2016)	Anti-inflammatory Upregulated	Atherosclerosis (Sung et al., 2012, Johnston et al., 2019)	Anti-inflammatory Increased lipid uptake

5.3.5. Identification of two novel trans-eQTLs

Next, we investigated whether TRIB1 non-coding variants have an effect on global gene expression. To do this, we used the microarray RNA data produced in the Cardiogenics Transcriptomic Study (CTS) (Heinig *et al.*, 2010, Schunkert *et al.*, 2011, Rotival *et al.*, 2011). We found that two non-coding SNPs in TRIB1, one located on the 3'UTR rs62521034 (previously discussed) and one in the 5'UTR rs3201475 are associated with a small, but significant reduction in the expression level of two distant genes: MRPS21 (Mitochondrial Ribosomal Protein S21) and NLRC4 (NLR family CARD domain containing 4), located on chromosome 1 and chromosome 2, respectively ($p=0.0000037$ and $p=0.000000134$) (**Table 5.5**). Rs62521034 and rs3201475 are then likely to be trans-eQTLs. To further substantiate this, we used a publicly available RNA-seq (GSE81046) of human monocyte-derived macrophage samples taken from 169 healthy individuals (Nedelec *et al.*, 2016). Rs62521034 was found in 20 individuals, whilst rs3201475 in 33 individuals; 10 of 169 donors carry both SNPs. We found that TRIB1 mRNA expression significantly correlates (negative correlation) with the expression of MRPS21 and NLRC4 ($p<0.0001$ and $p=0.0005$) (**Figure 5.7. B, C**). Although the low p-values indicate significance, the r squared values for both genes are low ($r^2= 0.20$ and $r^2=0.07$), suggesting that correlation of TRIB1 with MRPS21 and NLRC4 is weak, at least in this dataset. However, when we consider only those individuals carrying the SNPs (30 individuals for rs62521034 and 43 for rs3201475), there is a small improvement of the r squared values ($r^2= 0.30$ and $r^2=0.13$) (**Figure 5.7. D, E**). As TRIB1 has never been associated with these genes before, further work is required to confirm the role of the two non-coding SNPs rs62521034 and rs3201475 as trans-eQTLs.

Table 5.5. Identification of two novel trans-eQTLs

Illumina Human Ref-8 Bead Chip array of 849 monocyte and 684 macrophage samples collected from 459 individuals with cardiovascular disease (394 males and 65 females) and 458 controls (192 males and 266 females). Two SNPs located in the untranslated regions of TRIB1 are associated with a significant reduction in MRPS21 and NLRC4 genes. EA: effect allele; NEA: non-effect allele; EAF: effect allele frequency; beta:effect size estimate; beta_se: standard error of the beta; pvalue: statistical significance (cut off p value <0.05); rsq: r squared; FDR: false discovery rate.

SNP_ID	ILMN_Gene	EA	NEA	EAF	beta	beta_se	pvalue	Rsq	FDR
rs62521034	MRPS21	C	T	0.8247	-0.07555	0.016202	3.70E-06	0.4465	9.43E-01
rs3201475	NLRC4	C	T	0.6697	-0.073	0.013671	1.34E-07	0.8707	3.90E-01

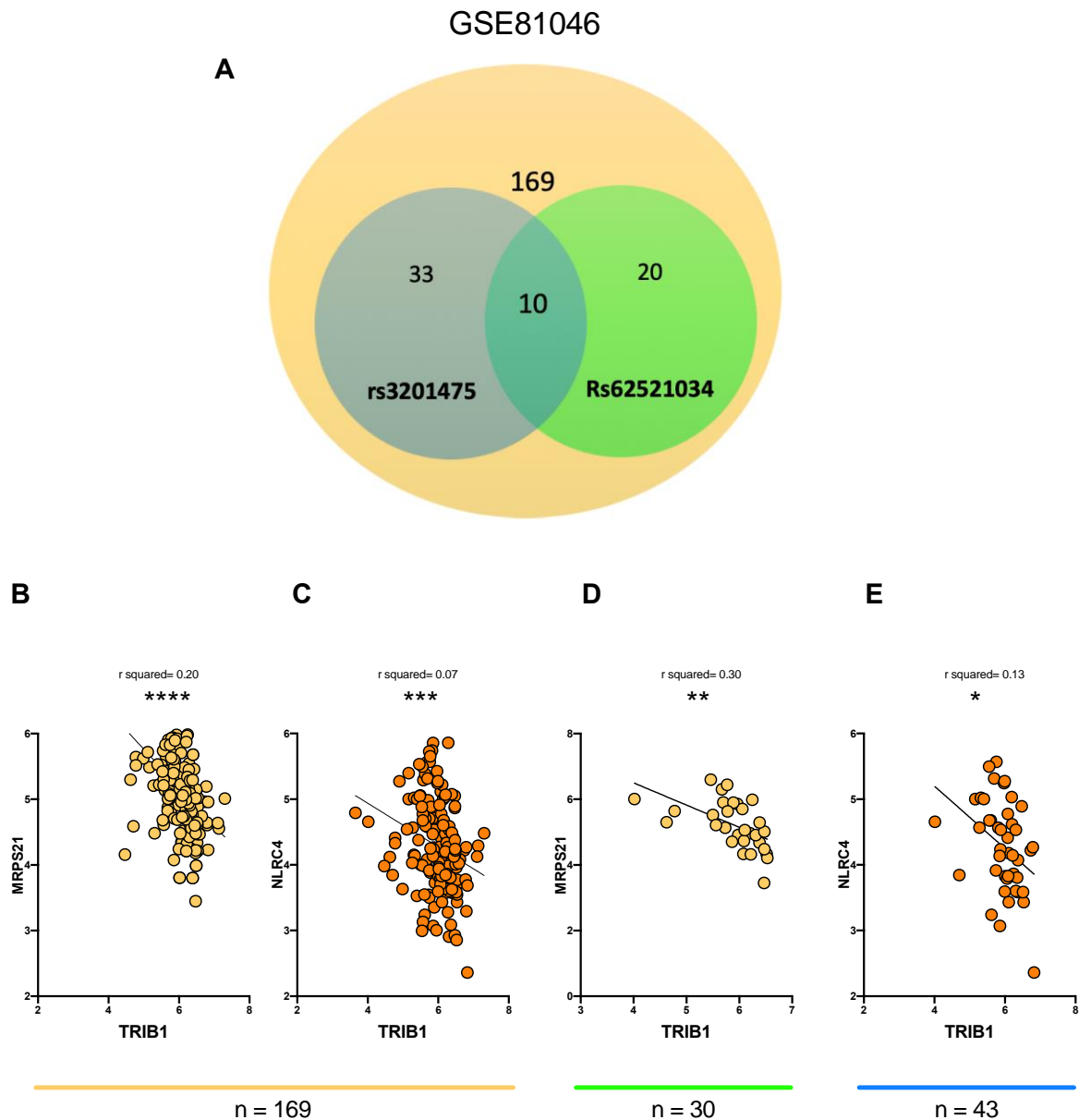


Figure 5.7. TRIB1 expression negatively correlates with MRSP21 and NLRC4 in GSE81046 dataset

Total number of individuals and number of individuals carrying TRIB1 SNPs in GSE81046 dataset (A); XY correlation between TRIB1 and MRSP21 (Counts per Million, n = 169, Pearson r test, **** p < 0.0001, $r^2=0.20$) (B); XY correlation between TRIB1 and NLRC4 (Counts per Million, n = 169, Pearson r test, *** p = 0.0005, $r^2=0.07$) (C); XY correlation between TRIB1 and MRSP21 (Counts per Million, n = 30, Pearson r test, ** p < 0.003, $r^2=0.30$) (D); XY correlation between TRIB1 and NLRC4 (Counts per Million, n = 43, Pearson r test, * p < 0.02, $r^2=0.13$) (E).

5.4. Summary

It is well appreciated that the 3'UTR of mRNA is fundamental in controlling the post-transcriptional fate of protein-coding genes (*Pesole et al., 2001*). It is also well known that any mutation in this regulatory region further impact gene expression outcomes, by either enhancing and inhibiting post-transcriptional events (*Chatterjee and Pal, 2009*). The importance of the 3'UTR relies on the presence of multiple regulatory sequences, including miRNA-binding sites, AU-rich elements and a poly(A) tail which mediate export, stability, decay and expression of a transcript (*Matoulkova et al., 2012*). Interestingly, what happens to the 3'UTR of a gene influence the expression of other genes (*Skeeles et al., 2013*) and this has been often linked to the presence of genetic polymorphisms and the activity of endogenous miRNAs (*Wilk et al., 2018*). Therefore, investigating the association between SNPs and miRNAs is essential to unravel the molecular mechanisms underlying the complex post-transcriptional regulation of eukaryotic genes. In this study, we focused on the TRIB1 gene. TRIB1 is characterized by a long (1934 bp) and conserved 3'UTR sequence and its mRNA has a half-life of less than 1 hour, hinting it is highly unstable and post-transcriptionally regulated (*Sharova et al., 2009*). In fact, we have previously reported that TRIB1 is negatively regulated by miR-101-3p, miR-132-3p and miR-214-5p in macrophages and in prostate cancer (see results Chapter 3 and Chapter 6). Here, we have shown that polymorphisms in the 3'UTR of TRIB1 has an impact on miRNA-mediate gene regulation, by creating novel binding-sites and modifying the affinity of existing ones. Using a luciferase reporter assay, we observed that the regulatory region of TRIB1 itself exerts a negative effect on gene stability and expression, causing a 42% reduction in the luciferase activity (see **Figure 5.1**). The presence of two SNPs (rs62521034 and rs56395423) further reduces the reporter activity, suggesting that these variants confer more instability to the TRIB1 gene (see **Figure 5.2**). Both SNPs have been predicted to create novel miRNA-binding sites, characterised by good alignment scores and free energy values (see **Figure 5.3**). As they affect TRIB1 expression, they are likely to be cis-eQTLs but we need more experimental evidence to make a conclusion. Also, in our experiment the negative effect of the TRIB1 SNPs is relatively small (17-20%) and this could depend on the endogenous expression level of regulatory proteins and factors (including miRNAs) within the host cell line, which have not been investigated in the present work. Moreover, performing this assay using a different microenvironment and employing multiple cell lines would perhaps give us more answers about the impact of rs62521034 and rs56395423 on TRIB1 expression and whether it strictly depends on the presence and level of tissue-specific regulators. In

addition, we identified a non-canonical seed region match between rs62521034 and miR-29a/b-3p and experimentally validated it as functional (see **Figure 5.4.**). This type of seed region is rare and to date only a few cases have been described (*Manzano et al., 2015*). According to published literature, either TRIB1 or miR-29a/b is implicated in acute myeloid leukemia (*Röthlisberger et al., 2007, Wang et al., 2012*) and in prostate cancer (*Moya et al., 2018, Zhu et al., 2018*), with contrasting roles: miR-29 is a tumour suppressing miRNA and it is usually downregulated, while TRIB1 plays the oncogene role. Whether they are correlated and whether their interaction is involved in these diseases, still remains to be investigated. Lastly, by using a published microarray dataset from myeloid cells, we identified two trans-eQTLs: TRIB1 non-coding SNPs rs3201475 (5'UTR, highest MAF 48%) and rs62521034 (3'UTR, highest MAF 22%) cause a small, but significant reduction in the expression of two distant genes (NLRC4 and MRPS21, respectively). By using a public transcriptomic dataset carried out on human monocyte-derived macrophages, we found that TRIB1 expression negatively correlates with these genes (see **Figure 5.5**). However, the low r^2 values indicate that the correlation is weak and there is no previous association of TRIB1 with NLRC4 and MRPS21. Therefore, a deeper investigation is required.

5.5. Limitations of the study

Although the association between TRIB1 SNPs and miRNAs has not been investigated before, the work presented in this Chapter has some limitations. First, we used only one miRNA-target prediction tool, miRanda, employing “relaxed” settings. On one hand, this allowed us to detect non-canonical binding sites which are recently emerging as functional. In fact, the non-canonical interaction that we have tested *in vitro* were functional, despite the small effect on the gene reporter activity (approximately 15%). On the other hand, miRanda is usually associated with a high number of false positives, so applying stringent parameters (i.e. reduce free energy threshold) and a second screening with a different algorithm (i.e. TargetScan) could improve the accuracy of the output, by reducing the number of positive interactions and narrowing down the list of SNPs and miRNAs. This will perhaps add a number of miRNA-binding sites abolished by the presence of SNPs, which we have not detected using miRanda algorithm. However, also the output generated by PolymiRTS do not show any abolished interaction for any of the minor alleles. We could further improve this analysis, by filtering the list of miRNA sequences and selecting only high-confidence miRNAs, which have been recently added in miRbase database, the “home” of miRNAs

(<ftp://mirbase.org/pub/mirbase/CURRENT/>). In fact, some of the novel miRNAs associated with TRIB1 SNPs are not confidentially annotated and often there is no knowledge about them. The second limitation of this study was the limited access to publicly available data and, above all, the lack of web-based tools enabling the correlation between miRNAs and their targets in a given tissue/disease using pre-existing data. For this reason, we could not investigate whether a correlation between TRIB1/rs62521034 and miR-29a-3p exists and if it could have an impact in acute myeloid leukaemia or in other types of cancer (see **Table 5.4**). Moreover, despite being confident about the identification of the two novel trans-eQTLs, we need more robust and convincing data. A good pilot experiment to understand whether those genes are somehow related will be a siRNA-mediated knockdown of TRIB1, followed by RT-qPCR and western blot for NLRC4 and MRPS21 gene and protein expression. Also, it would be useful to correlate the mRNA expression of TRIB1, NLRC4 and MRPS21 using different public transcriptomic data and perform an eQTL mapping.

Chapter 6. miRNAs targeting TRIB1 in Prostate Cancer

Declaration

The work presented in this chapter came from my own idea of integrating my PhD project into the main interest of the TRAIN ITN Consortium: investigating the role of Tribbles in the biology of prostate cancer. Both the *in silico* and *in vitro* part of this chapter have been entirely performed by me. A huge thanks to Swapna Satam and Ziyanda Shologu for sending me RNA samples from prostate cancer cell lines and also to Dr Alessandra Iscaro for giving me prostate tissues from mice.

Abstract

Prostate cancer (PCa) is one of the most common male cancers in the western world with a poor long-term prognosis. Current treatment for PCa is based on a combination of endocrine therapy, radical prostatectomy, standard cycles of chemotherapy and radiotherapy. However, as the disease progresses the majority of patients experience relapse. Hence, the identification of new molecular targets and the development of new therapeutic strategies is critical. It is well established that microRNAs (miRNAs) have pivotal roles in PCa development and progression, as they are frequently silenced by epigenetic modifications, thus perturbing the expression of multiple genes. Recent studies have shown that the pseudo-kinase Tribbles-1 (TRIB1) plays a crucial role in the proliferation and propagation of PCa. TRIB1 mRNA is overexpressed in PCa and regulates the ER chaperone GRP78, essential for prostate tumorigenesis. However, the mechanisms behind TRIB1 upregulation remain unclear. Here we investigate the potential association between TRIB1 overexpression and miRNA silencing in PCa, using both bioinformatics and experimental tools. Our results confirmed that TRIB1 is overexpressed in PCa cell lines, compared to cells derived from normal prostatic epithelium, as well as in a murine prostate cancer model. We identified 140 downregulated miRNAs in PCa and 21 of them are predicted to target the 3'UTR of TRIB1. We showed that miR-132-3p, an onco-suppressor miRNA, has two functional binding sites for the 3'UTR of TRIB1. miR-132-3p was able to negatively modulate TRIB1 expression *in vitro*, inducing a gene expression profile that recapitulated the TRIB1 knockdown phenotype. The latter was associated with changes in the expression of pro-inflammatory cytokines and tumour-related genes. The overexpression of TRIB1 in PCa may be explained by the downregulation of endogenous miRNAs, thus offering an interesting, novel therapeutic target. Further work is needed to investigate the role of additional microRNAs and their impact on PCa biology.

6.1. Introduction

PCa overview

Prostate cancer (PCa) is one of the most common solid cancers in elderly males worldwide. Each year over 1,500,000 men are diagnosed with PCa and over 360,000 men die (Rawla *et al.*, 2019). Established risk factors for PCa are age, genetics and family history, bad eating habits, sedentary life and lack of physical activity and also ethnicity. It has been reported that for African-American men both the incidence and mortality rates are higher compared to white men (Rawla *et al.*, 2019). The causes of this are not fully understood, but likely due to genetic diversity (Huang *et al.*, 2017). PCa is a slow-growing tumour: it starts in the prostate gland but over time it can spread throughout the body, most often in the bones and in lymph nodes. In patients affected by PCa, metastasis is the main cause of death (Rycaj *et al.*, 2017). From a pathological point of view, the majority of PCa (>95%) consist of adenocarcinomas, which is a tumour developing in the gland cells (Alizadeh *et al.*, 2014). Although the majority of cases are asymptomatic, patients suffering from PCa mainly experience urinary symptoms and sexual dysfunction (Merriel *et al.*, 2018). Treatment of PCa usually depends on the stage of the disease. For years, androgen deprivation therapy (ADT), via both surgery and drugs, was the gold standard for the treatment of both early stages and advanced metastatic PCa and it has also been successfully combined with radiation therapy (Gomella *et al.*, 2010). However, hormone suppression treatment inevitably leads to the development of castration-resistance within 18-36 months (Nakazawa *et al.*, 2017) and recently this treatment has also been associated with the risk of developing dementia and Alzheimer disease (Jayadevappa *et al.*, 2019). Therefore, further treatments are needed. At the moment available options include chemotherapy, radiotherapy, immunotherapy, cryosurgery and high-intensity focused ultrasound therapy (HIFU) (Vieweg *et al.*, 2007, Rodriguez *et al.*, 2014, Chaussy *et al.*, 2017, Nakazawa *et al.*, 2017). Immunotherapy and vaccines-based therapies are particularly promising in the treatment of PCa, because it naturally progresses slowly and provides enough time to activate immune responses (Janiczek *et al.*, 2017): for example, the vaccine Sipuleucel-T (Provenge®) has been associated with an increased survival of patients with castration-resistant PCa, reducing the risk of mortality by 22% (Kantoff *et al.*, 2010). The vaccine targets the prostatic acid phosphatase (PAP) which is upregulated in PCa and correlates with a poor prognosis and survival (Kantoff *et al.*, 2010, Kong *et al.*, 2013, Janiczek *et al.*, 2017).

Genetics of PCa

PCa is one of the most heterogeneous cancers and no single gene is responsible for it (*Yadav et al., 2018*). However, numerous genetic aberrations have been associated with primary and metastatic tumours, including mutations in the genes coding for androgen receptor (AR), phosphatase and tensin homolog (PTEN), proto-oncogene Myc (MYC), erythroblast transformation specific (ETS)-transcription factor (ERG), Homeobox Protein NK-3 Homolog A (NKX3-1), adenomatous polyposis coli (APC), breast cancer susceptibility genes (BRCA1 and BRCA2), ATM Serine/Threonine Kinase (ATM) and Speckle Type BTB/POZ Protein (SPOP) (*Wang et al., 2018*). It has been reported that the mutational burden in PCa is lower compared to other cancers. In fact, a recent genome cancer study showed that in PCa the median mutation frequency per megabase is lower (0.7) when compared to other malignancies (i.e. for bladder cancer is 7.1) (*Lawrence et al., 2014*). Besides genetic mutations, a large number of epigenetic modifications, including DNA and histone modifications, have been identified in PCa (*Baumgart et al., 2017*), as well as SNPs (*Benafif et al., 2018*). Interestingly, SNPs have been associated not only with the risk of developing PCa but also with cancer aggressiveness, survival and mortality (*Sullivan et al., 2015, Benafif et al., 2018, Moya et al., 2018*).

Downregulation of microRNAs in PCa

Aberrant expression of microRNAs (miRNAs) has been implicated in the development and progression of many cancers, including PCa (*Vanacore et al., 2017*). miRNAs control the expression of genes involved in proliferation and apoptosis, thus acting as oncogenes and tumour suppressors (*Zhang et al., 2007*). However, in PCa the majority of miRNAs appear to be downregulated and most often silenced by epigenetic modifications (*Ozen et al., 2007, Coppola et al., 2010, Ramassone et al., 2018*). Formosa and colleagues observed that miR-18b, miR-132, miR-34b/c, miR-148a, miR-450a and miR-542-3p were downregulated in PCa specimens compared to control samples and this was associated with promoter CpG island methylation, unmasked by 5-aza-2'-deoxycytidine treatment (*Formosa et al., 2013*). In particular, miR-132-3p has been shown to simultaneously target the 3'UTR of heparin-binding epidermal growth factor (HB-EGF) and TALIN2, thus impairing cellular motility, adhesion and proliferation (*Formosa et al., 2013*). HB-EGF and TALIN2 are usually overexpressed in PCa supporting invasion and metastasis (*Ongusaha et al., 2004, Desiniotis et al., 2011*). Similarly, the miR-145 promoter region is methylated in both tumour samples and prostate cancer cell lines and its loss correlates with a poor survival of PCa patients (*Zaman et al., 2010*,

Avgeris et al., 2013). Other examples of silenced miRNAs in PCa are miR-338-5p and miR-421, which have been shown to target the 3'UTR of SPINK1 (Serine Peptidase Inhibitor Kazal Type 1) (*Bhatia et al., 2019*), a gene usually upregulated in PCa and responsible for a more aggressive cancer subtype (*Tomlins et al., 2008*). The downregulation of miRNAs can be an important mechanism underlying the overexpression of genes involved in the prostate carcinogenesis, which are not necessarily altered by genetic mutations. Therefore, identifying and restoring the expression of de-regulated miRNAs could be a good approach to reduce the level of oncogenes and increase the expression of tumour suppressor genes.

The potential role of TRIB1 in PCa

As briefly explained in Chapter 1 (General Introduction), the TRIB1 gene has been implicated in PCa. To date only a few studies have been published covering this topic. Mashima and colleagues reported that TRIB1 was upregulated in prostate clinical tissues and in PCa cell line spheroid cultures (3D condition), compared to adherent cultures (2D condition). TRIB1 knockdown was associated with a decrease in cell proliferation, while TRIB1 overexpression increased tumour cells growth; by employing a soft agar assay, they also showed that TRIB1 knockdown impaired colony formation, while its overexpression significantly enhanced it. Moreover, overexpression of TRIB1 was linked to a significant reduction in the expression level of endoplasmic reticulum (ER) chaperones, including GRP78, GRP94 and GRP170 (*Mashima et al., 2014*). These are well known to promote carcinogenesis (*Gutiérrez et al., 2014*). Taken together these data suggest a fundamental role for TRIB1 in the growth and survival of PCa. However, no mutations in the gene have been described as causative of PCa and no mechanisms have been found responsible for its upregulation. However, a short tandem repeat (STR) was found in the 3'UTR of TRIB1 and it was significantly associated with prostate cancer risk and aggressiveness (*Moya et al., 2018*). The authors suggested that this STR could alter TRIB1 mRNA structure and stability, which in turn could affect TRIB1 expression in an allelic-dependent manner and it could also be linked to miRNA activity (*Moya et al., 2018*). Other evidence supporting the role of TRIB1 in PCa comes from the work published by Lin and colleagues in 2014: they found that TRIB1 is a direct target of miR-224, a miRNA downregulated in PCa. By forcing the expression of miR-224 in PCa cell lines, they observed a decrease in cell proliferation, invasion and migration which was TRIB1-dependent (*Lin et al., 2014*).

6.2. Hypothesis and aim of the study

The dysregulation of onco-suppressor miRNAs plays a central role in the development and progression of PCa. This is particularly true for miRNAs silenced by epigenetic modifications (i.e. promoter hypermethylation) that, in turn, cause the overexpression of their target genes. TRIB1 exerts an oncogenic role in PCa but the mechanisms underlying its upregulation are still unknown. Therefore, we hypothesize that the overexpression of TRIB1 gene in PCa is due to the downregulation of multiple microRNAs. The purpose of this study is to *in silico* identify and characterize downregulated miRNAs that potentially binds to the 3'UTR of TRIB1, post-transcriptionally regulating the gene.

6.3. Results

6.3.1. Data mining of PCa datasets: cBioPortal for Cancer Genomics

To understand the extent of TRIB1 contribution to PCa, we first carried out a data mining analysis using the cBioPortal for Cancer Genomics (<https://www.cbioportal.org/>). We investigated TRIB1 genomic alterations frequency, mRNA expression and overall survival in PCa patients, selecting 20 different studies for a total of 5051 patients and 5315 samples (details listed in **Table 6.1.**). 4952 of 5051 patients were profiled and TRIB1 alterations were found in 383 patients and in 414 samples, thus accounting for the 8% of the integrated dataset (**Figure 6.1.**). TRIB1 genomic alteration frequency was calculated in 15 of 20 datasets and ranged from 40% (Neuroendocrine Prostate Cancer, Multi-Institute, Nat Med 2016) to 1.75% (Prostate Adenocarcinoma, Broad/Cornell, Cell 2013) (**Figure 6.2. A**). When we filtered based on cancer type, TRIB1 was mostly mutated in castration-resistant PCa (41.43%) and neuroendocrine PCa (31.48%) (**Figure 6.2. B**). However, in all cases the most abundant alteration was genomic amplification. Transcriptomic data were available for 3 of 20 selected studies, consisting of tumour/normal pairs (baseline, normal = 0) and showed overexpression of TRIB1 mRNA, even in the absence of genomic amplification (**Figure 6.2. C**). Finally, the overall survival (Kaplan-Meier estimate, calculated in 7 of 20 studies) showed a significant ($p = 2.27e-13$) decrease in the survival of TRIB1 positive patients, compared to TRIB1 negative patients (**Figure 6.3.**).

Table 6.1. cBioPortal for Cancer genomics: selected studies

Twenty published studies were selected from cBioPortal for Cancer Genomics (2012-2019), they include genomic, transcriptomic and clinical data obtained from metastatic prostate carcinoma, metastatic prostate adenocarcinoma, prostate adenocarcinoma-derived organoids and neuroendocrine prostate cancer (<https://www.cbioportal.org/>).

Combined Studies from cBioPortal for Cancer Genomics	Number of Patients
Metastatic Prostate Adenocarcinoma (MCTP, Nature 2012)	119
Metastatic Prostate Adenocarcinoma (SU2C/PCF Dream Team, PNAS 2019)	429
Metastatic Prostate Cancer (SU2C/PCF Dream Team, Cell 2015)	150
Neuroendocrine Prostate Cancer (Multi-Institute, Nat Med 2016)	81
Prostate Adenocarcinoma (Broad/Cornell, Cell 2013)	82
Prostate Adenocarcinoma (Broad/Cornell, Nat Genet 2012)	123
Prostate Adenocarcinoma (CPC-GENE, Nature 2017)	477
Prostate Adenocarcinoma (Fred Hutchinson CRC, Nat Med 2016)	63
Prostate Adenocarcinoma (MSKCC, Cancer Cell 2010)	238
Prostate Adenocarcinoma (MSKCC, PNAS 2014)	104
Prostate Adenocarcinoma (MSKCC/DFCI, Nature Genetics 2018)	1013
Prostate Adenocarcinoma (SMMU, Eur Urol 2017)	65
Prostate Adenocarcinoma (TCGA, Cell 2015)	334
Prostate Adenocarcinoma (TCGA, Firehose Legacy)	500
Prostate Adenocarcinoma (TCGA, PanCancer Atlas)	494
Prostate Adenocarcinoma Organoids (MSKCC, Cell 2014)	7
Prostate Cancer (DKFZ, Cancer Cell 2018)	292
Prostate Cancer (MSK, 2019)	10
Prostate Cancer (MSKCC, JCO Precis Oncol 2017)	451
The Metastatic Prostate Cancer Project (Provisional, December 2018)	19

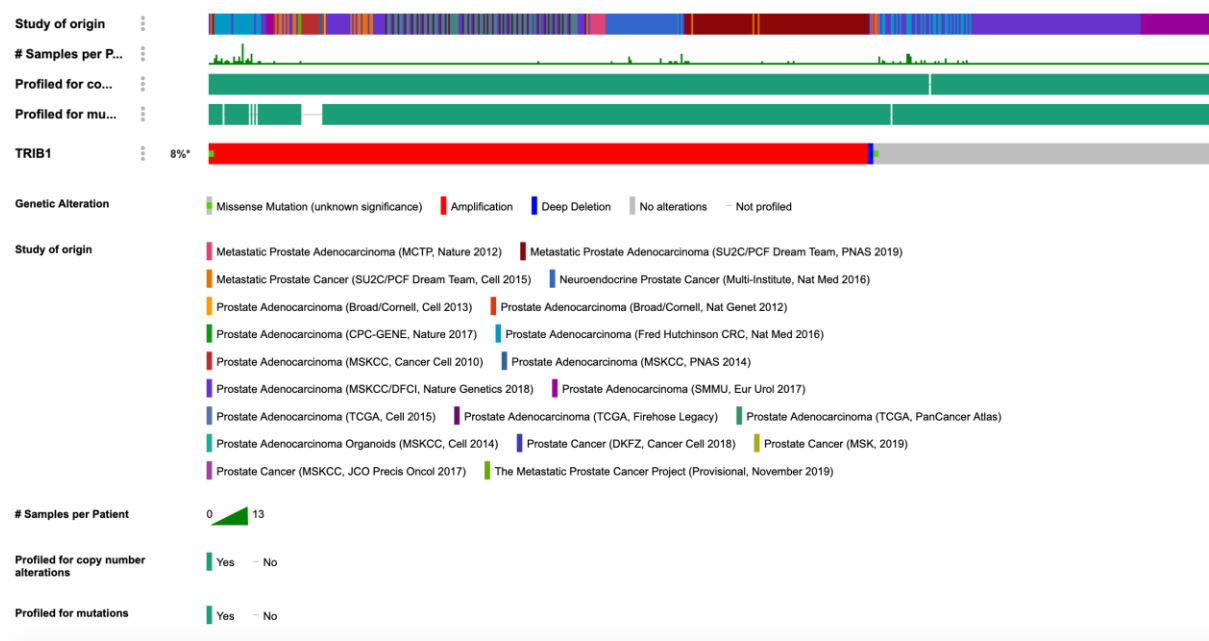


Figure 6.1. Screenshot of cBioPortal for Cancer Genomics showing the summary of TRIB1 alterations in PCa

The figure is a screenshot taken from cBioPortal for Cancer Genomics: 4952 of 5051 patients were profiled for TRIB1 and alterations were found in 383 patients and in 414 samples (8%). The major alteration is gene amplification (<https://www.cbioportal.org/>).

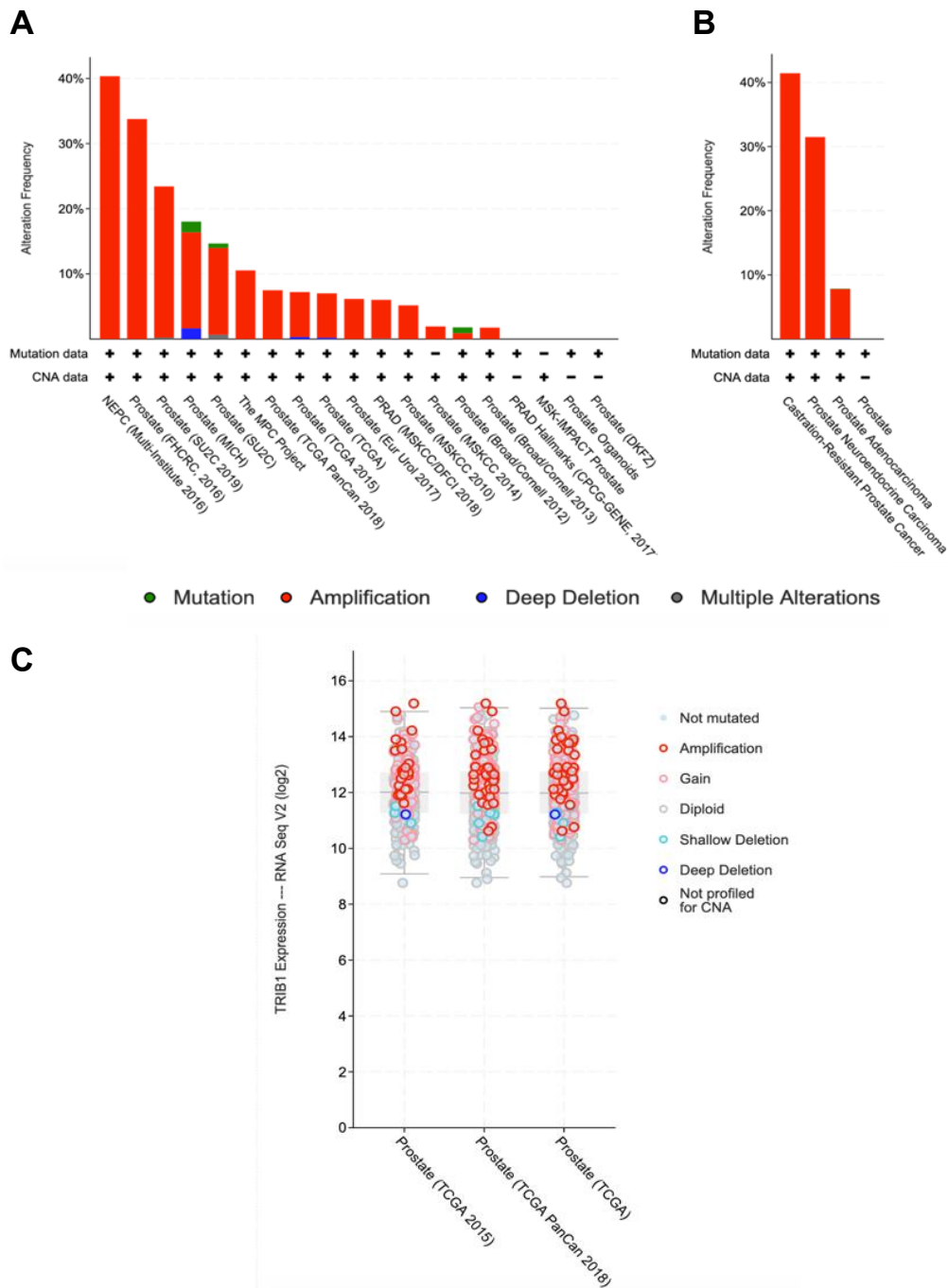
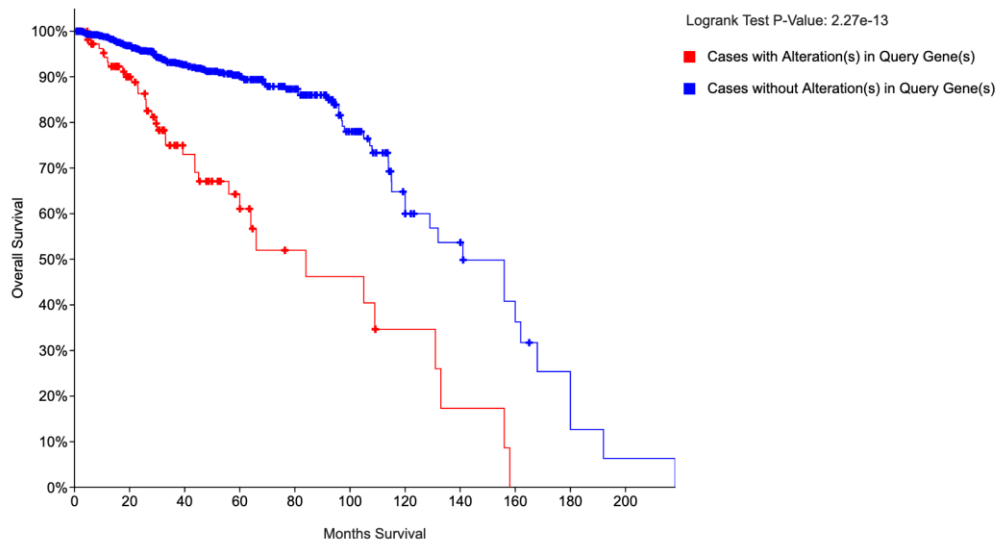


Figure 6.2. Data mining of PCa datasets show TRIB1 gene amplification

TRIB1 gene frequency alterations in 19 of 20 selected studies (A); TRIB1 gene frequency alterations filtered based on cancer types (4 of 5 categories shown) (B); TRIB1 RNA expression profile (RNA-seq) of 6 of 20 studies also showing the type of mutations (C). Graphs generated by cBioPortal for Cancer Genomics. CNA: copy number alterations; VUS: variance of uncertain significance (<https://www.cbioportal.org/>).



	Number of Cases, Total	Number of Cases, Deceased	Median Months Survival
Cases with Alteration(s) in Query Gene(s)	114	36	84
Cases without Alteration(s) in Query Gene(s)	1362	117	141

Figure 6.3. Overall Survival Kaplan-Meier estimate

Overall survival Kaplan-Meier estimate of prostate cancer cases with (red) and without (blue) TRIB1 alterations, calculated by cBioPortal for Cancer Genomics, shows a significant decrease in survival of patients between the two groups. However, the survival data of patients coming from different studies may have been defined by different criteria. Graph generated by cBioPortal for Cancer Genomics (<https://www.cbioportal.org/>).

6.3.2. Assessment of TRIB1 gene expression in human and mouse models of PCa by RT-qPCR

Next, we characterized the endogenous expression of TRIB1 mRNA in a panel of prostate cancer cell lines (described briefly in **Table 6.2.**) by using RT-qPCR. TRIB1 expression was significantly higher in PC3 (4-fold change, $p < 0.0001$), 22RV1 (3-fold change, $p = 0.03$) and LNCAP (2-fold change, $p = 0.02$) but not in DU145, which shows a TRIB1 expression similar to the controls ($p > 0.9$) (**Figure 6.4. A**) We also measured the level of murine Trib1 mRNA, isolated from prostate tumour of wild-type NU/J mice injected with either LNCAP cells or PBS as control (intra-prostatic injections). The cancer was allowed to grow for 30 days and prior to the RNA isolation, tumour development was assessed by gross examination. Despite LNCAP being human cells, Trib1 mRNA levels were significantly increased in LNCAP injected mice, compared to PBS control ($p = 0.03$) (**Figure 6.4. B**), suggesting that the tumour development and growth itself in the prostate gland may be responsible for upregulating Trib1 mRNA. We also checked the murine Trib1 RT-qPCR primers' target specificity by using the web-based tool BLAST (<https://www.ncbi.nlm.nih.gov/tools/primer-blast/>). As shown in **Figure 6.5.**, Trib1 primers specifically amplified the Trib1 mouse gene and not the human one, which does not come up as “predicted” off-target. A predicted off target activity of the primers is for the transcript variant X7 of the human gene FER1L6, but with 4 nucleotides mis-matches in both the forward and the reverse strands, therefore this is unlikely to happen.

Table 6.2. Overview of the human prostate cell lines used in the present study

A total of seven cell lines has been used: three metastatic cancer cells (PC3, DU145 and LNCAP), one xenograft (22RV1) and three immortalised epithelial cells derived from normal prostatic tissue (PWRE1, RWPE1 and PNT1A). PC3, DU145 and PNT1A do not express or express at low levels the androgen receptor. LNCAP cells have also been used to generate a prostate cancer mouse model (see **Figure 6.3 C**).

Cell line	Characteristics	Androgen Receptor
PC3	Human Prostatic Adenocarcinoma, Bone Metastasis	-
DU145	Human Prostatic Adenocarcinoma, Brain Metastasis	-
LNCAP	Human Prostate Carcinoma, Lymph Nodes Metastasis	+
22RV1	Human Prostate Carcinoma, Xenograft	+
PWRE1	Human Prostatic Epithelial Cells, Normal	+
RWPE1	Human Prostatic Epithelial Cells, Normal	+
PNT1A	Human Prostatic Epithelial Cells, Normal	-

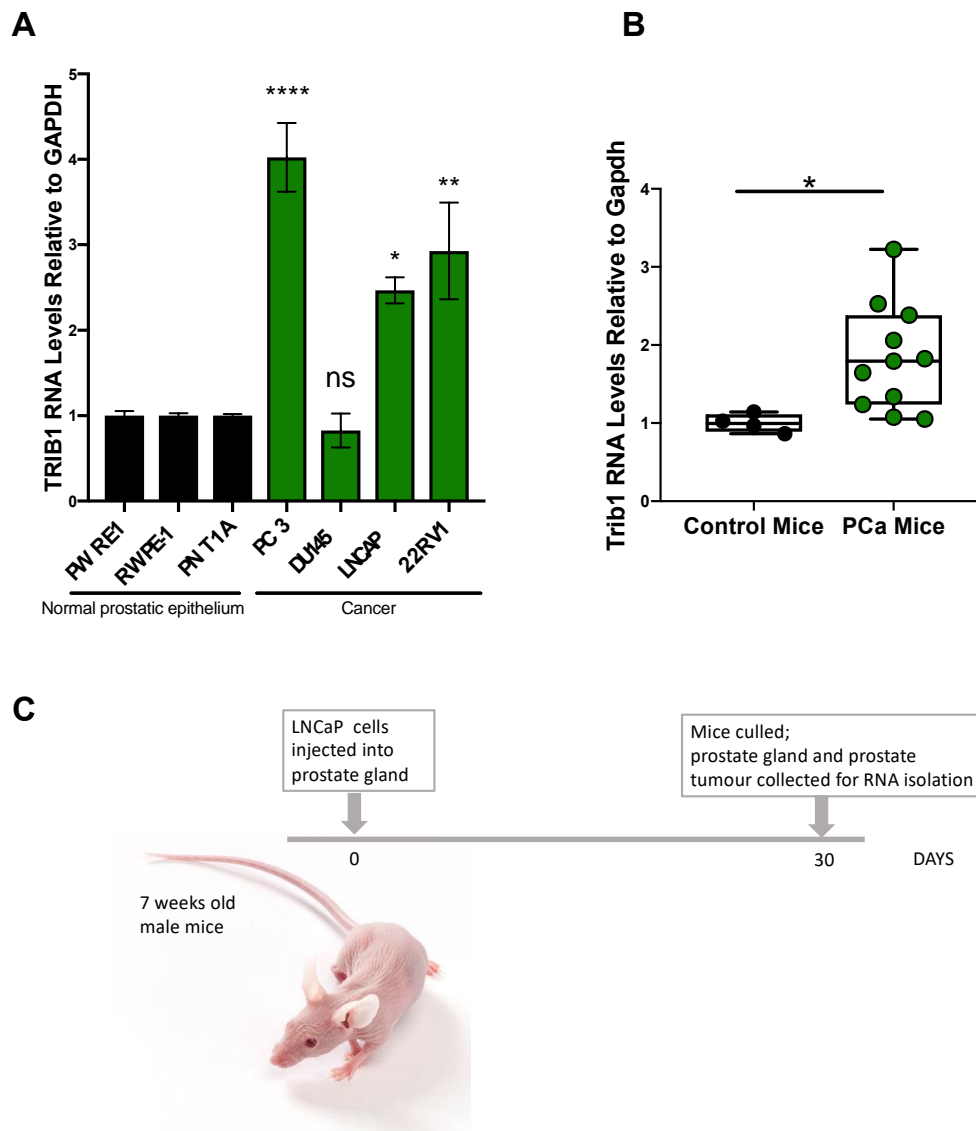


Figure 6.4. Assessment of TRIB1 RNA expression in human and mouse models of PCa

Relative level of TRIB1 RNA normalised to the housekeeping GAPDH in a panel of prostate cell lines (normal vs cancer) (mean \pm SEM, Ordinary One Way Anova, $n=3-6$, **** $p<0.0001$, ** $p<0.002$, * $p<0.05$, ns $p>0.05$) (A); relative level of murine Trib1 RNA normalised to the housekeeping Gapdh in prostate tissue from control mice and prostate tumour from mice injected with LNCaP cells (normal vs tumour) (mean \pm SEM, unpaired t-test, $n=4-11$, * $p<0.05$) (B); schematic illustration of the prostate cancer mouse model, obtained by injecting human cancer cells (LNCaP) in wild-type NU/J mice (C).

Primer pair 1

	Sequence (5'->3')	Length	Tm	GC%	Self complementarity
Forward primer	CTTACATCCAGCTGCCGTCC	20	60.81	60.00	6.00
Reverse primer	GTAGGCCTTGCTCTCACCAA	20	59.68	55.00	6.00

Products on target templates

>[NM_144549.4](#) Mus musculus tribbles pseudokinase 1 (Trib1), mRNA

```
product length = 74
Forward primer 1   CTTACATCCAGCTGCCGTCC 20
Template        907 ..... 926

Reverse primer 1   GTAGGCCTTGCTCTCACCAA 20
Template        980 ..... 961
```

>[XM_011517236.2](#) PREDICTED: Homo sapiens fer-1 like family member 6 (FER1L6), transcript variant X7, mRNA

```
product length = 1841
Reverse primer 1   GTAGGCCTTGCTCTCACCAA 20
Template        2230 ..C.AT....G..... 2211

Reverse primer 1   GTAGGCCTTGCTCTCACCAA 20
Template        390 C...A.T....A.....G 409
```

Figure 6.5. Assessment of murine Trib1 primers' target specificity using BLAST Primers tool

The figure is a screenshot taken from the BLAST Primers tool (<https://www.ncbi.nlm.nih.gov/tools/primer-blast/>), showing the specificity of murine Trib1 RT-qPCR primers.

6.3.2. Identification of downregulated miRNAs potentially targeting TRIB1

Once established that TRIB1 is amplified and overexpressed in different PCa datasets and upregulated at the RNA level in human and mouse models of PCa, we investigated whether miRNAs downregulated in PCa target the 3'UTR of TRIB1, causing its overexpression. We used miRCancer database (October 2019 release) (<http://mircancer.ecu.edu/index.jsp>) and found that a total of 168 distinct miRNAs are dysregulated in different models of PCa: 133 of 168 are downregulated, while 51 are upregulated (complete list is in Chapter 8, Appendix V). However, 16 miRNAs are listed as either down or up-regulated, according to different studies. We focused on the downregulated miRNAs and among them we found 21 miRNAs predicted to target TRIB1 according to three different miRNA-target prediction tools (miRanda, TargetScan and StarBase), as explained in Chapter 2 (**Figure 6.6**). **Table 6.3** lists the candidate miRNAs targeting TRIB1 and relevant publications. To understand the potential biological impact of these miRNAs on TRIB1, we further analysed the output generated by TargetScan (version 7.2, released in March 2018), shown in **Table 6.4** with a description of the scores and the main parameters of the algorithm in the table legend. All miRNAs are predicted to bind to the 3'UTR of TRIB1 and some of them have two different binding sites (let-7a-3p, miR-23a-3p, miR-101-3p, miR-130a-5p, miR-132-3p, miR-150-3p, miR-212-3p). They are characterized by a seed region pairing of 7-8 nucleotides (7-8mers) with different conformations (7mers 1A and M8). These two types of seed region strongly correlate with targeting efficiency and are selectively conserved (*Friedman et al., 2009*). The context++ and the weighted context++ scores, which are predictive of the efficacy of the sites (*Agarwal et al., 2015*) are low, negative numbers, suggesting a great predicted activity for all miRNAs. In addition, all the miRNAs, except for let-7a-3p, show a good context++ score percentile ranging from 62 to 99, suggesting that these sites on TRIB1 are more favourable than other sites of the same miRNA family. In fact, the context++ score percentile represents the percentile rank of each site compared to all sites of the same miRNA family: values between 50 and 100 indicates that that specific site is more favourable than most other sites of the same miRNA family. The context++ branch length, representing the site conservation, is also good, particularly for miR-23a-3p, miR-23b-3p, miR-101-3p, let-7a-5p, let-7c-5p and miR-144-3p (threshold: 8mer \geq 1.8; 7mer-m8 \geq 2.6; 7mer-1A \geq 3.6). Finally, the P_{CT}, calculated from the context++ branch length, indicates that some interactions are conserved due to their biological relevance. However, the algorithm calculates this only for highly conserved miRNA families. We previously have showed that miR-132-3p and miR-101-3p are able to modulate TRIB1

expression in both human and murine macrophages and miR-101/TRIB1 interaction was experimentally validated in our lab (see Chapter 3). Similarly, miR-224 was shown to modulate TRIB1 in a 3D model of PCa by Lin and colleagues (*Lin et al., 2014*). Therefore, we assessed the expression of these three miRNAs in prostate cancer cell lines by RT-qPCR. Consistent with published data, all the miRNAs were downregulated in cancer cells compared to control cells. miR-132-3p and miR-224-5p downregulation was the most robust in all cancer cell lines and miR-224-5p was not detected in PC3 and 22RV1 cell lines. miR-101 was significantly downregulated in PC3 ($p = 0.04$), but not in DU145, LNCAP and 22RV1 ($p = 0.7$, $p = 0.10$, $p = 0.09$) (**Figure 6.7.**). We next focused on the validation of miR-132-3p/TRIB1 interaction.

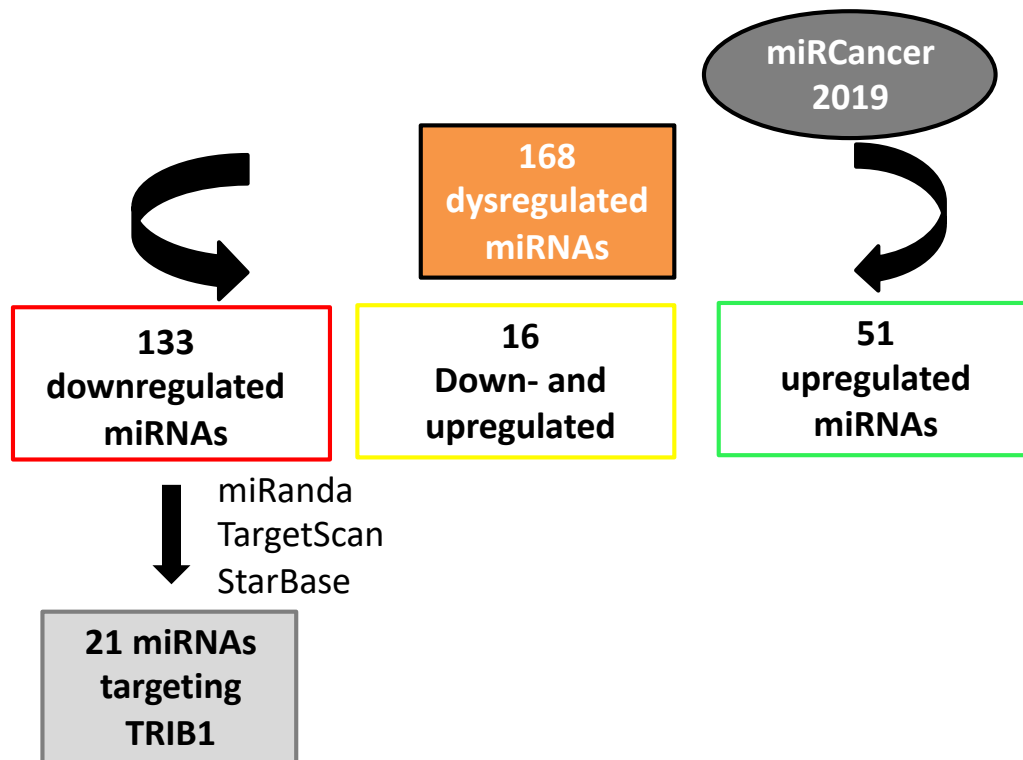


Figure 6.6. Identification of downregulated miRNAs targeting TRIB1

miRCaner database was used to identify dysregulated miRNAs in PCa. A total of 162 miRNAs was found to be altered: 133 of 168 are downregulated, 51 of 168 are upregulated and 16 have been reported by several groups to be either down- or upregulated. Among the downregulated miRNAs, we found 21 potential regulators of TRIB1 gene, which have been previously associated with other targets in PCa. The miR-target prediction analysis was carried out considering interactions present in three different databases (miRanda, TargetScan and StarBase).

Table 6.3. Candidate miRNAs downregulated in PCa and predicted to target the 3'UTR of TRIB1

List of miRNAs downregulated in PCa, predicted to target TRIB1 according to three different prediction tools (miRanda, TargetScan, StarBase) and relevant publications.

miRNAs	Cancer	Status	Publications
hsa-let-7a	Prostate Cancer	Downregulated	Dong et al., 2010, Tang et al., 2018
hsa-let-7c	Prostate Cancer	Downregulated	Nadiminty et al., 2012
hsa-miR-101	Prostate Cancer	Downregulated	Hao et al., 2011, Chakravarthi et al., 2016, Huang et al., 2017
hsa-miR-10a	Prostate Cancer	Downregulated	Mu et al., 2019
hsa-miR-129	Prostate Cancer	Downregulated	Xu et al., 2015, Xu et al., 2017
hsa-miR-130a	Prostate Cancer	Downregulated	Ramalho-Carvalho et al., 2017
hsa-miR-132	Prostate Cancer	Downregulated	Formosa et al., 2013, Qu et al., 2016, Li et al., 2018
hsa-miR-144-3p	Prostate Cancer	Downregulated	Zheng et al., 2018
hsa-miR-150	Prostate Cancer	Downregulated	Hong et al., 2019
hsa-miR-154	Prostate Cancer	Downregulated	Zhu et al., 2014
hsa-miR-212	Prostate Cancer	Downregulated	Borrego-Diaz et al., 2014, Ramalinga et al., 2015
hsa-miR-22	Prostate Cancer	Downregulated	Xin et al., 2016
hsa-miR-224	Prostate Cancer	Downregulated	Fu et al., 2015, Lin et al., 2014, Goto et al., 2014
hsa-miR-23a	Prostate Cancer	Downregulated	Cai et al., 2015
hsa-miR-23b	Prostate Cancer	Downregulated	Majid et al., 2012
hsa-miR-302a	Prostate Cancer	Downregulated	Zhang et al., 2015
hsa-miR-330	Prostate Cancer	Downregulated	Lee et al., 2009, Mao et al., 2013
hsa-miR-3619-5p	Prostate Cancer	Downregulated	Li et al., 2017
hsa-miR-372	Prostate Cancer	Downregulated	Kong et al., 2016
hsa-miR-373-3p	Prostate Cancer	Downregulated	Qu et al., 2018
hsa-miR-382	Prostate Cancer	Downregulated	Zhang et al., 2016

Table 6.4. TargetScan miRNA-TRIB1 analysis output

TargetScan Human 7 output for candidate miRNAs targeting TRIB1 showing the binding site position on the 3'UTR, the seed region type, the context⁺⁺ score (CS), the context⁺⁺ score percentile (CSP), the weighted context⁺⁺ score (WCS), the conserved branch length (CBL) and the probability of conserved targeting (P_{CT}). The CS for a specific site is the sum of the contribution of 14 features, described by Agarwal et al., 2015: the lowest CS is the most favourable; the CSP is the percentile rank of each site compared to all sites of the same miRNA family: values between 50 and 100 indicates that that specific site is more favourable than most other sites of the same miRNA family. The WCS represents the predicted efficacy of the sites: scores with lower negative values indicated greater predicted activity (Nam et al., 2014). The CBL represents the site conservation (threshold: 8mer \geq 1.8; 7mer-m8 \geq 2.6; 7mer-1A \geq 3.6). The P_{CT}, calculated only for the highly conserved miRNA families, ranges from 0 to 1 and it estimates that a site conserved to a particular branch length is conserved because of its targeting activity; it is then a measurement of the biological relevance of the interactions, as it correlates with the mean level of target destabilization, as reported by Friedman et al., 2009. The higher the P_{CT}, the higher the conservation and the biological relevance of the miRNA-target interaction.

miRNA	3'UTR position	Seed type	CS	CSP	WCS	CBL	Pct
hsa-let-7a-2-3p	1851-1857	7mer-m8	-0.14	86	-0.13	0.054	N/A
hsa-let-7a-3p	1113-1119	7mer-1A	-0.01	25	-0.01	0.054	N/A
hsa-let-7a-5p	1518-1524	7mer-1A	-0.22	78	-0.2	6.307	0.94
hsa-let-7c-3p	1538-1544	7mer-m8	-0.05	64	-0.05	1.01	N/A
hsa-let-7c-5p	1518-1524	7mer-1A	-0.22	78	-0.2	6.307	0.94
hsa-miR-101-3p.1	1526-1532	7mer-m8	-0.22	93	-0.21	4.444	0.84
hsa-miR-101-3p.1	1424-1430	7mer-1A	-0.04	69	-0.04	3.274	0.22
hsa-miR-10a-5p	391-397	7mer-m8	-0.2	92	-0.2	1.351	< 0.1
hsa-miR-129-1-3p	1467-1474	8mer	-0.43	99	-0.41	3.64	0.49
hsa-miR-130a-3p	630-636	7mer-1A	-0.12	82	-0.11	1.817	< 0.1
hsa-miR-130a-5p	1662-1669	8mer	-0.18	90	-0.17	6.643	0.63
hsa-miR-130a-5p	1869-1875	7mer-1A	-0.08	74	-0.07	2.746	0.12
hsa-miR-132-3p	554-560	7mer-m8	-0.05	77	-0.05	1.369	< 0.1
hsa-miR-132-3p	1763-1769	7mer-m8	-0.1	86	-0.09	1.264	< 0.1
hsa-miR-144-3p	1423-1430	8mer	-0.26	96	-0.24	3.196	0.28
hsa-miR-150-3p	79-85	7mer-1A	-0.19	79	-0.19	0.054	N/A
hsa-miR-150-5p	250-256	7mer-m8	-0.15	95	-0.15	0.154	< 0.1
hsa-miR-150-5p	336-342	7mer-1A	-0.2	97	-0.2	0.921	< 0.1
hsa-miR-154-5p	1635-1641	7mer-m8	-0.06	65	-0.05	2.541	N/A
hsa-miR-212-3p	554-560	7mer-m8	-0.03	67	-0.03	1.369	< 0.1
hsa-miR-212-3p	1763-1769	7mer-m8	-0.1	86	-0.09	1.264	< 0.1
hsa-miR-22-3p	458-464	7mer-m8	-0.13	78	-0.13	0	< 0.1
hsa-miR-224-5p	157-163	7mer-m8	-0.19	94	-0.19	2.321	N/A
hsa-miR-23a-3p	1662-1669	8mer	-0.21	91	-0.19	6.643	0.63
hsa-miR-23a-3p	1869-1875	7mer-1A	-0.07	70	-0.06	2.746	0.12
hsa-miR-23a-5p	221-227	7mer-m8	-0.29	96	-0.29	0	N/A
hsa-miR-23b-3p	1662-1669	8mer	-0.21	91	-0.19	6.643	0.63
hsa-miR-23b-5p	221-227	7mer-m8	-0.3	93	-0.3	0	N/A
hsa-miR-302a-3p	680-687	8mer	-0.18	91	-0.17	1.727	< 0.1
hsa-miR-330-3p	947-954	8mer	-0.03	65	-0.03	0.091	N/A
hsa-miR-330-5p	1281-1287	7mer-1A	-0.07	68	-0.06	2.089	N/A
hsa-miR-3619-3p	1027-1033	7mer-m8	-0.1	81	-0.1	0	N/A
hsa-miR-3619-5p	114-120	7mer-1A	-0.09	78	-0.09	0.348	N/A
hsa-miR-372-3p	680-687	8mer	-0.2	93	-0.19	1.727	< 0.1
hsa-miR-372-5p	169-175	7mer-m8	-0.02	63	-0.02	0.054	N/A
hsa-miR-373-3p	680-687	8mer	-0.13	91	-0.12	1.727	< 0.1
hsa-miR-382-3p	1667-1673	7mer-m8	-0.16	93	-0.15	2.545	N/A

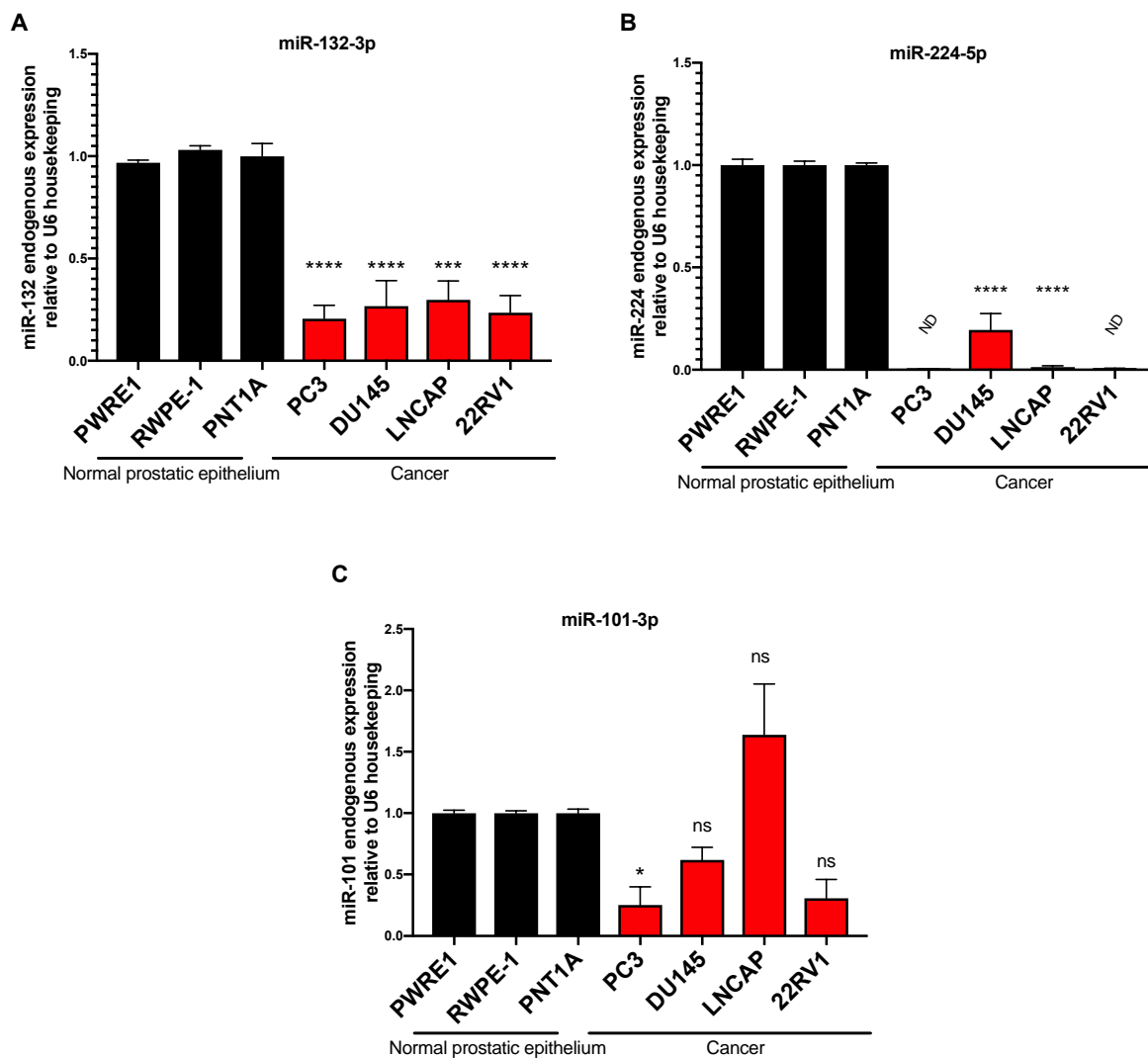


Figure 6.7. Assessment of candidate miRNAs expression in prostate cancer cell lines by RT-qPCR

Relative abundance of miR-132-3p (A), miR-224-5p (B) and miR-101-3p (C) normalised to the housekeeping U6 measured in a panel of prostate cancer cell lines by RT-qPCR (normal vs cancer) (mean \pm SEM, Ordinary One Way Anova, $n=3-6$, **** $p<0.0001$, *** $p<0.0002$, * $p<0.05$, ns $p>0.05$). ND: not detected.

6.3.3. Validation of miR-132-3p/TRIB1 interaction by gene reporter assay

According to TargetScan analysis, miR-132-3p has two binding sites for the 3'UTR of TRIB1. Despite it not being well conserved (CBL is 1.3 for binding site 1 and 1.2 for binding site 2), miR-132-3p/TRIB1 interaction shows a good CS; moreover, miR-132-3p is an established onco-suppressor in PCa with multiple targets and it is normally silenced by promoter hypermethylation. **Table 6.5.** lists the experimentally validated targets of miR-132-3p in the context of PCa. To investigate whether miR-132-3p binds to the 3'UTR of TRIB1 we used a dual luciferase reporter assay. We transiently transfected TRIB1 3'UTR renilla reporter plasmid and a firefly reporter plasmid together with miR-132-3p mimic or miR-132-3p inhibitor in HEK293T cell line. We observed that in the presence of the mimic the gene reporter activity significantly decreased compared to the negative control (38% decrease, $p=0.02$) (**Figure 6.8. A**), suggesting that the overexpression on miR-132-3p is responsible for TRIB1 3'UTR destabilization. Indeed, when miR-132-3p was inhibited there was a small increase of the luciferase activity (10% increase), meaning that the inhibition of the endogenous miR-132-3p enhanced TRIB1 expression. However, this was not statistically significant ($p=0.09$) (**Figure 6.8. B**). We did not perform miR-132-3p binding site mutagenesis, therefore we cannot conclude if the two binding sites are functional (see section 6.5. Limitations of the study).

Table 6.5. Experimentally validated targets of miR-132-3p and their effect on PCa

The table lists miR-132-3p target genes which have been experimentally validated, along with their biological effect in the context of PCa.

miR-132-3p target gene	Downstream effect	Reference
TALIN2	Impairment of cellular adhesion, cell death	Formosa et al., 2013
HB-EGF	Impairment of cellular adhesion, cell death	Formosa et al., 2013
E2F5	Reduction of cancer cells viability, increase in apoptosis	Li et al., 2018
GLUT1	Reduction of glycolysis and proliferation	Qu et al., 2016

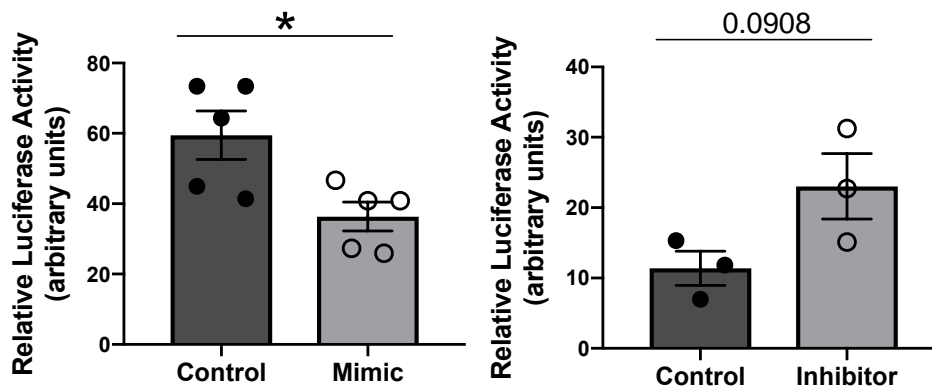


Figure 6.8. miR-132-3p/TRIB1 experimental validation

Relative luciferase activity measured in HEK293T cell line following 24 hours co-transfection of TRIB1 3'UTR-renilla reporter, firefly reporter and miR-132-3p mimic (50nM) (A) and inhibitor (25nM) (B) Total DNA transfected was 100ng/well (renilla/firefly readings, mean \pm SEM, unpaired t-test, n = 3-5, * p<0.05, ns p>0.05).

6.3.4. Impact of miR-132-3p and TRIB1 on PC3 gene expression

To evaluate the impact of miR-132-3p on PCa, we transiently overexpressed the miRNA in PC3 cell line by using a mimic and in parallel we knocked-down TRIB1 by using a siRNA. **Figure 6.9.** shows the TRIB1 mRNA level following miR-132 overexpression (**Figure 6.9. A**) and siRNA-mediated TRIB1 knockdown in PC3 cell line (**Figure 6.9. B**), which was reduced by 60% ($p=0.03$) and 80% ($p<0.0001$), respectively. We then used the same RNA samples to investigate the gene expression profile induced by either miR-132-3p mimic and TRIB1 knockdown and we found similar signatures. The genes we investigated are listed in **Table 6.6.**; all of them have been previously implicated in PCa biology, although the literature presents opposing and controversial data. We chose IL-1 β , IL-6 and IL-8 to evaluate the inflammatory status and PDL1, SPAR-C and VEGF as cancer-related genes for immunoregulation, metastasis and angiogenesis. We observed that the mRNA levels of pro-inflammatory cytokines IL-1 β , IL-6 and IL-8 increased in both conditions (**Figure 6.10.**). Specifically, IL-1 β significantly increased (1.4-fold change, $p=0.004$) in TRIB1 knockdown cells and in PC3 overexpressing miR-132-3p (1.2-fold change, $p=0.04$) (**Figure 6.10. A, D**). Both IL-6 and IL-8 mRNA expression was enhanced in TRIB1 knockdown samples (2.4-fold change, $p=0.001$, 1.6-fold change, $p=0.008$, respectively) (**Figure 6.10. E, F**). This is in line with what we have previously shown in macrophages in Chapter 3: TRIB1 manipulation affected IL-6 and IL-8 expression and secretion. Similarly, in PC3 treated with miR-132-3p mimic, IL-8 mRNA levels also increased (1.8-fold change, $p=0.03$), while the changes in IL-6 were not statistically significant ($p=0.2$). When we analysed the cancer genes, we also observed similar signatures: the expression of SPAR-C was significantly increased in TRIB1 knockdown cells by 1.6-fold change ($p=0.01$), but not in PC3 overexpressing miR-132-3p ($p=0.5$) (**Figure 6.11. A, D**); the expression of PD-L1 was significantly increased in both conditions (knockdown 1.9-fold change, $p=0.02$; mimic 2-fold change, $p=0.02$) (**Figure 6.11. B, E**). VEGF expression did not change in either condition (**Figure 6.11. C, F**).

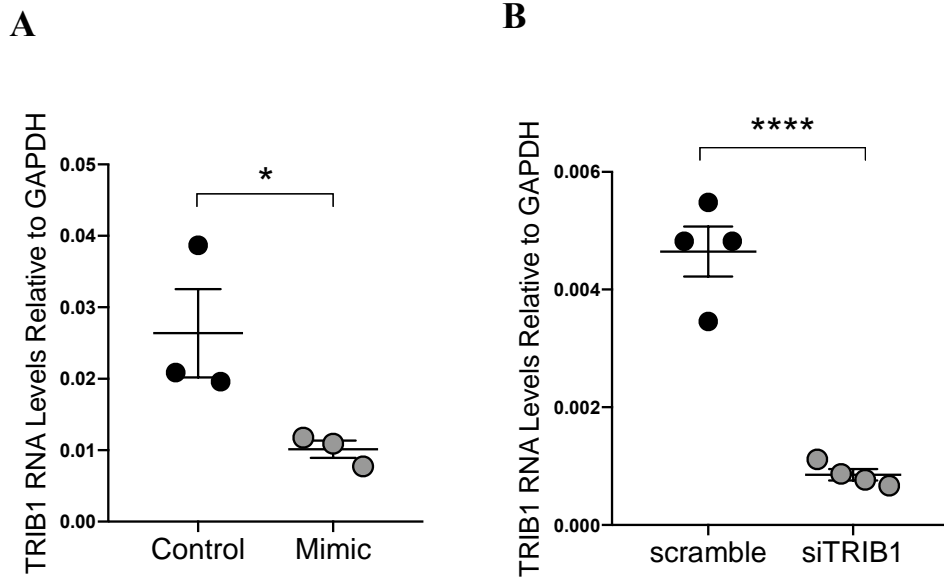


Figure 6.9. Assessment of TRIB1 RNA expression by RT-qPCR after miR-132-3p overexpression and TRIB1 knockdown in PC3 cell line

Relative TRIB1 RNA expression normalised to the housekeeping GAPDH, after 48 hours overexpression of miR-132-3p (50 nM) (**A**) and 48 hours TRIB1 knockdown (50 nM) (**B**) in PC3 cell line. Data are presented as mean \pm SEM (n = 3-4, unpaired t-test, * p<0.05, **** p < 0.0001).

Table 6.6. List of genes analysed in transfected PC3 cell line

The table lists the genes we analysed in transfected PC3 cell line along with their expression and function in PCa, according to published literature.

Gene	Expression in PCa	Role in PCa	Reference
IL-1β, Interleukin 1β	+++	Pro-inflammatory, tumorigenic, pro-metastatic	Liu et al., 2013, Shahriari et al., 2017
IL-6, Interleukin 6	+++	Pro-inflammatory, multifunctional	Culig et al., 2005, Nguyen et al., 2014
IL-8, Interleukin 8	+++	Pro-inflammatory, tumorigenic and pro-angiogenic	Kim et al., 2001, Guo et al., 2017
SPAR-C, Secreted Protein Acidic and Cysteine Rich	Variable	Controversial, inhibition/promotion of metastasis	Thomas et al., 2000, DeRosa et al., 2012, Ma et al., 2017, Liu et al., 2018
PD-L1, Programmed death-ligand 1	+++	Immunoregulatory, inhibition of anti-tumour immunity	Gevensleben et al., 2015
VEGF, Vascular Endothelial Growth Factor	+++	Angiogenesis	Botelho et al., 2010

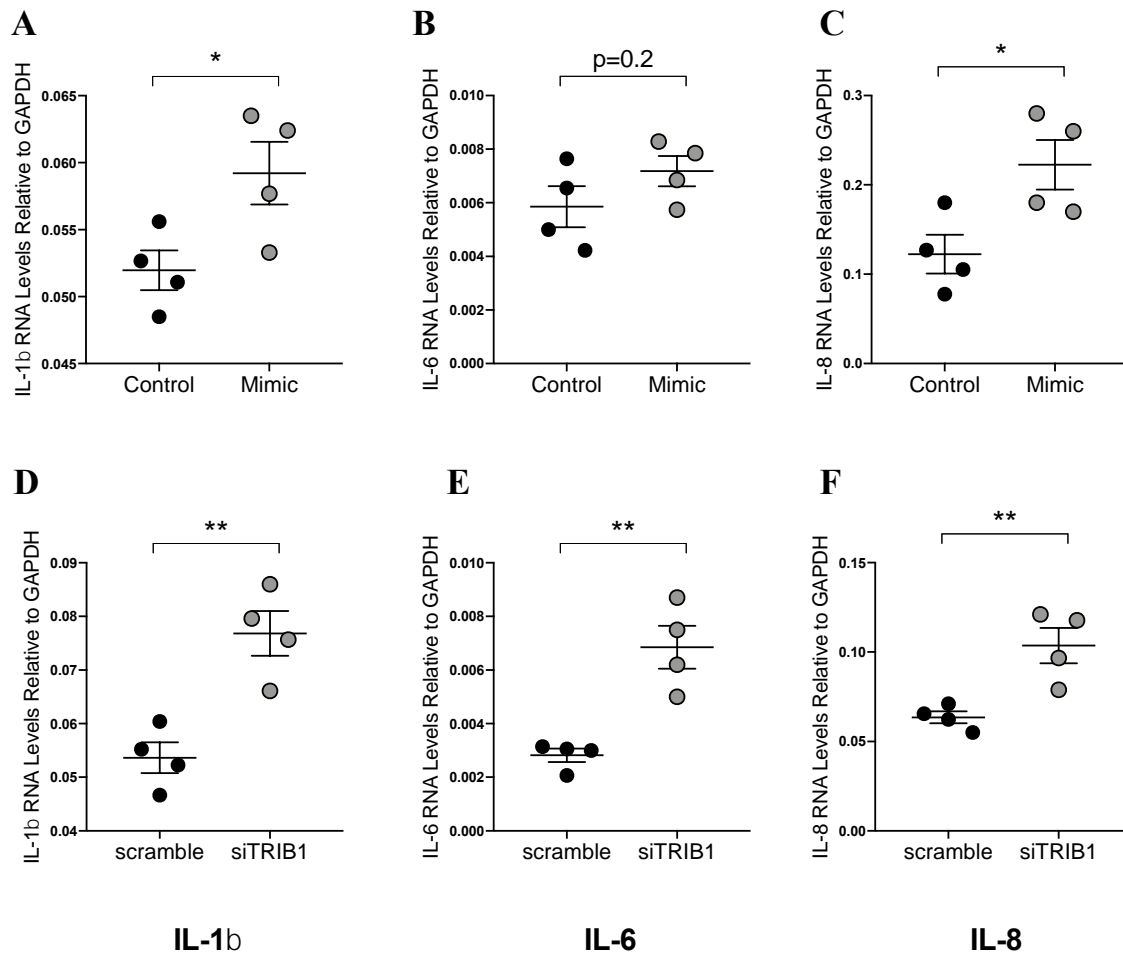


Figure 6.10. Impact of miR-132-3p and TRIB1 on pro-inflammatory cytokines in PC3 cell line

Relative RNA expression of pro-inflammatory cytokines IL-1 β , IL-6 and IL-8 normalised to the housekeeping GAPDH, after 48 hours overexpression of miR-132-3p (50 nM) (**A, B, C**) and 48 hours TRIB1 knockdown (50 nM) (**D, E, F**) in PC3 cell line. Data are presented as mean \pm SEM (n = 4, unpaired t-test, * p < 0.05, ** p < 0.005, **** p < 0.0001, ns p > 0.05).

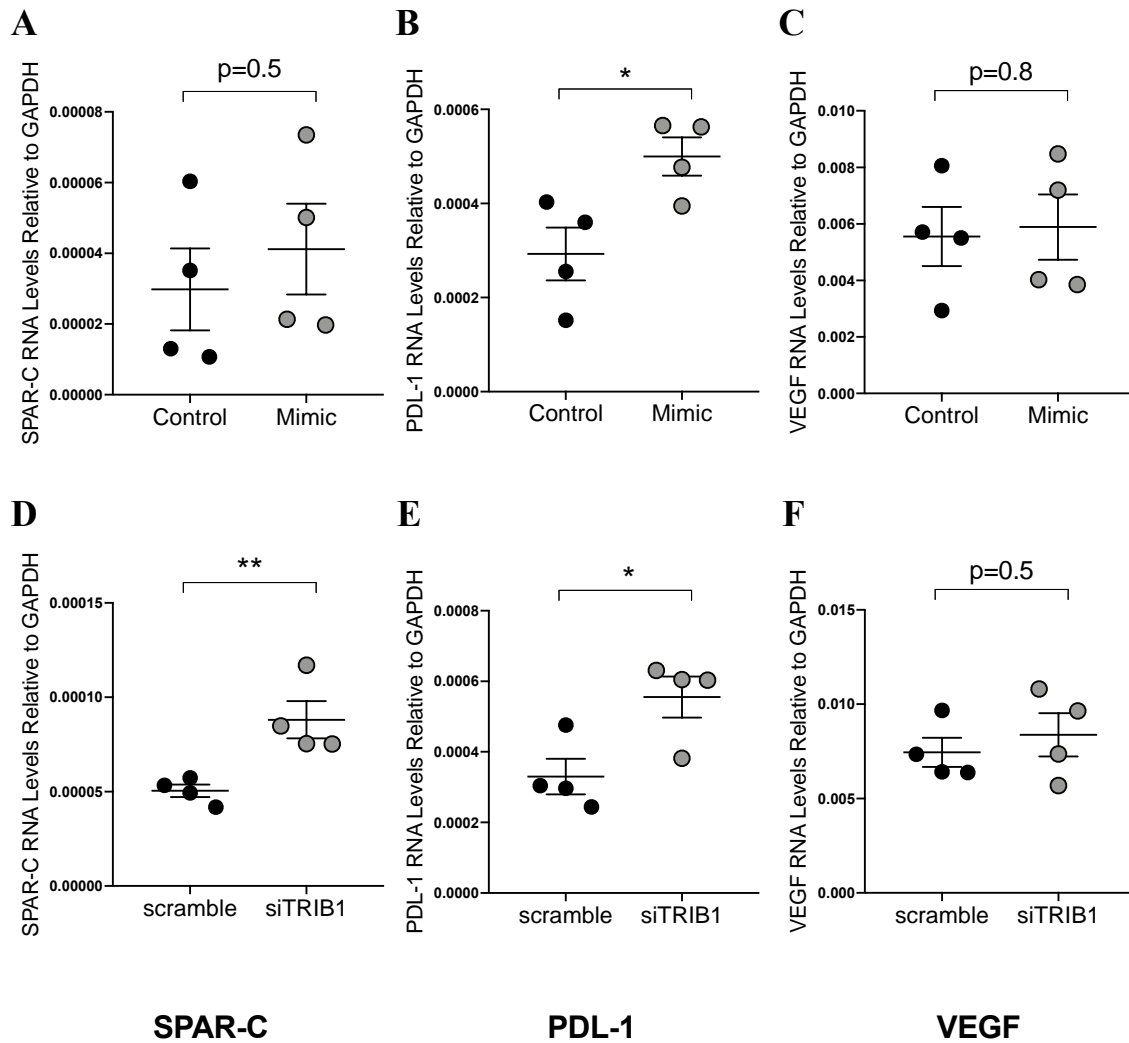


Figure 6.11. Impact of miR-132-3p and TRIB1 on cancer-related genes in PC3 cell line

Relative RNA expression of SPAR-C, PD-L1 and VEGF normalised to the housekeeping GAPDH, after 48 hours overexpression of miR-132-3p (50 nM) (**A**, **B**, **C**) and 48 hours TRIB1 knockdown (50 nM) (**D**, **E**, **F**) in PC3 cell line. Data are presented as mean \pm SEM (n = 4, unpaired t-test, * p < 0.05, ** p < 0.005, ns p > 0.05).

6.4. Summary

Considering the high rates of incidence and mortality of PCa, the identification of new molecular targets and therapeutic strategies appears critical (Rawla *et al.*, 2019). A growing number of cancer studies highlight the potential of miRNAs: given their ability to simultaneously control the expression of multiple genes in virtually all animal tissues, miRNAs represent attractive candidates through which we can modulate the expression of oncogenes and tumour suppressor genes (Shah *et al.*, 2016). It has been shown that in PCa the majority of miRNAs are downregulated and often silenced by epigenetic modifications (Ozen *et al.*, 2007, Coppola *et al.*, 2010, Ramassone *et al.*, 2018). As a consequence, the expression of their target genes increases. Here, we showed that TRIB1, an established oncogene in acute myeloid leukemia (Röthlisberger *et al.*, 2007) and in hepatocellular carcinoma (Ye *et al.*, 2017), is overexpressed in PCa and is a direct target of multiple downregulated/silenced miRNAs. Previous work showed that TRIB1 is upregulated in PCa both *in vitro* and *in vivo* and it supports prostate tumorigenesis via regulating ER chaperones (Lin *et al.*, 2014, Mashima *et al.*, 2014, Moya *et al.*, 2018). A short tandem repeat (STR) found in the 3'UTR of TRIB1 has also been linked to PCa risk, aggressiveness and survival (Moya *et al.*, 2018). Still, what is upstream of TRIB1 overexpression in PCa remains unclear. In this study, we hypothesised that the overexpression of TRIB1 in PCa can be explained by the downregulation of endogenous miRNAs. Our bioinformatics analysis of published cancer datasets showed that the most frequent alteration in TRIB1 is in genomic amplification; however, the gene is upregulated even in the absence of amplification. This was consistent with what was observed by Mashima and colleagues (Mashima *et al.*, 2014). We showed that TRIB1 mRNA is overexpressed in PC3, LNCAP and 22RV1 cancer cell lines, but not in DU145, compared to non-tumour controls (PWRE1, RWPE1 and PNT1A); interestingly, we also found that murine Trib1 mRNA tends to increase in mice injected with LNCAP cells, compared to control mice. LNCAP is a human derived cell line and this suggests that there might be intrinsic, environmental factors in the developed prostate tumour that, in turn, increase Trib1 transcription. However, this should be investigated further, using different models and also by looking at Trib1 protein levels. By using the miRCancer database and TargetScan prediction algorithm, we identified 21 downregulated miRNAs, predicted to target the 3'UTR of TRIB1 gene. The majority of predicted interactions are characterized by good score alignment, free energy and phylogenetic conservation, suggesting a potential biological relevance. We confirmed the downregulation of two candidate miRNAs (miR-132-3p and miR-224-5p) in a panel of PCa cell lines and

controls by using RT-qPCR and we further substantiated the interaction between miR-132-3p and TRIB1 through a luciferase gene reporter assay. We selected miR-132-3p as its expression was significantly downregulated in all cancer cell lines and we previously showed that it is able to modulate TRIB1 expression in human and murine macrophages (see Chapter 3). Moreover, miR-132-3p is well appreciated to be a tumour suppressor miRNA and several targets in PCa have already been experimentally validated (see **Table 6.5**). The gene reporter assay confirmed that miR-132-3p mimic exerts a negative effect on the 3'UTR of TRIB1. However, inhibiting miR-132-3p had no significant effect on gene reporter activity. This may be explained by the variability of transfection efficiency and the low number of biological replicates ($n = 3$). Although our *in-silico* prediction and luciferase assay data strongly suggest that miR-132-3p binds to the 3'UTR of the pseudo-kinase, we cannot conclude that the 2 binding sites are functional, due to the lack of mutagenesis experiment. Last, we evaluated the effect of both miR-132-3p overexpression and TRIB1 knockdown on PC3 gene expression profile and observed similar signatures. Specifically, the mRNA expression of IL-1 β , IL-6, IL-8, PD-L1 and SPAR-C is enhanced, suggesting that these genes might specifically respond to TRIB1 changes. We previously showed that overexpressing TRIB1 in human macrophages results in the reduction of IL-6 and IL-8 and we observed the opposite effect in cells treated with miR-101-3p mimic, regulator of TRIB1 (see Chapter 3). Furthermore, miR-132-3p has been already shown to increase IL-8 expression, via directly targeting SirT1 (nicotinamide adenine dinucleotide-dependent deacetylase) and modulating nuclear factor $\kappa\beta$ (NF $\kappa\beta$) in adipocytes (*Strum et al., 2009*). The expression of IL-1 β , IL-6, IL-8 is usually upregulated in PCa patients and it has been associated with poor prognosis of PCa and tumorigenic activity (*Kim et al., 2001, Culig et al., 2005, Liu et al., 2013, Nguyen et al., 2014, Guo et al., 2017, Shahriari et al., 2017*). The immunoregulatory protein PD-L1 is also highly expressed in prostate cancer, enabling the tumour to escape the immune system surveillance (*Gevensleben et al., 2015*), while the role of SPAR-C appears to be controversial. In fact, SPAR-C has been implicated in PCa and breast cancer bone metastasis with opposite effects: in PCa high expression of SPAR-C is correlated with a bad prognosis and predicts metastasis progression (*Thomas et al., 2000, Derosa et al., 2012*); in breast cancer it has been shown to inhibit migration and invasion (*Ma et al., 2017*). Interestingly, Liu and colleague observed that SPAR-C is downregulated in PCa by promoter hypermethylation and lower levels of SPAR-C mRNA and protein correlate with a poorer prognosis (*Liu et al., 2018*).

In conclusion, we demonstrated that TRIB1 is a target of multiple downregulated miRNAs in PCa that might represent the mechanisms behind TRIB1 overexpression. We experimentally demonstrated that miR-132-3p is able to negatively modulate TRIB1 expression. Although we observed similar transcriptional changes induced by miR-132-3p overexpression and TRIB1 knockdown, further experimental validation is needed to understand whether modulating TRIB1 can be beneficial or detrimental for the biology of PCa. In fact, the genes we analysed are considered “bad” for patient outcomes, despite the existence of controversial data (*Said et al., 2009, Kapinas et al., 2012, Shin et al., 2013*). Considering the context-dependent function of Tribbles proteins (see Chapter 1, **section 1.3.3.**) we do not exclude the possibility of a dual role for TRIB1, as well as “stage” dependent function. Therefore, *in vivo* experiments are also needed.

6.5. Limitations of the study

The work presented in this Chapter has some limitations. First of all, we have only tested miR-132-3p, but it would be interesting to investigate the activity of additional miRNAs targeting TRIB1, which are downregulated and/or silenced in PCa. This study was focussed on gene expression and RNA, but in future it should be also supported with protein data. The interaction between miR-132-3p and TRIB1 should be fully validated by involving the use of binding sites mutants, as well as a target-site blocker. In addition, the impact of miR-132-3p and TRIB1 manipulation on gene expression should be tested in animal models to see whether it changes in *in vivo* environments. More relevant genes should be included, as well as *in vitro*-based assay (proliferation, invasion, metastasis) to investigate the influence of miRNAs and TRIB1 on cancer behaviour.

Chapter 7. General discussion and conclusions

The work described in this thesis explored, for the first time, the post-transcriptional regulation of TRIB1 by miRNAs, with the main focus on macrophage and prostate cancer. By taking advantage of bioinformatics and miRNA-target prediction tools, we identified multiple miRNAs that could potentially target the 3'UTR of TRIB1, thus contributing to its variable expression in different tissues, as well as its short half-life and context-dependent function.

Below we discuss the main findings of this research and their potential biological impact. However, further work should be performed in the future, focussing on more mechanistic investigations and *in vivo* models.

TRIB1 is recognised to play a major role in polarising macrophages, by regulating the activation of the MAPK cascade and modulating the induction of inflammatory genes (*Satoh et al., 2013, Arndt et al., 2018*). More recently, the pseudo-kinase has been associated with the development and progression of prostate cancer (*Lin et al., 2014, Mashima et al., 2014, Moya et al., 2018, Liu et al., 2019*). In fact, TRIB1 is highly expressed in prostate cancer, compared to other types of malignancies (*Su et al., 2001, Ramaswamy et al., 2003*). It has been suggested that the mechanism by which TRIB1 affects prostate tumorigenesis involves the regulation of endoplasmic reticulum chaperone expression (*Mashima et al., 2014*). Nevertheless, whilst the downstream effectors of TRIB1 are well characterised, the molecular mechanisms by which TRIB1 expression itself is regulated are still largely unknown. TRIB1 mRNA has an unusually long 3'UTR and has previously been reported to be highly unstable, having a half-life shorter than 1 hour (*Sharova et al., 2009, Soubeyrand et al., 2016*). Therefore, we carried out a systematic analysis and experimental validation of the concept that TRIB1 expression is regulated via multiple miRNAs and that this, in turn, controls the expression of inflammatory genes. We have focussed our research on macrophages and prostate cancer models. We have shown that both human and murine TRIB1 are negatively regulated by miR-101-3p and miR-132-3p. To address the biological impact of these miRNAs, we performed an enrichment pathway analysis, using their predicted target genes. Among the top 10 enriched terms for miR-101-3p target genes we observed MAPK and chemokines mediated signalling pathways; for the genes targeted by miR-132-3p one of the most enriched term was prostate cancer. In fact, miR-132-3p is a well-established onco-suppressor miRNA and in prostate cancer has been shown to be silenced by DNA methylation (*Formosa et al., 2013*). Similarly, miR-101-3p has been documented to play important roles in macrophages, for example by direct interaction

with ABCA1 (Zhang *et al.*, 2015) and DUSP1 (Wei *et al.* 2015), thus controlling metabolic and inflammatory responses. Both miRNAs have not been associated with the TRIB1 gene before. We demonstrated that, via regulating TRIB1 expression, miR-101-3p and miR-132-3p affect inflammatory gene induction in both cellular systems. Specifically, miR-101-3p caused a significant increase in the expression of M1 macrophage markers, such as IL-6, IL-8, CD80 and CD86. However, it did not alter the levels of M2 polarisation markers. This suggests that the negative effect of miR-101-3p on TRIB1 is enough to drive an inflammatory phenotype, but not to switch off the genetic signatures typical of alternatively-activated macrophages. In fact, it is believed that the knockdown effect exerted by miRNAs on their target genes is small and seed region dependent (Liu *et al.*, 2019). On the contrary, the experimental overexpression of TRIB1 led to a robust increase of M2 macrophage markers, including CD163 and MSR-1. On one hand this confirms the crucial transcriptional role of the pseudo-kinase in M2 polarisation; on the other hand, low levels of TRIB1 promote the induction of M1 genes. Similarly, in PC3 cell line, forced expression of miR-132-3p led to an increase of pro-inflammatory genes, including IL-8 and the cancer related gene PD-L1. We confirmed that this was TRIB1-dependent, as the same directional changes were observed in cells treated with a TRIB1 siRNA. It has already been shown that TRIB1 overexpression affects the immune microenvironment of prostate cancer, promoting the infiltration of CD163⁺ macrophages (Liu *et al.*, 2019), but it has never been linked to the activity of PD-L1, which enables the tumour to escape the immune system surveillance (Gevensleben *et al.*, 2015). Therefore, our preliminary findings should be validated in the future to address whether TRIB1 has a role in influencing the immune escape, which is a well-known obstacle in cancer treatment.

Overall, the most consistent and robust effect of miRNAs regulating TRIB1 expression was the upregulation of IL-8, assessed in both cellular systems. Previously, Kiss-Toth and colleagues observed that TRIB1 was able to regulate the activity of the IL-8 promoter in a gene reporter assay, but this was not explored further (Kiss-Toth *et al.*, 2006). Similar to TRIB1, the IL-8 gene is a key player in numerous inflammatory diseases and cancers (Russo *et al.*, 2014, Alfaro *et al.*, 2017). Finding a link between the regulation of TRIB1 and IL-8 might be beneficial for the development of novel therapeutics, including miRNA-based strategies.

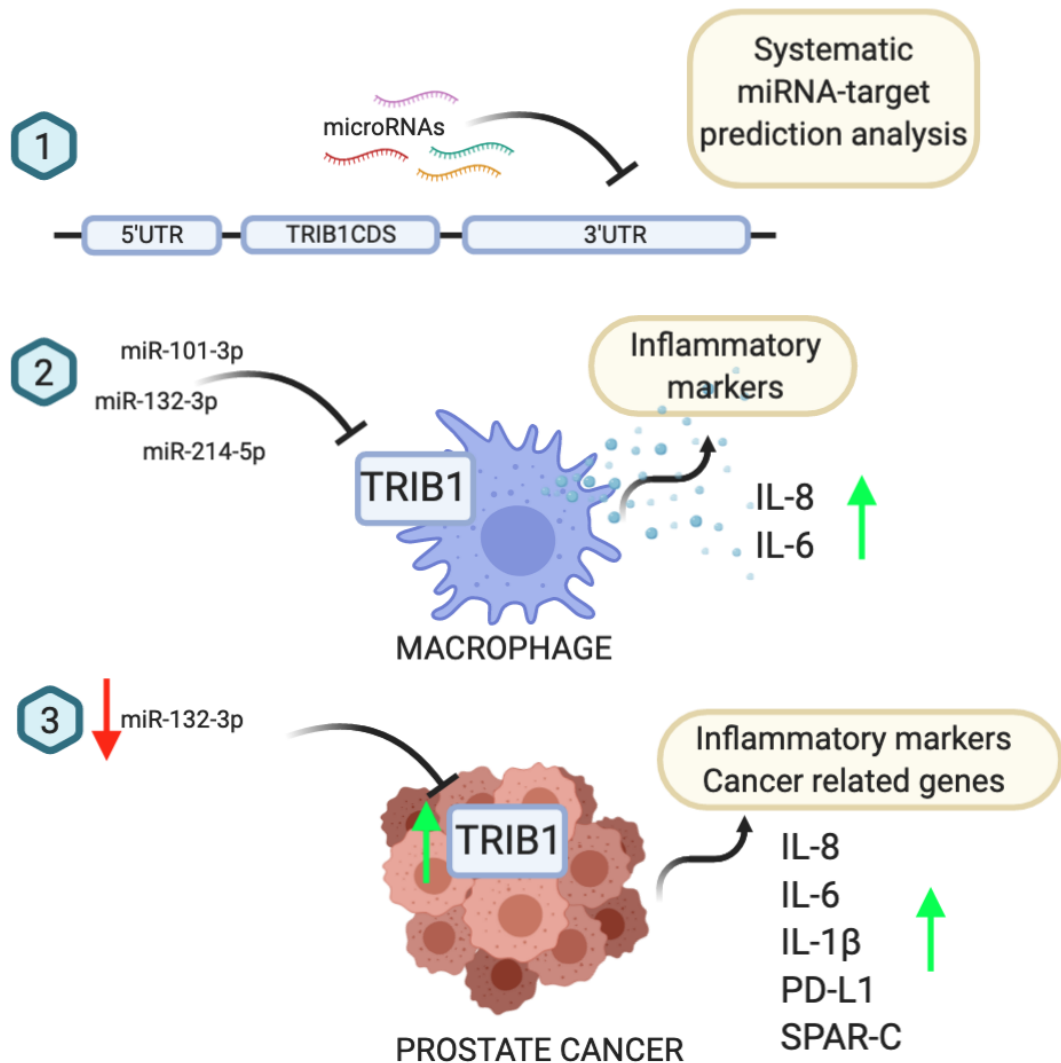


Figure 7.1. miRNAs targeting TRIB1 in macrophages and prostate cancer

The figure summarises the main findings described in this thesis. The 3'UTR of TRIB1 is enriched in miRNAs binding sites, detected by a systematic miRNA-target prediction analysis (1); miR-101-3p, miR-132-3p and miR-214-3p regulate TRIB1 expression and function in macrophages, thus altering the levels of pro-inflammatory cytokines (2); the onco-suppressor miR-132-3p regulates TRIB1 expression and function in prostate cancer, altering the levels of inflammatory and cancer-related genes (3).

A short research was conducted to investigate the impact of TRIB1 non-coding variants on miRNA-binding sites. TRIB1 variants have been associated with plasma triglycerides and cardiovascular disease risk by numerous independent studies (*Kathiresan et al., 2008, Willer et al., 2008, Teslovich et al., 2010, Deloukas et al., 2013, Nikpay et al., 2015, van der Harst et al., 2018*). However, nothing is known about the role of TRIB1 non-coding variants. The majority of SNPs in the GWAS catalogue are located in non-coding regions of the genome (*Tak et al., 2015*) and have been reported to be regulators of gene expression at the post-transcriptional level (*Hudson et al., 2003*). It has been demonstrated that non-coding SNPs can alter miRNA-mRNA interaction, by creating, abolishing or modifying their binding sites (*Moszyńska et al., 2017*). This has been often linked to human diseases or traits, such as prostate cancer (*Stageman et al., 2015*), coronary heart disease (*Hu et al., 2016*) and type 2 diabetes (*Goda et al., 2015*). Here we reported that multiple SNPs located in the 3'UTR of TRIB1 are predicted to alter miRNAs sites. By using a reporter assay, we demonstrated that 2 minor alleles, rs62521034 C>T and rs56395423 A>C, have a significant negative impact on TRIB1 mRNA stability, thus potentially acting as cis-eQTLs for the TRIB1 gene. In fact, rs62521034 and rs56395423 are predicted to create novel binding sites for 10 miRNAs, which have not been predicted to bind to the reference alleles. We validated as functional the interaction between rs62521034 C>T and miR-29a/b. This could have a biological impact in the pathogenesis and progression of multiple cancers, including acute myeloid leukaemia. In acute myeloid leukaemia, TRIB1 acts as an oncogene by promoting the degradation of C/EBP α (*Dedhia et al., 2010*). On the contrary, miR-29a/b is dysregulated and has been reported to have an onco-suppressor role, targeting apoptosis, cell cycle and proliferation (*Garzon et al., 2009*). Due to the lack of tools enabling the correlation between miRNAs and their targets in a given tissue/disease using pre-existing data, we could not investigate whether a correlation between TRIB1/rs62521034 and miR-29a/b exists and if it could have an impact in acute myeloid leukaemia or in other types of cancer. Therefore, further investigations are needed. In addition, by using the RNA microarray data produced by the Cardiogenics Consortium, we identified two potential TRIB1 trans-eQTLs: rs3201475 (5'UTR) and rs62521034 (3'UTR) were significantly associated with a small reduction in distant genes: NLRC4, activator of the inflammasome and MRPS21, a mitochondrial ribosomal protein. So far, there is no association between TRIB1 and these genes. However, considering the role of TRIB1 in inflammation (*Johnston et al., 2015*) and mitochondrial dysfunction (*Soubeyrand et al., 2013*), this should be further explored in the future.

Lastly, as a collaborative work, we performed a comprehensive, simultaneous analysis of miRNAs and mRNAs in human polarised macrophages by using multiple RNA sequencing experiments and downstream bioinformatics analysis. In fact, it is well established that miRNAs are master regulators of macrophage polarisation and inflammatory responses, controlling hundreds of key genes at the same time (*Essandoh et al., 2010*). However, the extent of miRNA-mRNA networks in macrophage polarisation have not been explored in a systematic, integrative manner. Here we have focussed on pro-inflammatory M1-like macrophage transcriptomic signatures, looking at both miRNAs and mRNAs. First, by using a small RNA seq, we detected 73 differentially expressed miRNAs between M0 and M1 macrophages, of which 47 were downregulated and 26 were upregulated. Among the upregulated miRNA we observed miR-155-5p, which has been previously reported to play a major role in regulating M1 macrophage polarisation (*Jablonski et al., 2016*). After identifying candidate miRNAs differentially expressed between M0 and M1 macrophages, we performed a target prediction analysis by using TargetScan. We filtered the list of target genes, selecting only those expressed by macrophages, using an RNA seq previously generated in our group. Interestingly, we found that 1573 genes upregulated in M1 polarised cells were predicted targets of 44 miRNAs, which were rather downregulated. Similarly, 1790 downregulated genes were predicted to be targeted by 26 upregulated miRNAs. This suggests that miRNAs contribute to the dysregulation of more than half of the genes differentially expressed between M0 and M1 polarised macrophages. Our pathway enrichment analysis indicated that the target genes of downregulated miRNAs participate to cytokine and chemokine signalling pathways, antigen presentation, T cell receptor signalling pathway, apoptosis, MAPK signalling pathway. On the contrary, the target genes of miRNAs upregulated in M1 cells are involved in DNA replication, cell cycle and metabolic pathways. Therefore, miRNAs control the two major events of the M1 macrophage activation: immune response and cell cycle. This was also consistent with a murine model of macrophage polarisation (*Jiang et al., 2017*), suggesting that the target genes of the differentially expressed miRNAs are conserved between human and mouse. In addition, our systematic approach allowed us to identify 9 miRNAs targeting more than 500 genes, which we named “super regulators”. None of them have been associated with this number of targets before. Therefore, we explored the effect of the experimental overexpression of two “super regulators” (miR-125a-3p and miR-186-5p), including miR-155-5p as a positive control, followed by an RNA-seq experiment. This was carried out on unpolarised macrophage and compared to the differential expression analysis previously done between M0 and M1 polarised cells. Although we did not observe many statistically significant

changes in gene expression, we did find gene overlapping and same directional changes. Gene Ontology analysis confirmed that the genes downregulated in response to “super regulators” miRNAs take part to the regulation of cell cycle and chromatin segregation. Taken together, our results indicate the existence of a macrophage-specific targetome that underlie many of the critical biological pathways involved in inflammation and in the classical activation of macrophages. Future work will focus on the experimental validation of these findings. This could certainly have an impact on the discovery and development of new strategies in the treatment of chronic inflammatory diseases using miRNA-based therapies.

References

- ◆ Abraham, S.M. and Clark, A.R. (2006). Dual-specificity phosphatase 1: a critical regulator of innate immune responses. *Biochem Soc Trans.* **34**(Pt 6), pp.1018-1023.
- ◆ Agarwal, V., Bell, G.W., Nam, J.W. and Bartel, D.P. (2015). Predicting effective microRNA target sites in mammalian mRNAs. *Elife.* **4**.
- ◆ Akira, S., Misawa, T., Satoh, T. and Saitoh, T. (2013). Macrophages control innate inflammation. *Diabetes Obes Metab.* **15 Suppl 3**, pp.10-18.
- ◆ Alfaro, C., Sanmamed, M.F., Rodríguez-Ruiz, M.E., Teijeira, Á., Oñate, C., González, Á., Ponz, M., Schalper, K.A., Pérez-Gracia, J.L. and Melero, I. (2017). Interleukin-8 in cancer pathogenesis, treatment and follow-up. *Cancer Treat Rev.* **60**, pp.24-31.
- ◆ Alizadeh, M. and Alizadeh, S. (2014). Survey of clinical and pathological characteristics and outcomes of patients with prostate cancer. *Glob J Health Sci.* **6**(7 Spec No), pp.49-57.
- ◆ Ambros, V. and Lee, R.C. (2004). Identification of microRNAs and other tiny noncoding RNAs by cDNA cloning. *Methods Mol Biol.* **265**, pp.131-158.
- ◆ Ambros, V., Lee, R.C., Lavanway, A., Williams, P.T. and Jewell, D. (2003). MicroRNAs and other tiny endogenous RNAs in *C. elegans*. *Curr Biol.* **13**(10), pp.807-818.
- ◆ Arab, A., Karimipoor, M., Irani, S., Kiani, A., Zeinali, S., Tafhiri, E. and Sheikhy, K. (2017). Potential circulating miRNA signature for early detection of NSCLC. *Cancer Genet.* **216-217**, pp.150-158.
- ◆ Ardekani, A.M. and Naeini, M.M. (2010). The Role of MicroRNAs in Human Diseases. *Avicenna J Med Biotechnol.* **2**(4), pp.161-179.
- ◆ Arndt, L., Dokas, J., Gericke, M., Kutzner, C.E., Müller, S., Jeromin, F., Thiery, J. and Burkhardt, R. (2018). Tribbles homolog 1 deficiency modulates function and polarization of murine bone marrow-derived macrophages. *J Biol Chem.* **293**(29), pp.11527-11536.
- ◆ Aulchenko, Y.S., Ripatti, S., Lindqvist, I., Boomsma, D., Heid, I.M., Pramstaller, P.P., Penninx, B.W., Janssens, A.C., Wilson, J.F., Spector, T., Martin, N.G., Pedersen, N.L., Kyvik, K.O., Kaprio, J., Hofman, A., Freimer, N.B., Jarvelin, M.R., Gyllenstein, U.,

Campbell, H., Rudan, I., Johansson, A., Marroni, F., Hayward, C., Vitart, V., Jonasson, I., Pattaro, C., Wright, A., Hastie, N., Pichler, I., Hicks, A.A., Falchi, M., Willemsen, G., Hottenga, J.J., de Geus, E.J., Montgomery, G.W., Whitfield, J., Magnusson, P., Saharinen, J., Perola, M., Silander, K., Isaacs, A., Sijbrands, E.J., Uitterlinden, A.G., Witteman, J.C., Oostra, B.A., Elliott, P., Ruukonen, A., Sabatti, C., Gieger, C., Meitinger, T., Kronenberg, F., Döring, A., Wichmann, H.E., Smit, J.H., McCarthy, M.I., van Duijn, C.M., Peltonen, L. and Consortium, E. (2009). Loci influencing lipid levels and coronary heart disease risk in 16 European population cohorts. *Nat Genet.* **41**(1), pp.47-55.

- ◆ Avgeris, M., Stravodimos, K., Fragoulis, E.G. and Scorilas, A. (2013). The loss of the tumour-suppressor miR-145 results in the shorter disease-free survival of prostate cancer patients. *Br J Cancer.* **108**(12), pp.2573-2581.
- ◆ Bardi, G.T., Smith, M.A. and Hood, J.L. (2018). Melanoma exosomes promote mixed M1 and M2 macrophage polarization. *Cytokine.* **105**, pp.63-72.
- ◆ Bartel, D.P. (2004). MicroRNAs: genomics, biogenesis, mechanism, and function. *Cell.* **116**(2), pp.281-297.
- ◆ Bartel, D.P. (2009). MicroRNAs: target recognition and regulatory functions. *Cell.* **136**(2), pp.215-233.
- ◆ Bauer, R.C., Yenilmez, B.O. and Rader, D.J. (2015). Tribbles-1: a novel regulator of hepatic lipid metabolism in humans. *Biochem Soc Trans.* **43**(5), pp.1079-1084.
- ◆ Baumgart, S.J. and Haendler, B. (2017). Exploiting Epigenetic Alterations in Prostate Cancer. *Int J Mol Sci.* **18**(5).
- ◆ Benafif, S., Kote-Jarai, Z., Eeles, R.A. and Consortium, P. (2018). A Review of Prostate Cancer Genome-Wide Association Studies (GWAS). *Cancer Epidemiol Biomarkers Prev.* **27**(8), pp.845-857.
- ◆ Bernstein, E., Kim, S.Y., Carmell, M.A., Murchison, E.P., Alcorn, H., Li, M.Z., Mills, A.A., Elledge, S.J., Anderson, K.V. and Hannon, G.J. (2003). Dicer is essential for mouse development. *Nat Genet.* **35**(3), pp.215-217.
- ◆ Betel, D., Wilson, M., Gabow, A., Marks, D.S. and Sander, C. (2008). The microRNA.org resource: targets and expression. *Nucleic Acids Res.* **36**(Database issue), pp.D149-153.

- ◆ Bhatia, V., Yadav, A., Tiwari, R., Nigam, S., Goel, S., Carskadon, S., Gupta, N., Goel, A., Palanisamy, N. and Ateeq, B. (2019). Epigenetic Silencing of miRNA-338-5p and miRNA-421 Drives SPINK1-Positive Prostate Cancer. *Clin Cancer Res.* **25**(9), pp.2755-2768.
- ◆ Bhattacharya, A., Ziebarth, J.D. and Cui, Y. (2014). PolymiRTS Database 3.0: linking polymorphisms in microRNAs and their target sites with human diseases and biological pathways. *Nucleic Acids Res.* **42**(Database issue), pp.D86-91.
- ◆ Billack, B. (2006). Macrophage activation: role of toll-like receptors, nitric oxide, and nuclear factor kappa B. *Am J Pharm Educ.* **70**(5), p102.
- ◆ Bolger, A.M., Lohse, M. and Usadel, B. (2014). Trimmomatic: a flexible trimmer for Illumina sequence data. *Bioinformatics.* **30**(15), pp.2114-2120.
- ◆ Borchert, G.M., Lanier, W. and Davidson, B.L. (2006). RNA polymerase III transcribes human microRNAs. *Nat Struct Mol Biol.* **13**(12), pp.1097-1101.
- ◆ Borrego-Diaz, E., Powers, B.C., Azizov, V., Lovell, S., Reyes, R., Chapman, B., Tawfik, O., McGregor, D., Diaz, F.J., Wang, X. and Veldhuizen, P.V. (2014). A potential regulatory loop between Lin28B:miR-212 in androgen-independent prostate cancer. *Int J Oncol.* **45**(6), pp.2421-2429.
- ◆ Bronte, V. and Zanovello, P. (2005). Regulation of immune responses by L-arginine metabolism. *Nat Rev Immunol.* **5**(8), pp.641-654.
- ◆ Brookes, A.J. (1999). The essence of SNPs. *Gene.* **234**(2), pp.177-186.
- ◆ Broughton, J.P., Lovci, M.T., Huang, J.L., Yeo, G.W. and Pasquinelli, A.E. (2016a). Pairing beyond the Seed Supports MicroRNA Targeting Specificity. *Mol Cell.* **64**(2), pp.320-333.
- ◆ Bruno, A.E., Li, L., Kalabus, J.L., Pan, Y., Yu, A. and Hu, Z. (2012). miRdSNP: a database of disease-associated SNPs and microRNA target sites on 3'UTRs of human genes. *BMC Genomics.* **13**, p44.
- ◆ Bubendorf, L., Schöpfer, A., Wagner, U., Sauter, G., Moch, H., Willi, N., Gasser, T.C. and Mihatsch, M.J. (2000). Metastatic patterns of prostate cancer: an autopsy study of 1,589 patients. *Hum Pathol.* **31**(5), pp.578-583.

- ◆ Caescu, C.I., Guo, X., Tesfa, L., Bhagat, T.D., Verma, A., Zheng, D. and Stanley, E.R. (2015). Colony stimulating factor-1 receptor signaling networks inhibit mouse macrophage inflammatory responses by induction of microRNA-21. *Blood*. **125**(8), pp.e1-13.
- ◆ Cai, S., Chen, R., Li, X., Cai, Y., Ye, Z., Li, S., Li, J., Huang, H., Peng, S., Wang, J., Tao, Y., Wen, X., Mo, J., Deng, Z., Zhang, Y. and Gao, X. (2015). Downregulation of microRNA-23a suppresses prostate cancer metastasis by targeting the PAK6-LIMK1 signaling pathway. *Oncotarget*. **6**(6), pp.3904-3917.
- ◆ Calin, G.A. and Croce, C.M. (2006). MicroRNA signatures in human cancers. *Nat Rev Cancer*. **6**(11), pp.857-866.
- ◆ Chakravarthi, B.V., Goswami, M.T., Pathi, S.S., Robinson, A.D., Cieřlik, M., Chandrashekar, D.S., Agarwal, S., Siddiqui, J., Daignault, S., Carskadon, S.L., Jing, X., Chinnaiyan, A.M., Kunju, L.P., Palanisamy, N. and Varambally, S. (2016). MicroRNA-101 regulated transcriptional modulator SUB1 plays a role in prostate cancer. *Oncogene*. **35**(49), pp.6330-6340.
- ◆ Chatterjee, S. and Pal, J.K. (2009). Role of 5'- and 3'-untranslated regions of mRNAs in human diseases. *Biol Cell*. **101**(5), pp.251-262.
- ◆ Chaussy, C.G. and Thüroff, S. (2017). High-Intensity Focused Ultrasound for the Treatment of Prostate Cancer: A Review. *J Endourol*. **31**(S1), pp.S30-S37.
- ◆ Chen, K., Song, F., Calin, G.A., Wei, Q., Hao, X. and Zhang, W. (2008). Polymorphisms in microRNA targets: a gold mine for molecular epidemiology. *Carcinogenesis*. **29**(7), pp.1306-1311.
- ◆ Chen, K.C., Wang, Y.S., Hu, C.Y., Chang, W.C., Liao, Y.C., Dai, C.Y. and Juo, S.H. (2011). OxLDL up-regulates microRNA-29b, leading to epigenetic modifications of MMP-2/MMP-9 genes: a novel mechanism for cardiovascular diseases. *FASEB J*. **25**(5), pp.1718-1728.
- ◆ Chen, Y. and Wang, X. (2020). miRDB: an online database for prediction of functional microRNA targets. *Nucleic Acids Res*. **48**(D1), pp.D127-D131.
- ◆ Clària, J., González-Pérez, A., López-Vicario, C., Rius, B. and Titos, E. (2011a). New insights into the role of macrophages in adipose tissue inflammation and Fatty liver

disease: modulation by endogenous omega-3 Fatty Acid-derived lipid mediators. *Front Immunol.* **2**, p49.

- ◆ Cobos Jiménez, V., Bradley, E.J., Willemsen, A.M., van Kampen, A.H., Baas, F. and Kootstra, N.A. (2014). Next-generation sequencing of microRNAs uncovers expression signatures in polarized macrophages. *Physiol Genomics.* **46**(3), pp.91-103.
- ◆ Comabella, M., Craig, D.W., Camiña-Tato, M., Morcillo, C., Lopez, C., Navarro, A., Rio, J., Montalban, X., Martin, R. and Group, B.S. (2008). Identification of a novel risk locus for multiple sclerosis at 13q31.3 by a pooled genome-wide scan of 500,000 single nucleotide polymorphisms. *PLoS One.* **3**(10), pe3490.
- ◆ Consortium, G. (2013). The Genotype-Tissue Expression (GTEx) project. *Nat Genet.* **45**(6), pp.580-585.
- ◆ Consortium, W.T.C.C. (2007). Genome-wide association study of 14,000 cases of seven common diseases and 3,000 shared controls. *Nature.* **447**(7145), pp.661-678.
- ◆ Coppola, V., De Maria, R. and Bonci, D. (2010). MicroRNAs and prostate cancer. *Endocr Relat Cancer.* **17**(1), pp.F1-17.
- ◆ Cui, C., Yang, W., Shi, J., Zhou, Y., Yang, J. and Cui, Q. (2018). Identification and Analysis of Human Sex-biased MicroRNAs. *Genomics Proteomics Bioinformatics.* **16**(3), pp.200-211.
- ◆ Culig, Z., Steiner, H., Bartsch, G. and Hobisch, A. (2005). Interleukin-6 regulation of prostate cancer cell growth. *J Cell Biochem.* **95**(3), pp.497-505.
- ◆ Curtale, G., Rubino, M. and Locati, M. (2019a). MicroRNAs as Molecular Switches in Macrophage Activation. *Front Immunol.* **10**, p799.
- ◆ Dai, R. and Ahmed, S.A. (2014). Sexual dimorphism of miRNA expression: a new perspective in understanding the sex bias of autoimmune diseases. *Ther Clin Risk Manag.* **10**, pp.151-163.
- ◆ Davies, L.C. and Taylor, P.R. (2015). Tissue-resident macrophages: then and now. *Immunology.* **144**(4), pp.541-548.
- ◆ de Gaetano, M., Crean, D., Barry, M. and Belton, O. (2016). M1- and M2-Type Macrophage Responses Are Predictive of Adverse Outcomes in Human Atherosclerosis. *Front Immunol.* **7**, p275.

- ◆ de la Morena, M.T., Eitson, J.L., Dozmorov, I.M., Belkaya, S., Hoover, A.R., Anguiano, E., Pascual, M.V. and van Oers, N.S.C. (2013). Signature MicroRNA expression patterns identified in humans with 22q11.2 deletion/DiGeorge syndrome. *Clin Immunol.* **147**(1), pp.11-22.
- ◆ Dedhia, P.H., Keeshan, K., Uljon, S., Xu, L., Vega, M.E., Shestova, O., Zaks-Zilberman, M., Romany, C., Blacklow, S.C. and Pear, W.S. (2010). Differential ability of Tribbles family members to promote degradation of C/EBPalpha and induce acute myelogenous leukemia. *Blood.* **116**(8), pp.1321-1328.
- ◆ Deiluiis, J.A. (2016). MicroRNAs as regulators of metabolic disease: pathophysiologic significance and emerging role as biomarkers and therapeutics. *Int J Obes (Lond).* **40**(1), pp.88-101.
- ◆ Deloukas, P., Kanoni, S., Willenborg, C., Farrall, M., Assimes, T.L., Thompson, J.R., Ingelsson, E., Saleheen, D., Erdmann, J., Goldstein, B.A., Stirrups, K., König, I.R., Cazier, J.B., Johansson, A., Hall, A.S., Lee, J.Y., Willer, C.J., Chambers, J.C., Esko, T., Folkersen, L., Goel, A., Grundberg, E., Havulinna, A.S., Ho, W.K., Hopewell, J.C., Eriksson, N., Kleber, M.E., Kristiansson, K., Lundmark, P., Lyytikäinen, L.P., Rafelt, S., Shungin, D., Strawbridge, R.J., Thorleifsson, G., Tikkanen, E., Van Zuydam, N., Voight, B.F., Waite, L.L., Zhang, W., Ziegler, A., Absher, D., Altshuler, D., Balmforth, A.J., Barroso, I., Braund, P.S., Burgdorf, C., Claudi-Boehm, S., Cox, D., Dimitriou, M., Do, R., Doney, A.S., El Mokhtari, N., Eriksson, P., Fischer, K., Fontanillas, P., Franco-Cereceda, A., Gigante, B., Groop, L., Gustafsson, S., Hager, J., Hallmans, G., Han, B.G., Hunt, S.E., Kang, H.M., Illig, T., Kessler, T., Knowles, J.W., Kolovou, G., Kuusisto, J., Langenberg, C., Langford, C., Leander, K., Lokki, M.L., Lundmark, A., McCarthy, M.I., Meisinger, C., Melander, O., Mihailov, E., Maouche, S., Morris, A.D., Müller-Nurasyid, M., Nikus, K., Peden, J.F., Rayner, N.W., Rasheed, A., Rosinger, S., Rubin, D., Rumpf, M.P., Schäfer, A., Sivananthan, M., Song, C., Stewart, A.F., Tan, S.T., Thorgeirsson, G., van der Schoot, C.E., Wagner, P.J., Wells, G.A., Wild, P.S., Yang, T.P., Amouyel, P., Arveiler, D., Basart, H., Boehnke, M., Boerwinkle, E., Brambilla, P., Cambien, F., Cupples, A.L., de Faire, U., Dehghan, A., Diemert, P., Epstein, S.E., Evans, A., Ferrario, M.M., Ferrières, J., Gauguier, D., Go, A.S., Goodall, A.H., Gudnason, V., Hazen, S.L., Holm, H., Iribarren, C., Jang, Y., Kähönen, M., Kee,

F., Kim, H.S., Klopp, N., Koenig, W., Kratzer, W., Kuulasmaa, K., Laakso, M., Laaksonen, R., Lind, L., Ouwehand, W.H., Parish, S., Park, J.E., Pedersen, N.L., Peters, A., Quertermous, T., Rader, D.J., Salomaa, V., Schadt, E., Shah, S.H., Sinisalo, J., Stark, K., Stefansson, K., Trégouët, D.A., Virtamo, J., Wallentin, L., Wareham, N., Zimmermann, M.E., Nieminen, M.S., Hengstenberg, C., Sandhu, M.S., Pastinen, T., Syvänen, A.C., Hovingh, G.K., Dedoussis, G., Franks, P.W., Lehtimäki, T., Metspalu, A., Zalloua, P.A., Siegbahn, A., Schreiber, S., Ripatti, S., Blankenberg, S.S., Perola, M., Clarke, R., Boehm, B.O., O'Donnell, C., Reilly, M.P., März, W., Collins, R., Kathiresan, S., Hamsten, A., Kooner, J.S., Thorsteinsdottir, U., Danesh, J., Palmer, C.N., Roberts, R., Watkins, H., Schunkert, H., Samani, N.J., Consortium, C.D., Consortium, D., Consortium, C., Consortium, M. and Consortium, W.T.C.C. (2013). Large-scale association analysis identifies new risk loci for coronary artery disease. *Nat Genet.* **45**(1), pp.25-33.

- ◆ Derosa, C.A., Furusato, B., Shaheduzzaman, S., Srikantan, V., Wang, Z., Chen, Y., Seifert, M., Siefert, M., Ravindranath, L., Young, D., Nau, M., Dobi, A., Werner, T., McLeod, D.G., Vahey, M.T., Sesterhenn, I.A., Srivastava, S. and Petrovics, G. (2012). Elevated osteonectin/SPARC expression in primary prostate cancer predicts metastatic progression. *Prostate Cancer Prostatic Dis.* **15**(2), pp.150-156.
- ◆ Desiniotis, A. and Kyprianou, N. (2011). Significance of talin in cancer progression and metastasis. *Int Rev Cell Mol Biol.* **289**, pp.117-147.
- ◆ Di Pietro, V., Porto, E., Ragusa, M., Barbagallo, C., Davies, D., Forcione, M., Logan, A., Di Pietro, C., Purrello, M., Grey, M., Hammond, D., Sawlani, V., Barbey, A.K. and Belli, A. (2018). Salivary MicroRNAs: Diagnostic Markers of Mild Traumatic Brain Injury in Contact-Sport. *Front Mol Neurosci.* **11**, p290.
- ◆ Doench, J.G., Petersen, C.P. and Sharp, P.A. (2003). siRNAs can function as miRNAs. *Genes Dev.* **17**(4), pp.438-442.
- ◆ Dong, Q., Meng, P., Wang, T., Qin, W., Wang, F., Yuan, J., Chen, Z., Yang, A. and Wang, H. (2010). MicroRNA let-7a inhibits proliferation of human prostate cancer cells in vitro and in vivo by targeting E2F2 and CCND2. *PLoS One.* **5**(4), pe10147.

- ◆ Dong, S., Xia, J., Wang, H., Sun, L., Wu, Z., Bin, J., Liao, Y., Li, N. and Liao, W. (2016). Overexpression of TRIB3 promotes angiogenesis in human gastric cancer. *Oncol Rep.* **36**(4), pp.2339-2348.
- ◆ Du, K., Herzig, S., Kulkarni, R.N. and Montminy, M. (2003). TRB3: a tribbles homolog that inhibits Akt/PKB activation by insulin in liver. *Science.* **300**(5625), pp.1574-1577.
- ◆ Du, T. and Zamore, P.D. (2005). microPrimer: the biogenesis and function of microRNA. *Development.* **132**(21), pp.4645-4652.
- ◆ Duffield, J.S. (2010). Macrophages and immunologic inflammation of the kidney. *Semin Nephrol.* **30**(3), pp.234-254.
- ◆ Dugast, E., Kiss-Toth, E., Soulillou, J.P., Brouard, S. and Ashton-Chess, J. (2013). The Tribbles-1 protein in humans: roles and functions in health and disease. *Curr Mol Med.* **13**(1), pp.80-85.
- ◆ Dweep, H. and Gretz, N. (2015). miRWalk2.0: a comprehensive atlas of microRNA-target interactions. *Nat Methods.* **12**(8), p697.
- ◆ Dweep, H., Sticht, C., Pandey, P. and Gretz, N. (2011). miRWalk--database: prediction of possible miRNA binding sites by "walking" the genes of three genomes. *J Biomed Inform.* **44**(5), pp.839-847.
- ◆ El-Brolosy, M.A. and Stainier, D.Y.R. (2017). Genetic compensation: A phenomenon in search of mechanisms. *PLoS Genet.* **13**(7), pe1006780.
- ◆ Elefant, N., Berger, A., Shein, H., Hofree, M., Margalit, H. and Altuvia, Y. (2011a). RepTar: a database of predicted cellular targets of host and viral miRNAs. *Nucleic Acids Res.* **39**(Database issue), pp.D188-194.
- ◆ Epelman, S., Lavine, K.J. and Randolph, G.J. (2014). Origin and functions of tissue macrophages. *Immunity.* **41**(1), pp.21-35.
- ◆ Erlich, Y., Mitra, P.P., delaBastide, M., McCombie, W.R. and Hannon, G.J. (2008). Alta-Cyclic: a self-optimizing base caller for next-generation sequencing. *Nat Methods.* **5**(8), pp.679-682.
- ◆ Essandoh, K., Li, Y., Huo, J. and Fan, G.C. (2016). MiRNA-Mediated Macrophage Polarization and its Potential Role in the Regulation of Inflammatory Response. *Shock.* **46**(2), pp.122-131.

- ◆ Ewels, P., Magnusson, M., Lundin, S. and Källér, M. (2016). MultiQC: summarize analysis results for multiple tools and samples in a single report. *Bioinformatics*. **32**(19), pp.3047-3048.
- ◆ Eyers, P.A., Keeshan, K. and Kannan, N. (2017). Tribbles in the 21st Century: The Evolving Roles of Tribbles Pseudokinases in Biology and Disease. *Trends Cell Biol.* **27**(4), pp.284-298.
- ◆ Fan, X., Zhang, H., Cheng, Y., Jiang, X., Zhu, J. and Jin, T. (2016). Double Roles of Macrophages in Human Neuroimmune Diseases and Their Animal Models. *Mediators Inflamm.* **2016**, p8489251.
- ◆ Fang, Z. and Rajewsky, N. (2011). The impact of miRNA target sites in coding sequences and in 3'UTRs. *PLoS One.* **6**(3), pe18067.
- ◆ Faruq, O. and Vecchione, A. (2015). microRNA: Diagnostic Perspective. *Front Med (Lausanne)*. **2**, p51.
- ◆ Fernández-Hernando, C. (2013). Emerging role of microRNAs in the regulation of lipid metabolism. *Hepatology.* **57**(2), pp.432-434.
- ◆ Fontana, L., Pelosi, E., Greco, P., Racanicchi, S., Testa, U., Liuzzi, F., Croce, C.M., Brunetti, E., Grignani, F. and Peschle, C. (2007). MicroRNAs 17-5p-20a-106a control monocytopoiesis through AML1 targeting and M-CSF receptor upregulation. *Nat Cell Biol.* **9**(7), pp.775-787.
- ◆ Formosa, A., Lena, A.M., Markert, E.K., Cortelli, S., Miano, R., Mauriello, A., Croce, N., Vandesompele, J., Mestdagh, P., Finazzi-Agrò, E., Levine, A.J., Melino, G., Bernardini, S. and Candi, E. (2013). DNA methylation silences miR-132 in prostate cancer. *Oncogene.* **32**(1), pp.127-134.
- ◆ Friedman, R.C., Farh, K.K., Burge, C.B. and Bartel, D.P. (2009). Most mammalian mRNAs are conserved targets of microRNAs. *Genome Res.* **19**(1), pp.92-105.
- ◆ Fu, H., He, H.C., Han, Z.D., Wan, Y.P., Luo, H.W., Huang, Y.Q., Cai, C., Liang, Y.X., Dai, Q.S., Jiang, F.N. and Zhong, W.D. (2015). MicroRNA-224 and its target CAMKK2 synergistically influence tumor progression and patient prognosis in prostate cancer. *Tumour Biol.* **36**(3), pp.1983-1991.

- ◆ Fu, Y., Zhao, Y. and Huang, B. (2017). Tribbles homolog 1 enhances cholesterol efflux from oxidized low-density lipoprotein-loaded THP-1 macrophages. *Exp Ther Med.* **14**(1), pp.862-866.
- ◆ Fujisaka, S., Usui, I., Nawaz, A., Takikawa, A., Kado, T., Igarashi, Y. and Tobe, K. (2016). M2 macrophages in metabolism. *Diabetol Int.* **7**(4), pp.342-351.
- ◆ Fuxman Bass, J.I., Diallo, A., Nelson, J., Soto, J.M., Myers, C.L. and Walhout, A.J. (2013). Using networks to measure similarity between genes: association index selection. *Nat Methods.* **10**(12), pp.1169-1176.
- ◆ Garzon, R., Heaphy, C.E., Havelange, V., Fabbri, M., Volinia, S., Tsao, T., Zanesi, N., Kornblau, S.M., Marcucci, G., Calin, G.A., Andreeff, M. and Croce, C.M. (2009). MicroRNA 29b functions in acute myeloid leukemia. *Blood.* **114**(26), pp.5331-5341.
- ◆ Geng, Q., Fan, T., Zhang, B., Wang, W., Xu, Y. and Hu, H. (2014). Five microRNAs in plasma as novel biomarkers for screening of early-stage non-small cell lung cancer. *Respir Res.* **15**, p149.
- ◆ Gevensleben, H., Dietrich, D., Golletz, C., Steiner, S., Jung, M., Thiesler, T., Majores, M., Stein, J., Uhl, B., Müller, S., Ellinger, J., Stephan, C., Jung, K., Brossart, P. and Kristiansen, G. (2016). The Immune Checkpoint Regulator PD-L1 Is Highly Expressed in Aggressive Primary Prostate Cancer. *Clin Cancer Res.* **22**(8), pp.1969-1977.
- ◆ Ghani, S., Riemke, P., Schönheit, J., Lenze, D., Stumm, J., Hoogenkamp, M., Lagendijk, A., Heinz, S., Bonifer, C., Bakkers, J., Abdelilah-Seyfried, S., Hummel, M. and Rosenbauer, F. (2011). Macrophage development from HSCs requires PU.1-coordinated microRNA expression. *Blood.* **118**(8), pp.2275-2284.
- ◆ Gilad, Y., Rifkin, S.A. and Pritchard, J.K. (2008). Revealing the architecture of gene regulation: the promise of eQTL studies. *Trends Genet.* **24**(8), pp.408-415.
- ◆ Gomella, L.G., Singh, J., Lallas, C. and Trabulsi, E.J. (2010). Hormone therapy in the management of prostate cancer: evidence-based approaches. *Ther Adv Urol.* **2**(4), pp.171-181.
- ◆ Gordon, S., Plüddemann, A. and Martinez Estrada, F. (2014). Macrophage heterogeneity in tissues: phenotypic diversity and functions. *Immunol Rev.* **262**(1), pp.36-55.

- ◆ Goto, Y., Nishikawa, R., Kojima, S., Chiyomaru, T., Enokida, H., Inoguchi, S., Kinoshita, T., Fuse, M., Sakamoto, S., Nakagawa, M., Naya, Y., Ichikawa, T. and Seki, N. (2014). Tumour-suppressive microRNA-224 inhibits cancer cell migration and invasion via targeting oncogenic TPD52 in prostate cancer. *FEBS Lett.* **588**(10), pp.1973-1982.
- ◆ Grimson, A., Farh, K.K., Johnston, W.K., Garrett-Engele, P., Lim, L.P. and Bartel, D.P. (2007). MicroRNA targeting specificity in mammals: determinants beyond seed pairing. *Mol Cell.* **27**(1), pp.91-105.
- ◆ Guan, H., Shuaib, A., Leon, D.D., Angyal, A., Salazar, M., Velasco, G., Holcombe, M., Dower, S.K. and Kiss-Toth, E. (2016). Competition between members of the tribbles pseudokinase protein family shapes their interactions with mitogen activated protein kinase pathways. *Sci Rep.* **6**, p32667.
- ◆ Guo, Y., Zang, Y., Lv, L., Cai, F., Qian, T., Zhang, G. and Feng, Q. (2017). IL-8 promotes proliferation and inhibition of apoptosis via STAT3/AKT/NF- κ B pathway in prostate cancer. *Mol Med Rep.* **16**(6), pp.9035-9042.
- ◆ Gutiérrez, T. and Simmen, T. (2014). Endoplasmic reticulum chaperones and oxidoreductases: critical regulators of tumor cell survival and immunorecognition. *Front Oncol.* **4**, p291.
- ◆ Hao, Y., Gu, X., Zhao, Y., Greene, S., Sha, W., Smoot, D.T., Califano, J., Wu, T.C. and Pang, X. (2011). Enforced expression of miR-101 inhibits prostate cancer cell growth by modulating the COX-2 pathway in vivo. *Cancer Prev Res (Phila).* **4**(7), pp.1073-1083.
- ◆ Hatfield, S.D., Shcherbata, H.R., Fischer, K.A., Nakahara, K., Carthew, R.W. and Ruohola-Baker, H. (2005). Stem cell division is regulated by the microRNA pathway. *Nature.* **435**(7044), pp.974-978.
- ◆ He, L. and Hannon, G.J. (2004). MicroRNAs: small RNAs with a big role in gene regulation. *Nat Rev Genet.* **5**(7), pp.522-531.
- ◆ Hegedus, Z., Czibula, A. and Kiss-Toth, E. (2006). Tribbles: novel regulators of cell function; evolutionary aspects. *Cell Mol Life Sci.* **63**(14), pp.1632-1641.
- ◆ Hegedus, Z., Czibula, A. and Kiss-Toth, E. (2007). Tribbles: a family of kinase-like proteins with potent signalling regulatory function. *Cell Signal.* **19**(2), pp.238-250.

- ◆ Heinig, M., Petretto, E., Wallace, C., Bottolo, L., Rotival, M., Lu, H., Li, Y., Sarwar, R., Langley, S.R., Bauerfeind, A., Hummel, O., Lee, Y.A., Paskas, S., Rintisch, C., Saar, K., Cooper, J., Buchan, R., Gray, E.E., Cyster, J.G., Erdmann, J., Hengstenberg, C., Maouche, S., Ouwehand, W.H., Rice, C.M., Samani, N.J., Schunkert, H., Goodall, A.H., Schulz, H., Roider, H.G., Vingron, M., Blankenberg, S., Münzel, T., Zeller, T., Szymczak, S., Ziegler, A., Tiret, L., Smyth, D.J., Pravenec, M., Aitman, T.J., Cambien, F., Clayton, D., Todd, J.A., Hubner, N., Cook, S.A. and Consortium, C. (2010). A trans-acting locus regulates an anti-viral expression network and type 1 diabetes risk. *Nature*. **467**(7314), pp.460-464.
- ◆ Hong, X. and Yu, J.J. (2019). MicroRNA-150 suppresses epithelial-mesenchymal transition, invasion, and metastasis in prostate cancer through the TRPM4-mediated β -catenin signaling pathway. *Am J Physiol Cell Physiol*. **316**(4), pp.C463-C480.
- ◆ Hornung, V., Bauernfeind, F., Halle, A., Samstad, E.O., Kono, H., Rock, K.L., Fitzgerald, K.A. and Latz, E. (2008). Silica crystals and aluminum salts activate the NALP3 inflammasome through phagosomal destabilization. *Nat Immunol*. **9**(8), pp.847-856.
- ◆ Hsu, J.B., Chiu, C.M., Hsu, S.D., Huang, W.Y., Chien, C.H., Lee, T.Y. and Huang, H.D. (2011). miRTar: an integrated system for identifying miRNA-target interactions in human. *BMC Bioinformatics*. **12**, p300.
- ◆ Hu, S.L., Cui, G.L., Huang, J., Jiang, J.G. and Wang, D.W. (2016a). An APOC3 3'UTR variant associated with plasma triglycerides levels and coronary heart disease by creating a functional miR-4271 binding site. *Sci Rep*. **6**, p32700.
- ◆ Hua, F., Shang, S., Yang, Y.W., Zhang, H.Z., Xu, T.L., Yu, J.J., Zhou, D.D., Cui, B., Li, K., Lv, X.X., Zhang, X.W., Liu, S.S., Yu, J.M., Wang, F., Zhang, C., Huang, B. and Hu, Z.W. (2019). TRIB3 Interacts With β -Catenin and TCF4 to Increase Stem Cell Features of Colorectal Cancer Stem Cells and Tumorigenesis. *Gastroenterology*. **156**(3), pp.708-721.e715.
- ◆ Huang, F.W., Mosquera, J.M., Garofalo, A., Oh, C., Baco, M., Amin-Mansour, A., Rabasha, B., Bahl, S., Mullane, S.A., Robinson, B.D., Aldubayan, S., Khani, F., Karir, B., Kim, E., Chimene-Weiss, J., Hofree, M., Romanel, A., Osborne, J.R., Kim, J.W., Azabdaftari, G., Woloszynska-Read, A., Sfanos, K., De Marzo, A.M., Demichelis, F.,

- Gabriel, S., Van Allen, E.M., Mesirov, J., Tamayo, P., Rubin, M.A., Powell, I.J. and Garraway, L.A. (2017). Exome Sequencing of African-American Prostate Cancer Reveals Loss-of-Function. *Cancer Discov.* **7**(9), pp.973-983.
- ◆ Huang, S., Yang, Z., Ma, Y., Yang, Y. and Wang, S. (2017). miR-101 Enhances Cisplatin-Induced DNA Damage Through Decreasing Nicotinamide Adenine Dinucleotide Phosphate Levels by Directly Repressing Tp53-Induced Glycolysis and Apoptosis Regulator Expression in Prostate Cancer Cells. *DNA Cell Biol.* **36**(4), pp.303-310.
 - ◆ Huang, S., Zou, C., Tang, Y., Wa, Q., Peng, X., Chen, X., Yang, C., Ren, D., Huang, Y., Liao, Z., Zou, X. and Pan, J. (2019). miR-582-3p and miR-582-5p Suppress Prostate Cancer Metastasis to Bone by Repressing TGF- β Signaling. *Mol Ther Nucleic Acids.* **16**, pp.91-104.
 - ◆ Huang, Y.Q., Cai, A.P., Chen, J.Y., Huang, C., Li, J. and Feng, Y.Q. (2016). The Relationship of Plasma miR-29a and Oxidized Low Density Lipoprotein with Atherosclerosis. *Cell Physiol Biochem.* **40**(6), pp.1521-1528.
 - ◆ Hudson, T.J. (2003). Wanted: regulatory SNPs. *Nat Genet.* **33**(4), pp.439-440.
 - ◆ Hutvagner, G. and Zamore, P.D. (2002). A microRNA in a multiple-turnover RNAi enzyme complex. *Science.* **297**(5589), pp.2056-2060.
 - ◆ Iizuka, M., Ogawa, T., Enomoto, M., Motoyama, H., Yoshizato, K., Ikeda, K. and Kawada, N. (2012). Induction of microRNA-214-5p in human and rodent liver fibrosis. *Fibrogenesis Tissue Repair.* **5**(1), p12.
 - ◆ Ismail, N., Wang, Y., Dakhllallah, D., Moldovan, L., Agarwal, K., Batte, K., Shah, P., Wisler, J., Eubank, T.D., Tridandapani, S., Paulaitis, M.E., Piper, M.G. and Marsh, C.B. (2013). Macrophage microvesicles induce macrophage differentiation and miR-223 transfer. *Blood.* **121**(6), pp.984-995.
 - ◆ Iwakawa, H.O. and Tomari, Y. (2015a). The Functions of MicroRNAs: mRNA Decay and Translational Repression. *Trends Cell Biol.* **25**(11), pp.651-665.
 - ◆ Izrailit, J., Berman, H.K., Datti, A., Wrana, J.L. and Reedijk, M. (2013). High throughput kinase inhibitor screens reveal TRB3 and MAPK-ERK/TGF β pathways as fundamental Notch regulators in breast cancer. *Proc Natl Acad Sci U S A.* **110**(5), pp.1714-1719.

- ◆ Jablonski, K.A., Amici, S.A., Webb, L.M., Ruiz-Rosado, J.e.D., Popovich, P.G., Partida-Sanchez, S. and Guerau-de-Arellano, M. (2015). Novel Markers to Delineate Murine M1 and M2 Macrophages. *PLoS One*. **10**(12), pe0145342.
- ◆ Jablonski, K.A., Gaudet, A.D., Amici, S.A., Popovich, P.G. and Guerau-de-Arellano, M. (2016). Control of the Inflammatory Macrophage Transcriptional Signature by miR-155. *PLoS One*. **11**(7), pe0159724.
- ◆ Jackute, J., Zemaitis, M., Pranys, D., Sitkauskiene, B., Miliauskas, S., Vaitkiene, S. and Sakalauskas, R. (2018). Distribution of M1 and M2 macrophages in tumor islets and stroma in relation to prognosis of non-small cell lung cancer. *BMC Immunol*. **19**(1), p3.
- ◆ Janiczek, M., Szyllberg, Ł., Kasperska, A., Kowalewski, A., Parol, M., Antosik, P., Radecka, B. and Marszałek, A. (2017). Immunotherapy as a Promising Treatment for Prostate Cancer: A Systematic Review. *J Immunol Res*. **2017**, p4861570.
- ◆ Jayadevappa, R., Chhatre, S., Malkowicz, S.B., Parikh, R.B., Guzzo, T. and Wein, A.J. (2019). Association Between Androgen Deprivation Therapy Use and Diagnosis of Dementia in Men With Prostate Cancer. *JAMA Netw Open*. **2**(7), pe196562.
- ◆ Jiang, L., Li, X., Zhang, Y., Zhang, M., Tang, Z. and Lv, K. (2017). Microarray and bioinformatics analyses of gene expression profiles in BALB/c murine macrophage polarization. *Mol Med Rep*. **16**(5), pp.7382-7390.
- ◆ Jiang, L., Schlesinger, F., Davis, C.A., Zhang, Y., Li, R., Salit, M., Gingeras, T.R. and Oliver, B. (2011). Synthetic spike-in standards for RNA-seq experiments. *Genome Res*. **21**(9), pp.1543-1551.
- ◆ Johnston, J.M., Angyal, A., Bauer, R.C., Hamby, S., Suvarna, S.K., Baidžajevs, K., Hegedus, Z., Dear, T.N., Turner, M., Wilson, H.L., Goodall, A.H., Rader, D.J., Shoulders, C.C., Francis, S.E., Kiss-Toth, E. and Consortium, C. (2019). Myeloid Tribbles 1 induces early atherosclerosis via enhanced foam cell expansion. *Sci Adv*. **5**(10), peax9183.
- ◆ Jonas, S. and Izaurralde, E. (2015). Towards a molecular understanding of microRNA-mediated gene silencing. *Nat Rev Genet*. **16**(7), pp.421-433.
- ◆ Jones, G.E. (2000). Cellular signaling in macrophage migration and chemotaxis. *J Leukoc Biol*. **68**(5), pp.593-602.

- ◆ Kantoff, P.W., Higano, C.S., Shore, N.D., Berger, E.R., Small, E.J., Penson, D.F., Redfern, C.H., Ferrari, A.C., Dreicer, R., Sims, R.B., Xu, Y., Frohlich, M.W., Schellhammer, P.F. and Investigators, I.S. (2010). Sipuleucel-T immunotherapy for castration-resistant prostate cancer. *N Engl J Med.* **363**(5), pp.411-422.
- ◆ Kapinas, K., Lowther, K.M., Kessler, C.B., Tilbury, K., Lieberman, J.R., Tirnauer, J.S., Campagnola, P. and Delany, A.M. (2012). Bone matrix osteonectin limits prostate cancer cell growth and survival. *Matrix Biol.* **31**(5), pp.299-307.
- ◆ Karagkouni, D., Paraskevopoulou, M.D., Chatzopoulos, S., Vlachos, I.S., Tastsoglou, S., Kanellos, I., Papadimitriou, D., Kavakiotis, I., Maniou, S., Skoufos, G., Vergoulis, T., Dalamagas, T. and Hatzigeorgiou, A.G. (2018b). DIANA-TarBase v8: a decade-long collection of experimentally supported miRNA-gene interactions. *Nucleic Acids Res.* **46**(D1), pp.D239-D245.
- ◆ Kathiresan, S., Melander, O., Guiducci, C., Surti, A., Burt, N.P., Rieder, M.J., Cooper, G.M., Roos, C., Voight, B.F., Havulinna, A.S., Wahlstrand, B., Hedner, T., Corella, D., Tai, E.S., Ordovas, J.M., Berglund, G., Vartiainen, E., Jousilahti, P., Hedblad, B., Taskinen, M.R., Newton-Cheh, C., Salomaa, V., Peltonen, L., Groop, L., Altshuler, D.M. and Orho-Melander, M. (2008). Six new loci associated with blood low-density lipoprotein cholesterol, high-density lipoprotein cholesterol or triglycerides in humans. *Nat Genet.* **40**(2), pp.189-197.
- ◆ Keeshan, K., He, Y., Wouters, B.J., Shestova, O., Xu, L., Sai, H., Rodriguez, C.G., Maillard, I., Tobias, J.W., Valk, P., Carroll, M., Aster, J.C., Delwel, R. and Pear, W.S. (2006). Tribbles homolog 2 inactivates C/EBPalpha and causes acute myelogenous leukemia. *Cancer Cell.* **10**(5), pp.401-411.
- ◆ Kertesz, M., Iovino, N., Unnerstall, U., Gaul, U. and Segal, E. (2007). The role of site accessibility in microRNA target recognition. *Nat Genet.* **39**(10), pp.1278-1284.
- ◆ Khan, A.A., Betel, D., Miller, M.L., Sander, C., Leslie, C.S. and Marks, D.S. (2009). Transfection of small RNAs globally perturbs gene regulation by endogenous microRNAs. *Nat Biotechnol.* **27**(6), pp.549-555.
- ◆ Khan, D., Sharathchandra, A., Ponnuswamy, A., Grover, R. and Das, S. (2013). Effect of a natural mutation in the 5' untranslated region on the translational control of p53 mRNA. *Oncogene.* **32**(35), pp.4148-4159.

- ◆ Kim, S.J., Uehara, H., Karashima, T., Mccarty, M., Shih, N. and Fidler, I.J. (2001). Expression of interleukin-8 correlates with angiogenesis, tumorigenicity, and metastasis of human prostate cancer cells implanted orthotopically in nude mice. *Neoplasia*. **3**(1), pp.33-42.
- ◆ Kim, V.N. (2004). MicroRNA precursors in motion: exportin-5 mediates their nuclear export. *Trends Cell Biol.* **14**(4), pp.156-159.
- ◆ Kim, V.N. and Nam, J.W. (2006). Genomics of microRNA. *Trends Genet.* **22**(3), pp.165-173.
- ◆ Kinne, R.W., Bräuer, R., Stuhlmüller, B., Palombo-Kinne, E. and Burmester, G.R. (2000). Macrophages in rheumatoid arthritis. *Arthritis Res.* **2**(3), pp.189-202.
- ◆ Kishi, H., Sato, M., Shibata, Y., Sato, K., Inoue, S., Abe, S., Kimura, T., Nishiwaki, M., Yamauchi, K., Nemoto, T., Igarashi, A., Tokairin, Y., Nakajima, O. and Kubota, I. (2016). Role of chemokine C-C motif ligand-1 in acute and chronic pulmonary inflammations. *Springerplus.* **5**(1), p1241.
- ◆ Kiss-Toth, E. (2011). Tribbles: 'puzzling' regulators of cell signalling. *Biochem Soc Trans.* **39**(2), pp.684-687.
- ◆ Kiss-Toth, E., Bagstaff, S.M., Sung, H.Y., Jozsa, V., Dempsey, C., Caunt, J.C., Oxley, K.M., Wyllie, D.H., Polgar, T., Harte, M., O'neill, L.A., Qwarnstrom, E.E. and Dower, S.K. (2004). Human tribbles, a protein family controlling mitogen-activated protein kinase cascades. *J Biol Chem.* **279**(41), pp.42703-42708.
- ◆ Kiss-Toth, E., Wyllie, D.H., Holland, K., Marsden, L., Jozsa, V., Oxley, K.M., Polgar, T., Qwarnstrom, E.E. and Dower, S.K. (2006). Functional mapping and identification of novel regulators for the Toll/Interleukin-1 signalling network by transcription expression cloning. *Cell Signal.* **18**(2), pp.202-214.
- ◆ Kloosterman, W.P., Wienholds, E., Ketting, R.F. and Plasterk, R.H. (2004). Substrate requirements for let-7 function in the developing zebrafish embryo. *Nucleic Acids Res.* **32**(21), pp.6284-6291.
- ◆ Koh, T.J. and DiPietro, L.A. (2011). Inflammation and wound healing: the role of the macrophage. *Expert Rev Mol Med.* **13**, pe23.
- ◆ Kong, H.Y. and Byun, J. (2013). Emerging roles of human prostatic Acid phosphatase. *Biomol Ther (Seoul).* **21**(1), pp.10-20.

- ◆ Kong, X., Qian, X., Duan, L., Liu, H., Zhu, Y. and Qi, J. (2016). microRNA-372 Suppresses Migration and Invasion by Targeting p65 in Human Prostate Cancer Cells. *DNA Cell Biol.* **35**(12), pp.828-835.
- ◆ Kozomara, A., Birgaoanu, M. and Griffiths-Jones, S. (2019). miRBase: from microRNA sequences to function. *Nucleic Acids Res.* **47**(D1), pp.D155-D162.
- ◆ Kubota, Y., Takubo, K., Shimizu, T., Ohno, H., Kishi, K., Shibuya, M., Saya, H. and Suda, T. (2009). M-CSF inhibition selectively targets pathological angiogenesis and lymphangiogenesis. *J Exp Med.* **206**(5), pp.1089-1102.
- ◆ Kurtz, C.L., Fannin, E.E., Toth, C.L., Pearson, D.S., Vickers, K.C. and Sethupathy, P. (2015). Inhibition of miR-29 has a significant lipid-lowering benefit through suppression of lipogenic programs in liver. *Sci Rep.* **5**, p12911.
- ◆ Lagos-Quintana, M., Rauhut, R., Lendeckel, W. and Tuschl, T. (2001). Identification of novel genes coding for small expressed RNAs. *Science.* **294**(5543), pp.853-858.
- ◆ Lahortiga, I., De Keersmaecker, K., Van Vlierberghe, P., Graux, C., Cauwelier, B., Lambert, F., Mentens, N., Beverloo, H.B., Pieters, R., Speleman, F., Odero, M.D., Bauters, M., Froyen, G., Marynen, P., Vandenberghe, P., Wlodarska, I., Meijerink, J.P. and Cools, J. (2007). Duplication of the MYB oncogene in T cell acute lymphoblastic leukemia. *Nat Genet.* **39**(5), pp.593-595.
- ◆ Laing, R.E., Hess, P., Shen, Y., Wang, J. and Hu, S.X. (2011). The role and impact of SNPs in pharmacogenomics and personalized medicine. *Curr Drug Metab.* **12**(5), pp.460-486.
- ◆ Landthaler, M., Yalcin, A. and Tuschl, T. (2004). The human DiGeorge syndrome critical region gene 8 and Its D. melanogaster homolog are required for miRNA biogenesis. *Curr Biol.* **14**(23), pp.2162-2167.
- ◆ Langmead, B. and Salzberg, S.L. (2012). Fast gapped-read alignment with Bowtie 2. *Nat Methods.* **9**(4), pp.357-359.
- ◆ Laoui, D., Van Overmeire, E., Movahedi, K., Van den Bossche, J., Schoupe, E., Mommer, C., Nikolaou, A., Morias, Y., De Baetselier, P. and Van Ginderachter, J.A. (2011). Mononuclear phagocyte heterogeneity in cancer: different subsets and activation states reaching out at the tumor site. *Immunobiology.* **216**(11), pp.1192-1202.

- ◆ Laviron, M. and Boissonnas, A. (2019). Ontogeny of Tumor-Associated Macrophages. *Front Immunol.* **10**, p1799.
- ◆ Lawrence, M.S., Stojanov, P., Mermel, C.H., Robinson, J.T., Garraway, L.A., Golub, T.R., Meyerson, M., Gabriel, S.B., Lander, E.S. and Getz, G. (2014). Discovery and saturation analysis of cancer genes across 21 tumour types. *Nature.* **505**(7484), pp.495-501.
- ◆ Lee, K.H., Chen, Y.L., Yeh, S.D., Hsiao, M., Lin, J.T., Goan, Y.G. and Lu, P.J. (2009). MicroRNA-330 acts as tumor suppressor and induces apoptosis of prostate cancer cells through E2F1-mediated suppression of Akt phosphorylation. *Oncogene.* **28**(38), pp.3360-3370.
- ◆ Lee, R.C., Feinbaum, R.L. and Ambros, V. (1993). The *C. elegans* heterochronic gene *lin-4* encodes small RNAs with antisense complementarity to *lin-14*. *Cell.* **75**(5), pp.843-854.
- ◆ Lee, Y.C., Wang, W.L., Chang, W.C., Huang, Y.H., Hong, G.C., Wang, H.L., Chou, Y.H., Tseng, H.C., Lee, H.T., Li, S.T., Chen, H.L., Wu, C.C., Yang, H.F., Wang, B.Y. and Chang, W.W. (2019). Tribbles Homolog 3 Involved in Radiation Response of Triple Negative Breast Cancer Cells by Regulating Notch1 Activation. *Cancers (Basel).* **11**(2).
- ◆ Leinders, M., Üçeyler, N., Pritchard, R.A., Sommer, C. and Sorkin, L.S. (2016). Increased miR-132-3p expression is associated with chronic neuropathic pain. *Exp Neurol.* **283**(Pt A), pp.276-286.
- ◆ Lewis, B.P., Shih, I.H., Jones-Rhoades, M.W., Bartel, D.P. and Burge, C.B. (2003). Prediction of mammalian microRNA targets. *Cell.* **115**(7), pp.787-798.
- ◆ Li, H., Handsaker, B., Wysoker, A., Fennell, T., Ruan, J., Homer, N., Marth, G., Abecasis, G., Durbin, R. and Subgroup, G.P.D.P. (2009). The Sequence Alignment/Map format and SAMtools. *Bioinformatics.* **25**(16), pp.2078-2079.
- ◆ Li, H., Jiang, T., Li, M.Q., Zheng, X.L. and Zhao, G.J. (2018). Transcriptional Regulation of Macrophages Polarization by MicroRNAs. *Front Immunol.* **9**, p1175.
- ◆ Li, J.H., Liu, S., Zhou, H., Qu, L.H. and Yang, J.H. (2014a). starBase v2.0: decoding miRNA-ceRNA, miRNA-ncRNA and protein-RNA interaction networks from large-scale CLIP-Seq data. *Nucleic Acids Res.* **42**(Database issue), pp.D92-97.

- ◆ Li, J.H., Liu, S., Zhou, H., Qu, L.H. and Yang, J.H. (2014b). starBase v2.0: decoding miRNA-ceRNA, miRNA-ncRNA and protein-RNA interaction networks from large-scale CLIP-Seq data. *Nucleic Acids Res.* **42**(Database issue), pp.D92-97.
- ◆ Li, S., Wang, C., Yu, X., Wu, H., Hu, J., Wang, S. and Ye, Z. (2017). miR-3619-5p inhibits prostate cancer cell growth by activating CDKN1A expression. *Oncol Rep.* **37**(1), pp.241-248.
- ◆ Li, S.L., Sui, Y., Sun, J., Jiang, T.Q. and Dong, G. (2018). Identification of tumor suppressive role of microRNA-132 and its target gene in tumorigenesis of prostate cancer. *Int J Mol Med.* **41**(4), pp.2429-2433.
- ◆ Li, Y. and Kowdley, K.V. (2012). MicroRNAs in common human diseases. *Genomics Proteomics Bioinformatics.* **10**(5), pp.246-253.
- ◆ Lin, Z.Y., Huang, Y.Q., Zhang, Y.Q., Han, Z.D., He, H.C., Ling, X.H., Fu, X., Dai, Q.S., Cai, C., Chen, J.H., Liang, Y.X., Jiang, F.N., Zhong, W.D., Wang, F. and Wu, C.L. (2014a). MicroRNA-224 inhibits progression of human prostate cancer by downregulating TRIB1. *Int J Cancer.* **135**(3), pp.541-550.
- ◆ Lindow, M. and Kauppinen, S. (2012). Discovering the first microRNA-targeted drug. *J Cell Biol.* **199**(3), pp.407-412.
- ◆ Lingel, A. and Sattler, M. (2005). Novel modes of protein-RNA recognition in the RNAi pathway. *Curr Opin Struct Biol.* **15**(1), pp.107-115.
- ◆ Litwin, M.S. and Tan, H.J. (2017). The Diagnosis and Treatment of Prostate Cancer: A Review. *JAMA.* **317**(24), pp.2532-2542.
- ◆ Liu, J., Wu, X., Franklin, J.L., Messina, J.L., Hill, H.S., Moellering, D.R., Walton, R.G., Martin, M. and Garvey, W.T. (2010). Mammalian Tribbles homolog 3 impairs insulin action in skeletal muscle: role in glucose-induced insulin resistance. *Am J Physiol Endocrinol Metab.* **298**(3), pp.E565-576.
- ◆ Liu, Q., Russell, M.R., Shahriari, K., Jernigan, D.L., Lioni, M.I., Garcia, F.U. and Fatatis, A. (2013). Interleukin-1 β promotes skeletal colonization and progression of metastatic prostate cancer cells with neuroendocrine features. *Cancer Res.* **73**(11), pp.3297-3305.
- ◆ Liu, R., Zhang, C., Hu, Z., Li, G., Wang, C., Yang, C., Huang, D., Chen, X., Zhang, H., Zhuang, R., Deng, T., Liu, H., Yin, J., Wang, S., Zen, K., Ba, Y. and Zhang, C.Y.

- (2011). A five-microRNA signature identified from genome-wide serum microRNA expression profiling serves as a fingerprint for gastric cancer diagnosis. *Eur J Cancer*. **47**(5), pp.784-791.
- ◆ Liu, T., Qiu, X., Zhao, X., Yang, R., Lian, H., Qu, F., Li, X. and Guo, H. (2018). Hypermethylation of the SPARC promoter and its prognostic value for prostate cancer. *Oncol Rep*. **39**(2), pp.659-666.
 - ◆ Liu, W. and Wang, X. (2019). Prediction of functional microRNA targets by integrative modeling of microRNA binding and target expression data. *Genome Biol*. **20**(1), p18.
 - ◆ Liu, X., Lv, X., Yang, Q., Jin, H., Zhou, W. and Fan, Q. (2018). MicroRNA-29a Functions as a Tumor Suppressor and Increases Cisplatin Sensitivity by Targeting NRAS in Lung Cancer. *Technol Cancer Res Treat*. **17**, p1533033818758905.
 - ◆ Liu, Y.H., Tan, K.A., Morrison, I.W., Lamb, J.R. and Argyle, D.J. (2013). Macrophage migration is controlled by Tribbles 1 through the interaction between C/EBP β and TNF- α . *Vet Immunol Immunopathol*. **155**(1-2), pp.67-75.
 - ◆ Liu, Z.Z., Han, Z.D., Liang, Y.K., Chen, J.X., Wan, S., Zhuo, Y.J., Cai, Z.D., Deng, Y.L., Lin, Z.Y., Mo, R.J., He, H.C. and Zhong, W.D. (2019). TRIB1 induces macrophages to M2 phenotype by inhibiting IKB-zeta in prostate cancer. *Cell Signal*. **59**, pp.152-162.
 - ◆ Logothetis, C.J. and Lin, S.H. (2005). Osteoblasts in prostate cancer metastasis to bone. *Nat Rev Cancer*. **5**(1), pp.21-28.
 - ◆ Lohan, F. and Keeshan, K. (2013). The functionally diverse roles of tribbles. *Biochem Soc Trans*. **41**(4), pp.1096-1100.
 - ◆ Lorenz, R., Bernhart, S.H., Höner Zu Siederdisen, C., Tafer, H., Flamm, C., Stadler, P.F. and Hofacker, I.L. (2011a). ViennaRNA Package 2.0. *Algorithms Mol Biol*. **6**, p26.
 - ◆ Love, M.I., Huber, W. and Anders, S. (2014). Moderated estimation of fold change and dispersion for RNA-seq data with DESeq2. *Genome Biol*. **15**(12), p550.
 - ◆ Low, H., Hoang, A. and Sviridov, D. (2012). Cholesterol efflux assay. *J Vis Exp*. (61), pe3810.
 - ◆ Lytle, J.R., Yario, T.A. and Steitz, J.A. (2007). Target mRNAs are repressed as efficiently by microRNA-binding sites in the 5' UTR as in the 3' UTR. *Proc Natl Acad Sci U S A*. **104**(23), pp.9667-9672.

- ◆ Ma, J., Gao, S., Xie, X., Sun, E., Zhang, M., Zhou, Q. and Lu, C. (2017). SPARC inhibits breast cancer bone metastasis and may be a clinical therapeutic target. *Oncol Lett.* **14**(5), pp.5876-5882.
- ◆ Majid, S., Dar, A.A., Saini, S., Arora, S., Shahryari, V., Zaman, M.S., Chang, I., Yamamura, S., Tanaka, Y., Deng, G. and Dahiya, R. (2012). miR-23b represses proto-oncogene Src kinase and functions as methylation-silenced tumor suppressor with diagnostic and prognostic significance in prostate cancer. *Cancer Res.* **72**(24), pp.6435-6446.
- ◆ Mangravite, L.M., Engelhardt, B.E., Medina, M.W., Smith, J.D., Brown, C.D., Chasman, D.I., Mecham, B.H., Howie, B., Shim, H., Naidoo, D., Feng, Q., Rieder, M.J., Chen, Y.D., Rotter, J.I., Ridker, P.M., Hopewell, J.C., Parish, S., Armitage, J., Collins, R., Wilke, R.A., Nickerson, D.A., Stephens, M. and Krauss, R.M. (2013). A statin-dependent QTL for GATM expression is associated with statin-induced myopathy. *Nature.* **502**(7471), pp.377-380.
- ◆ Mantovani, A., Allavena, P. and Sica, A. (2004). Tumour-associated macrophages as a prototypic type II polarised phagocyte population: role in tumour progression. *Eur J Cancer.* **40**(11), pp.1660-1667.
- ◆ Mantovani, A. and Locati, M. (2013). Tumor-associated macrophages as a paradigm of macrophage plasticity, diversity, and polarization: lessons and open questions. *Arterioscler Thromb Vasc Biol.* **33**(7), pp.1478-1483.
- ◆ Mantovani, A., Sica, A. and Locati, M. (2005). Macrophage polarization comes of age. *Immunity.* **23**(4), pp.344-346.
- ◆ Manzano, M., Forte, E., Raja, A.N., Schipma, M.J. and Gottwein, E. (2015a). Divergent target recognition by coexpressed 5'-isomiRs of miR-142-3p and selective viral mimicry. *RNA.* **21**(9), pp.1606-1620.
- ◆ Mao, Y., Chen, H., Lin, Y., Xu, X., Hu, Z., Zhu, Y., Wu, J., Zheng, X. and Xie, L. (2013). microRNA-330 inhibits cell motility by downregulating Sp1 in prostate cancer cells. *Oncol Rep.* **30**(1), pp.327-333.
- ◆ Martin, C.J., Peters, K.N. and Behar, S.M. (2014). Macrophages clean up: efferocytosis and microbial control. *Curr Opin Microbiol.* **17**, pp.17-23.

- ◆ Martinez, F.O. and Gordon, S. (2014). The M1 and M2 paradigm of macrophage activation: time for reassessment. *F1000Prime Rep.* **6**, p13.
- ◆ Martinez, F.O., Gordon, S., Locati, M. and Mantovani, A. (2006). Transcriptional profiling of the human monocyte-to-macrophage differentiation and polarization: new molecules and patterns of gene expression. *J Immunol.* **177**(10), pp.7303-7311.
- ◆ Martinez, F.O., Sica, A., Mantovani, A. and Locati, M. (2008). Macrophage activation and polarization. *Front Biosci.* **13**, pp.453-461.
- ◆ Marín, R.M. and Vaníček, J. (2011). Efficient use of accessibility in microRNA target prediction. *Nucleic Acids Res.* **39**(1), pp.19-29.
- ◆ Mashima, T., Soma-Nagae, T., Migita, T., Kinoshita, R., Iwamoto, A., Yuasa, T., Yonese, J., Ishikawa, Y. and Seimiya, H. (2014). TRIB1 supports prostate tumorigenesis and tumor-propagating cell survival by regulation of endoplasmic reticulum chaperone expression. *Cancer Res.* **74**(17), pp.4888-4897.
- ◆ Mata, J., Curado, S., Ephrussi, A. and Rørth, P. (2000). Tribbles coordinates mitosis and morphogenesis in *Drosophila* by regulating string/CDC25 proteolysis. *Cell.* **101**(5), pp.511-522.
- ◆ Mathews, D.H., Burkard, M.E., Freier, S.M., Wyatt, J.R. and Turner, D.H. (1999). Predicting oligonucleotide affinity to nucleic acid targets. *RNA.* **5**(11), pp.1458-1469.
- ◆ Matoulkova, E., Michalova, E., Vojtesek, B. and Hrstka, R. (2012). The role of the 3' untranslated region in post-transcriptional regulation of protein expression in mammalian cells. *RNA Biol.* **9**(5), pp.563-576.
- ◆ Merriel, S.W.D., Funston, G. and Hamilton, W. (2018). Prostate Cancer in Primary Care. *Adv Ther.* **35**(9), pp.1285-1294.
- ◆ Mills, C.D. (2012). M1 and M2 Macrophages: Oracles of Health and Disease. *Crit Rev Immunol.* **32**(6), pp.463-488.
- ◆ Mitsi, E., Kamng'ona, R., Rylance, J., Solórzano, C., Jesus Reiné, J., Mwandumba, H.C., Ferreira, D.M. and Jambo, K.C. (2018). Human alveolar macrophages predominately express combined classical M1 and M2 surface markers in steady state. *Respir Res.* **19**(1), p66.

- ◆ Monteleone, K., Selvaggi, C., Cacciotti, G., Falasca, F., Mezzaroma, I., D'Ettorre, G., Turriziani, O., Vullo, V., Antonelli, G. and Scagnolari, C. (2015). MicroRNA-29 family expression and its relation to antiviral immune response and viro-immunological markers in HIV-1-infected patients. *BMC Infect Dis.* **15**, p51.
- ◆ Moore, K.J., Sheedy, F.J. and Fisher, E.A. (2013). Macrophages in atherosclerosis: a dynamic balance. *Nat Rev Immunol.* **13**(10), pp.709-721.
- ◆ Mosser, D.M. and Edwards, J.P. (2008). Exploring the full spectrum of macrophage activation. *Nat Rev Immunol.* **8**(12), pp.958-969.
- ◆ Moszyńska, A., Gebert, M., Collawn, J.F. and Bartoszewski, R. (2017). SNPs in microRNA target sites and their potential role in human disease. *Open Biol.* **7**(4).
- ◆ Moya, L., Lai, J., Hoffman, A., Srinivasan, S., Panchadsaram, J., Chambers, S., Clements, J.A., Batra, J. and BioResource, A.P.C. (2018). Association Analysis of a Microsatellite Repeat in the. *Front Genet.* **9**, p428.
- ◆ Mu, H., Xiang, L., Li, S., Rao, D., Wang, S. and Yu, K. (2019). MiR-10a functions as a tumor suppressor in prostate cancer via targeting KDM4A. *J Cell Biochem.* **120**(4), pp.4987-4997.
- ◆ Munshi, S.U., Panda, H., Holla, P., Rewari, B.B. and Jameel, S. (2014). MicroRNA-150 is a potential biomarker of HIV/AIDS disease progression and therapy. *PLoS One.* **9**(5), pe95920.
- ◆ Murray, P.J. (2017). Macrophage Polarization. *Annu Rev Physiol.* **79**, pp.541-566.
- ◆ Nadiminty, N., Tummala, R., Lou, W., Zhu, Y., Shi, X.B., Zou, J.X., Chen, H., Zhang, J., Chen, X., Luo, J., deVere White, R.W., Kung, H.J., Evans, C.P. and Gao, A.C. (2012). MicroRNA let-7c is downregulated in prostate cancer and suppresses prostate cancer growth. *PLoS One.* **7**(3), pe32832.
- ◆ Naiki, T., Saijou, E., Miyaoka, Y., Sekine, K. and Miyajima, A. (2007). TRB2, a mouse Tribbles ortholog, suppresses adipocyte differentiation by inhibiting AKT and C/EBPbeta. *J Biol Chem.* **282**(33), pp.24075-24082.
- ◆ Nakazawa, M., Paller, C. and Kyprianou, N. (2017). Mechanisms of Therapeutic Resistance in Prostate Cancer. *Curr Oncol Rep.* **19**(2), p13.

- ◆ Nam, J.W., Rissland, O.S., Koppstein, D., Abreu-Goodger, C., Jan, C.H., Agarwal, V., Yildirim, M.A., Rodriguez, A. and Bartel, D.P. (2014). Global analyses of the effect of different cellular contexts on microRNA targeting. *Mol Cell*. **53**(6), pp.1031-1043.
- ◆ Nguyen, D.P., Li, J. and Tewari, A.K. (2014). Inflammation and prostate cancer: the role of interleukin 6 (IL-6). *BJU Int*. **113**(6), pp.986-992.
- ◆ Nguyen, N., Vishwakarma, B.A., Oakley, K., Han, Y., Przychodzen, B., Maciejewski, J.P. and Du, Y. (2016). Myb expression is critical for myeloid leukemia development induced by Setbp1 activation. *Oncotarget*. **7**(52), pp.86300-86312.
- ◆ Nikpay, M., Goel, A., Won, H.H., Hall, L.M., Willenborg, C., Kanoni, S., Saleheen, D., Kyriakou, T., Nelson, C.P., Hopewell, J.C., Webb, T.R., Zeng, L., Dehghan, A., Alver, M., Armasu, S.M., Auro, K., Bjornes, A., Chasman, D.I., Chen, S., Ford, I., Franceschini, N., Gieger, C., Grace, C., Gustafsson, S., Huang, J., Hwang, S.J., Kim, Y.K., Kleber, M.E., Lau, K.W., Lu, X., Lu, Y., Lytikäinen, L.P., Mihailov, E., Morrison, A.C., Pervjakova, N., Qu, L., Rose, L.M., Salfati, E., Saxena, R., Scholz, M., Smith, A.V., Tikkanen, E., Uitterlinden, A., Yang, X., Zhang, W., Zhao, W., de Andrade, M., de Vries, P.S., van Zuydam, N.R., Anand, S.S., Bertram, L., Beutner, F., Dedoussis, G., Frossard, P., Gauguier, D., Goodall, A.H., Gottesman, O., Haber, M., Han, B.G., Jalilzadeh, S., Kessler, T., König, I.R., Lannfelt, L., Lieb, W., Lind, L., Lindgren, C.M., Lokki, M.L., Magnusson, P.K., Mallick, N.H., Mehra, N., Meitinger, T., Memon, F.U., Morris, A.P., Nieminen, M.S., Pedersen, N.L., Peters, A., Rallidis, L.S., Rasheed, A., Samuel, M., Shah, S.H., Sinisalo, J., Stirrups, K.E., Trompet, S., Wang, L., Zaman, K.S., Ardisino, D., Boerwinkle, E., Borecki, I.B., Bottinger, E.P., Buring, J.E., Chambers, J.C., Collins, R., Cupples, L.A., Danesh, J., Demuth, I., Elosua, R., Epstein, S.E., Esko, T., Feitosa, M.F., Franco, O.H., Franzosi, M.G., Granger, C.B., Gu, D., Gudnason, V., Hall, A.S., Hamsten, A., Harris, T.B., Hazen, S.L., Hengstenberg, C., Hofman, A., Ingelsson, E., Iribarren, C., Jukema, J.W., Karhunen, P.J., Kim, B.J., Kooner, J.S., Kullo, I.J., Lehtimäki, T., Loos, R.J.F., Melander, O., Metspalu, A., März, W., Palmer, C.N., Perola, M., Quertermous, T., Rader, D.J., Ridker, P.M., Ripatti, S., Roberts, R., Salomaa, V., Sanghera, D.K., Schwartz, S.M., Sedorf, U., Stewart, A.F., Stott, D.J., Thiery, J., Zalloua, P.A., O'Donnell, C.J., Reilly, M.P., Assimes, T.L., Thompson, J.R., Erdmann, J., Clarke, R., Watkins, H., Kathiresan,

- S., McPherson, R., Deloukas, P., Schunkert, H., Samani, N.J. and Farrall, M. (2015). A comprehensive 1,000 Genomes-based genome-wide association meta-analysis of coronary artery disease. *Nat Genet.* **47**(10), pp.1121-1130.
- ◆ Nishida, N., Mimori, K., Fabbri, M., Yokobori, T., Sudo, T., Tanaka, F., Shibata, K., Ishii, H., Doki, Y. and Mori, M. (2011). MicroRNA-125a-5p is an independent prognostic factor in gastric cancer and inhibits the proliferation of human gastric cancer cells in combination with trastuzumab. *Clin Cancer Res.* **17**(9), pp.2725-2733.
 - ◆ Nédélec, Y., Sanz, J., Baharian, G., Szpiech, Z.A., Pacis, A., Dumaine, A., Grenier, J.C., Freiman, A., Sams, A.J., Hebert, S., Pagé Sabourin, A., Luca, F., Blekhan, R., Hernandez, R.D., Pique-Regi, R., Tung, J., Yotova, V. and Barreiro, L.B. (2016). Genetic Ancestry and Natural Selection Drive Population Differences in Immune Responses to Pathogens. *Cell.* **167**(3), pp.657-669.e621.
 - ◆ O'Brien, J., Hayder, H., Zayed, Y. and Peng, C. (2018). Overview of MicroRNA Biogenesis, Mechanisms of Actions, and Circulation. *Front Endocrinol (Lausanne).* **9**, p402.
 - ◆ Odegaard, J.I. and Chawla, A. (2013). The immune system as a sensor of the metabolic state. *Immunity.* **38**(4), pp.644-654.
 - ◆ Odegaard, J.I., Ganeshan, K. and Chawla, A. (2013). Adipose tissue macrophages: Amicus adipem? *Cell Metab.* **18**(6), pp.767-768.
 - ◆ Ohoka, N., Hattori, T., Kitagawa, M., Onozaki, K. and Hayashi, H. (2007). Critical and functional regulation of CHOP (C/EBP homologous protein) through the N-terminal portion. *J Biol Chem.* **282**(49), pp.35687-35694.
 - ◆ Ohoka, N., Yoshii, S., Hattori, T., Onozaki, K. and Hayashi, H. (2005). TRB3, a novel ER stress-inducible gene, is induced via ATF4-CHOP pathway and is involved in cell death. *EMBO J.* **24**(6), pp.1243-1255.
 - ◆ Ohri, C.M., Shikotra, A., Green, R.H., Waller, D.A. and Bradding, P. (2009). Macrophages within NSCLC tumour islets are predominantly of a cytotoxic M1 phenotype associated with extended survival. *Eur Respir J.* **33**(1), pp.118-126.
 - ◆ Ongusaha, P.P., Kwak, J.C., Zwible, A.J., Macip, S., Higashiyama, S., Taniguchi, N., Fang, L. and Lee, S.W. (2004). HB-EGF is a potent inducer of tumor growth and angiogenesis. *Cancer Res.* **64**(15), pp.5283-5290.

- ◆ Orr, N. and Chanock, S. (2008). Common genetic variation and human disease. *Adv Genet.* **62**, pp.1-32.
- ◆ Ostertag, A., Jones, A., Rose, A.J., Liebert, M., Kleinsorg, S., Reimann, A., Vegiopoulos, A., Berriel Diaz, M., Strzoda, D., Yamamoto, M., Satoh, T., Akira, S. and Herzig, S. (2010a). Control of adipose tissue inflammation through TRB1. *Diabetes.* **59**(8), pp.1991-2000.
- ◆ Ozen, M., Creighton, C.J., Ozdemir, M. and Ittmann, M. (2008). Widespread deregulation of microRNA expression in human prostate cancer. *Oncogene.* **27**(12), pp.1788-1793.
- ◆ Papagregoriou, G., Erguler, K., Dweep, H., Voskarides, K., Koupepidou, P., Athanasiou, Y., Pierides, A., Gretz, N., Felekis, K.N. and Deltas, C. (2012). A miR-1207-5p binding site polymorphism abolishes regulation of HBEGF and is associated with disease severity in CFHR5 nephropathy. *PLoS One.* **7**(2), pe31021.
- ◆ Paraskevopoulou, M.D., Georgakilas, G., Kostoulas, N., Vlachos, I.S., Vergoulis, T., Reczko, M., Filippidis, C., Dalamagas, T. and Hatzigeorgiou, A.G. (2013). DIANA-microT web server v5.0: service integration into miRNA functional analysis workflows. *Nucleic Acids Res.* **41**(Web Server issue), pp.W169-173.
- ◆ Parker, J.S., Roe, S.M. and Barford, D. (2004). Crystal structure of a PIWI protein suggests mechanisms for siRNA recognition and slicer activity. *EMBO J.* **23**(24), pp.4727-4737.
- ◆ Patro, R., Duggal, G., Love, M.I., Irizarry, R.A. and Kingsford, C. (2017). Salmon provides fast and bias-aware quantification of transcript expression. *Nat Methods.* **14**(4), pp.417-419.
- ◆ Pattabiraman, D.R. and Gonda, T.J. (2013). Role and potential for therapeutic targeting of MYB in leukemia. *Leukemia.* **27**(2), pp.269-277.
- ◆ Pesole, G., Mignone, F., Gissi, C., Grillo, G., Licciulli, F. and Liuni, S. (2001). Structural and functional features of eukaryotic mRNA untranslated regions. *Gene.* **276**(1-2), pp.73-81.
- ◆ Peterson, S.M., Thompson, J.A., Ufkin, M.L., Sathyanarayana, P., Liaw, L. and Congdon, C.B. (2014a). Common features of microRNA target prediction tools. *Front Genet.* **5**, p23.

- ◆ Petrov, A.I., Kay, S.J.E., Kalvari, I., Howe, K.L., Gray, K.A., Bruford, E.A., Kersey, P.J., Cochrane, G., Finn, R.D., Bateman, A., Kozomara, A., Griffiths-Jones, S., Frankish, A., Zwieb, C.W., Lau, B.Y., Williams, K.P., Chan, P.P., Lowe, T.M., Cannone, J.J., Gutell, R., Machnicka, M.A., Bujnicki, J.M., Yoshihama, M., Kenmochi, N., Chai, B., Cole, J.R., Szymanski, M., Karlowski, W.M., Wood, V., Huala, E., Berardini, T.Z., Zhao, Y., Chen, R., Zhu, W., Paraskevopoulou, M.D., Vlachos, I.S., Hatzigeorgiou, A.G., Ma, L., Zhang, Z., Puetz, J., Stadler, P.F., McDonald, D., Basu, S., Fey, P., Engel, S.R., Cherry, J.M., Volders, P.J., Mestdagh, P., Wower, J., Clark, M.B., Quek, X.C., Dinger, M.E. and The RNAcentral Consortium. (2017). RNAcentral: a comprehensive database of non-coding RNA sequences. *Nucleic Acids Res.* **45**(D1), pp.D128-D134.
- ◆ Pfeiffer, F., Gröber, C., Blank, M., Händler, K., Beyer, M., Schultze, J.L. and Mayer, G. (2018). Systematic evaluation of error rates and causes in short samples in next-generation sequencing. *Sci Rep.* **8**(1), p10950.
- ◆ Pratt, A.J. and MacRae, I.J. (2009). The RNA-induced silencing complex: a versatile gene-silencing machine. *J Biol Chem.* **284**(27), pp.17897-17901.
- ◆ Pyonteck, S.M., Gadea, B.B., Wang, H.W., Gocheva, V., Hunter, K.E., Tang, L.H. and Joyce, J.A. (2012). Deficiency of the macrophage growth factor CSF-1 disrupts pancreatic neuroendocrine tumor development. *Oncogene.* **31**(11), pp.1459-1467.
- ◆ Qi, L., Heredia, J.E., Altarejos, J.Y., Screatton, R., Goebel, N., Niessen, S., Macleod, I.X., Liew, C.W., Kulkarni, R.N., Bain, J., Newgard, C., Nelson, M., Evans, R.M., Yates, J. and Montminy, M. (2006). TRB3 links the E3 ubiquitin ligase COP1 to lipid metabolism. *Science.* **312**(5781), pp.1763-1766.
- ◆ Qian, B.Z. and Pollard, J.W. (2010). Macrophage diversity enhances tumor progression and metastasis. *Cell.* **141**(1), pp.39-51.
- ◆ Qu, H.W., Jin, Y., Cui, Z.L. and Jin, X.B. (2018). MicroRNA-373-3p inhibits prostate cancer progression by targeting AKT1. *Eur Rev Med Pharmacol Sci.* **22**(19), pp.6252-6259.
- ◆ Qu, W., Ding, S.M., Cao, G., Wang, S.J., Zheng, X.H. and Li, G.H. (2016). miR-132 mediates a metabolic shift in prostate cancer cells by targeting Glut1. *FEBS Open Bio.* **6**(7), pp.735-741.

- ◆ Quatromoni, J.G. and Eruslanov, E. (2012). Tumor-associated macrophages: function, phenotype, and link to prognosis in human lung cancer. *Am J Transl Res.* **4**(4), pp.376-389.
- ◆ Ramalho-Carvalho, J., Martins, J.B., Cekaite, L., Sveen, A., Torres-Ferreira, J., Graça, I., Costa-Pinheiro, P., Eilertsen, I.A., Antunes, L., Oliveira, J., Lothe, R.A., Henrique, R. and Jerónimo, C. (2017). Epigenetic disruption of miR-130a promotes prostate cancer by targeting SEC23B and DEPDC1. *Cancer Lett.* **385**, pp.150-159.
- ◆ Ramalinga, M., Roy, A., Srivastava, A., Bhattarai, A., Harish, V., Suy, S., Collins, S. and Kumar, D. (2015). MicroRNA-212 negatively regulates starvation induced autophagy in prostate cancer cells by inhibiting SIRT1 and is a modulator of angiogenesis and cellular senescence. *Oncotarget.* **6**(33), pp.34446-34457.
- ◆ Ramassone, A., Pagotto, S., Veronese, A. and Visone, R. (2018). Epigenetics and MicroRNAs in Cancer. *Int J Mol Sci.* **19**(2).
- ◆ Ramaswamy, S., Ross, K.N., Lander, E.S. and Golub, T.R. (2003). A molecular signature of metastasis in primary solid tumors. *Nat Genet.* **33**(1), pp.49-54.
- ◆ Rath, M., Müller, I., Kropf, P., Closs, E.I. and Munder, M. (2014). Metabolism via Arginase or Nitric Oxide Synthase: Two Competing Arginine Pathways in Macrophages. *Front Immunol.* **5**, p532.
- ◆ Rawla, P. (2019). Epidemiology of Prostate Cancer. *World J Oncol.* **10**(2), pp.63-89.
- ◆ Reczko, M., Maragkakis, M., Alexiou, P., Grosse, I. and Hatzigeorgiou, A.G. (2012). Functional microRNA targets in protein coding sequences. *Bioinformatics.* **28**(6), pp.771-776.
- ◆ Remmerie, A. and Scott, C.L. (2018). Macrophages and lipid metabolism. *Cell Immunol.* **330**, pp.27-42.
- ◆ Riffo-Campos, Á., Riquelme, I. and Brebi-Mieville, P. (2016). Tools for Sequence-Based miRNA Target Prediction: What to Choose? *Int J Mol Sci.* **17**(12).
- ◆ Ritchie, M.E., Phipson, B., Wu, D., Hu, Y., Law, C.W., Shi, W. and Smyth, G.K. (2015). limma powers differential expression analyses for RNA-sequencing and microarray studies. *Nucleic Acids Res.* **43**(7), pe47.

- ◆ Rodríguez, S.A., Arias Fúnez, F., Bueno Bravo, C., Rodríguez-Patrón Rodríguez, R., Sanz Mayayo, E., Palacios, V.H. and Burgos Revilla, F.J. (2014). Cryotherapy for primary treatment of prostate cancer: intermediate term results of a prospective study from a single institution. *Prostate Cancer*. **2014**, p571576.
- ◆ Rotival, M., Zeller, T., Wild, P.S., Maouche, S., Szymczak, S., Schillert, A., Castagné, R., Deiseroth, A., Proust, C., Brocheton, J., Godefroy, T., Perret, C., Germain, M., Eleftheriadis, M., Sinning, C.R., Schnabel, R.B., Lubos, E., Lackner, K.J., Rossmann, H., Münzel, T., Rendon, A., Erdmann, J., Deloukas, P., Hengstenberg, C., Diemert, P., Montalescot, G., Ouwehand, W.H., Samani, N.J., Schunkert, H., Tregouet, D.A., Ziegler, A., Goodall, A.H., Cambien, F., Tiret, L., Blankenberg, S. and Consortium, C. (2011). Integrating genome-wide genetic variations and monocyte expression data reveals trans-regulated gene modules in humans. *PLoS Genet*. **7**(12), pe1002367.
- ◆ Roy, S. (2016). miRNA in Macrophage Development and Function. *Antioxid Redox Signal*. **25**(15), pp.795-804.
- ◆ Ru, P., Steele, R., Newhall, P., Phillips, N.J., Toth, K. and Ray, R.B. (2012). miRNA-29b suppresses prostate cancer metastasis by regulating epithelial-mesenchymal transition signaling. *Mol Cancer Ther*. **11**(5), pp.1166-1173.
- ◆ Russo, R.C., Garcia, C.C., Teixeira, M.M. and Amaral, F.A. (2014). The CXCL8/IL-8 chemokine family and its receptors in inflammatory diseases. *Expert Rev Clin Immunol*. **10**(5), pp.593-619.
- ◆ Rycaj, K. and Tang, D.G. (2017). Molecular determinants of prostate cancer metastasis. *Oncotarget*. **8**(50), pp.88211-88231.
- ◆ Ryder, M., Gild, M., Hohl, T.M., Pamer, E., Knauf, J., Ghossein, R., Joyce, J.A. and Fagin, J.A. (2013). Genetic and pharmacological targeting of CSF-1/CSF-1R inhibits tumor-associated macrophages and impairs BRAF-induced thyroid cancer progression. *PLoS One*. **8**(1), pe54302.
- ◆ Röthlisberger, B., Heizmann, M., Bargetzi, M.J. and Huber, A.R. (2007). TRIB1 overexpression in acute myeloid leukemia. *Cancer Genet Cytogenet*. **176**(1), pp.58-60.
- ◆ Said, N., Frierson, H.F., Chernauskas, D., Conaway, M., Motamed, K. and Theodorescu, D. (2009). The role of SPARC in the TRAMP model of prostate carcinogenesis and progression. *Oncogene*. **28**(39), pp.3487-3498.

- ◆ Salazar, M., Lorente, M., García-Taboada, E., Pérez Gómez, E., Dávila, D., Zúñiga-García, P., María Flores, J., Rodríguez, A., Hegedus, Z., Mosén-Ansorena, D., Aransay, A.M., Hernández-Tiedra, S., López-Valero, I., Quintanilla, M., Sánchez, C., Iovanna, J.L., Dusetti, N., Guzmán, M., Francis, S.E., Carracedo, A., Kiss-Toth, E. and Velasco, G. (2015). Loss of Tribbles pseudokinase-3 promotes Akt-driven tumorigenesis via FOXO inactivation. *Cell Death Differ.* **22**(1), pp.131-144.
- ◆ Satoh, T., Kidoya, H., Naito, H., Yamamoto, M., Takemura, N., Nakagawa, K., Yoshioka, Y., Morii, E., Takakura, N., Takeuchi, O. and Akira, S. (2013). Critical role of Trib1 in differentiation of tissue-resident M2-like macrophages. *Nature.* **495**(7442), pp.524-528.
- ◆ Schulz, C., Gomez Perdiguero, E., Chorro, L., Szabo-Rogers, H., Cagnard, N., Kierdorf, K., Prinz, M., Wu, B., Jacobsen, S.E., Pollard, J.W., Frampton, J., Liu, K.J. and Geissmann, F. (2012). A lineage of myeloid cells independent of Myb and hematopoietic stem cells. *Science.* **336**(6077), pp.86-90.
- ◆ Schunkert, H., König, I.R., Kathiresan, S., Reilly, M.P., Assimes, T.L., Holm, H., Preuss, M., Stewart, A.F., Barbalic, M., Gieger, C., Absher, D., Aherrahrou, Z., Allayee, H., Altshuler, D., Anand, S.S., Andersen, K., Anderson, J.L., Ardissino, D., Ball, S.G., Balmforth, A.J., Barnes, T.A., Becker, D.M., Becker, L.C., Berger, K., Bis, J.C., Boekholdt, S.M., Boerwinkle, E., Braund, P.S., Brown, M.J., Burnett, M.S., Buyschaert, I., Carlquist, J.F., Chen, L., Cichon, S., Codd, V., Davies, R.W., Dedoussis, G., Dehghan, A., Demissie, S., Devaney, J.M., Diemert, P., Do, R., Doering, A., Eifert, S., Mokhtari, N.E., Ellis, S.G., Elosua, R., Engert, J.C., Epstein, S.E., de Faire, U., Fischer, M., Folsom, A.R., Freyer, J., Gigante, B., Girelli, D., Gretarsdottir, S., Gudnason, V., Gulcher, J.R., Halperin, E., Hammond, N., Hazen, S.L., Hofman, A., Horne, B.D., Illig, T., Iribarren, C., Jones, G.T., Jukema, J.W., Kaiser, M.A., Kaplan, L.M., Kastelein, J.J., Khaw, K.T., Knowles, J.W., Kolovou, G., Kong, A., Laaksonen, R., Lambrechts, D., Leander, K., Lettre, G., Li, M., Lieb, W., Loley, C., Lotery, A.J., Mannucci, P.M., Maouche, S., Martinelli, N., McKeown, P.P., Meisinger, C., Meitinger, T., Melander, O., Merlini, P.A., Mooser, V., Morgan, T., Mühleisen, T.W., Muhlestein, J.B., Münzel, T., Musunuru, K., Nahrstaedt, J., Nelson, C.P., Nöthen, M.M., Olivieri, O., Patel, R.S., Patterson, C.C., Peters, A., Peyvandi, F., Qu, L.,

Quyyumi, A.A., Rader, D.J., Rallidis, L.S., Rice, C., Rosendaal, F.R., Rubin, D., Salomaa, V., Sampietro, M.L., Sandhu, M.S., Schadt, E., Schäfer, A., Schillert, A., Schreiber, S., Schrezenmeir, J., Schwartz, S.M., Siscovick, D.S., Sivananthan, M., Sivapalaratnam, S., Smith, A., Smith, T.B., Snoep, J.D., Soranzo, N., Spertus, J.A., Stark, K., Stirrups, K., Stoll, M., Tang, W.H., Tennstedt, S., Thorgeirsson, G., Thorleifsson, G., Tomaszewski, M., Uitterlinden, A.G., van Rij, A.M., Voight, B.F., Wareham, N.J., Wells, G.A., Wichmann, H.E., Wild, P.S., Willenborg, C., Witteman, J.C., Wright, B.J., Ye, S., Zeller, T., Ziegler, A., Cambien, F., Goodall, A.H., Cupples, L.A., Quertermous, T., März, W., Hengstenberg, C., Blankenberg, S., Ouwehand, W.H., Hall, A.S., Deloukas, P., Thompson, J.R., Stefansson, K., Roberts, R., Thorsteinsdottir, U., O'Donnell, C.J., McPherson, R., Erdmann, J., Samani, N.J., Cardiogenics and Consortium, C. (2011a). Large-scale association analysis identifies 13 new susceptibility loci for coronary artery disease. *Nat Genet.* **43**(4), pp.333-338.

- ◆ Seok, H., Ham, J., Jang, E.S. and Chi, S.W. (2016a). MicroRNA Target Recognition: Insights from Transcriptome-Wide Non-Canonical Interactions. *Mol Cells.* **39**(5), pp.375-381.
- ◆ Sethupathy, P. and Collins, F.S. (2008). MicroRNA target site polymorphisms and human disease. *Trends Genet.* **24**(10), pp.489-497.
- ◆ Shah, M.Y., Ferrajoli, A., Sood, A.K., Lopez-Berestein, G. and Calin, G.A. (2016). microRNA Therapeutics in Cancer - An Emerging Concept. *EBioMedicine.* **12**, pp.34-42.
- ◆ Shahriari, K., Shen, F., Worrede-Mahdi, A., Liu, Q., Gong, Y., Garcia, F.U. and Fatatis, A. (2017). Cooperation among heterogeneous prostate cancer cells in the bone metastatic niche. *Oncogene.* **36**(20), pp.2846-2856.
- ◆ Shaked, I., Meerson, A., Wolf, Y., Avni, R., Greenberg, D., Gilboa-Geffen, A. and Soreq, H. (2009). MicroRNA-132 potentiates cholinergic anti-inflammatory signaling by targeting acetylcholinesterase. *Immunity.* **31**(6), pp.965-973.
- ◆ Sharda, D.R., Yu, S., Ray, M., Squadrito, M.L., De Palma, M., Wynn, T.A., Morris, S.M. and Hankey, P.A. (2011). Regulation of macrophage arginase expression and tumor growth by the Ron receptor tyrosine kinase. *J Immunol.* **187**(5), pp.2181-2192.

- ◆ Sharova, L.V., Sharov, A.A., Nedorezov, T., Piao, Y., Shaik, N. and Ko, M.S. (2009). Database for mRNA half-life of 19 977 genes obtained by DNA microarray analysis of pluripotent and differentiating mouse embryonic stem cells. *DNA Res.* **16**(1), pp.45-58.
- ◆ Sheedy, F.J. (2015). Turning 21: Induction of miR-21 as a Key Switch in the Inflammatory Response. *Front Immunol.* **6**, p19.
- ◆ Shen, M.M. and Abate-Shen, C. (2010). Molecular genetics of prostate cancer: new prospects for old challenges. *Genes Dev.* **24**(18), pp.1967-2000.
- ◆ Shin, M., Mizokami, A., Kim, J., Ofude, M., Konaka, H., Kadono, Y., Kitagawa, Y., Miwa, S., Kumaki, M., Keller, E.T. and Namiki, M. (2013). Exogenous SPARC suppresses proliferation and migration of prostate cancer by interacting with integrin β 1. *Prostate.* **73**(11), pp.1159-1170.
- ◆ Shiohama, A., Sasaki, T., Noda, S., Minoshima, S. and Shimizu, N. (2003). Molecular cloning and expression analysis of a novel gene DGCR8 located in the DiGeorge syndrome chromosomal region. *Biochem Biophys Res Commun.* **304**(1), pp.184-190.
- ◆ Sinha, P., Clements, V.K. and Ostrand-Rosenberg, S. (2005). Interleukin-13-regulated M2 macrophages in combination with myeloid suppressor cells block immune surveillance against metastasis. *Cancer Res.* **65**(24), pp.11743-11751.
- ◆ Skeeles, L.E., Fleming, J.L., Mahler, K.L. and Toland, A.E. (2013). The impact of 3'UTR variants on differential expression of candidate cancer susceptibility genes. *PLoS One.* **8**(3), pe58609.
- ◆ Song, J.J., Smith, S.K., Hannon, G.J. and Joshua-Tor, L. (2004). Crystal structure of Argonaute and its implications for RISC slicer activity. *Science.* **305**(5689), pp.1434-1437.
- ◆ Soubeyrand, S., Martinuk, A., Lau, P. and McPherson, R. (2016). TRIB1 Is Regulated Post-Transcriptionally by Proteasomal and Non-Proteasomal Pathways. *PLoS One.* **11**(3), pe0152346.
- ◆ Soubeyrand, S., Naing, T., Martinuk, A. and McPherson, R. (2013). ERK1/2 regulates hepatocyte Trib1 in response to mitochondrial dysfunction. *Biochim Biophys Acta.* **1833**(12), pp.3405-3414.

- ◆ Starczynowski, D.T., Kuchenbauer, F., Wegrzyn, J., Rouhi, A., Petriv, O., Hansen, C.L., Humphries, R.K. and Karsan, A. (2011). MicroRNA-146a disrupts hematopoietic differentiation and survival. *Exp Hematol.* **39**(2), pp.167-178.e164.
- ◆ Stark, A., Brennecke, J., Bushati, N., Russell, R.B. and Cohen, S.M. (2005). Animal MicroRNAs confer robustness to gene expression and have a significant impact on 3'UTR evolution. *Cell.* **123**(6), pp.1133-1146.
- ◆ Stegeman, S., Moya, L., Selth, L.A., Spurdle, A.B., Clements, J.A. and Batra, J. (2015a). A genetic variant of MDM4 influences regulation by multiple microRNAs in prostate cancer. *Endocr Relat Cancer.* **22**(2), pp.265-276.
- ◆ Steggerda, S.M., Bennett, M.K., Chen, J., Emberley, E., Huang, T., Janes, J.R., Li, W., MacKinnon, A.L., Makkouk, A., Marguier, G., Murray, P.J., Neou, S., Pan, A., Parlati, F., Rodriguez, M.L.M., Van de Velde, L.A., Wang, T., Works, M., Zhang, J., Zhang, W. and Gross, M.I. (2017). Inhibition of arginase by CB-1158 blocks myeloid cell-mediated immune suppression in the tumor microenvironment. *J Immunother Cancer.* **5**(1), p101.
- ◆ Sticht, C., De La Torre, C., Parveen, A. and Gretz, N. (2018). miRWalk: An online resource for prediction of microRNA binding sites. *PLoS One.* **13**(10), pe0206239.
- ◆ Strum, J.C., Johnson, J.H., Ward, J., Xie, H., Feild, J., Hester, A., Alford, A. and Waters, K.M. (2009). MicroRNA 132 regulates nutritional stress-induced chemokine production through repression of SirT1. *Mol Endocrinol.* **23**(11), pp.1876-1884.
- ◆ Su, A.I., Welsh, J.B., Sapinoso, L.M., Kern, S.G., Dimitrov, P., Lapp, H., Schultz, P.G., Powell, S.M., Moskaluk, C.A., Frierson, H.F. and Hampton, G.M. (2001). Molecular classification of human carcinomas by use of gene expression signatures. *Cancer Res.* **61**(20), pp.7388-7393.
- ◆ Sullivan, J., Kopp, R., Stratton, K., Manschreck, C., Corines, M., Rau-Murthy, R., Hayes, J., Lincon, A., Ashraf, A., Thomas, T., Schrader, K., Gallagher, D., Hamilton, R., Scher, H., Lilja, H., Scardino, P., Eastham, J., Offit, K., Vijai, J. and Klein, R.J. (2015). An analysis of the association between prostate cancer risk loci, PSA levels, disease aggressiveness and disease-specific mortality. *Br J Cancer.* **113**(1), pp.166-172.

- ◆ Sumner, R., Crawford, A., Mucenski, M. and Frampton, J. (2000). Initiation of adult myelopoiesis can occur in the absence of c-Myb whereas subsequent development is strictly dependent on the transcription factor. *Oncogene*. **19**(30), pp.3335-3342.
- ◆ Sung, H.Y., Francis, S.E., Arnold, N.D., Holland, K., Ernst, V., Angyal, A. and Kiss-Toth, E. (2012). Enhanced macrophage tribbles-1 expression in murine experimental atherosclerosis. *Biology (Basel)*. **1**(1), pp.43-57.
- ◆ Sung, H.Y., Francis, S.E., Crossman, D.C. and Kiss-Toth, E. (2006). Regulation of expression and signalling modulator function of mammalian tribbles is cell-type specific. *Immunol Lett*. **104**(1-2), pp.171-177.
- ◆ Sung, H.Y., Guan, H., Czibula, A., King, A.R., Eder, K., Heath, E., Suvarna, S.K., Dower, S.K., Wilson, A.G., Francis, S.E., Crossman, D.C. and Kiss-Toth, E. (2007). Human tribbles-1 controls proliferation and chemotaxis of smooth muscle cells via MAPK signaling pathways. *J Biol Chem*. **282**(25), pp.18379-18387.
- ◆ Tak, Y.G. and Farnham, P.J. (2015a). Making sense of GWAS: using epigenomics and genome engineering to understand the functional relevance of SNPs in non-coding regions of the human genome. *Epigenetics Chromatin*. **8**, p57.
- ◆ Tak, Y.G. and Farnham, P.J. (2015b). Making sense of GWAS: using epigenomics and genome engineering to understand the functional relevance of SNPs in non-coding regions of the human genome. *Epigenetics Chromatin*. **8**, p57.
- ◆ Takahashi, Y., Ohoka, N., Hayashi, H. and Sato, R. (2008). TRB3 suppresses adipocyte differentiation by negatively regulating PPARgamma transcriptional activity. *J Lipid Res*. **49**(4), pp.880-892.
- ◆ Tang, G., Du, R., Tang, Z. and Kuang, Y. (2018). MiRNAlet-7a mediates prostate cancer PC-3 cell invasion, migration by inducing epithelial-mesenchymal transition through CCR7/MAPK pathway. *J Cell Biochem*. **119**(4), pp.3725-3731.
- ◆ Teijeiro, V., Yang, D., Majumdar, S., González, F., Rickert, R.W., Xu, C., Koche, R., Verma, N., Lai, E.C. and Huangfu, D. (2018). DICER1 Is Essential for Self-Renewal of Human Embryonic Stem Cells. *Stem Cell Reports*. **11**(3), pp.616-625.
- ◆ Teslovich, T.M., Musunuru, K., Smith, A.V., Edmondson, A.C., Stylianou, I.M., Koseki, M., Pirruccello, J.P., Ripatti, S., Chasman, D.I., Willer, C.J., Johansen, C.T., Fouchier, S.W., Isaacs, A., Peloso, G.M., Barbalic, M., Ricketts, S.L., Bis, J.C.,

Aulchenko, Y.S., Thorleifsson, G., Feitosa, M.F., Chambers, J., Orho-Melander, M., Melander, O., Johnson, T., Li, X., Guo, X., Li, M., Shin Cho, Y., Jin Go, M., Jin Kim, Y., Lee, J.Y., Park, T., Kim, K., Sim, X., Twee-Hee Ong, R., Croteau-Chonka, D.C., Lange, L.A., Smith, J.D., Song, K., Hua Zhao, J., Yuan, X., Luan, J., Lamina, C., Ziegler, A., Zhang, W., Zee, R.Y., Wright, A.F., Witteman, J.C., Wilson, J.F., Willemsen, G., Wichmann, H.E., Whitfield, J.B., Waterworth, D.M., Wareham, N.J., Waeber, G., Vollenweider, P., Voight, B.F., Vitart, V., Uitterlinden, A.G., Uda, M., Tuomilehto, J., Thompson, J.R., Tanaka, T., Surakka, I., Stringham, H.M., Spector, T.D., Soranzo, N., Smit, J.H., Sinisalo, J., Silander, K., Sijbrands, E.J., Scuteri, A., Scott, J., Schlessinger, D., Sanna, S., Salomaa, V., Saharinen, J., Sabatti, C., Ruukonen, A., Rudan, I., Rose, L.M., Roberts, R., Rieder, M., Psaty, B.M., Pramstaller, P.P., Pichler, I., Perola, M., Penninx, B.W., Pedersen, N.L., Pattaro, C., Parker, A.N., Pare, G., Oostra, B.A., O'Donnell, C.J., Nieminen, M.S., Nickerson, D.A., Montgomery, G.W., Meitinger, T., McPherson, R., McCarthy, M.I., McArdle, W., Masson, D., Martin, N.G., Marroni, F., Mangino, M., Magnusson, P.K., Lucas, G., Luben, R., Loos, R.J., Lokki, M.L., Lettre, G., Langenberg, C., Launer, L.J., Lakatta, E.G., Laaksonen, R., Kyvik, K.O., Kronenberg, F., König, I.R., Khaw, K.T., Kaprio, J., Kaplan, L.M., Johansson, A., Jarvelin, M.R., Janssens, A.C., Ingelsson, E., Igl, W., Kees Hovingh, G., Hottenga, J.J., Hofman, A., Hicks, A.A., Hengstenberg, C., Heid, I.M., Hayward, C., Havulinna, A.S., Hastie, N.D., Harris, T.B., Haritunians, T., Hall, A.S., Gyllensten, U., Guiducci, C., Groop, L.C., Gonzalez, E., Gieger, C., Freimer, N.B., Ferrucci, L., Erdmann, J., Elliott, P., Ejebe, K.G., Döring, A., Dominiczak, A.F., Demissie, S., Deloukas, P., de Geus, E.J., de Faire, U., Crawford, G., Collins, F.S., Chen, Y.D., Caulfield, M.J., Campbell, H., Burt, N.P., Bonnycastle, L.L., Boomsma, D.I., Boekholdt, S.M., Bergman, R.N., Barroso, I., Bandinelli, S., Ballantyne, C.M., Assimes, T.L., Quertermous, T., Altshuler, D., Seielstad, M., Wong, T.Y., Tai, E.S., Feranil, A.B., Kuzawa, C.W., Adair, L.S., Taylor, H.A., Borecki, I.B., Gabriel, S.B., Wilson, J.G., Holm, H., Thorsteinsdottir, U., Gudnason, V., Krauss, R.M., Mohlke, K.L., Ordovas, J.M., Munroe, P.B., Kooner, J.S., Tall, A.R., Hegele, R.A., Kastelein, J.J., Schadt, E.E., Rotter, J.I., Boerwinkle, E., Strachan, D.P., Mooser, V., Stefansson, K., Reilly, M.P., Samani, N.J., Schunkert, H., Cupples, L.A., Sandhu, M.S., Ridker,

- P.M., Rader, D.J., van Duijn, C.M., Peltonen, L., Abecasis, G.R., Boehnke, M. and Kathiresan, S. (2010). Biological, clinical and population relevance of 95 loci for blood lipids. *Nature*. **466**(7307), pp.707-713.
- ◆ Testa, U., Castelli, G. and Pelosi, E. (2019). Cellular and Molecular Mechanisms Underlying Prostate Cancer Development: Therapeutic Implications. *Medicines (Basel)*. **6**(3).
 - ◆ Thomas, A.C. and Mattila, J.T. (2014). "Of mice and men": arginine metabolism in macrophages. *Front Immunol*. **5**, p479.
 - ◆ Thomas, S.L., Alam, R., Lemke, N., Schultz, L.R., Gutiérrez, J.A. and Rempel, S.A. (2010). PTEN augments SPARC suppression of proliferation and inhibits SPARC-induced migration by suppressing SHC-RAF-ERK and AKT signaling. *Neuro Oncol*. **12**(9), pp.941-955.
 - ◆ Tomari, Y. and Zamore, P.D. (2005). MicroRNA biogenesis: drosha can't cut it without a partner. *Curr Biol*. **15**(2), pp.R61-64.
 - ◆ Tomlins, S.A., Rhodes, D.R., Yu, J., Varambally, S., Mehra, R., Perner, S., Demichelis, F., Helgeson, B.E., Laxman, B., Morris, D.S., Cao, Q., Cao, X., Andrén, O., Fall, K., Johnson, L., Wei, J.T., Shah, R.B., Al-Ahmadie, H., Eastham, J.A., Eggener, S.E., Fine, S.W., Hotakainen, K., Stenman, U.H., Tsodikov, A., Gerald, W.L., Lilja, H., Reuter, V.E., Kantoff, P.W., Scardino, P.T., Rubin, M.A., Bjartell, A.S. and Chinnaiyan, A.M. (2008). The role of SPINK1 in ETS rearrangement-negative prostate cancers. *Cancer Cell*. **13**(6), pp.519-528.
 - ◆ Trombetta, A.C., Soldano, S., Contini, P., Tomatis, V., Ruaro, B., Paolino, S., Brizzolara, R., Montagna, P., Sulli, A., Pizzorni, C., Smith, V. and Cutolo, M. (2018). A circulating cell population showing both M1 and M2 monocyte/macrophage surface markers characterizes systemic sclerosis patients with lung involvement. *Respir Res*. **19**(1), p186.
 - ◆ Tugal, D., Liao, X. and Jain, M.K. (2013). Transcriptional control of macrophage polarization. *Arterioscler Thromb Vasc Biol*. **33**(6), pp.1135-1144.
 - ◆ Valinezhad Orang, A., Safaralizadeh, R. and Kazemzadeh-Bavili, M. (2014). Mechanisms of miRNA-Mediated Gene Regulation from Common Downregulation to mRNA-Specific Upregulation. *Int J Genomics*. **2014**, p970607.

- ◆ van Dalen, F.J., van Stevendaal, M.H.M.E., Fennemann, F.L., Verdoes, M. and Ilina, O. (2018). Molecular Repolarisation of Tumour-Associated Macrophages. *Molecules*. **24**(1).
- ◆ van der Harst, P. and Verweij, N. (2018). Identification of 64 Novel Genetic Loci Provides an Expanded View on the Genetic Architecture of Coronary Artery Disease. *Circ Res*. **122**(3), pp.433-443.
- ◆ Vanacore, D., Boccellino, M., Rossetti, S., Cavaliere, C., D'Aniello, C., Di Franco, R., Romano, F.J., Montanari, M., La Mantia, E., Piscitelli, R., Nocerino, F., Cappuccio, F., Grimaldi, G., Izzo, A., Castaldo, L., Pepe, M.F., Malzone, M.G., Iovane, G., Ametrano, G., Stiuso, P., Quagliuolo, L., Barberio, D., Perdonà, S., Muto, P., Montella, M., Maiolino, P., Veneziani, B.M., Botti, G., Caraglia, M. and Facchini, G. (2017). Micrnas in prostate cancer: an overview. *Oncotarget*. **8**(30), pp.50240-50251.
- ◆ Vasudevan, S., Tong, Y. and Steitz, J.A. (2007). Switching from repression to activation: microRNAs can up-regulate translation. *Science*. **318**(5858), pp.1931-1934.
- ◆ Veremeyko, T., Siddiqui, S., Sotnikov, I., Yung, A. and Ponomarev, E.D. (2013). IL-4/IL-13-dependent and independent expression of miR-124 and its contribution to M2 phenotype of monocytic cells in normal conditions and during allergic inflammation. *PLoS One*. **8**(12), pe81774.
- ◆ Vieweg, J. (2007). The evolving therapeutic landscape of prostate cancer. *Curr Opin Urol*. **17**(3), p156.
- ◆ Viola, A., Munari, F., Sánchez-Rodríguez, R., Scolaro, T. and Castegna, A. (2019). The Metabolic Signature of Macrophage Responses. *Front Immunol*. **10**, p1462.
- ◆ Wang, G., Zhao, D., Spring, D.J. and DePinho, R.A. (2018). Genetics and biology of prostate cancer. *Genes Dev*. **32**(17-18), pp.1105-1140.
- ◆ Wang, N., Liang, H. and Zen, K. (2014). Molecular mechanisms that influence the macrophage m1-m2 polarization balance. *Front Immunol*. **5**, p614.
- ◆ Wang, S., Wang, L., Wu, C., Sun, S. and Pan, J.H. (2018). E2F2 directly regulates the STAT1 and PI3K/AKT/NF-κB pathways to exacerbate the inflammatory phenotype in rheumatoid arthritis synovial fibroblasts and mouse embryonic fibroblasts. *Arthritis Res Ther*. **20**(1), p225.

- ◆ Wang, X., Liu, S., Cao, L., Zhang, T., Yue, D., Wang, L., Ping, Y., He, Q., Zhang, C., Wang, M., Chen, X., Gao, Q., Wang, D., Zhang, Z., Wang, F., Yang, L., Li, J., Huang, L., Zhang, B. and Zhang, Y. (2017). miR-29a-3p suppresses cell proliferation and migration by downregulating IGF1R in hepatocellular carcinoma. *Oncotarget*. **8**(49), pp.86592-86603.
- ◆ Wang, X.S., Gong, J.N., Yu, J., Wang, F., Zhang, X.H., Yin, X.L., Tan, Z.Q., Luo, Z.M., Yang, G.H., Shen, C. and Zhang, J.W. (2012). MicroRNA-29a and microRNA-142-3p are regulators of myeloid differentiation and acute myeloid leukemia. *Blood*. **119**(21), pp.4992-5004.
- ◆ Wang, Z., Brandt, S., Medeiros, A., Wang, S., Wu, H., Dent, A. and Serezani, C.H. (2015). MicroRNA 21 is a homeostatic regulator of macrophage polarization and prevents prostaglandin E2-mediated M2 generation. *PLoS One*. **10**(2), pe0115855.
- ◆ Wang, Z., Sha, H.H. and Li, H.J. (2019). Functions and mechanisms of miR-186 in human cancer. *Biomed Pharmacother*. **119**, p109428.
- ◆ Ward, L.D. and Kellis, M. (2012). HaploReg: a resource for exploring chromatin states, conservation, and regulatory motif alterations within sets of genetically linked variants. *Nucleic Acids Res*. **40**(Database issue), pp.D930-934.
- ◆ Wei, R., Yang, F., Urban, T.J., Li, L., Chalasani, N., Flockhart, D.A. and Liu, W. (2012). Impact of the Interaction between 3'-UTR SNPs and microRNA on the Expression of Human Xenobiotic Metabolism Enzyme and Transporter Genes. *Front Genet*. **3**, p248.
- ◆ Wei, X., Tang, C., Lu, X., Liu, R., Zhou, M., He, D., Zheng, D., Sun, C. and Wu, Z. (2015a). MiR-101 targets DUSP1 to regulate the TGF- β secretion in sorafenib inhibits macrophage-induced growth of hepatocarcinoma. *Oncotarget*. **6**(21), pp.18389-18405.
- ◆ Wienholds, E., Koudijs, M.J., van Eeden, F.J., Cuppen, E. and Plasterk, R.H. (2003). The microRNA-producing enzyme Dicer1 is essential for zebrafish development. *Nat Genet*. **35**(3), pp.217-218.
- ◆ Wightman, B., Ha, I. and Ruvkun, G. (1993). Posttranscriptional regulation of the heterochronic gene *lin-14* by *lin-4* mediates temporal pattern formation in *C. elegans*. *Cell*. **75**(5), pp.855-862.

- ◆ Wilk, G. and Braun, R. (2018a). regQTLs: Single nucleotide polymorphisms that modulate microRNA regulation of gene expression in tumors. *PLoS Genet.* **14**(12), pe1007837.
- ◆ Willer, C.J., Sanna, S., Jackson, A.U., Scuteri, A., Bonnycastle, L.L., Clarke, R., Heath, S.C., Timpson, N.J., Najjar, S.S., Stringham, H.M., Strait, J., Duren, W.L., Maschio, A., Busonero, F., Mulas, A., Albai, G., Swift, A.J., Morcken, M.A., Narisu, N., Bennett, D., Parish, S., Shen, H., Galan, P., Meneton, P., Hercberg, S., Zelenika, D., Chen, W.M., Li, Y., Scott, L.J., Scheet, P.A., Sundvall, J., Watanabe, R.M., Nagaraja, R., Ebrahim, S., Lawlor, D.A., Ben-Shlomo, Y., Davey-Smith, G., Shuldiner, A.R., Collins, R., Bergman, R.N., Uda, M., Tuomilehto, J., Cao, A., Collins, F.S., Lakatta, E., Lathrop, G.M., Boehnke, M., Schlessinger, D., Mohlke, K.L. and Abecasis, G.R. (2008). Newly identified loci that influence lipid concentrations and risk of coronary artery disease. *Nat Genet.* **40**(2), pp.161-169.
- ◆ Wynn, T.A., Chawla, A. and Pollard, J.W. (2013). Macrophage biology in development, homeostasis and disease. *Nature.* **496**(7446), pp.445-455.
- ◆ Xi, J., Huang, Q., Wang, L., Ma, X., Deng, Q., Kumar, M., Zhou, Z., Li, L., Zeng, Z., Young, K.H., Zhang, M. and Li, Y. (2018). miR-21 depletion in macrophages promotes tumoricidal polarization and enhances PD-1 immunotherapy. *Oncogene.* **37**(23), pp.3151-3165.
- ◆ Xie, B., Ding, Q., Han, H. and Wu, D. (2013). miRCancer: a microRNA-cancer association database constructed by text mining on literature. *Bioinformatics.* **29**(5), pp.638-644.
- ◆ Xin, H., Zhang, C., Herrmann, A., Du, Y., Figlin, R. and Yu, H. (2009). Sunitinib inhibition of Stat3 induces renal cell carcinoma tumor cell apoptosis and reduces immunosuppressive cells. *Cancer Res.* **69**(6), pp.2506-2513.
- ◆ Xin, M., Qiao, Z., Li, J., Liu, J., Song, S., Zhao, X., Miao, P., Tang, T., Wang, L., Liu, W., Yang, X., Dai, K. and Huang, G. (2016). miR-22 inhibits tumor growth and metastasis by targeting ATP citrate lyase: evidence in osteosarcoma, prostate cancer, cervical cancer and lung cancer. *Oncotarget.* **7**(28), pp.44252-44265.

- ◆ Xu, G., Zhang, Z., Xing, Y., Wei, J., Ge, Z., Liu, X., Zhang, Y. and Huang, X. (2014). MicroRNA-149 negatively regulates TLR-triggered inflammatory response in macrophages by targeting MyD88. *J Cell Biochem.* **115**(5), pp.919-927.
- ◆ Xu, H., Wang, P., You, J., Zheng, Y., Fu, Y., Tang, Q., Zhou, L., Wei, Z., Lin, B., Shu, Y., Zhu, Y., Hu, L. and Kong, X. (2010). Screening of Kozak-motif-located SNPs and analysis of their association with human diseases. *Biochem Biophys Res Commun.* **392**(1), pp.89-94.
- ◆ Xu, S., Ge, J., Zhang, Z. and Zhou, W. (2017). MiR-129 inhibits cell proliferation and metastasis by targeting ETS1 via PI3K/AKT/mTOR pathway in prostate cancer. *Biomed Pharmacother.* **96**, pp.634-641.
- ◆ Xu, S., Yi, X.M., Zhou, W.Q., Cheng, W., Ge, J.P. and Zhang, Z.Y. (2015). Downregulation of miR-129 in peripheral blood mononuclear cells is a diagnostic and prognostic biomarker in prostate cancer. *Int J Clin Exp Pathol.* **8**(11), pp.14335-14344.
- ◆ Xuan, W., Qu, Q., Zheng, B., Xiong, S. and Fan, G.H. (2015). The chemotaxis of M1 and M2 macrophages is regulated by different chemokines. *J Leukoc Biol.* **97**(1), pp.61-69.
- ◆ Yadav, S.S., Stockert, J.A., Hackert, V., Yadav, K.K. and Tewari, A.K. (2018). Intratumor heterogeneity in prostate cancer. *Urol Oncol.* **36**(8), pp.349-360.
- ◆ Yamamoto, M., Uematsu, S., Okamoto, T., Matsuura, Y., Sato, S., Kumar, H., Satoh, T., Saitoh, T., Takeda, K., Ishii, K.J., Takeuchi, O., Kawai, T. and Akira, S. (2007). Enhanced TLR-mediated NF-IL6 dependent gene expression by Trib1 deficiency. *J Exp Med.* **204**(9), pp.2233-2239.
- ◆ Yang, J.K., Liu, H.J., Wang, Y., Li, C., Yang, J.P., Yang, L., Qi, X.J., Zhao, Y.L., Shi, X.F., Li, J.C., Sun, G.Z. and Jiao, B.H. (2019). Exosomal miR-214-5p Released from Glioblastoma Cells Modulates Inflammatory Response of Microglia after Lipopolysaccharide Stimulation through Targeting CXCR5. *CNS Neurol Disord Drug Targets.* **18**(1), pp.78-87.
- ◆ Yang, L. and Zhang, Y. (2017). Tumor-associated macrophages, potential targets for cancer treatment. *Biomark Res.* **5**, p25.

- ◆ Ye, Y., Wang, G., Zhuang, J., He, S., Song, Y., Ni, J., Xia, W. and Wang, J. (2017). The Oncogenic Role of Tribbles 1 in Hepatocellular Carcinoma Is Mediated by a Feedback Loop Involving microRNA-23a and p53. *Front Physiol.* **8**, p789.
- ◆ Yokoyama, T. and Nakamura, T. (2011). Tribbles in disease: Signaling pathways important for cellular function and neoplastic transformation. *Cancer Sci.* **102**(6), pp.1115-1122.
- ◆ Yona, S., Kim, K.W., Wolf, Y., Mildner, A., Varol, D., Breker, M., Strauss-Ayali, D., Viukov, S., Guilliams, M., Misharin, A., Hume, D.A., Perlman, H., Malissen, B., Zelzer, E. and Jung, S. (2013). Fate mapping reveals origins and dynamics of monocytes and tissue macrophages under homeostasis. *Immunity.* **38**(1), pp.79-91.
- ◆ Yoshida, A., Kato, J.Y., Nakamae, I. and Yoneda-Kato, N. (2013). COP1 targets C/EBP α for degradation and induces acute myeloid leukemia via Trib1. *Blood.* **122**(10), pp.1750-1760.
- ◆ Young, M.D., Wakefield, M.J., Smyth, G.K. and Oshlack, A. (2010). Gene ontology analysis for RNA-seq: accounting for selection bias. *Genome Biol.* **11**(2), pR14.
- ◆ Yu, J.M., Sun, W., Wang, Z.H., Liang, X., Hua, F., Li, K., Lv, X.X., Zhang, X.W., Liu, Y.Y., Yu, J.J., Liu, S.S., Shang, S., Wang, F., Yang, Z.N., Zhao, C.X., Hou, X.Y., Li, P.P., Huang, B., Cui, B. and Hu, Z.W. (2019a). TRIB3 supports breast cancer stemness by suppressing FOXO1 degradation and enhancing SOX2 transcription. *Nat Commun.* **10**(1), p5720.
- ◆ Yue, D., Liu, H. and Huang, Y. (2009a). Survey of Computational Algorithms for MicroRNA Target Prediction. *Curr Genomics.* **10**(7), pp.478-492.
- ◆ Zaman, M.S., Chen, Y., Deng, G., Shahryari, V., Suh, S.O., Saini, S., Majid, S., Liu, J., Khatri, G., Tanaka, Y. and Dahiya, R. (2010). The functional significance of microRNA-145 in prostate cancer. *Br J Cancer.* **103**(2), pp.256-264.
- ◆ Zeng, Y. and Cullen, B.R. (2003). Sequence requirements for micro RNA processing and function in human cells. *RNA.* **9**(1), pp.112-123.
- ◆ Zeng, Y., Wagner, E.J. and Cullen, B.R. (2002). Both natural and designed micro RNAs can inhibit the expression of cognate mRNAs when expressed in human cells. *Mol Cell.* **9**(6), pp.1327-1333.

- ◆ Zeng, Y., Yi, R. and Cullen, B.R. (2003). MicroRNAs and small interfering RNAs can inhibit mRNA expression by similar mechanisms. *Proc Natl Acad Sci U S A.* **100**(17), pp.9779-9784.
- ◆ Zhang, B., Pan, X., Cobb, G.P. and Anderson, T.A. (2007). microRNAs as oncogenes and tumor suppressors. *Dev Biol.* **302**(1), pp.1-12.
- ◆ Zhang, B., Pan, X., Wang, Q., Cobb, G.P. and Anderson, T.A. (2006). Computational identification of microRNAs and their targets. *Comput Biol Chem.* **30**(6), pp.395-407.
- ◆ Zhang, D.E., Hetherington, C.J., Chen, H.M. and Tenen, D.G. (1994). The macrophage transcription factor PU.1 directs tissue-specific expression of the macrophage colony-stimulating factor receptor. *Mol Cell Biol.* **14**(1), pp.373-381.
- ◆ Zhang, F., Parayath, N.N., Ene, C.I., Stephan, S.B., Koehne, A.L., Coon, M.E., Holland, E.C. and Stephan, M.T. (2019). Genetic programming of macrophages to perform anti-tumor functions using targeted mRNA nanocarriers. *Nat Commun.* **10**(1), p3974.
- ◆ Zhang, G.M., Bao, C.Y., Wan, F.N., Cao, D.L., Qin, X.J., Zhang, H.L., Zhu, Y., Dai, B., Shi, G.H. and Ye, D.W. (2015). MicroRNA-302a Suppresses Tumor Cell Proliferation by Inhibiting AKT in Prostate Cancer. *PLoS One.* **10**(4), pe0124410.
- ◆ Zhang, N., Lei, J., Lei, H., Ruan, X., Liu, Q., Chen, Y. and Huang, W. (2015). MicroRNA-101 overexpression by IL-6 and TNF- α inhibits cholesterol efflux by suppressing ATP-binding cassette transporter A1 expression. *Exp Cell Res.* **336**(1), pp.33-42.
- ◆ Zhang, W., Liu, J., Qiu, J., Fu, X., Tang, Q., Yang, F., Zhao, Z. and Wang, H. (2016). MicroRNA-382 inhibits prostate cancer cell proliferation and metastasis through targeting COUP-TFII. *Oncol Rep.* **36**(6), pp.3707-3715.
- ◆ Zhang, X., Zhong, N., Li, X. and Chen, M.B. (2019a). TRIB3 promotes lung cancer progression by activating β -catenin signaling. *Eur J Pharmacol.* **863**, p172697.
- ◆ Zhang, Y., Sui, J., Shen, X., Li, C., Yao, W., Hong, W., Peng, H., Pu, Y., Yin, L. and Liang, G. (2017). Differential expression profiles of microRNAs as potential biomarkers for the early diagnosis of lung cancer. *Oncol Rep.* **37**(6), pp.3543-3553.
- ◆ Zhang, Y., Zhang, M., Zhong, M., Suo, Q. and Lv, K. (2013). Expression profiles of miRNAs in polarized macrophages. *Int J Mol Med.* **31**(4), pp.797-802.

- ◆ Zhao, G.J., Yin, K., Fu, Y.C. and Tang, C.K. (2012). The interaction of ApoA-I and ABCA1 triggers signal transduction pathways to mediate efflux of cellular lipids. *Mol Med.* **18**, pp.149-158.
- ◆ Zhou, H., Luo, Y., Chen, J.H., Hu, J., Luo, Y.Z., Wang, W., Zeng, Y. and Xiao, L. (2013). Knockdown of TRB3 induces apoptosis in human lung adenocarcinoma cells through regulation of Notch 1 expression. *Mol Med Rep.* **8**(1), pp.47-52.
- ◆ Zhu, C., Hou, X., Zhu, J., Jiang, C. and Wei, W. (2018). Expression of miR-30c and miR-29b in prostate cancer and its diagnostic significance. *Oncol Lett.* **16**(3), pp.3140-3144.
- ◆ Zhu, C., Shao, P., Bao, M., Li, P., Zhou, H., Cai, H., Cao, Q., Tao, L., Meng, X., Ju, X., Qin, C., Li, J. and Yin, C. (2014). miR-154 inhibits prostate cancer cell proliferation by targeting CCND2. *Urol Oncol.* **32**(1), pp.31.e39-16.
- ◆ Zhu, Y., Herndon, J.M., Sojka, D.K., Kim, K.W., Knolhoff, B.L., Zuo, C., Cullinan, D.R., Luo, J., Bearden, A.R., Lavine, K.J., Yokoyama, W.M., Hawkins, W.G., Fields, R.C., Randolph, G.J. and DeNardo, D.G. (2017). Tissue-Resident Macrophages in Pancreatic Ductal Adenocarcinoma Originate from Embryonic Hematopoiesis and Promote Tumor Progression. *Immunity.* **47**(3), p597.
- ◆ Zonari, E., Pucci, F., Saini, M., Mazzieri, R., Politi, L.S., Gentner, B. and Naldini, L. (2013). A role for miR-155 in enabling tumor-infiltrating innate immune cells to mount effective antitumor responses in mice. *Blood.* **122**(2), pp.243-252.

Chapter 8, Supporting Information

Appendix I, Chapter 2, General Materials and Methods

A1.1. List of reagents and kits

Reagent/Kit	Company	Cat. No
iScript cDNA Synthesis Kit	Biorad	1708891
miRCURY LNA RT Kit	Qiagen	339340
miRCURY LNA SYBR Green PCR Kit	Qiagen	339345
miRNeasy Mini Kit	Qiagen	217004
RNase-Free DNase Set	Qiagen	79256
Precision Plus 2x qPCR Master Mix with SYBR Green	Primer Design	PPLUS-SY-20ML
GenElute™ HP Plasmid Midiprep Kit	Sigma-Aldrich	NA0200-1KT
GenElute™ HP Plasmid Miniprep Kit	Sigma-Aldrich	NA0160
Dual Luciferase Reporter Assay Kit	Promega	E1910
Human IL-8 DuoSet ELISA	R & D	DY208
RealTime-Glo™ MT Cell Viability Assay	Promega	G9711
QuikChange II-Site-directed mutagenesis	Agilent	200521
pENTR/D-TOPO directional cloning	Invitrogen	K240020
Gateway LR Clonase II enzyme mix	Invitrogen	11791020
E.Coli C2987H	NEB	C2987I
Human Recombinant M-CSF	PrepoTech	300-25
Human Recombinant IL-4	PrepoTech	200-04
Human Recombinant IL-10	PrepoTech	200-10
Human Recombinant IFN- γ	PrepoTech	300-02
Human Recombinant M-CSF	ImmunoTools	11343117
E.Coli Lipopolysaccharide	Enzo Life Sciences	ALX-581-007-L001
miR-101-3p mimic	Horizon Discovery	C-300518-07-0005
miR-132-3p mimic	Horizon Discovery	C-300599-06-0005
miR-214-5p mimic	Horizon Discovery	C-301153-01-0005
miR-101-3p inhibitor	Horizon Discovery	IH-300518-08-0005
miR-132-3p inhibitor	Horizon Discovery	IH-300599-05-0005
Mimic Negative Control	Horizon Discovery	CN-001000-01-05
Inhibitor Negative Control	Horizon Discovery	IN-001005-01-05
miR-155-5p primer mix	Qiagen	339306
miR-125a-3p primer mix	Qiagen	339306
miR-186-5p primer mix	Qiagen	339306
miR-149-5p primer mix	Qiagen	339306
miR-766-3p primer mix	Qiagen	339306
miR-1343-3p primer mix	Qiagen	339306
TRIB1 siRNA	Horizon Discovery	L-003633-00-0005
DICER1 siRNA	Horizon Discovery	L-003483-00-0005
AGO2 siRNA	Horizon Discovery	L-004639-00-0005
siRNA negative control (scramble)	Horizon Discovery	D-001810-01-05
siGLO Green Transfection Indicator	Horizon Discovery	D-001630
MIR-101/TRIB1 Target Site Blocker	Qiagen	339199
Negative Control Target Site Blocker	Qiagen	339199
Viomer Green	Cambridge Bioscience	VG-01LB-01
Viomer Blue	Cambridge Bioscience	VG-01LB-01
Dharmafect DUO	Horizon Discovery	T-2010-03

Lipofectamine 3000 Reagent	Invitrogen	L3000008, L3000015
Ficoll Paque Plus	GE Healthcare	171440-02
DMEM media	Gibco	11885084
RMPI 1640 media	Gibco	21875034
Keratinocyte SF media	Gibco	17005042
NEAA	Gibco	11140050
Sodium Pyruvate	Gibco	11360070
Penicillin/Streptomycin	Gibco	15070-063
L-glutamine	Gibco	17-605E
Trypsin	Lonza	BE02-007E
Low-endotoxin heat inactivated FBS	PAN Biotech	P40-37500
Bovine Serum Albumin	Sigma-Aldrich	A7906
Bovine Serum Albumin, fatty acid free	Sigma-Aldrich	A8806
Protease Inhibitor Cocktail	Sigma-Aldrich	P8340
RIPA Lysis Buffer	Sigma-Aldrich	R0278
Pierce BCA Protein Assay	Thermo Fisher Scientific	23225
Tris Buffered Saline pH 8.0, powder	Sigma-Aldrich	T6664-10PAK
MOPS SDS Running Buffer (20X)	Invitrogen	NP0001
MES SDS Running Buffer (20X)	Invitrogen	NP0002
NuPAGE 4-12% Bis-Tris Protein Gels 10 wells, 15 wells	Invitrogen	NP0323PK2, NP0335PK2
NuPAGE Antioxidant	Invitrogen	NP0005
Protein Ladder	Invitrogen	LC5925
Re-blot stripping solution	Merck	2504
TopFluor Cholesterol	Avanti Polar Lipids	810255
CD14+ microbeads	Miltenyi Biotech	130-050-201
High Density Lipoprotein	Biorad	5685-2004
Substrate Reagent ELISA	R & D	DY999

A1.2. List of machines and equipment

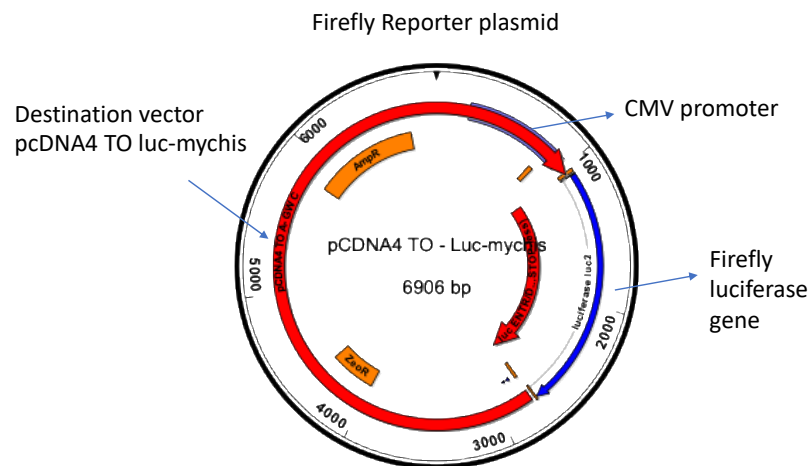
Machine/Equipment	Company
Nanodrop Spectrophotometer	Thermo Fisher Scientific
Flow Cytometer, LSR II	BD Bioscience
CFX384 C1000 Touch Thermal Cycler	Biorad
ChemiDoc™ XRS+	Biorad
C-DiGit® Blot Scanner, LI-COR	LI-COR Biosciences
Microplate Reader, Varioskan Flash	Thermo Fisher Scientific
Transilluminator UV InGenius3	Syngene

A1.3. List of antibodies used in western blot and immunofluorescence

Antibody	Company and Cat. Number	Working Dilution
Trib1	Millipore, 09-126	1:1000 WB, 1:200 IF
Alpha-tubulin	Santa Cruz Biotech, sc-5286	1:5000 WB, 1:500 IF
Heat Shock Protein 90	Abcam, ab13495	1:5000 WB
Mouse IgG, Isotype Control	Invitrogen, 10400C	1:500 IF
Rabbit IgG, Isotype Control	Invitrogen, 10500C	1:500 IF
Anti-Mouse	Dako, P0447	1:5000 WB, 1:1000 IF
Anti-Rabbit	Dako, P0448	1:5000 WB, 1:1000 IF
DAPI solution	Thermo Fisher Scientific, 62248	1:1000 IF

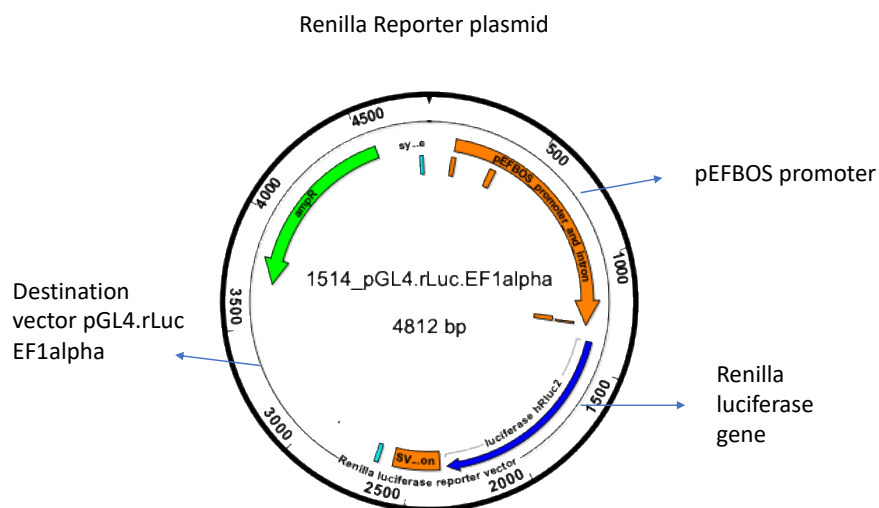
A1.4. Plasmids maps

Plasmids were generated in our lab, as described in Chapter 2. Entry plasmids and destination vectors were purchased by Prof. Endre Kiss-Toth. Below the maps of each plasmid used in this thesis.



A1.4.1. Firefly reporter plasmid map

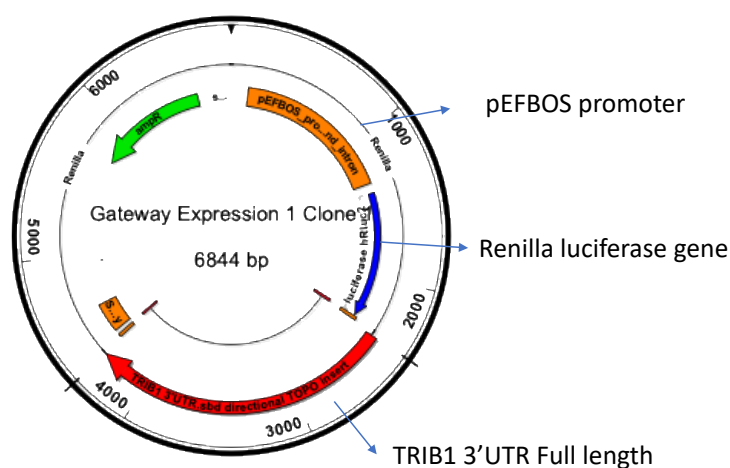
Firefly reporter plasmid used in the dual luciferase reporter assay, as internal control, for data normalisation. Map generated using DNASTar, Laser gene (<https://www.dnastar.com>).



A1.4.2. Renilla reporter plasmid map

Renilla reporter plasmid used in the dual luciferase reporter assay, as “NO UTR” control. Map generated using DNASTar, Laser gene (<https://www.dnastar.com>).

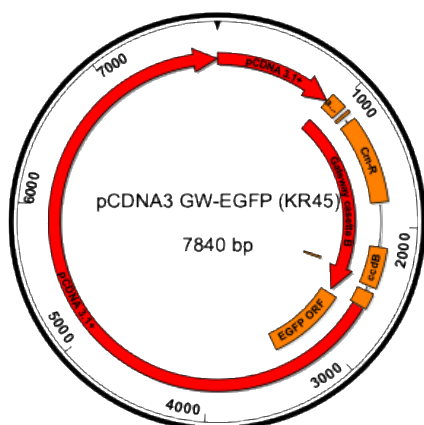
TRIB1 3'UTR Renilla Reporter plasmid



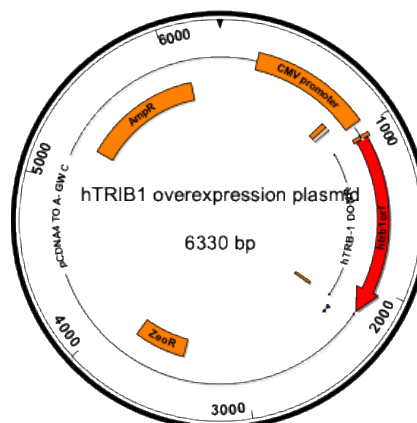
A1.4.3. TRIB1 3'UTR renilla reporter plasmid map

TRIB1 3'UTR renilla reporter plasmid used in the dual luciferase reporter assay, as test plasmid. The same plasmid was used to generate miRNA-binding site mutant and SNPs. Map generated using DNASTar, Laser gene (<https://www.dnastar.com>).

GFP overexpression plasmid



hTRIB1 overexpression plasmid



A1.4.4. Plasmids used for overexpression experiment

Expression plasmid used for overexpressing GFP (left) and TRIB1 (right) in MDMs by transient transfection (<https://www.dnastar.com>)

A1.5. List of RT-qPCR primers

Gene	Forward primer	Reverse primer
hTRIB1	CTCCACGGAGGAGAGAACCC	GACAAAGCATCATCTTCCCCC
hGAPDH	ATTGCCCTCAACGACCACTTT	CCCTGTTGCTGTAGCCAAATTC
hIL-4	TCCGATTCCTGAAACGGCTC	TGGTTGGCTTCCTTCACAGG
hIL-6	ACCCCCAGGAGAAGATTCCA	GATGCCGTCGAGGATGTACC
hIL-8	TGCCAAGGAGTGCTAAAG	CTCCACAACCCTCTGCAC
hMSR-1	CGAGGTCCCCTGGAGAAAGT	CAATTGCTCCCCGATCACCTTT
hCD36	TCTGTCCTATTGGGAAAGTCACT G	GAACTGCAATACCTGGCTTTTC TC
hCD163	AGGAGAGAACTTAGTCCACCA	TCAGAATGGCCTCCTTTTCCA
hSPAR-C	TGATGGTGCAGAGGAAACCG	TGTTCTCATCCAGCTCGCAC
hPD-L1	AGGGCATTCCAGAAAGATGAGG	GGTCCTTGGGAACCGTGAC
hVEGF	ATGCGGATCAAACCTCACCA	GCTCTATCTTTCTTTGGTCTGC
hTNF- α	CCTGCTGCACTTTGGAGTGA	CTTGTCACCTCGGGGTTCGAG
hCD80	TGCCTGACCTACTGCTTTGC	GGCGTACACTTTCCTTCTCA
hCD86	CCCAGACCACATTCCTTGGAT	TCCCTCTCCATTGTGTTGGT
hFAM26 F	GAGGGCTCGCATCCAAAAGA	GTACTIONGGCCTTCGGATTGAA
hDICER1	ACCAATCTCAACCAGCCACT	TCAAAAGGCAGTGAAGGCGA
hAGO2	GTCACCAAACATTCCCCTG	GTGTTTCTGCTCCTGTCCGA
hABCA1	TACATCTCCCTTCCCAGCA	GGGCCAGAGTCCCAAGACTA
hDUSP1	CCCCACTCTACGATCAGGGT	CCTTGCGGGAAGCGTGATA
mTrib1	CTTACATCCAGCTGCCGTCC	GTAGGCCTTGCTCTCACCAA
mGapdh	TGGCAAAGTGGAGATTGTTGCC	AAGATGGTGATGGGCTTCCCG

A1.6. Site-directed mutagenesis primers

Primer sequences:

Primer Name	Primer Sequence (5' to 3')
del1526-1532	5'-gagaatgccgtgtataacctcagctactttgtacatatattttacc-3'
del1526-1532-antisense	5'-ggtaaaatatatgtacaaagtagctgaggatatacacggcattctc-3'

Oligonucleotide information:

Primer Name	Length (nt.)	Tm	Duplex Energy at 68 °C	Energy Cost of Mismatches
del1526-1532	45	79.77°C	-38.93 kcal/mole	29.69%
del1526-1532-antisense	45	79.77°C	-41.48 kcal/mole	30.10%

Primer-template duplexes:

Primer Name	Primer-Template Duplex
del1526-1532	5'-gagaatgccgtgtataacctcac-----gtactttgtacatatattttacc-3' acactcttaacggcacatatggagtgcatgacacatgaaacatgtatataaaaatggaaa tgtgagaatgccgtgtataacctcagctactgtgtactttgtacatatattttacccttt
del1526-1532-antisense	 3'-ctcttaacggcacatatggagtg-----catgaaacatgtatataaaaatgg-5'

A1.6.1. Forward and reverse primers used for site-directed mutagenesis of miR-101-3p binding site

Mutagenesis primers used for deleting miR-101-3p binding site in the 3'UTR of TRIB1 luciferase reporter plasmid. Primers were designed using Agilent website (<https://www.agilent.com/store/primerDesignProgram.jsp>).

A

*

Forward: 5' CTGCTGAACTCGGCATGGTGCCTCCTCTTCTCTGTTG 3'
Reverse: 5' CAACAGAGAAGAGGAGGCACCATGCCGAGTTCAGCAG 3'

*

GC content: 56.76%	Location: 114-150
Melting temp: 83.6°C	Mismatched bases: 1
Length: 37 bp	Mutation: Substitution
5' flanking region: 18 bp	Forward primer MW: 11265.42 Da
3' flanking region: 18 bp	Reverse primer MW: 11475.58 Da

B

Forward: 5' CCCTTCACCTCCCCAAA CCTCAGAAACC 3'
Reverse: 5' GGTTCCTGAGGTTTGGGGGAGGTGAAGGG 3'

*

GC content: 58.62%	Location: 100-128
Melting temp: 79.4°C	Mismatched bases: 1
Length: 29 bp	Mutation: Substitution
5' flanking region: 14 bp	Forward primer MW: 8616.75 Da
3' flanking region: 14 bp	Reverse primer MW: 9181.01 Da

C

Forward: 5' CCCTTCACCTCCCCGAAA CCTCAGAAACC 3'
Reverse: 5' GGTTCCTGAGGTTTCGGGGAGGTGAAGGG 3'

*

GC content: 58.62%	Location: 100-128
Melting temp: 79.4°C	Mismatched bases: 1
Length: 29 bp	Mutation: Substitution
5' flanking region: 14 bp	Forward primer MW: 8656.77 Da
3' flanking region: 14 bp	Reverse primer MW: 9140.99 Da

A1.6.2. Forward and reverse primers used to generate SNPs in the 3'UTR of TRIB1

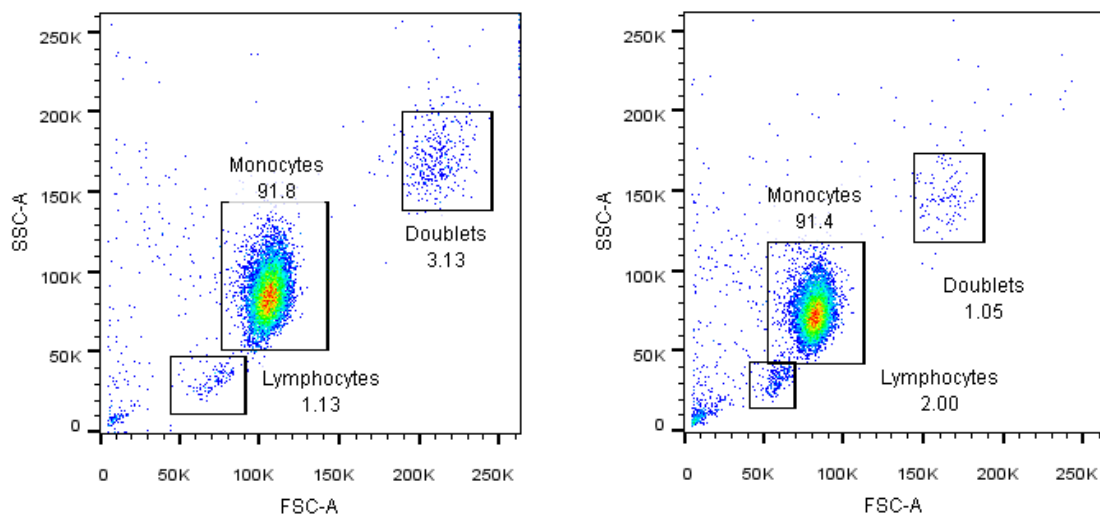
Mutagenesis primers used for generating rs62521034(A) and rs56395423 (B, C) in 3'UTR of TRIB1 renilla luciferase reporter plasmid. Primers were designed using Primer X (<https://www.bioinformatics.org/primerx/>).

Appendix II, Supplementary data for Chapter 3

This section contains supporting data for Chapter 3, miR-101-3p negatively regulates Tribbles-1 expression in primary human macrophages.

A2.1. Assessment of CD14⁺ monocyte purity: flow cytometry

The specificity of the PBMCs isolation protocol was previously confirmed in our group by using Flow Cytometry (LSR II flow cytometer, BD Bioscience). Monocytes were stained for both purity and activation by Dr Yang Li (PhD thesis submitted in 2019). More than 90% of monocytes were detected in total CD14⁺ PBMCs fraction with minor proportions of cell debris, lymphocytes and monocyte doublets. **Figure 8.2.1.** shows the proportion of CD14⁺ monocytes (>90%) isolated by myself from two different donors.

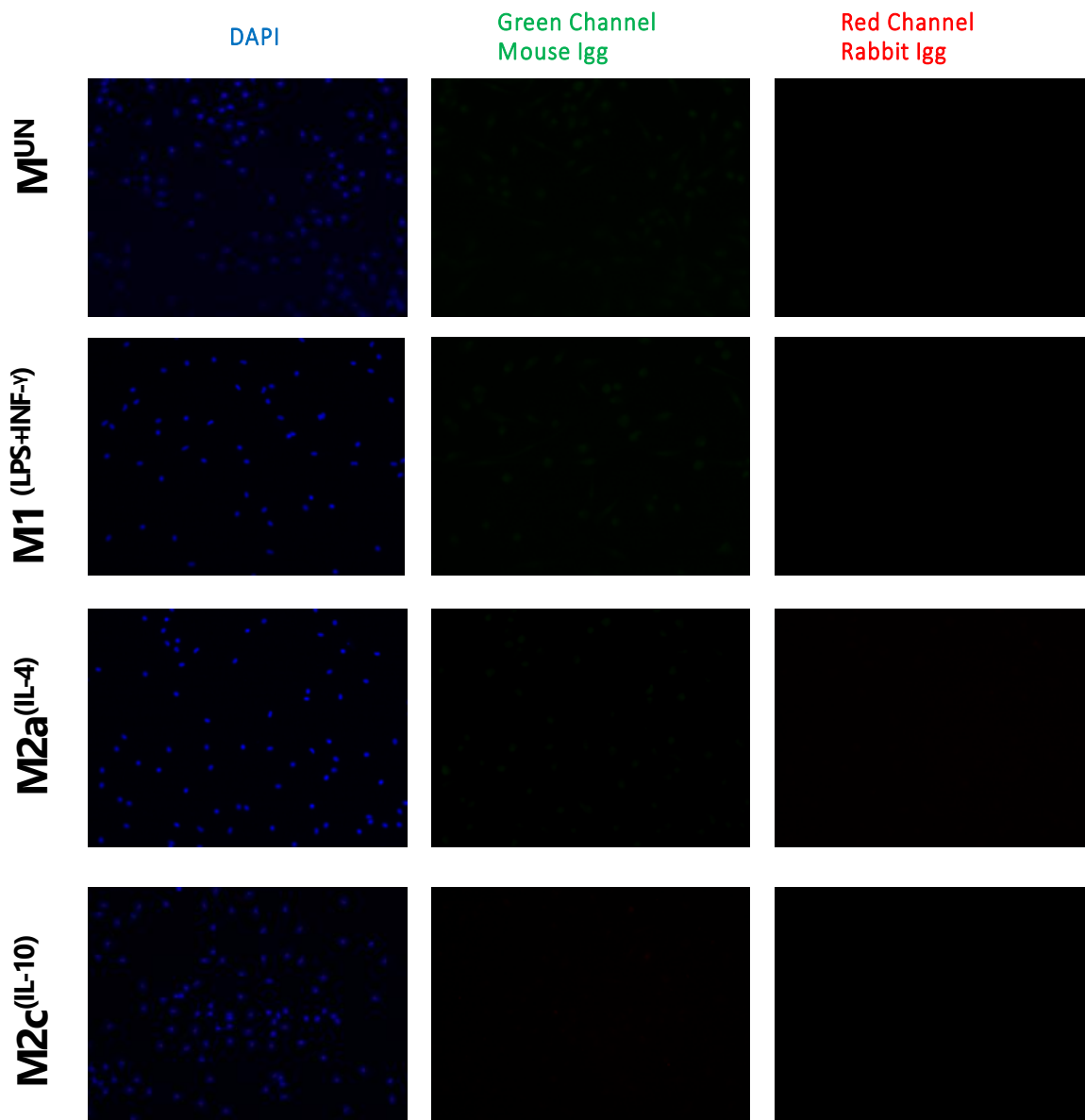


A2.1. Assessment of CD14⁺ monocyte population purity

Flow Cytometry was performed after the positive selection of CD14⁺ monocytes (human CD14⁺ beads- conjugated antibody) to assess the purity of the isolated population (> 90 %). The figures show two representative experiments. Gating was performed using the intrinsic parameters of cell size and granularity (SSC and FSC), according to previous gating generated in our lab.

A2.2. Immunofluorescence: isotype controls

For each condition tested in the immunofluorescence we included isotype controls that did not show any strong signal. Below images taken from a representative sample, the same showed in Chapter 3.

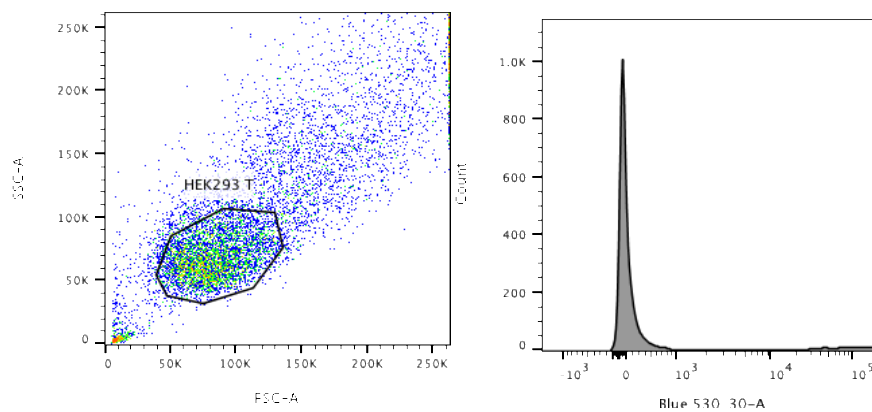


A2.2. Immunofluorescence isotype controls

Representative immunofluorescence images for Donor B showing polarised MDMs stained for dapi (blue) mouse Igg (green), rabbit Igg (red). Images were acquired using a 20x objective magnification.

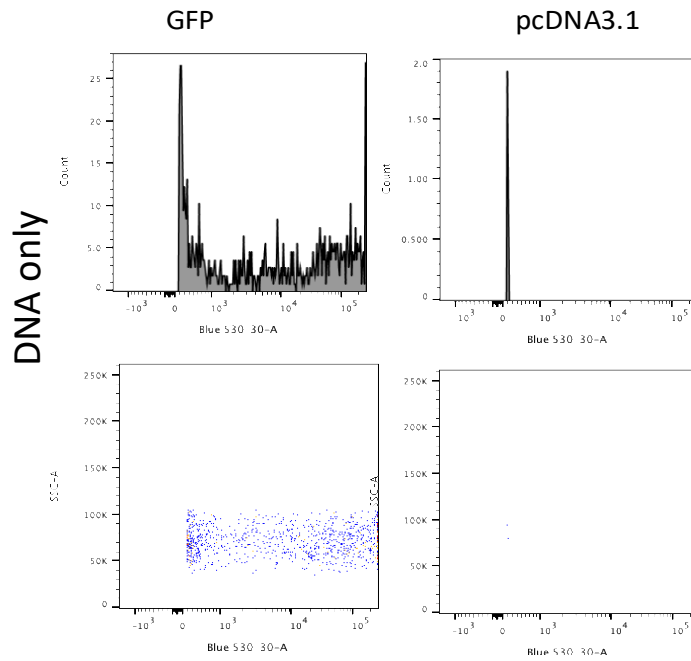
A2.3. Assessment of co-transfection efficiency

Transfection efficiency was assessed for the DNA/RNA co-transfection in HEK293T cell line (Dharmafect DUO kit) by using Flow Cytometry and evaluating fluorescence signal. To this aim, we used GFP and an empty plasmid (pcDNA3.1) and a fluorescent RNA (siGLO) and its negative control. Transfection was carried out for 24 hours (2 biological experiments, 3 technical replicates each). Cells were washed in PBS, removed from tissue culture plate and resuspended in MACs buffer (500-1000uL). **Figure 8.2.3.1-4** show representative flow cytometry images, while **Figure 8.2.3.5.** shows the quantification as percentage and mean fluorescent intensity (MFI). The percentage of live/dead cells and GFP positive/negative is specified in each figure legend. The percentage of efficiency, measured through fluorescence, was approximately 30% (GFP + siGLO). We believe that this is due to cell death occurring during the collection and the preparation of the samples, prior to the flow cytometry analysis. The transfection of both DNA and RNA was successful. Transient transfections using Lipofectamine 3000 and Viromer kits were previously optimised in our lab by other PhD students (data not shown).



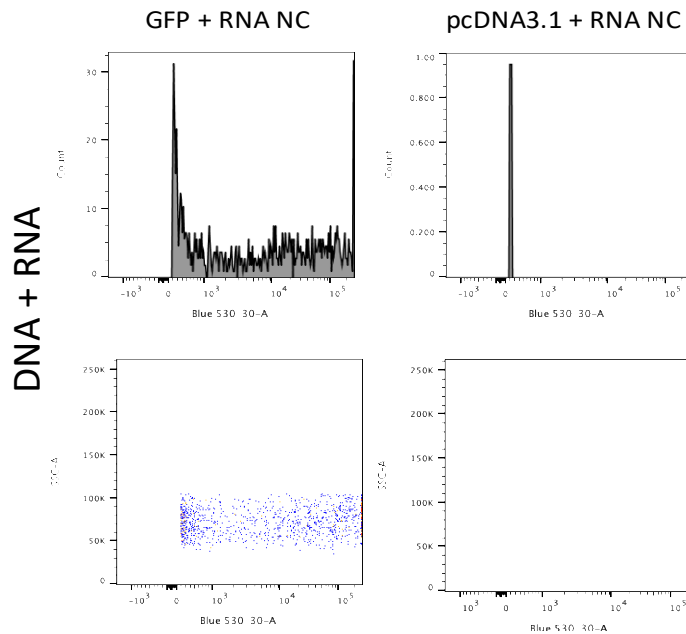
A2.3.1. Flow cytometry: non-transfected HEK293T cells

The graphs show the main cell population in dot plots (SSC/FSC) (left) and blue emission as histogram (Count/530-30) (right), stained with TO-PRO-1. Live cells were 54%.



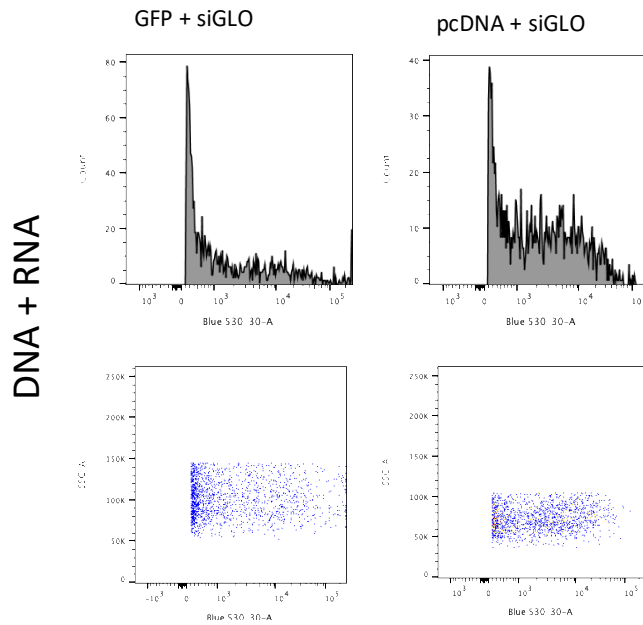
A2.3.2. Flow cytometry: DNA transfection in HEK293T cells

Histogram and dot plot for GFP (left) and an empty plasmid vector pcDNA3.1 (right). GFP positive cells were 20%. No blue emission for pcDNA3.1 transfected cells.



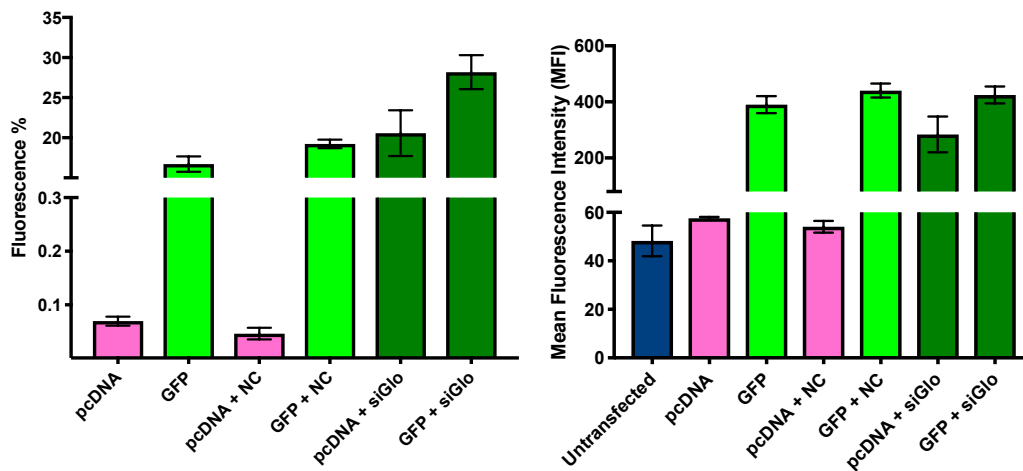
A2.3.3. Flow cytometry: DNA and RNA co-transfection in HEK293T cells

Histogram and dot plot for GFP and RNA negative control (left) and an empty plasmid vector pcDNA3.1 and RNA negative control (right). GFP positive cells were 20%. No blue emission for pcDNA3.1/RNA control transfection.



A2.3.4. Flow cytometry: DNA and RNA siGLO co-transfection in HEK293T cells

Histogram and dot plot for GFP and RNA siGLO (left) and an empty plasmid vector pcDNA3.1 and RNA siGLO (right). GFP/siGLO positive cells were 30%; pcDNA3.1/siGLO positive cells were 15%.



A2.3.5. Flow cytometry: fluorescence percentage and MFI

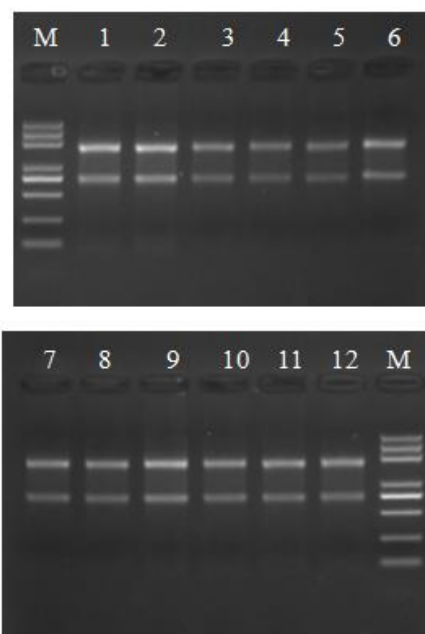
The graphs show the % of the fluorescence (left) and the mean fluorescence intensity (right) for each transfection condition. No statistical analysis was performed.

Appendix III, Supplementary data for Chapter 4

This section contains supporting data for Chapter 4, Integrated transcriptome analysis of small non-coding RNAs and mRNAs in pro-inflammatory macrophages.

A3.1. RNA quality and concentration: representative samples

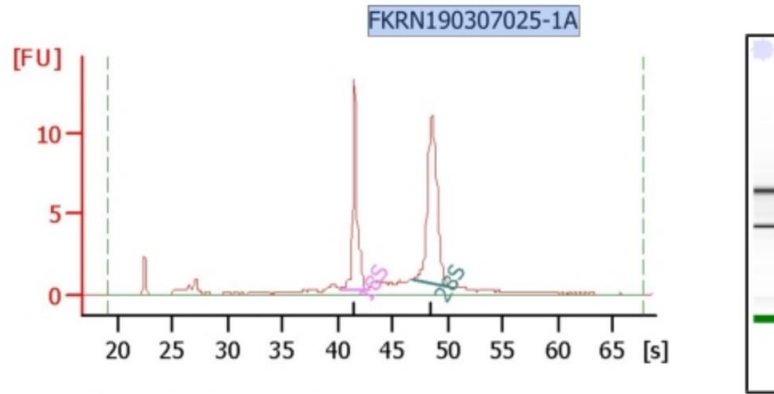
Prior to RNA-seq experiments, RNA was checked for quality and concentration by the company Novogene, using agarose gel electrophoresis, nanodrop and the bioanalyser Agilent 2100. Below some representative samples.



Remark: M: Trans 2K Plus DNA ladder; 1-12: samples ranged in the order of upper table (1-2、 5、 11-12 loaded 1ul, 3-4、 6-10 loaded 2ul).

A3.1.1. RNA agarose gel electrophoresis: RNA quality assessment

Agarose gel electrophoresis of RNA samples isolated from MDMs and sent for small non-coding RNA sequencing experiment (GelConc:1%; Voltage:180v; Run Time:16min). The 18S and 28S ribosomal are clear and RNA appears intact (no additional bands).



Overall Results for sample 12 : FKRN190307025-1A

RNA Area: 62.9
 RNA Concentration: 177 ng/μl
 rRNA Ratio [28s / 18s]: 1.5
 RNA Integrity Number (RIN): 9.5 (B.02.09)
 Result Flagging Color:
 Result Flagging Label: RIN: 9.50

Fragment table for sample 12 : FKRN190307025-1A

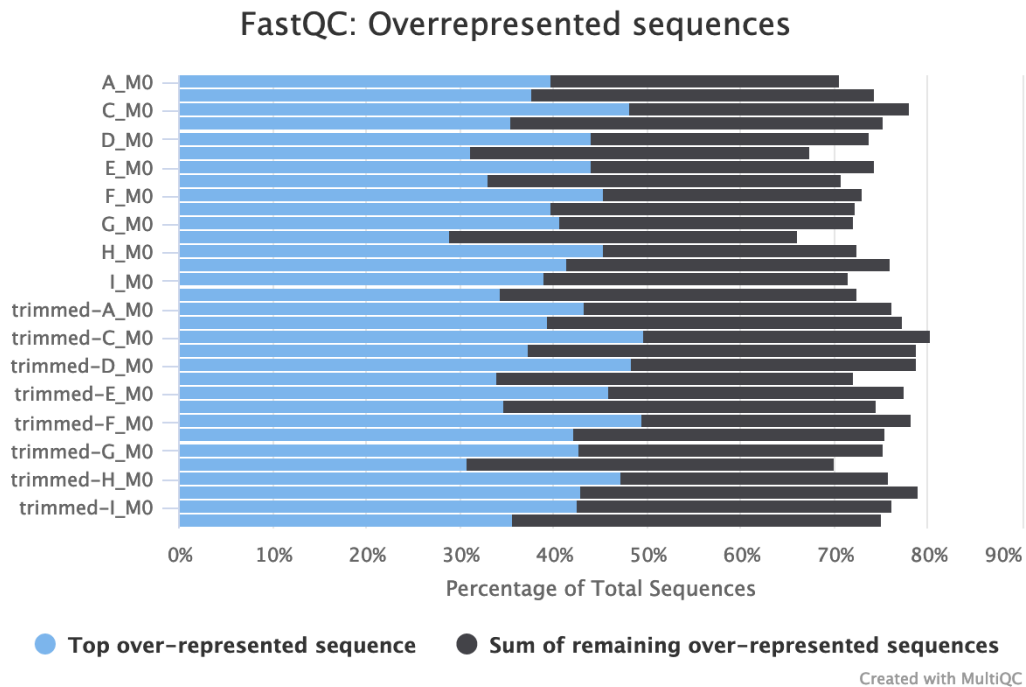
Name	Start Time [s]	End Time [s]	Area	% of total Area
18S	40.19	42.79	14.5	23.1
28S	46.87	50.31	22.0	35.1

A3.1.2. Agilent 2100 bioanalyser: RNA quality assessment

RNA quality assessment of a representative sample sent for small non-coding RNA sequencing experiment: the plot, generated by Agilent 2100 bioanalyser, shows two distinct peaks corresponding to the S18 and S28 ribosomal subunits. The small peak between 20s and 25s represents the marker. The RNA Integrity Number (RIN) is 9.5 and indicates that the sample is intact (RIN is a number between 1 and 10, 1 being the most degraded and 10 the most intact).

A3.2. miRNA-seq: overrepresented sequence

As mentioned in Chapter 4, before analysing the small RNA seq, we removed an overrepresented sequence, corresponding to miR-21. The plot below, generated during the quality check, shows the % of miR-21 sequence in samples before and after the trimming phase.



A3.2. MultiQC report: overrepresented sequences

MultiQC report plot showing overrepresented sequences in small RNA sequencing experiment. Blue bars represent miR-21, which was removed from the analysis.

A3.3. List of differentially expressed small RNAs

The tables below list small RNAs differentially expressed between M0 and M1 macrophages, including miRNAs, sorted according the adjusted p values (>0.05).

BaseMean is the average of the normalised count values; log2FoldChange represents the effect size estimate: how much the expression of a gene changed due to the treatment (M0 vs M1); lfcSE is the standard error estimate for the log2FoldChange; stat represents the wald statistics; pvalue is attained by the wald test; padj is the pvalue corrected for multiple testing using the Benjamini and Hochberg method.

A3.3.1. List of small RNAs upregulated in M1 macrophages

RNACentral ID	baseMean	log2FoldChange	lfcSE	stat	pvalue	padj
URS0000287398	87.07	1.01	0.26	3.81	1.42E-04	2.05E-03
URS00005E1F00	137.17	1.01	0.24	4.12	3.74E-05	7.05E-04
URS00000C18F2	477.18	1.01	0.24	4.28	1.91E-05	4.09E-04
URS0000386F92	423.37	1.01	0.22	4.51	6.54E-06	1.75E-04
URS0000EC0861	25.55	1.01	0.31	3.21	1.35E-03	1.32E-02
URS0000682FB0	717.09	1.01	0.23	4.42	9.81E-06	2.37E-04
URS00006C8EDF	97.24	1.01	0.25	3.97	7.31E-05	1.22E-03
URS0000624312	1048.65	1.01	0.21	4.77	1.88E-06	5.96E-05
URS00006FCBA3	47.56	1.01	0.32	3.21	1.34E-03	1.32E-02
URS00002D40C8	486.68	1.01	0.24	4.18	2.88E-05	5.75E-04
URS00006CF521	86.93	1.02	0.29	3.50	4.62E-04	5.54E-03
URS0000A8472C	1036.60	1.02	0.21	4.76	1.96E-06	6.15E-05
URS0000EC0779	10.35	1.02	0.36	2.83	4.72E-03	3.49E-02
URS000043D1A9	93.87	1.03	0.27	3.84	1.23E-04	1.82E-03
URS00005A0236	26.99	1.04	0.31	3.34	8.45E-04	9.35E-03
URS000067843B	318.62	1.04	0.23	4.46	8.26E-06	2.08E-04
URS000072BBEB	72.89	1.04	0.34	3.03	2.46E-03	2.11E-02
URS0000728B3E	25.49	1.04	0.36	2.88	3.99E-03	3.05E-02
URS00001672F3	103.12	1.05	0.20	5.17	2.39E-07	1.04E-05
URS0000635FFC	43.61	1.05	0.37	2.88	3.99E-03	3.05E-02
URS0000640661	711.17	1.05	0.23	4.61	3.98E-06	1.17E-04
URS0000EA616E	22.62	1.05	0.28	3.74	1.84E-04	2.53E-03
URS00006C2A6C	660.71	1.06	0.23	4.57	4.78E-06	1.33E-04
URS00006F59B4	45.68	1.06	0.23	4.68	2.86E-06	8.52E-05
URS000072540A	468.42	1.06	0.22	4.93	8.27E-07	3.18E-05
URS0000D588F3	23.51	1.06	0.39	2.70	6.90E-03	4.66E-02
URS00006744D5	454.29	1.06	0.24	4.33	1.51E-05	3.41E-04
URS00002154C2	240.85	1.06	0.24	4.33	1.50E-05	3.41E-04
URS00000FC8EB	1694.09	1.06	0.22	4.84	1.32E-06	4.60E-05

URS000015A6F8	483.64	1.06	0.25	4.18	2.97E-05	5.89E-04
URS0000521091	497.31	1.07	0.23	4.57	4.77E-06	1.33E-04
URS0000685E74	43.95	1.07	0.27	4.01	6.08E-05	1.06E-03
URS000064074C	84.35	1.08	0.33	3.27	1.08E-03	1.14E-02
URS0000739B5B	81.70	1.08	0.32	3.38	7.29E-04	8.22E-03
URS000020CB8F	473.69	1.08	0.25	4.35	1.33E-05	3.11E-04
URS00006100A0	30.79	1.08	0.33	3.23	1.23E-03	1.23E-02
URS000069A1F2	26.78	1.09	0.30	3.66	2.52E-04	3.32E-03
URS00001AD596	762.43	1.09	0.37	2.94	3.32E-03	2.63E-02
URS000062AA63	30.47	1.10	0.38	2.86	4.25E-03	3.21E-02
URS0000EC1AE8	21.81	1.11	0.39	2.88	3.93E-03	3.02E-02
URS0000659544	397.57	1.11	0.29	3.79	1.53E-04	2.18E-03
URS0000AA94DC	8.77	1.12	0.38	2.94	3.27E-03	2.59E-02
URS0000E82BA2	586.88	1.12	0.29	3.84	1.21E-04	1.80E-03
URS00006F4537	48.47	1.13	0.23	4.83	1.40E-06	4.64E-05
URS000061B694	12821.77	1.13	0.19	5.86	4.72E-09	3.13E-07
URS00006E7A67	36.36	1.13	0.27	4.16	3.24E-05	6.34E-04
URS00002F039B	123.40	1.13	0.41	2.78	5.44E-03	3.88E-02
URS0000311FB0	78.60	1.14	0.23	4.92	8.60E-07	3.26E-05
URS000029EF95	559.55	1.14	0.27	4.21	2.53E-05	5.10E-04
URS00000A8253	123.43	1.14	0.42	2.69	7.12E-03	4.77E-02
URS00006F58F8	27.10	1.14	0.37	3.10	1.94E-03	1.74E-02
URS000022B8AA	557.92	1.14	0.25	4.48	7.35E-06	1.88E-04
URS000065EBC0	32.18	1.14	0.36	3.17	1.50E-03	1.43E-02
URS0000D5EDDD	13.50	1.15	0.35	3.26	1.13E-03	1.17E-02
URS00008B5862	34.04	1.15	0.38	3.03	2.46E-03	2.11E-02
URS00006174C2	167.42	1.15	0.35	3.33	8.70E-04	9.54E-03
URS00004F5239	90.36	1.16	0.30	3.79	1.50E-04	2.15E-03
URS00004A2461	588.86	1.17	0.27	4.29	1.80E-05	3.89E-04
URS0000D5C559	988.23	1.17	0.26	4.54	5.69E-06	1.55E-04
URS000005A7A9	21.94	1.18	0.33	3.62	2.99E-04	3.87E-03
URS00005F7694	770.70	1.18	0.37	3.15	1.62E-03	1.52E-02
URS000045533A	125.06	1.18	0.43	2.74	6.15E-03	4.26E-02
URS000044BAE3	842.59	1.18	0.31	3.78	1.59E-04	2.23E-03
URS0000EA7AA7	248.63	1.18	0.23	5.07	3.89E-07	1.64E-05
URS00000FB60D	171.46	1.18	0.25	4.70	2.56E-06	7.70E-05
URS00004DC6D6	874.55	1.19	0.31	3.87	1.10E-04	1.66E-03
URS0000EBEE05	903.19	1.19	0.33	3.61	3.10E-04	3.98E-03
URS00002F2AEC	896.33	1.19	0.31	3.87	1.09E-04	1.66E-03
URS000006E1E3	906.31	1.20	0.33	3.69	2.28E-04	3.08E-03
URS0000527A9F	238.06	1.21	0.27	4.49	7.24E-06	1.87E-04
URS00006D74B2	106.96	1.21	0.38	3.18	1.49E-03	1.43E-02
URS0000815951	119.39	1.21	0.42	2.86	4.26E-03	3.22E-02

URS00003177B8	125.08	1.22	0.40	3.08	2.04E-03	1.81E-02
URS0000DC002B	118.26	1.22	0.45	2.74	6.09E-03	4.24E-02
URS00006C58BC	472.72	1.23	0.34	3.64	2.70E-04	3.52E-03
URS00003E8921	120.23	1.23	0.46	2.70	7.02E-03	4.71E-02
URS000069B369	963.37	1.25	0.29	4.32	1.57E-05	3.48E-04
URS00000A7517	113.71	1.25	0.45	2.75	5.98E-03	4.20E-02
URS000001A289	451.63	1.25	0.32	3.91	9.09E-05	1.45E-03
URS000065BD15	408.85	1.25	0.21	5.89	3.94E-09	2.76E-07
URS00004F76B3	30.79	1.25	0.46	2.74	6.16E-03	4.26E-02
URS0000AEC348	119.35	1.26	0.44	2.86	4.20E-03	3.18E-02
URS000064FAB6	12.52	1.26	0.37	3.40	6.74E-04	7.71E-03
URS000029D0D3	113.47	1.26	0.43	2.95	3.21E-03	2.57E-02
URS0000E53B55	119.19	1.27	0.45	2.79	5.32E-03	3.84E-02
URS00004B70B9	114.28	1.27	0.44	2.87	4.04E-03	3.08E-02
URS000062C4DE	124.52	1.27	0.28	4.57	4.80E-06	1.33E-04
URS00001C308D	1258.45	1.28	0.29	4.34	1.44E-05	3.30E-04
URS00006B2647	21.86	1.28	0.38	3.38	7.27E-04	8.22E-03
URS00005C3DDD	119.56	1.29	0.42	3.09	1.98E-03	1.77E-02
URS00003ECA54	106.19	1.29	0.38	3.40	6.64E-04	7.63E-03
URS00006C8412	10.30	1.29	0.40	3.25	1.17E-03	1.21E-02
URS00006C721A	36.46	1.30	0.36	3.59	3.29E-04	4.15E-03
URS00006C06E6	33.15	1.30	0.40	3.24	1.19E-03	1.21E-02
URS00006914B1	7.58	1.31	0.48	2.71	6.80E-03	4.61E-02
URS0000DC92B6	121.89	1.32	0.44	2.96	3.07E-03	2.49E-02
URS00006A9AE8	128.39	1.33	0.28	4.73	2.22E-06	6.89E-05
URS000064A807	20.27	1.33	0.48	2.81	4.99E-03	3.64E-02
URS0000EBF1EC	998.21	1.34	0.21	6.26	3.95E-10	2.95E-08
URS000066C003	478.34	1.34	0.23	5.73	1.02E-08	6.21E-07
URS0000677B31	16.23	1.34	0.33	4.02	5.90E-05	1.04E-03
URS0000190FE5	275.18	1.35	0.26	5.24	1.59E-07	7.62E-06
URS000074CBFD	760.51	1.36	0.21	6.41	1.48E-10	1.17E-08
URS00006D1B55	32.18	1.36	0.40	3.38	7.37E-04	8.27E-03
URS000040DCFF	1826.38	1.36	0.17	8.09	6.10E-16	1.11E-13
URS000068668E	21.52	1.36	0.36	3.83	1.29E-04	1.90E-03
URS000042F13F	169.74	1.37	0.24	5.69	1.28E-08	7.61E-07
URS0000B01320	114.06	1.38	0.44	3.13	1.72E-03	1.59E-02
URS00000AA464	22.03	1.39	0.40	3.50	4.59E-04	5.53E-03
URS00003361F9	21.05	1.39	0.52	2.69	7.14E-03	4.77E-02
URS000063FB43	2232.93	1.40	0.52	2.71	6.68E-03	4.57E-02
URS00005EA0AD	137.27	1.41	0.29	4.83	1.36E-06	4.61E-05
URS00001123BD	24.72	1.41	0.33	4.24	2.20E-05	4.59E-04
URS0000147B41	24.96	1.42	0.30	4.72	2.39E-06	7.26E-05
URS0000AC252C	107.78	1.43	0.45	3.14	1.67E-03	1.55E-02

URS0000591950	298.69	1.44	0.21	6.80	1.07E-11	1.08E-09
URS00003496BE	71.05	1.44	0.25	5.82	5.88E-09	3.81E-07
URS00006E357A	31.67	1.45	0.36	4.05	5.18E-05	9.40E-04
URS0000A9690B	8.42	1.46	0.46	3.17	1.51E-03	1.43E-02
URS0000158189	7.96	1.46	0.49	2.99	2.78E-03	2.32E-02
URS00007362AD	32.78	1.46	0.32	4.55	5.36E-06	1.48E-04
URS00007063CB	7.55	1.46	0.49	2.98	2.86E-03	2.35E-02
URS00006A9C77	15.10	1.47	0.35	4.23	2.29E-05	4.67E-04
URS0000244A71	5.05	1.47	0.55	2.67	7.57E-03	4.97E-02
URS0000757938	33.15	1.47	0.38	3.83	1.31E-04	1.91E-03
URS00004B1671	1602.06	1.48	0.31	4.83	1.34E-06	4.61E-05
URS0000E13005	60.86	1.49	0.51	2.93	3.39E-03	2.66E-02
URS00006B6C08	5.28	1.51	0.52	2.91	3.61E-03	2.80E-02
URS00006CFACA	32.52	1.51	0.46	3.27	1.07E-03	1.13E-02
URS000013899F	122.72	1.53	0.30	5.05	4.36E-07	1.77E-05
URS0000758A62	26.41	1.55	0.40	3.90	9.43E-05	1.48E-03
URS0000648E1F	27.93	1.56	0.38	4.08	4.54E-05	8.28E-04
URS0000DEECO	16.29	1.58	0.52	3.02	2.54E-03	2.15E-02
URS000068FD04	697.14	1.60	0.28	5.63	1.79E-08	1.02E-06
URS00004208C5	1644.39	1.60	0.18	8.89	5.88E-19	1.77E-16
URS000038D768	14.98	1.60	0.41	3.90	9.81E-05	1.51E-03
URS000073124E	82.23	1.61	0.29	5.63	1.82E-08	1.02E-06
URS0000697465	79.61	1.61	0.28	5.78	7.31E-09	4.64E-07
URS000069E2A5	4.75	1.62	0.60	2.69	7.17E-03	4.78E-02
URS000047C79B	15.64	1.62	0.34	4.81	1.53E-06	4.97E-05
URS000068C733	7.54	1.63	0.51	3.17	1.51E-03	1.43E-02
URS000071ED2F	32.58	1.65	0.44	3.75	1.74E-04	2.42E-03
URS00004F0321	6947.27	1.67	0.39	4.24	2.19E-05	4.59E-04
URS00005402A5	14.84	1.67	0.63	2.67	7.54E-03	4.95E-02
URS000011CFE8	5919.12	1.67	0.45	3.70	2.18E-04	2.97E-03
URS0000635088	6939.36	1.69	0.39	4.31	1.66E-05	3.61E-04
URS0000593537	178.13	1.70	0.26	6.48	9.34E-11	7.58E-09
URS0000282AB2	17.19	1.70	0.40	4.24	2.27E-05	4.67E-04
URS00001B460B	13.16	1.72	0.43	3.99	6.67E-05	1.14E-03
URS000037F5E2	14.04	1.73	0.38	4.51	6.39E-06	1.73E-04
URS0000D6E1B0	13.80	1.74	0.47	3.71	2.11E-04	2.87E-03
URS00007F742E	17.76	1.76	0.65	2.70	6.89E-03	4.66E-02
URS00007EC19C	15.95	1.77	0.66	2.69	7.23E-03	4.81E-02
URS000057E781	11.63	1.78	0.63	2.83	4.69E-03	3.47E-02
URS0000DE23D7	20.05	1.81	0.67	2.70	6.91E-03	4.66E-02
URS0000381B86	5.17	1.82	0.60	3.05	2.32E-03	2.02E-02
URS000038C474	12.65	1.85	0.45	4.14	3.41E-05	6.60E-04
URS0000804A0D	17.53	1.86	0.69	2.71	6.76E-03	4.60E-02

URS000031B6ED	8.28	1.87	0.45	4.13	3.58E-05	6.78E-04
URS0000807EA6	15.59	1.89	0.61	3.10	1.93E-03	1.74E-02
URS00004AC6E6	12.04	1.92	0.64	3.02	2.56E-03	2.16E-02
URS00004AA2FO	16.02	1.92	0.66	2.91	3.61E-03	2.80E-02
URS00003130BD	257.42	1.93	0.42	4.60	4.25E-06	1.23E-04
URS0000DDA3BB	18.37	1.93	0.64	3.01	2.64E-03	2.21E-02
URS000042B8BF	8.61	1.94	0.48	4.03	5.55E-05	9.88E-04
URS0000DC3018	15.45	1.97	0.72	2.75	5.90E-03	4.15E-02
URS00007E8E68	16.95	2.01	0.65	3.10	1.91E-03	1.73E-02
URS00006D3DD2	13.22	2.03	0.45	4.50	6.89E-06	1.83E-04
URS000034E9D0_63221	17.02	2.08	0.65	3.19	1.42E-03	1.38E-02
URS0000DE2957	15.57	2.09	0.65	3.23	1.26E-03	1.25E-02
URS000075BEBE	35.93	2.09	0.37	5.64	1.75E-08	1.02E-06
URS0000E339B7	232.38	2.09	0.41	5.11	3.31E-07	1.42E-05
URS000048FEBE	16.21	2.16	0.58	3.75	1.80E-04	2.48E-03
URS00001F5B39	15.61	2.16	0.42	5.18	2.17E-07	9.59E-06
URS00008EE2B1	9.42	2.20	0.68	3.24	1.21E-03	1.22E-02
URS000070BF11	7.11	2.27	0.56	4.03	5.51E-05	9.88E-04
URS00001F0C23	55.30	2.32	0.35	6.70	2.05E-11	1.93E-09
URS00006E19EA	397.35	2.33	0.30	7.85	4.14E-15	6.72E-13
URS0000424278	300.29	2.37	0.32	7.37	1.69E-13	2.15E-11
URS000023FB43	6.16	2.45	0.72	3.42	6.19E-04	7.17E-03
URS0000338542	35900.61	2.52	0.22	11.34	8.78E-30	8.54E-27
URS000019676E	23.14	2.83	0.42	6.72	1.88E-11	1.83E-09
URS0000D54CAD	211862.08	2.83	0.23	12.05	1.89E-33	2.76E-30
URS00002198F3	16.15	2.95	0.45	6.58	4.59E-11	3.83E-09
URS0000199B53	6.45	2.95	0.90	3.27	1.08E-03	1.14E-02
URS00006E0DAF	5.89	3.11	0.68	4.60	4.20E-06	1.23E-04
URS0000688DD3	32.64	3.13	0.43	7.29	3.17E-13	3.70E-11
URS0000CFBCCA	6.30	3.16	0.64	4.93	8.17E-07	3.18E-05
URS00006BACE4	33.42	3.24	0.36	8.92	4.66E-19	1.70E-16
URS000034309A	8.34	3.31	0.87	3.79	1.54E-04	2.18E-03
URS00003D4175	66.96	3.59	0.44	8.17	3.01E-16	5.87E-14
URS0000054224	69.14	3.77	0.45	8.30	1.06E-16	2.21E-14
URS0000EBB7A5	4.98	3.90	0.95	4.10	4.20E-05	7.81E-04
URS000001C659	7.14	4.50	0.93	4.83	1.40E-06	4.64E-05
URS00002DABEA	13.47	4.97	0.74	6.67	2.56E-11	2.27E-09
URS0000410073	11.84	6.73	0.86	7.82	5.47E-15	8.40E-13

A3.3.2. List of small RNAs downregulated in M1 macrophages

RNACentral ID	baseMean	log2FoldChange	lfcSE	stat	pvalue	padj
URS00002B2B5C	15.60	-4.75	0.61	-7.85	4.02E-15	6.72E-13
URS000002103A	11.92	-4.60	0.63	-7.33	2.22E-13	2.70E-11
URS00000DA3DF	8.82	-4.13	0.79	-5.24	1.65E-07	7.75E-06
URS000056B04E	240.87	-3.61	0.30	12.13	7.05E-34	2.06E-30
URS00006E0B8F	14.77	-3.30	0.55	-5.95	2.64E-09	1.93E-07
URS00004FCB5F	6.12	-3.24	0.72	-4.48	7.60E-06	1.93E-04
URS00001C770D	15.83	-3.04	0.41	-7.47	8.12E-14	1.08E-11
URS000075E96D	35.02	-2.97	0.39	-7.62	2.60E-14	3.62E-12
URS00006E020B	15.90	-2.86	0.45	-6.36	2.00E-10	1.54E-08
URS000007ACA1	6.30	-2.71	0.69	-3.91	9.36E-05	1.48E-03
URS000064426B	5.29	-2.62	0.62	-4.24	2.27E-05	4.67E-04
URS0000237FB8	64.70	-2.52	0.28	-9.01	2.06E-19	8.58E-17
URS00008B5FCF	5.79	-2.40	0.76	-3.15	1.61E-03	1.51E-02
URS000003ABC4	22.32	-2.37	0.55	-4.32	1.56E-05	3.47E-04
URS0000E9F36E	6.20	-2.32	0.62	-3.78	1.60E-04	2.23E-03
URS00006F9520	5.46	-2.25	0.65	-3.44	5.79E-04	6.82E-03
URS000005D4F5	407.73	-2.21	0.24	-9.16	5.00E-20	2.43E-17
URS00001597DC	11.68	-2.18	0.39	-5.57	2.56E-08	1.41E-06
URS000067E5FF	5.14	-2.17	0.64	-3.38	7.23E-04	8.21E-03
URS0000CB6503	11.29	-2.16	0.51	-4.25	2.16E-05	4.58E-04
URS00006C0B51	371.11	-2.13	0.23	-9.24	2.44E-20	1.43E-17
URS0000CA62EF	12.80	-2.00	0.38	-5.32	1.07E-07	5.27E-06
URS000075AEBC	5.52	-1.99	0.60	-3.32	9.02E-04	9.76E-03
URS0000564C39	76.06	-1.93	0.20	-9.55	1.33E-21	9.70E-19
URS00002CBC6D	280.84	-1.87	0.21	-8.72	2.78E-18	7.38E-16
URS00006E4867	9.68	-1.85	0.63	-2.95	3.19E-03	2.57E-02
URS00003FFA6C	20.68	-1.84	0.33	-5.51	3.51E-08	1.90E-06
URS0000045DBD	163.60	-1.80	0.20	-8.89	6.07E-19	1.77E-16
URS0000D55DFB	14.74	-1.73	0.52	-3.33	8.53E-04	9.40E-03
URS000075C34D	288.28	-1.71	0.29	-5.89	3.97E-09	2.76E-07
URS00004E57E7	65.82	-1.66	0.23	-7.11	1.16E-12	1.28E-10
URS0000BB15D5	18.11	-1.66	0.39	-4.25	2.12E-05	4.52E-04
URS0000241987	172.07	-1.65	0.29	-5.76	8.52E-09	5.29E-07
URS00006DF24F	39564.84	-1.64	0.25	-6.67	2.57E-11	2.27E-09
URS0000080D0A	809.22	-1.63	0.20	-8.32	8.94E-17	2.01E-14
URS00002F8148	9.54	-1.62	0.45	-3.58	3.43E-04	4.29E-03
URS0000384021	23.54	-1.60	0.29	-5.45	5.04E-08	2.67E-06
URS00005092C2	8.62	-1.59	0.41	-3.86	1.12E-04	1.69E-03
URS00001012BC	58.79	-1.56	0.22	-7.11	1.19E-12	1.28E-10
URS0000EA6322	11.91	-1.56	0.43	-3.64	2.75E-04	3.57E-03

URS0000065D58	18.51	-1.52	0.42	-3.60	3.18E-04	4.05E-03
URS000006CE6B7	10.59	-1.50	0.42	-3.55	3.88E-04	4.78E-03
URS0000052AB63	14.50	-1.49	0.38	-3.90	9.82E-05	1.51E-03
URS00000EBB075	6.86	-1.47	0.50	-2.93	3.35E-03	2.64E-02
URS0000075C652	7.78	-1.46	0.49	-2.99	2.79E-03	2.32E-02
URS000006AFF4E	8.22	-1.43	0.46	-3.10	1.96E-03	1.76E-02
URS000008230A	7.19	-1.40	0.51	-2.75	6.05E-03	4.22E-02
URS0000015D23B	22.22	-1.39	0.31	-4.50	6.96E-06	1.83E-04
URS000004B2A47	49.73	-1.37	0.29	-4.81	1.51E-06	4.96E-05
URS00000079D48	196.05	-1.36	0.28	-4.90	9.73E-07	3.55E-05
URS0000066288D	8.32	-1.36	0.43	-3.14	1.67E-03	1.55E-02
URS00000662807	466.45	-1.33	0.15	-8.64	5.50E-18	1.34E-15
URS000000BD1DE	24.48	-1.30	0.36	-3.66	2.54E-04	3.33E-03
URS000001C85C7	12.23	-1.29	0.42	-3.04	2.34E-03	2.02E-02
URS000004C9052	100.63	-1.26	0.28	-4.45	8.43E-06	2.09E-04
URS0000023BE29	154.63	-1.26	0.30	-4.14	3.41E-05	6.60E-04
URS0000044EF2B	29.80	-1.25	0.42	-2.96	3.05E-03	2.48E-02
URS00000424D74	25.17	-1.24	0.25	-4.89	1.01E-06	3.65E-05
URS0000060AABB	428.54	-1.22	0.16	-7.63	2.36E-14	3.45E-12
URS000000CF1D2	827.74	-1.22	0.18	-6.63	3.38E-11	2.90E-09
URS00000EABDD4	23.02	-1.21	0.30	-4.03	5.59E-05	9.88E-04
URS0000062982B	12.85	-1.18	0.42	-2.83	4.63E-03	3.44E-02
URS00000383E7F	9.07	-1.18	0.44	-2.68	7.44E-03	4.91E-02
URS000003E16E5	140.82	-1.15	0.23	-5.07	4.08E-07	1.68E-05
URS00000246356	23.42	-1.14	0.34	-3.32	8.91E-04	9.70E-03
URS00000554A4F	33.16	-1.09	0.28	-3.93	8.49E-05	1.38E-03
URS000002CDFCA	32.60	-1.08	0.30	-3.59	3.34E-04	4.21E-03
URS0000023133F	31.81	-1.08	0.34	-3.16	1.58E-03	1.49E-02
URS0000003F252	1081.27	-1.07	0.20	-5.35	8.95E-08	4.58E-06
URS0000071E3CB	24.12	-1.06	0.33	-3.24	1.20E-03	1.22E-02
URS000000451A1	131428.28	-1.05	0.21	-5.07	3.93E-07	1.64E-05
URS00000679788	220.26	-1.04	0.24	-4.31	1.63E-05	3.58E-04
URS00000156390	43.49	-1.04	0.35	-2.99	2.80E-03	2.32E-02
URS00000629ECF	14.16	-1.03	0.37	-2.74	6.18E-03	4.27E-02
URS00000259CF4	116.17	-1.02	0.21	-4.90	9.60E-07	3.55E-05
URS0000050E4BA	1798.91	-1.00	0.19	-5.22	1.81E-07	8.37E-06
URS00000644074	2342.84	-1.00	0.19	-5.35	8.87E-08	4.58E-06

A3.4. List of differentially expressed genes

The tables below list the genes differentially expressed in response to miRNAs overexpression, sorted according to the adjusted p values (>0.05).

LogFC represents the log₂ fold change, AveExpr is the average expression over all samples (CPM values); stat represents the wald statistics; pvalue is attained by the wald test; padj is the pvalue corrected for multiple testing using the Benjamini and Hochberg method.

A3.4.1. List of genes significantly downregulated in miR-155-5p overexpressing macrophages

Gene	logFC	AveExpr	stat	P.Value	adj.P.Val
SLC1A3	-1.02	8.12	-11.97	1.47E-10	4.62E-07
ARHGAP18	-1.14	6.22	-10.84	8.33E-10	9.56E-07
CSF1R	-1.20	7.47	-10.61	1.19E-09	1.19E-06
MOCS2	-1.34	4.19	-10.50	1.44E-09	1.27E-06
MPEG1	-2.30	6.53	-10.48	1.47E-09	1.27E-06
MARCHF1	-1.62	6.33	-9.63	6.07E-09	3.35E-06
PICALM	-1.13	8.00	-9.16	1.39E-08	5.73E-06
ANXA2	-0.81	11.04	-9.01	1.83E-08	6.60E-06
PTPN22	-1.64	4.00	-8.71	3.15E-08	9.17E-06
SPRED1	-1.65	4.28	-8.71	3.11E-08	9.17E-06
GATM	-1.51	4.00	-8.19	8.32E-08	1.75E-05
TBC1D14	-1.19	5.54	-8.00	1.20E-07	2.22E-05
MARVELD1	-1.32	3.46	-7.97	1.26E-07	2.27E-05
NRP1	-1.12	7.36	-7.90	1.44E-07	2.48E-05
CSE1L	-0.65	5.42	-7.90	1.45E-07	2.48E-05
NME4	-0.95	3.70	-7.83	1.66E-07	2.68E-05
IKBIP	-1.23	3.72	-7.79	1.78E-07	2.76E-05
ABHD6	-1.31	4.13	-7.68	2.22E-07	2.98E-05
MRPS27	-0.75	4.73	-7.64	2.42E-07	3.13E-05
MEX3B	-1.29	1.98	-7.58	2.69E-07	3.38E-05
TM6SF1	-1.32	5.12	-7.46	3.43E-07	3.93E-05
TGFBR1	-1.30	5.53	-7.36	4.17E-07	4.54E-05
OPRL1	-1.79	0.28	-7.24	5.36E-07	5.31E-05
FMNL2	-0.46	7.31	-6.97	9.21E-07	7.88E-05
S1PR3	-2.86	-2.86	-6.95	9.68E-07	8.14E-05
POLE3	-0.63	5.17	-6.90	1.08E-06	8.87E-05
SLC25A43	-0.70	4.58	-6.84	1.22E-06	9.39E-05
RCBTB2	-0.57	6.46	-6.78	1.38E-06	1.03E-04
CD36	-1.08	9.03	-6.66	1.79E-06	1.26E-04
BACH1	-0.86	6.54	-6.59	2.05E-06	1.36E-04
FGD5	-2.51	2.00	-6.54	2.30E-06	1.48E-04
AGTRAP	-0.71	6.09	-6.35	3.43E-06	1.93E-04

RAB6A	-0.35	6.98	-6.29	3.92E-06	2.11E-04
AP1B1	-0.49	7.30	-6.28	3.99E-06	2.13E-04
NBPF1	-0.83	5.37	-6.19	4.88E-06	2.44E-04
GPD1L	-1.28	2.67	-5.98	7.72E-06	3.31E-04
CDC25A	-2.83	-0.45	-5.93	8.46E-06	3.53E-04
UROS	-0.65	5.05	-5.94	8.46E-06	3.53E-04
FITM2	-0.97	1.99	-5.92	8.69E-06	3.58E-04
E2F2	-2.53	-1.26	-5.75	1.27E-05	4.70E-04
IL16	-1.82	3.25	-5.74	1.31E-05	4.80E-04
PFKFB2	-0.87	3.48	-5.73	1.33E-05	4.86E-04
RXRA	-0.74	6.21	-5.67	1.52E-05	5.37E-04
RGS18	-2.53	-0.16	-5.65	1.60E-05	5.56E-04
CIAO1	-0.53	6.12	-5.63	1.66E-05	5.72E-04
DUSP10	-0.56	5.23	-5.63	1.66E-05	5.72E-04
VWA8	-0.58	4.86	-5.62	1.70E-05	5.78E-04
TGFBR2	-0.84	6.01	-5.59	1.81E-05	6.05E-04
NDUFV3	-0.58	4.76	-5.57	1.91E-05	6.28E-04
LGI2	-3.03	-1.97	-5.54	2.04E-05	6.54E-04
CLINT1	-0.47	5.94	-5.51	2.17E-05	6.88E-04
PARVB	-0.75	5.99	-5.46	2.41E-05	7.40E-04
HMGCR	-0.92	5.67	-5.37	2.98E-05	8.57E-04
PCCA	-1.11	3.30	-5.37	2.99E-05	8.59E-04
MYO1D	-0.80	4.96	-5.36	3.05E-05	8.71E-04
BRI3BP	-0.87	4.38	-5.34	3.16E-05	8.95E-04
SORL1	-1.34	3.76	-5.34	3.20E-05	9.03E-04
DIS3L	-0.91	3.88	-5.34	3.22E-05	9.07E-04
INPP5A	-1.02	2.34	-5.30	3.46E-05	9.59E-04
PTDSS1	-0.34	6.63	-5.27	3.72E-05	1.01E-03
PRKDC	-1.01	6.51	-5.22	4.18E-05	1.09E-03
SPARC	-1.12	8.18	-5.20	4.42E-05	1.13E-03
HSPA5	-0.61	9.61	-5.19	4.46E-05	1.14E-03
SGK3	-0.71	6.76	-5.15	4.94E-05	1.23E-03
SGK3	-0.71	6.76	-5.15	4.94E-05	1.23E-03
ANKH	-1.17	3.96	-5.11	5.36E-05	1.30E-03
FXN	-0.98	2.36	-5.11	5.44E-05	1.32E-03
RNF166	-1.08	4.28	-5.10	5.47E-05	1.32E-03
RAB11FIP2	-0.62	4.19	-5.09	5.60E-05	1.34E-03
MXI1	-0.62	3.76	-5.04	6.25E-05	1.46E-03
RRM2	-2.21	1.69	-5.04	6.35E-05	1.47E-03
USP31	-0.68	3.16	-4.99	7.09E-05	1.58E-03
SFXN2	-1.84	1.13	-4.92	8.38E-05	1.78E-03
MRS2	-0.54	5.27	-4.90	8.71E-05	1.84E-03
SNX29	-0.58	5.18	-4.81	1.06E-04	2.10E-03
TP53INP1	-0.54	4.76	-4.78	1.14E-04	2.21E-03
MBNL3	-0.93	3.51	-4.75	1.23E-04	2.32E-03
HACD1	-1.12	0.95	-4.64	1.58E-04	2.80E-03

SLC26A11	-0.51	8.52	-4.63	1.64E-04	2.87E-03
LRP12	-0.77	5.14	-4.60	1.75E-04	3.02E-03
HLTF	-1.09	3.20	-4.59	1.77E-04	3.04E-03
EEPD1	-0.99	4.98	-4.57	1.88E-04	3.17E-03
CCT2	-0.35	6.55	-4.56	1.92E-04	3.22E-03
MMD	-1.09	3.38	-4.51	2.13E-04	3.48E-03
RBFA	-0.63	2.75	-4.48	2.30E-04	3.64E-03
FASTKD1	-0.56	4.84	-4.48	2.31E-04	3.65E-03
EEFSEC	-0.61	3.64	-4.47	2.35E-04	3.70E-03
OTULINL	-1.20	2.89	-4.36	3.06E-04	4.49E-03
SLC7A11	-0.88	7.33	-4.34	3.23E-04	4.68E-03
DOK2	-1.20	2.82	-4.33	3.26E-04	4.72E-03
TM7SF3	-0.53	5.89	-4.31	3.42E-04	4.90E-03
CYP7B1	-1.93	-2.26	-4.23	4.10E-04	5.67E-03
DENND2B	-1.55	1.89	-4.23	4.12E-04	5.70E-03
OXA1L	-0.39	6.66	-4.23	4.14E-04	5.72E-03
STRN3	-0.55	4.22	-4.23	4.15E-04	5.73E-03
NOLC1	-0.38	5.26	-4.22	4.23E-04	5.82E-03
RAB32	-0.65	4.78	-4.21	4.31E-04	5.89E-03
EPAS1	-0.69	7.17	-4.20	4.45E-04	6.01E-03
CMTM4	-0.88	2.81	-4.20	4.48E-04	6.04E-03
SYT1	-2.77	-1.98	-4.15	4.96E-04	6.53E-03
LIN7A	-3.05	-0.96	-4.15	5.02E-04	6.59E-03
CRHBP	-1.53	-1.27	-4.13	5.17E-04	6.72E-03
AMIGO1	-1.70	-0.05	-4.10	5.64E-04	7.17E-03
ACVR1	-0.39	4.81	-4.08	5.87E-04	7.39E-03
EBPL	-0.79	1.32	-4.06	6.19E-04	7.70E-03
ARFGAP3	-0.33	6.40	-4.05	6.23E-04	7.74E-03
MPI	-0.75	3.59	-4.05	6.31E-04	7.82E-03
TMED3	-0.56	6.39	-4.03	6.63E-04	8.09E-03
ELL2	-0.50	6.26	-3.98	7.44E-04	8.81E-03
HIF1A	-0.32	7.18	-3.96	7.68E-04	9.04E-03
TRIM32	-0.59	2.20	-3.94	8.05E-04	9.35E-03
ABHD2	-0.74	7.87	-3.86	9.80E-04	1.08E-02
ABAT	-0.82	2.52	-3.83	1.05E-03	1.13E-02
TMEM218	-0.53	3.96	-3.79	1.17E-03	1.23E-02
CD84	-0.67	9.68	-3.78	1.17E-03	1.23E-02
CHAF1A	-0.67	3.63	-3.77	1.21E-03	1.26E-02
GRHPR	-0.43	5.04	-3.74	1.29E-03	1.33E-02
RNF26	-0.34	4.42	-3.74	1.30E-03	1.33E-02
DTNA	-1.02	1.70	-3.66	1.55E-03	1.52E-02
PCLAF	-1.60	-0.42	-3.65	1.58E-03	1.55E-02
KDM5B	-0.52	4.98	-3.63	1.66E-03	1.60E-02
SLC2A9	-0.60	3.54	-3.63	1.67E-03	1.61E-02
CLCN4	-1.85	-1.36	-3.58	1.89E-03	1.78E-02
ANTXR1	-2.26	-2.39	-3.56	1.98E-03	1.84E-02

DUSP7	-0.86	4.56	-3.54	2.05E-03	1.89E-02
PSMG1	-0.46	3.84	-3.51	2.23E-03	2.01E-02
KCNJ1	-0.71	3.96	-3.46	2.49E-03	2.17E-02
KLHL32	-1.58	0.01	-3.42	2.70E-03	2.31E-02
MEGF6	-0.95	1.94	-3.39	2.90E-03	2.44E-02
GMNN	-0.62	2.85	-3.39	2.92E-03	2.45E-02
METR1	-0.65	2.24	-3.37	3.07E-03	2.54E-02
ZHX3	-1.12	3.40	-3.36	3.15E-03	2.59E-02
ATP5F1A	-0.45	8.59	-3.35	3.20E-03	2.62E-02
CTDSPL	-0.79	3.32	-3.32	3.46E-03	2.78E-02
TNIK	-0.39	6.21	-3.31	3.50E-03	2.81E-02
CDCA3	-1.45	-0.95	-3.31	3.53E-03	2.83E-02
GATB	-0.37	4.60	-3.29	3.64E-03	2.89E-02
TMEM236	-1.47	-0.75	-3.29	3.65E-03	2.90E-02
PPP5C	-0.28	5.17	-3.22	4.33E-03	3.30E-02
NME2	-0.40	7.37	-3.21	4.36E-03	3.31E-02
ITGAV	-0.52	6.69	-3.21	4.42E-03	3.34E-02
PLXDC2	-0.45	7.19	-3.20	4.52E-03	3.40E-02
RAPH1	-0.62	3.64	-3.17	4.87E-03	3.60E-02
NDUFAF6	-0.60	2.91	-3.14	5.20E-03	3.79E-02
RASSF8	-0.72	2.43	-3.13	5.28E-03	3.83E-02
VKORC1L1	-0.24	5.36	-3.12	5.40E-03	3.89E-02
TRIP13	-1.25	0.30	-3.10	5.60E-03	4.00E-02
OTUB2	-0.66	2.90	-3.10	5.66E-03	4.04E-02
GOLGA3	-0.42	6.13	-3.09	5.81E-03	4.11E-02
GFPT1	-0.47	5.76	-3.07	6.09E-03	4.27E-02
PLD1	-0.43	5.61	-3.05	6.32E-03	4.40E-02
DHFR	-0.64	3.04	-3.02	6.76E-03	4.63E-02
METAP1	-0.27	5.14	-3.00	7.02E-03	4.77E-02
MECR	-0.52	2.74	-3.00	7.04E-03	4.78E-02
LGALS1	-0.69	2.52	-2.99	7.18E-03	4.85E-02
PDHX	-0.24	4.90	-2.98	7.46E-03	4.99E-02
MMP8	-1.79	-2.61	-2.98	7.47E-03	4.99E-02
UBXN2B	-0.49	4.48	-2.98	7.47E-03	4.99E-02

A3.4.2. List of genes significantly downregulated in miR-125a-3p overexpressing macrophages

Gene	logFC	AveExpr	stat	P.Value	adj.P.Val
DTX4	-0.57	6.31	-5.51	2.20E-05	1.77E-02
DUSP1	-0.80	5.64	-5.39	2.84E-05	2.10E-02
INF2	-0.29	6.69	-5.05	6.23E-05	3.60E-02
EHD1	-0.81	5.84	-4.92	8.38E-05	3.99E-02

A3.4.3. List of genes significantly downregulated in miR-186-5p overexpressing macrophages

Gene	logFC	AveExpr	stat	P.Value	adj.P.Val
CRTAP	-0.73	6.05	-5.65	1.58E-05	1.59E-02

Appendix IV, Supplementary data for Chapter 5

This section contains supporting data for Chapter 5, miRNAs targeting TRIB1 non-coding variants and identification of two novel eQTLs.

A4.1. TRIB1 non-coding variants

TRIB1 non-coding variants affecting the 3'UTR were downloaded from <https://www.ncbi.nlm.nih.gov/snp>. Table A4.1.1. lists the ID of the 90 SNPs/INDELs analysed in Chapter 5. We selected the following parameters:

- annotations: nucleotide;
- functional class: 3'UTR;
- validation status: by frequency.

A4.1. List of TRIB1 non-coding variants

rs544226392	rs17405319	rs762994344	rs564442600	rs145010344	rs777776886
rs546022723	rs56395423	rs764331355	rs566209806	rs145449131	rs780519373
rs546479447	rs62521034	rs764779399	rs568362286	rs149107463	rs777112667
rs546842228	rs72647345	rs765360657	rs568453644	rs367637074	rs575452977
rs548263380	rs72647346	rs766250927	rs568845890	rs372324007	rs372022826
rs548386397	rs72647347	rs767431696	rs570838123	rs375565353	rs144434073
rs550925842	rs72647348	rs768403240	rs573109640	rs529150647	rs756175087
rs550939781	rs72647349	rs770137661	rs575121683	rs529289692	rs756397904
rs552692797	rs73704997	rs771645792	rs575198443	rs530681133	rs757344260
rs554138846	rs74486799	rs772580999	rs577356981	rs530790403	rs757466992
rs554972862	rs80023284	rs775715767	rs751789944	rs533208547	rs758576660
rs555208281	rs138055464	rs775724040	rs754065243	rs536284997	rs758819773
rs555485182	rs140611687	rs776325924	rs755860381	rs537301973	rs759347835
rs557685029	rs140952648	rs776449618	rs540547779	rs539767360	rs761444485
rs560408937	rs143673595	rs777539484	rs544175527	rs2235108	rs761488304

A4.2. SNPs analysis with miRanda algorithm: workflow and scripts

I. Input files pre-processing scripts

miRanda algorithm works with sequences printed in one line. Alignment of FASTA sequences (TRIB1 3'UTR, reference sequence) was performed using the following command:

```
awk '!/^>/ { printf "%s", $0; n = "\n" } /^>/ { print n $0; n = "" }END { printf "%s", n }'  
input_file.txt > output_file.txt
```

SNPs sequences were pre-processed using the Python scripts. These scripts require Biopython as extension (<http://biopython.org/wiki/Download>). Pre-processing was performed in order to generate sequences of the same length as the reference sequence. As mentioned in Chapter 5, SNPs were downloaded as short sequences containing IUPAC ambiguity codes. The first script uses the TRIB1 3'UTR reference sequence to complete the regions flanking the polymorphism; warning messages will alert the user that the flanking region (upstream or downstream or both) contains errors due to poor annotations. Those sequences have been generated manually.

```
import re  
from Bio.Seq import Seq  
import sys  
  
def IUPAC_SNP(fasta):  
    IUPAC_dic = {"M": "A/C", "R": "A/G", "W": "A/T", "S": "C/G", "Y": "C/T", "K": "G/T", "V": "A/C/G", "H": "A/C/T", "D": "A/G/T", "B": "C/G/T", "N": "G/A/T/C"}  
  
    old_header = fasta["header"]  
    field = fasta["header"].split('|')[8]  
    alleles = fasta["header"].split('|')[8].split(' ')[1].split('/')  
    for nt in fasta["sequence"]:  
        if nt not in ['A', 'C', 'G', 'T']:  
  
            new_allele = IUPAC_dic[nt]  
            new_header = fasta["header"]  
            new_header = re.sub(field, 'alleles="%s" % new_allele, new_header)  
            fasta["header"] = new_header  
  
    return fasta  
        #print old_header  
        #print new_header, exit()  
  
def new_fasta(header, sequence):  
    return {  
        'header': header.replace('\n', '').replace(' ', ''),  
        'sequence': sequence.replace('\n', '').replace(' ', '')  
    }  
  
def parse_header_line(line):  
    header = line  
    sequence = ''  
    return header, sequence  
  
with open(sys.argv[1], 'r') as f:  
    fastas = []  
    line = f.readline()  
    header, sequence = parse_header_line(line)  
    for line in f.readlines():  
        if line[0] == '>':  
            fastas.append(new_fasta(header, sequence))  
            header, sequence = parse_header_line(line)  
            continue  
  
        sequence += line  
  
    fastas.append(new_fasta(header, sequence))  
  
with open(sys.argv[2], "r") as f_ref:  
    fasta_ref = {}  
    for line in f_ref.readlines():  
        if line[0] == ">":  
            fasta_ref["header"] = line  
        else:  
            fasta_ref["sequence"] = line.replace('\n', '')  
  
    #print fasta_ref  
with open(sys.argv[3], "w") as f_out:
```

```

for fasta in fastas:
    #ref_seq = fasta_ref["sequence"]
    for indx, nucleotide in enumerate(fasta["sequence"]):
        if nucleotide not in ['A', 'C', 'G', 'T']:
            lock = False
            m = re.search(fasta["sequence"][0:indx], fasta_ref["sequence"])
            n = re.search(fasta["sequence"][(indx + 1):], fasta_ref["sequence"])
            #print fasta["sequence"][0:indx]
            if m == None and n == None:
                print "Warning! The SNP %s doesn't match with the reference FASTA " % fasta["header"].split('|')[2], "\n"
                ## Try to reverse
                print "SEQ BEFORE THE REVERSE", fasta["sequence"], "\n"
                fasta["sequence"] = str(Seq(fasta["sequence"]).reverse_complement())
                fasta = IUPAC_SNP(fasta)

            print "SEQ AFTER THE REVERSE", fasta["sequence"], "\n"
            for indx_reverse, nt_rv in enumerate(fasta["sequence"]):
                if nt_rv not in ['A', 'C', 'G', 'T']:
                    lock = False
                    m_inv = re.search(fasta["sequence"][0:indx_reverse], fasta_ref["sequence"])
                    n_inv = re.search(fasta["sequence"][(indx_reverse + 1):], fasta_ref["sequence"])

                    if m_inv == None and n_inv == None:
                        print "WARNING!! Doing the complementary doesn't change anything (REMOVED SNP %s) " % fasta["header"].split('|')[2]
                    if m_inv == None:
                        print "SNP: ", fasta["header"], "bind partially to the sequence WARNING"
                        print "Check the sequence: ", fasta["sequence"][0:indx_reverse]
                    if n_inv == None:
                        print "SNP: ", fasta["header"], "bind partially to the sequence WARNING"
                        print "Check the sequence: ", fasta["sequence"][(indx_reverse+1):]

                    else:
                        fasta["sequence"] = fasta_ref["sequence"][0: (m_inv.span()[0])] + fasta["sequence"] + fasta_ref["sequence"][(n_inv.span()[1]): ]

                        lock = True

            if m == None:
                print "SNP: ", fasta["header"], "bind partially to the sequence WARNING", "\n"
                print "Check the sequence: ", fasta["sequence"][0:indx]
                #fasta["sequence"] = fasta_ref["sequence"][0: (m.span()[0])] + fasta["sequence"] + fasta_ref["sequence"][(m.span()[1]+2): ]
            if n == None:
                print "SNP: ", fasta["header"], "bind partially to the sequence WARNING", "\n"
                print "Check the sequence: ", fasta["sequence"][(indx+1):]
                #fasta["sequence"] = fasta_ref["sequence"][0: (m.span()[0])] + fasta["sequence"] + fasta_ref["sequence"][(n.span()[1]+2): ]

            else:
                fasta["sequence"] = fasta_ref["sequence"][0: (m.span()[0])] + fasta["sequence"] + fasta_ref["sequence"][(n.span()[1]): ]

            lock = True

        if lock:
            print >> f_out, fasta["header"]
            print >> f_out, fasta["sequence"]

```

The second script adds a flag at the end of the header of each sequence (i.e. 'trib1_hsa'):

```

import sys

trib1_snp = open(sys.argv[1], "r")

lines_trib1= trib1_snp.readlines()
trib1_snp.close()

trib_snp = open(sys.argv[2], "w")

name= "|"+ (sys.argv[3])
#mutation_list = ["M", "W", "S", "Y", "R", "D", "K", "B", "V", "H", "N"]
for line in lines_trib1:
    #if line.startswith('>')
    if line[0] == ">":
        line_up = line.strip() + name + '\n'
        trib_snp.write(line_up)
    else:
        #print line.split()
        # for letter in line:
        #     if letter in mutation_list:

        trib_snp.write(line)
    #print line
trib_snp.close()

```

The third script reads the header of each sequence (the header contains information about the SNP/INDEL) and replaces the IUPAC letters with the correspondent nucleotides. The nucleotide inserted in the sequence is also added at the end of the header.

```

import sys

def new_fasta(header, sequence, alleles):
    return {
        'header': header.replace('\n', '').replace(' ', ''),
        'sequence': sequence.replace('\n', '').replace(' ', ''),
        'alleles': alleles
    }

def parse_header_line(line):
    header = line
    sequence = ''
    alleles = line.split('|')[8].split('')[1].split('/')
    return header, sequence, alleles

def replace_snps(in_file_path, out_file_path):
    fastas = []
    with open(in_file_path, 'r') as f:
        line = f.readline()
        header, sequence, alleles = parse_header_line(line)
        for line in f.readlines():
            if line[0] == '>':
                fastas.append(new_fasta(header, sequence, alleles))
                header, sequence, alleles = parse_header_line(line)
                continue

            sequence += line

        fastas.append(new_fasta(header, sequence, alleles))

    with open(out_file_path, 'w') as fout:
        for fasta in fastas:
            for nucleotide in fasta['sequence']:
                if nucleotide not in ['A', 'C', 'G', 'T']:
                    for allele in fasta['alleles']:
                        index = fasta['alleles'].index(allele)
                        #print fasta['header'] + "_%s" %(allele)
                        #print fasta['header']
                        #print fasta['sequence']
                        fout.write(fasta['header'] + "_%s" %(allele) + "\n")
                        fout.write(fasta['sequence'].replace(nucleotide, allele) + "\n")
                        # print >> fout, fasta['header']
                    # print >> fout, fasta['sequence'].replace(nucleotide, allele)
                    print >> fout

            #print fasta['header']
            #print fasta['sequence'].replace(nucleotide, allele)

replace_snps(sys.argv[1], sys.argv[2])

```

II. Output file post-processing script

After generating the input files, we run miRanda algorithm, following default settings. The output generated contains all the information about the target-prediction scan, but it does not have a specific format.

```

Read Sequence:hsa-miR-101-3p MIMAT0000099(21 nt)
Read Sequence:htrib1_utr (1948 nt)
-----
Performing Scan: hsa-miR-101-3p vs htrib1_utr
-----

Forward: Score: 151.000000 Q:2 to 18 R:1511 to 1533 Align Len (18) (77.78%) (77.78%)

Query: 3' aaguCA-AUAGUGU-CAUGACAu 5'
      || || | || |||||
Ref: 5' ccgtGTATACCTCACGTACTGTg 3'

Energy: -16.070000 kCal/Mol

```

For this reason, we post-processed the original output to organise the data in a table, using the script below.

```

import re
import sys

with open(sys.argv[1], 'r') as finput:
    start_analysis = re.compile("Performing Scan")

    bindings= []

    for line in finput.readlines():
        # bind = {"miRNA" : mirna,
        #         "mrna": mrna_name,
        #         "Seed_i": position1,
        #         "Seed_f": position2,
        #         "Score": score
        #        }
        if start_analysis.match(line):

            info =[]
            mirna_name = line.split()[2]
            mrna_name = line.split()[4]
            #bind["miRNA"] = mirna_name
            #bind["UTR"] = utr_name
            #print mirna_name
            #print line
            if "Forward:" in line.split():
                bind ={}
                sequence=[]
                position1 = line.split()[6][2:]
                position2= line.split()[8]
                score = line.split()[2]
                bind["miRNA"] = mirna_name
                bind["mRNA"] = mrna_name
                bind["Position_i"] = position1
                bind["Position_f"] = position2
                bind["Score"] = score

                #print "SCORE", score
                continue

                #info.append([position1,position2])

            if "Ref:" in line.split():
                #print "REF", line.split()
                sequence = line.split()[2]
                bind["Sequence"] = sequence
                #print sequence
                bindings.append(bind)
            if "Energy:" in line.split():
                energy = line.split()[1]
                bind ["Energy"] = energy
                bindings.append(bind)

with open("post_processing.txt", 'w') as fout:
    print >> fout, ("miRNA" + "\t" + "mRNA_name" + "\t" + "Seed_i" + "\t" + "Seed_f" + "\t" + "Sequence" + "\t" + "Score" + "\t" + "Energy")
    for hit in bindings:
        print >> fout, hit["miRNA"]+ "\t" + hit["mRNA"] + "\t" + hit["Position_i"] + "\t" + hit["Position_f"] + "\t" + hit["Sequence"] + "\t" + hit["Score"] + "\t" + hit["Energy"]

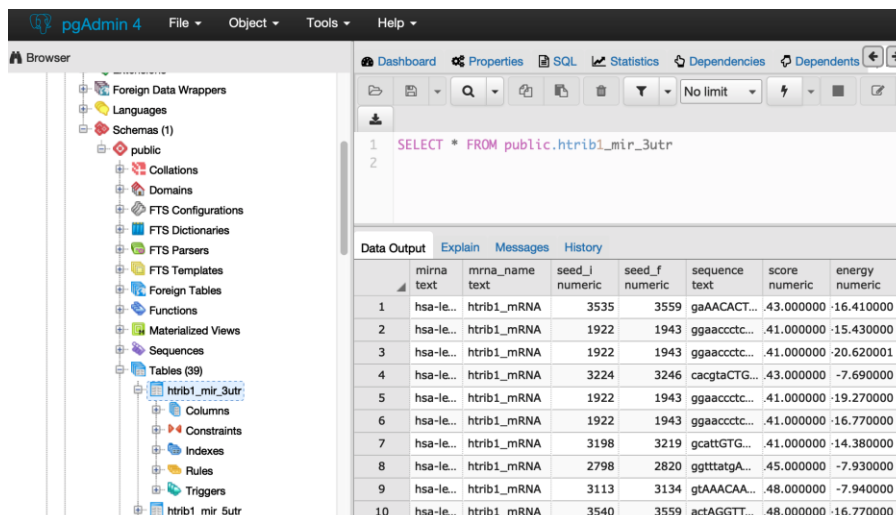
```

After applying the script, miRanda output looks like a table that can be exported in different formal, including .xlsx, .txt and .csv. It contains the miRNA name (column 1), the target region (column 2), the start and the end of the alignment (column 3, 4), the sequence aligned with the miRNA (column 5), the score (column 6) and the free energy value (column 7).

	A	B	C	D	E	F	G	H
5	hsa-let-7c-3p	htrib1_utr	1523	1545	cacgtaCTGTGTACTTTGTACAt	143	-7.09	
1	hsa-let-7c-5p	htrib1_utr	221	242	ggaaccctcACCAACTATCTCt	141	-19.27	
0	hsa-let-7c-5p	htrib1_utr	221	242	ggaaccctcACCAACTATCTCt	141	-19.27	
1	hsa-let-7d-5p	htrib1_utr	221	242	ggaaccctcACCAACTATCTCt	141	-16.77	
2	hsa-let-7d-5p	htrib1_utr	221	242	ggaaccctcACCAACTATCTCt	141	-16.77	
3	hsa-let-7e-3p	htrib1_utr	1497	1518	gcattGTGAGAATGCCGTGTAt	141	-14.38	
4	hsa-let-7e-3p	htrib1_utr	1497	1518	gcattGTGAGAATGCCGTGTAt	141	-14.38	
5	hsa-let-7f-2-3p	htrib1_utr	1412	1433	gtAAACAAAATATACTGTATt	148	-7.94	
6	hsa-let-7f-2-3p	htrib1_utr	1412	1433	gtAAACAAAATATACTGTATt	148	-7.94	
7	hsa-let-7f-2-3p	htrib1_utr	1097	1119	ggtttatgAATACGCTGTATAa	145	-7.93	
8	hsa-let-7f-2-3p	htrib1_utr	1097	1119	ggtttatgAATACGCTGTATAa	145	-7.93	
9	hsa-let-7g-3p	htrib1_utr	1839	1858	actAGGTTCT-TCCTGTACAt	148	-16.77	
0	hsa-let-7g-3p	htrib1_utr	1839	1858	actAGGTTCT-TCCTGTACAt	148	-16.77	
1	hsa-miR-101-3p	htrib1_utr	1511	1533	ccgtGTATACCTCAGTACTGTg	151	-16.07	
2	hsa-miR-101-3p	htrib1_utr	1511	1533	ccgtGTATACCTCAGTACTGTg	151	-16.07	
3	hsa-miR-103b	htrib1_utr	1454	1477	ggCAGTCATCTTA-AGGGCTATGc	165	-24.639999	
4	hsa-miR-103b	htrib1_utr	1454	1477	ggCAGTCATCTTA-AGGGCTATGc	165	-24.639999	
5	hsa-miR-106a-5p	htrib1_utr	1517	1540	atACCTCAGTACTGT--GTACTTTg	145	-20.34	
6	hsa-miR-106a-5p	htrib1_utr	1517	1540	atACCTCAGTACTGT--GTACTTTg	145	-20.34	
7	hsa-miR-106b-5p	htrib1_utr	1522	1540	tcacGACTGT--GTACTTTg	142	-17.74	
8	hsa-miR-106b-5p	htrib1_utr	1522	1540	tcacGACTGT--GTACTTTg	142	-17.74	
9	hsa-miR-10a-5p	htrib1_utr	373	398	gtaATAACCGTATTTTCACAGGGTg	147	-16.52	
0	hsa-miR-10a-5p	htrib1_utr	373	398	gtaATAACCGTATTTTCACAGGGTg	147	-16.52	
1	hsa-miR-10b-5p	htrib1_utr	379	398	acCGTATTT--TTC-ACAGGGTg	152	-17.040001	
2	hsa-miR-10b-5p	htrib1_utr	379	398	acCGTATTT--TTC-ACAGGGTg	152	-17.040001	

III. Output analysis: mySQL

Post-processed outputs from miRanda algorithm were imported as tables in mySQL and analysed by SELECT, INTERSECT, EXCEPT and UNION functions. These allow the users to select distinct interactions using desired parameters (score, energy etc..) and intersect data from different datasets (different tables), for example intersection of miRNAs targeting the reference allele and miRNAs targeting SNPs to find shared interactions. Below a screenshot of MySQL database containing miRanda post-processed output.



Appendix V, Supplementary data for Chapter 6

This section contains supporting data for Chapter 6, miRNAs targeting TRIB1 in Prostate Cancer.

A5.1. miRCancer database output

The output of miRCancer database can be accessed at this link <http://mircancer.ecu.edu/search.jsp?mirId=&logic=&condition=Or&cancerName=prostate+cancer&buttonSearch>. The tables below list the dysregulated miRNAs in PCa, based on published literature (downregulated miRNAs are shown in red, upregulated in green). Some miRNAs have been identified as either down- or upregulated in different studies. The number of distinct miRNAs is 168.

A5.1. miRCancer Output: dysregulated miRNAs in PCA

hsa-miR-3619-5p	hsa-let-7a-3p	hsa-miR-218	hsa-miR-628-5p	hsa-miR-615	hsa-miR-125b	hsa-miR-21
hsa-miR-486-5p	hsa-let-7c	hsa-miR-221	hsa-miR-642a-5p	hsa-miR-1246	hsa-miR-1301	hsa-miR-210-3p
hsa-miR-382	hsa-miR-100	hsa-miR-222	hsa-miR-7	hsa-miR-493-3p	hsa-miR-1301-3p	hsa-miR-22
hsa-miR-1297	hsa-miR-101	hsa-miR-224	hsa-miR-765	hsa-miR-132	hsa-miR-1307	hsa-miR-221
hsa-miR-372	hsa-miR-105	hsa-miR-23a	hsa-miR-940	hsa-miR-491-5p	hsa-miR-141	hsa-miR-222
hsa-miR-186	hsa-miR-124	hsa-miR-23b	hsa-miR-223	hsa-miR-185-5p	hsa-miR-141-3p	hsa-miR-223-3p
hsa-miR-27a	hsa-miR-128	hsa-miR-25	hsa-miR-125b	hsa-miR-1266-5p	hsa-miR-146b	hsa-miR-301a
hsa-miR-509-5p	hsa-miR-1296	hsa-miR-26a	hsa-miR-573	hsa-miR-126	hsa-miR-150	hsa-miR-301b
hsa-miR-802	hsa-miR-130b	hsa-miR-26b	hsa-miR-340	hsa-miR-1	hsa-miR-152-3p	hsa-miR-30d
hsa-miR-466	hsa-miR-133b	hsa-miR-29b	hsa-miR-378	hsa-miR-152	hsa-miR-153	hsa-miR-30e*
hsa-miR-141	hsa-miR-135a	hsa-miR-302a	hsa-miR-135b	hsa-miR-29c	hsa-miR-155	hsa-miR-31
hsa-miR-34b-3p	hsa-miR-143	hsa-miR-30a	hsa-miR-24	hsa-miR-17	hsa-miR-181a	hsa-miR-323
hsa-miR-130a	hsa-miR-145	hsa-miR-30b	hsa-miR-421	hsa-miR-452-5p	hsa-miR-181b	hsa-miR-429
hsa-miR-194	hsa-miR-146a	hsa-miR-30d	hsa-miR-103	hsa-miR-206	hsa-miR-181c	hsa-miR-454
hsa-miR-1271	hsa-miR-154	hsa-miR-30e	hsa-miR-613	hsa-miR-1180	hsa-miR-181d	hsa-miR-483-5p
hsa-miR-501-3p	hsa-miR-15a	hsa-miR-31	hsa-miR-335	hsa-miR-211	hsa-miR-182	hsa-miR-486-5p
hsa-miR-196a-5p	hsa-miR-15b	hsa-miR-323	hsa-miR-543	hsa-miR-144-3p	hsa-miR-182-5p	hsa-miR-500
hsa-miR-33a	hsa-miR-16	hsa-miR-330	hsa-miR-146b	hsa-miR-202	hsa-miR-183	hsa-miR-543
hsa-miR-618	hsa-miR-187	hsa-miR-331-3p	hsa-miR-129	hsa-miR-133a-3p	hsa-miR-18a	hsa-miR-588
hsa-miR-30c	hsa-miR-188-5p	hsa-miR-345	hsa-miR-138	hsa-miR-99a	hsa-miR-191	hsa-miR-590-3p
hsa-let-7a	hsa-miR-195	hsa-miR-34a	hsa-miR-204-5p	hsa-miR-410-3p	hsa-miR-192	hsa-miR-652
hsa-miR-199a	hsa-miR-199b	hsa-miR-34b	hsa-miR-26a-5p	hsa-miR-139-5p	hsa-miR-194	hsa-miR-671
hsa-miR-141-3p	hsa-miR-200b	hsa-miR-34c	hsa-miR-204	hsa-miR-519d	hsa-miR-204	
hsa-miR-205-5p	hsa-miR-203	hsa-miR-374b	hsa-miR-22	hsa-miR-150	hsa-miR-206	
hsa-miR-193a-3p	hsa-miR-205	hsa-miR-449a	hsa-miR-154-5p	hsa-miR-373-3p	hsa-miR-20a	
hsa-miR-493-5p	hsa-miR-212	hsa-miR-4723-5p	hsa-miR-452	hsa-miR-744	hsa-miR-20b	
hsa-miR-539	hsa-miR-497	hsa-miR-503	hsa-miR-10a	hsa-miR-93	hsa-miR-96	